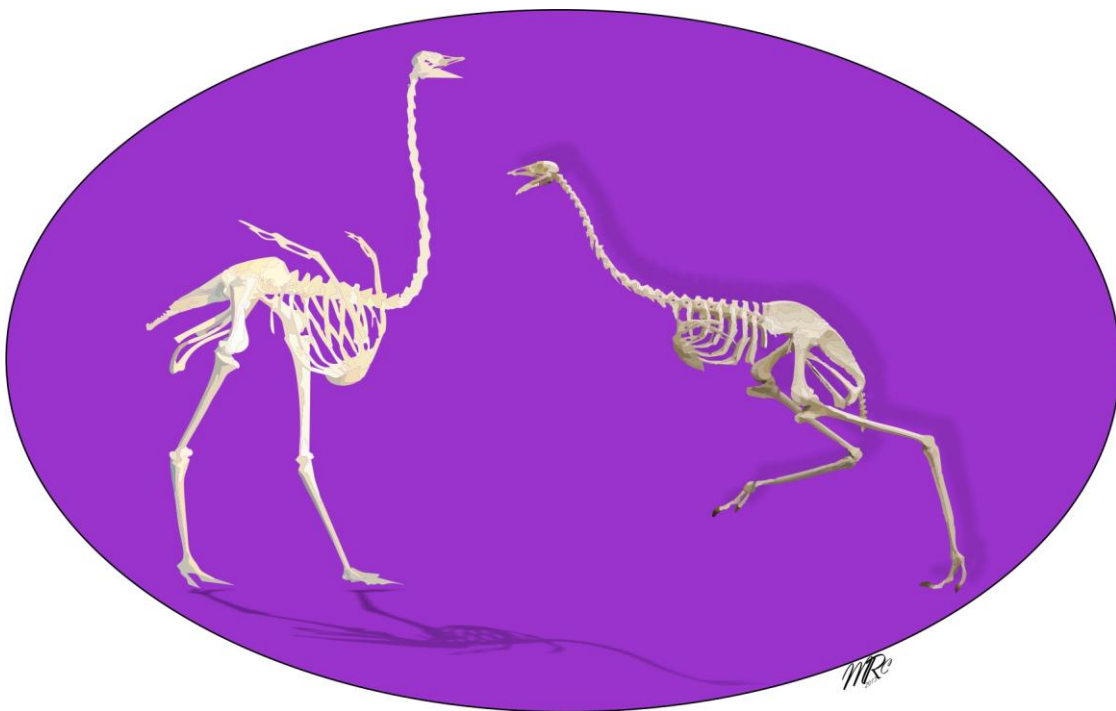


**Comparative morphology
and functional significance of mechanical and
sensory structures in the upper digestive tract of
the ostrich (*Struthio camelus*) and emu
(*Dromaius novaehollandiae*)**



by

MARTINA RACHEL CROLE
BVSc (Hons) MSc (*Cum laude*) PGCHE

Submitted in partial fulfilment of the requirements for the degree Doctor of Philosophy

**DEPARTMENT OF ANATOMY AND PHYSIOLOGY
FACULTY OF VETERINARY SCIENCE
UNIVERSITY OF PRETORIA
PRETORIA
2013**

Promoter:

**Professor Doctor John Thomson Soley
BA (Hons)(UNISA) MSc (Witwatersrand) PhD (Pretoria)
Department of Anatomy and Physiology
Faculty of Veterinary Science
University of Pretoria
Pretoria**

DECLARATION

I declare that the thesis which I hereby submit for the degree Doctor of Philosophy (PhD) (Veterinary Sciences) at the University of Pretoria is my own work and has not been submitted by me for a degree at another university.

DEDICATION

To my Ouma, Elizabeth Crole.

To my family, who despite being far away, have over the years never forgotten about me. My parents: Louis and Susan Crole. My sisters and bother-in-laws: Emma and Gary Pardoe, Elizabeth and Robert Lavies and Louise and Nicholas Groenewald. And, of course, all my favourite nieces and nephews: Rebecca, Sarah, Hannah and James Pardoe and Jessica, Daniel and Benjamin Lavies.

My Aunt, Tersia Venter. Thank you for always being there for me. To the remainder of my Aunts, Uncles and cousins: the Osler's and Harris' thank you for all the good times, parties, camping and great family get-togethers.

To Deon: your love for life and your love for me are truly uplifting and inspiring.

The enigmatic ostrich and emu

Flapping their wings the ostrich tribe cannot fly;
Whereas those of most birds take them high in the sky.
The ostrich she leaves her eggs on the ground,
Where there in the dust their warmth can be found.
She forgets that a foot may step on and break them,
Or indeed that a beast may find them and take them.
She treats her young harshly, as though they weren't hers,
And labours in vain without thinking for years.
For her wisdoms' deprived by the Great God Jehovah,
As He did not bestow her with wisdom all over.
Yet when she arises and lifts herself high,
She scorns horse and rider as she goes by.

CONTENTS

ACKNOWLEDGEMENTS	ii
SUMMARY	iii
<u>CHAPTER 1:</u> GENERAL INTRODUCTION	1
<u>CHAPTER 2:</u> THE LINGUO-LARYNGEAL APPARATUS	9
<u>CHAPTER 3:</u> DISTRIBUTION AND STRUCTURE OF INTRA-ORAL HERBST CORPUSCLES	27
<u>CHAPTER 4:</u> MORPHOLOGY AND SENSORY SPECIALISATIONS OF THE BILL. I. EPIDERMIS AND DERMIS	84
<u>CHAPTER 5:</u> MORPHOLOGY AND SENSORY SPECIALISATIONS OF THE BILL. II. THE OSSEOUS COMPONENT OF THE BILL TIP	114
<u>CHAPTER 6:</u> MORPHOLOGY AND SENSORY SPECIALISATIONS OF THE BILL. III. THE TRIGEMINAL NERVE BRANCHES SUPPLYING THE BILL TIP	156
<u>CHAPTER 7:</u> MORPHOLOGY AND SENSORY SPECIALISATIONS OF THE BILL. IV. THE BILL TIP ORGAN	184
<u>CHAPTER 8:</u> DISTRIBUTION AND STRUCTURE OF TASTE BUDS	214
<u>CHAPTER 9:</u> GENERAL CONCLUSIONS	235
APPENDICES	241

ACKNOWLEDGEMENTS

To my promoter, colleague and friend, John Soley. You have taught me excellence and through your patience and effort have provided me with a solid foundation in research. You are a dedicated teacher and I look forward to many more lessons and adventures together in the world of teaching and academia. Thank you for all the time and effort you have poured into this thesis.

The Head of Department, Anatomy and Physiology, Faculty of Veterinary Science, Herman Groenewald. Thank you for your continued support.

Adriaan Olivier (Klein Karoo Ostrich Abattoir), Tanya Claassen (Oryx Ostrich Abattoir), Petra Rough (Emu Ranch, Rustenburg) and Peter Duncan (Krugersdorp) for providing the ostrich and emu specimens. Without your interest and co-operation none of this study would have been possible.

Erna van Wilpe and Lizette du Plessis (Electron Microscopy Unit, Department, of Anatomy and Physiology); Sarah Clift, Raphima Phaswane, Naomi Timmerman and Joey Breedt (Histopathology Laboratory, Department of Paraclinical Sciences) for the processing of specimens; Lizette du Plessis for the electron micrographs of Herbst corpuscles; The librarians from the Jotella F. Soga Library, Faculty of Veterinary Science; Charmaine Vermeulen for the beautiful photography; Fritz Huchzermeyer and Elizabeth Lavies for German translations.

Wilma Olivier and Support staff of the Department of Anatomy and Physiology, Faculty of Veterinary Science; Andre Ganswindt for assistance with statistical analysis.

The University of Pretoria for financial support of this project.

Rob and Yvonne Sinclair, René, Quinton and Shane Sutherland, Marja Soley, Kirstin, Gerhard, Damién and Carly van den Berg; thank you for all the fun times, love, care and support.

SUMMARY

Comparative morphology and functional significance of mechanical and sensory structures in the upper digestive tract of the ostrich (*Struthio camelus*) and emu (*Dromaius novaehollandiae*)

by

MARTINA RACHEL CROLE

PROMOTER: Professor Doctor John Thomson Soley

DEPARTMENT: Department of Anatomy and Physiology, Faculty of Veterinary Science, University of Pretoria, Private Bag X04, Onderstepoort, 0110, Republic of South Africa.

DEGREE: Doctor of Philosophy (PhD)

This study describes, on a comparative basis, the morphology of mechanical (the linguo-laryngeal apparatus) and sensory (Herbst corpuscles and taste buds) specialisations in the upper digestive tract (bill and oropharynx) of the ostrich and emu, with a view to a better understanding of the functional significance of these structures. The ostrich and emu are commercial entities that constitute important niche industries and are farmed intensively throughout South Africa. A lack of information on the mechanical and sensory specialisations of the upper digestive tract in these two birds hampers a sound understanding of food selection and intake.

A total of 48 adult (12-14 months) ostrich heads and 48 adult emu (12-14 months) heads obtained from birds at slaughter at commercial abattoirs and farms, as well as 5 ostrich chick (2-4 weeks) heads and 1 emu chick (8 weeks) head, obtained from previous research projects, were used for this study. Morphological features were described using basic gross anatomical (dissection and stereomicroscopy) and histological techniques (H&E staining), supplemented by differential staining for cartilage and bone, transmission electron microscopy and immunohistochemistry. The findings of the study were compared with the relevant literature and hypotheses for functional significance were formed.

The avian glottis channels air from the oropharynx to the trachea and is situated on an elevated structure, the laryngeal mound. It is imperative that the glottis be protected and closed during swallowing, which in mammals is achieved by covering the glottis with the epiglottis, as well as by adduction of the arytenoid cartilages. An epiglottis, however, is reportedly absent in birds. Ratites such as the ostrich and emu possess a very wide glottis in comparison to other birds. The question therefore arises as to how these large birds avoid inhalation of food particles through a wide glottis, with apparently little protection, particularly as their feeding method involves throwing the food over the glottis to land in the proximal esophagus. In the ostrich, when the glottis was closed and the tongue body retracted, the smooth tongue root became highly folded and the rostral portion of the laryngeal mound was encased by the pocket in the base of the \cap -shaped tongue body. In this position the lingual papillae also hooked over the most rostral laryngeal projections. However, in the emu, retraction of the tongue body over the closed glottis resulted in the prominent, triangular tongue root sliding over the rostral portion of the laryngeal mound. In both the ostrich and emu these actions resulted in the rostral portion of the laryngeal mound and weakest point of the adducted glottis being enclosed and stabilised. Only after conducting a comparative study between these two birds using fresh specimens did it become clear how specific morphological peculiarities were perfectly specialised to assist in the closure and protection of the wide glottis. A unique anatomical mechanism in ratites was identified, described and proposed, which may functionally replace an epiglottis; the linguo-laryngeal apparatus.

The oropharynx of the ostrich and emu is richly supplied with Herbst corpuscles. This widespread distribution of these mechanoreceptors has not previously been reported in

birds. Specific concentrations of Herbst corpuscles within the oropharynx, which differ between the ostrich and emu, assist in the accurate positioning of the tongue and laryngeal mound for cleaning the choana (internal nares). The Herbst corpuscles are strategically located to aid in the handling and transport of food and the median palatine and ventral ridges in the ostrich display a concentration of Herbst corpuscles which denote these structures as sensory organs, namely the palatal and interramal organs. Three specific arrangements of Herbst corpuscles were noted in the oropharynx. The first arrangement consisted of groups of corpuscles located peripherally around a myelinated nerve and was present in the bill tip. The second arrangement, possibly linked to the first, was that of individual or groups of corpuscles without an obvious associated nerve and was present throughout the remaining regions of the oropharynx. The third arrangement was that of corpuscles associated with large, simple branched tubular mucus-secreting glands. The basic structure of Herbst corpuscles in the ostrich and emu, observed by light and transmission electron microscopy, of a capsule (with cellular and acellular lamella), an outer zone (collagen fibrils, fibroblasts and a fluid matrix), an inner core (formed by bilaterally symmetrical specialised Schwann cells) and a receptor axon, is similar to that noted for other avian species. However, unlike in other birds, the capsule of the Herbst corpuscle in the ostrich and emu is formed by myofibroblasts which indicates contractile properties for this component of the corpuscle in ratites. Sensory cilia were noted in the myofibroblasts of the capsule and fibroblasts of the outer zone of the ostrich Herbst corpuscle which may assist in regulating the tension of the capsule. These features have not been reported in other avian species.

Although the structure of the palaeognathous palate has been widely studied, relatively little information is available on the morphology of the ratite bill. The kiwi possesses a bill tip organ and the present study confirmed the existence of this somatosensory organ in the ostrich and emu. Examination of the rhamphotheca of these two birds demonstrated numerous specialisations. In the emu, rhamphothecal serrations with intervening keratinised pegs on the rostral mandibular tomia resembled a form of pseudo-teeth. These structures may share a similar embryological origin to teeth; however, they would appear to function by channelling and enhancing vibratory stimuli to Herbst corpuscles in nearby bony pits. In the ostrich, epidermal troughs were present in the regions overlying the bill tip organ and functioned to enhance vibratory stimuli to the underlying Herbst corpuscles. Additionally, in the ostrich only, and not related to the

structure or functioning of the bill tip organ, the rostral tomia and maxillary and mandibular nails were composed of typical tubular and inter-tubular horn. This may represent a unique feature in birds. The structure of the mandible and premaxilla was similar to that described previously for these birds. However, the persistence of Meckel's cartilage through to the adult bird in the ostrich and emu is a novel avian feature not previously reported.

The bony bill tips were adorned with numerous sensory (bony) pits which displayed similar distribution patterns in the ostrich and emu and indicated the presence, macroscopically, of a bill tip organ. The total number of pits in the bill tip of the ostrich and emu did not differ significantly, although regional differences did occur. The subdivisions of the trigeminal nerve (*N. ophthalmicus*, *N. medialis* and *N. intramandibularis*) innervating the bill tip were well developed in both birds and displayed extensive branching. The emu displayed more myelinated nerve fibres in both nerves than in the ostrich. As myelinated nerve fibres supply Herbst corpuscles, the number of nerve fibres is correlated to the number of corpuscles. No correlation could be made between the number of pits in a particular region and the number of nerve fibres or with the relative percentage of Herbst corpuscles in that region. The bill tip organ in both species was basically similar except for the epidermal specialisations noted above. Two parts of the bill tip organ were recognised; the bony bill tip organ (Herbst corpuscles stacked in bony cavities and pits) and the peripheral bill tip organ (Herbst corpuscles in sheets or chains in the connective tissue between the epithelium and bone). The morphology of the bill tip organ in the ostrich and emu indicates that it is an organ that functions by direct touch. These two ratite species appear to possess the most elaborate bill tip organ of any pecking bird. The existence of a bill tip organ in the ostrich and emu is an enigma and points to the possibility that a bill tip organ is a basal structure in all palaeognathous birds (living and extinct). Furthermore, it is evident by observing the exploratory behaviour of the ostrich and emu, that they use their bill tip organ extensively as a tool for exploring and interpreting their environment as well as for discriminating food.

The sense of taste in birds is an important motivator for feeding as well as initial food selection. The existence of this sense in ratites has remained largely speculative. In the present study taste buds were only identified in the emu and were predominantly located in the caudal region of the non-pigmented oropharyngeal roof and sparsely

located on the oropharyngeal floor. The taste buds extended the full width of the epithelium in which they were located and were ovoid structures. The taste bud was composed of centrally located, vertically oriented light and dark cells (representing both receptor cells and supporting elements) and peripherally situated follicular cells which were continuous with the surrounding *Str. germinativum* of the stratified squamous epithelium. Positive IHC labelling for neurofilament demonstrated numerous fine nerve fibres (*Neurofibra gustatoria*) within the connective tissue immediately surrounding the taste bud. Taste bud morphology in the emu was similar to that described in other birds. However, when sectioned tangentially they were indistinguishable from the surrounding epithelium with H&E staining. By using IHC labelling, concentrations of nerve fibres could be demonstrated beneath apparently nondescript epidermal structures, thus indicating the presence of a taste bud. The distribution of taste buds in the oropharynx could be linked to the particular feeding method of the emu. Based on information from GenBank, it would appear that the relatively few taste buds present in the emu oropharynx would mainly function in distinguishing bitter taste. As bitter-tasting compounds can cause a negative association with a particular food type, it would appear that the sense of taste in the emu would predominantly function for protection and not food selection.

This study revealed various unique findings regarding the mechanical and sensory specialisations in the upper digestive tract of the ostrich and emu.

- The ostrich and emu possess a combination of structures which functionally replace an epiglottis, namely the linguo-laryngeal apparatus.
- Herbst corpuscles are widely distributed in the oropharynx of the ostrich and emu and their distribution is related to the particular feeding habits of these birds.
- The capsule of Herbst corpuscles in the ostrich and emu is composed of contractile elements, a feature not reported in other birds.
- The ostrich and emu possess a well-developed bill tip organ, which is an unusual feature amongst pecking birds.
- Taste buds are present in the emu and no structures resembling taste buds were identified in the ostrich.

CHAPTER 1

GENERAL INTRODUCTION

The ostrich (*Struthio camelus*) and emu (*Dromaius novaehollandiae*) are, respectively, the largest and second largest extant birds in the world (Amadon, 1947). Both are members of the *Ratidae* and are farmed extensively throughout the world for their feathers, meat and skin (the ostrich) and fat, meat and skin (the emu). There is a continued and increasing world-wide interest in ratites as these birds are farmed to meet potential demand (Tully and Shane, 1996) thus making both species commercially important. Despite the global focus of ostrich production residing in South Africa (Tully and Shane, 1996), emu farming in this country is assuming an ever increasing importance as a valuable niche enterprise, focussing attention on the need for an improved understanding of the basic biology of these birds. Ratites, together with the tinamous (*Tinamiformes*), belong to the superorder *Palaeognathae*, which represents the much smaller of only two extant superorders within the class *Aves*; the other superorder being the *Neognathae*. Pycraft (1900) first used the term palaeognathous (meaning ancient palate) which refers to the difference in palatal conformation between palaeognathous and neognathous birds (Johnston, 2011). The palaeognaths represent a monophyletic group (Johnston, 2011) and their distinct differences from neognathous birds have prompted a large degree of academic and taxonomic interest. Despite the amount of data available, there has been little agreement regarding the phylogeny of palaeognathous birds or their position within the avian phylogenetic tree. This is emphasized by the conflicting information presented by molecular and morphological studies (see Johnston (2011) for a review of the literature). Part of the fascination with ratites is their close relation to the extinct moas and elephant birds, the largest known birds to have ever walked the earth, with the Elephant-bird (*Aepyornis maximus*) of Madagascar estimated at 438 kg and the larger Moas (*Dinornis*) of New Zealand estimated at 236 kg, compared to the mass of approximately 100 kg in an ostrich (Amadon, 1947).

The upper digestive tract (bill, oropharynx and esophagus) is of considerable importance in birds. Positioned at the end of a long and highly mobile neck, the bill may serve many purposes of a human hand (Wight *et al.*, 1970) which would include defense, feeding, preening, nest building and exploration. The basic morphology of the oropharynx and esophagus has been extensively described in both the ostrich (Tivane, 2008) and emu (Crole, 2009). Both of these studies reveal an underlying complexity of this region and the structures therein such as the presence of Herbst corpuscles (both species) and taste buds (in the emu). Preliminary studies on the oropharynx have further indicated interesting differences and or similarities in the distribution and structure of Herbst corpuscles in the ostrich and emu (Crole and Soley, 2009a; Crole *et al.*, 2009), further strengthening the need to fully understand the morphology of this region in ratites. There is a notable body of literature available on the upper digestive tract of ratites (Meckel, 1829; Owen, 1835; Cuvier, 1836; MacAlister, 1864; Gadow, 1879; Owen, 1879; Parker, 1891; Pycraft, 1900; Göppert, 1903; Duerden, 1912; Faraggiana, 1933; Roach, 1952; Parkes and Clark, 1966; Feder, 1972; McCann, 1973; Cho *et al.*, 1984; Herd, 1985; Fowler, 1991; Bonga Tomlinson, 2000; Gussekloo and Bout, 2005; Tivane *et al.*, 2006; Cunningham *et al.*, 2007; Guimarães *et al.*, 2007; Porcescu, 2007; Jackowiak and Ludwig, 2008; Tadjalli *et al.*, 2008; Tivane, 2008; Crole, 2009; Crole and Soley, 2009a, b, c; Crole *et al.*, 2009; Guimarães *et al.*, 2009; Poost Pasand *et al.*, 2010; Crole and Soley, 2010a, b, 2011a, b; Santos *et al.* 2011; Crole and Soley, 2012a, b, c; Crole *et al.*, 2013) which, although appearing exhaustive, contains, with few exceptions, inadequate anatomical detail. Additionally, the scattered nature of this information has resulted in difficulty regarding interpretation of the data (Sales, 2006). Despite being based on scant anatomical information, the feeding pattern of ratites has been documented in some detail (Bonga Tomlinson, 2000; Gussekloo and Bout, 2005). This information has subsequently been linked to specialized anatomical structures (Crole and Soley, 2009a, b, c, 2010a, b, c, 2011, 2012b, c).

Select previous studies on the upper digestive tract of the ostrich (Tivane, 2008; Crole *et al.*, 2009; Crole and Soley, 2012c) and emu (Crole, 2009; Crole *et al.*, 2009; Crole and Soley, 2009a, b, c, 2010a, b, c, 2011, 2012a, c) have identified a number of aspects (see below) which require further exploration, explanation and characterization, and which, when compared on a comparative basis, will allow more clear and accurate interpretations of anatomical peculiarities. It is already apparent that palaeognathous

birds (including the ostrich and emu) differ considerably, with respect to anatomy and feeding, from neognathous birds (Bonga Tomlinson, 2000; Gussekloo and Bout, 2005). A more detailed understanding of the morphology of mechanical and sensory structures in palaeognaths may further distinguish this small superorder of birds and consolidate their status not only as a commercial entity (ostrich and emu), but also as a unique, monophyletic group of birds. An understanding of the basic anatomy of structures in the oropharynx of the ostrich and emu will assist in recognizing pathology in this region. For example, the pharyngeal folds and associated tonsils (Crole and Soley, 2010a, 2012a) have been linked to an important disease, avian mycobacteriosis, whereby the infection was apparently localized within these structures in the ostrich (Crole *et al.*, 2013). This finding has implications for flock and human health and could possibly be incorporated in meat inspection protocols to identify birds with similar lesions which may potentially be infected.

The provision of previously unknown comparative data on the morphology and related function of mechanical and sensory structures in the upper digestive tract of commercially important ratites (ostrich and emu) could positively impact on the ratite industry by providing an improved understanding of diet selection as well as serving as an aid in pathological studies. The morphological data provided by the study would be of academic value in allowing future comparisons to be made between members of the *Ratidae* as well as providing further insight into their phylogeny. A more detailed introduction is supplied for each individual topic addressed in the various chapters of the thesis.

This study aims to:

- Describe the linguo-laryngeal apparatus in the ostrich and emu and provide a comprehensive comparative analysis of its function based on distinct morphological features.
- Provide a comparative description of the distribution and morphological features of Herbst corpuscles in the oropharynx of the ostrich and emu.
- Characterise the innervation of the bill in the ostrich and emu and provide a comprehensive comparative morphological description.
- Describe, on a comparative basis, the distribution and structure of taste buds in the upper digestive tract of the ostrich and emu.
- Link microscopic findings to the gross morphology and formulate postulations for function.
- Critically appraise the existing literature on the above mentioned topics.
- Gather data for future studies.

The envisaged benefits arising from this study are the following:

- Characterisation of a novel anatomical mechanism (the linguo-laryngeal apparatus) in ratites.
- Mapping and comparison of sensory structures (Herbst corpuscles and taste buds) in the upper digestive tract of the ostrich and emu.
- Characterisation of bill structure and innervation in the ostrich and emu.
- Determination and characterisation of the sense of taste in the ostrich and emu which could have implications for the composition of feed.
- Provision of a more accurate appreciation of the structure of the upper digestive tract of commercially important ratites which will provide a greater insight into food selection and feeding behaviour of these birds.

References

- Amadon, D. 1947. An estimated weight of the largest known bird. *The Condor*. **49**: 159-164.
- Bonga Tomlinson, C.A. 2000. *Feeding in Paleognathous Birds*. In: Feeding: Form, Function, and Evolution in Tetrapod Vertebrates. Edited by K. Schwenk. San Diego: Academic Press. pp. 359-394.
- Cho, P., Brown, B. and Anderson, M. 1984. Comparative gross anatomy of ratites. *Zoo Biology*. **3**: 133-144.
- Crole, M.R. 2009. A gross anatomical and histological study of the oropharynx and proximal oesophagus of the emu (*Dromaius novaehollandiae*). MSc dissertation, University of Pretoria, South Africa.
- Crole, M.R. and Soley, J.T. 2009a. Comparative distribution of Herbst corpuscles within the oropharyngeal cavity of the ostrich (*Struthio camelus*) and emu (*Dromaius novaehollandiae*). *17th Congress of the International Federation of Associations of Anatomists*, Cape Town, South Africa. p. 361.
- Crole, M.R. and Soley, J.T. 2009b. Morphology of the tongue of the emu (*Dromaius novaehollandiae*). I. Gross anatomical features and topography. *Onderstepoort Journal of Veterinary Research*. **76**: 335-345.
- Crole, M.R. and Soley, J.T. 2009c. Morphology of the tongue of the emu (*Dromaius novaehollandiae*). II. Histological features. *Onderstepoort Journal of Veterinary Research*. **76**: 347-361.
- Crole, M.R. and Soley, J.T. 2010a. Distribution and structure of lymphoid tissue in the upper digestive tract of the emu (*Dromaius novaehollandiae*). *Proceedings of the Microscopy Society of Southern Africa*. **40**: 18.
- Crole, M.R. and Soley, J.T. 2010b. Gross morphology of the intra-oral *rhamphotheca*, oropharynx and proximal esophagus of the emu (*Dromaius novaehollandiae*). *Anatomia Histologia Embryologia*. **39**: 207-218.
- Crole, M.R. and Soley, J.T. 2010c. Surface features of the emu (*Dromaius novaehollandiae*) tongue. *Anatomia Histologia Embryologia*. **39**: 355-365.
- Crole, M.R. and Soley, J.T. 2011. Gland distribution and structure in the oropharynx and proximal oesophagus of the emu (*Dromaius novaehollandiae*). *Acta Zoologica (Stockholm)*. **92**: 206-215.
- Crole, M.R. and Soley, J.T. 2012a. Evidence of a true pharyngeal tonsil in birds: A novel lymphoid organ in *Dromaius novaehollandiae* and *Struthio camelus* (Palaeognathae). *Frontiers in Zoology*. **9**: 21.

Crole, M.R. and Soley, J.T. 2012b. Gross anatomical features of the tongue, lingual skeleton and laryngeal mound of *Rhea americana* (Palaeognathae, Aves): morpho-functional considerations. *Zoomorphology*. **131**: 265-273.

Crole, M.R. and Soley, J.T. 2012c. What prevents *Struthio camelus* and *Dromaius novaehollandiae* (Palaeognathae) from choking? A novel anatomical mechanism in ratites, the linguo-laryngeal apparatus. *Frontiers in Zoology*. **9**: 11.

Crole, M.R., Soley, J.T. and Clift, S.J. 2013. Incidental *Mycobacterium*-induced granulomatous inflammation of the follicular pharyngeal tonsils in a South African farmed ostrich (*Struthio camelus*). *Journal of the South African Veterinary Association*. **84** (1): Art. #961, 9 pages. <http://dx.doi.org/10.4102/jsava.v84i1.961>

Crole, M.R., Soley, J.T. and du Plessis, L. 2009. The ultrastructure of Herbst corpuscles in the oropharynx of the emu (*Dromaius novaehollandiae*) and ostrich (*Struthio camelus*). *Proceedings of the Microscopy Society of Southern Africa*. **39**: 27.

Cunningham, S., Castro, I. and Alley, M. 2007. A new prey-detection mechanism for kiwi (*Apteryx* spp.) suggests convergent evolution between paleognathous and neognathous birds. *Journal of Anatomy*. **211**: 493-502.

Cuvier, G. 1836. *Leçons d'anatomie comparée*, Third edition. Vol. 1 & 2. Edited by M. Duméril. Bruxelles: Dumont.

Duerden, J.E. 1912. Experiments with ostriches XVIII. The anatomy and physiology of the ostrich. A. The external characters. *Agricultural Journal of the Union of South Africa*. **3**: 1-27.

Faraggiana, R. 1933. Sulla morfologia della lingua e del rialzo laringeo di alcune specie di uccelli Ratiti e Carenati non comuni. *Bollettino dei Musei di Zoologia e Anatomia Comparata*. **43**: 313-323.

Feder, F.-H. 1972. Zur mikroskopischen Anatomie des Verdauungsapparates beim Nandu (*Rhea americana*). *Anatomischer Anzeiger*. **132**: 250-265.

Fowler, M.E. 1991. Comparative clinical anatomy of ratites. *Journal of Zoo and Wildlife Medicine*. **22**: 204-227.

Gadow, H. 1879. Versuch einer vergleichenden Anatomie des Verdauungssystemes der Vögel. *Jenaische Zeitschrift für Medizin und Naturwissenschaft*. **13**: 92-171.

Göppert, E. 1903. Die Bedeutung der Zunge für den sekundären Gaumen und den Ductus nasopharyngeus. *Morphologisches Jahrbuch*. **31**: 311-359.

Guimarães, J.P., Mari, R.B., De Carvalho, H.S. and Watanabe, L. 2009. Fine structure of the dorsal surface of ostrich's (*Struthio camelus*) tongue. *Zoological Science*. **26**: 153-156.

Guimarães, J.P., Mari, R.B., Miglino, M.A., Hernandez-Blasquez, F.J. and Watanabe, I. 2007. Mecanorreceptores da mucosa palatine de avestruz (*Struthio camelus*): estudo ao microscópio luz. *Pesquisa Veterinária Brasileira*. **27**: 491-494.

Gusseklou, S.W.S. and Bout, R.G. 2005. The kinematics of feeding and drinking in palaeognathous birds in relation to cranial morphology. *The Journal of Experimental Biology*. **208**: 3395–3407.

Herd, R.M. 1985. Anatomy and histology of the gut of the emu *Dromaius novaehollandiae*. *Emu*. **85**: 43-46.

Jackowiak, H. and Ludwig, M. 2008. Light and scanning electron microscopic study of the structure of the ostrich (*Struthio camelus*) tongue. *Zoological Science*. **25**: 188-194.

Johnston, P. 2011. New morphological evidence supports congruent phylogenies and Gondwana vicariance for palaeognathous birds. *Zoological Journal of the Linnean Society*. **163**: 959-982.

MacAlister, A. 1864. On the anatomy of the ostrich (*Struthio camelus*). *Proceedings of the Royal Irish Academy*. **9**: 1-24.

McCann, C. 1973. The tongues of kiwis. *Notornis*. **20**: 123-127.

Meckel, J.F. 1829. *System der vergleichenden Anatomie*. Halle: Der Rehgerschen Buchhandlung.

Owen, R. 1835. Division I. Organs in plants and animals for the special purposes of the individual. Subdivision VIII. Organs of sense. Series II. Organ of taste. In birds, in *Royal College of Surgeons of England. Museum, Owen R (ed) Descriptive and illustrated catalogue of the physiological series of comparative anatomy contained in the museum of the Royal College of Surgeons in London. Vol. 3. Part 1. Nervous system and organs of sense*. London: Richard Taylor.

Owen, R. 1879. *Memoirs on the extinct and wingless birds of New Zealand; with an appendix of those of England, Australia, Newfoundland, Mauritius and Rodriguez*. Vol. 1. London: John van Voorst.

Parkes, K.C. and Clark, G.A. 1966. An additional character linking ratites and tinamous, and an interpretation of their monophyly. *The Condor*. **68**: 459-471.

- Parker, T.J. 1891. Observations on the anatomy and development of apteryx. *Philosophical Transactions of the Royal Society of London, B*. **182**: 25-134.
- Poost Pasand, A., Tadjalli, M. and Mansouri, H. 2010. Microscopic study on the tongue of male ostrich. *European Journal of Biological Sciences*. **2**: 24-31.
- Porcescu, G. 2007. Comparative morphology of the digestive tract of the Black African ostrich, hen and turkey. Ph.D. thesis, Agrarian State University of Moldova, Moldova.
- Pycraft, W.P. 1900. On the morphology and phylogeny of the palaeognathae (*Ratitae and Crypturi*) and neognathae (*Carinatae*). *Transactions of the Zoological Society of London*. **15**: 149-290.
- Roach, R.W. 1952. Notes on the New Zealand kiwis (1). *New Zealand Veterinary Journal*. **1**: 38-39.
- Santos, T.C., Fukuda, K.Y., Guimarães, J.P., Oliveira, M.F., Miglino, M.A. and Watanabe, I.-S. 2011. Light and scanning electron microcopy study of the tongue in *Rhea americana*. *Zoological Science*. **28**: 41-46.
- Sales, J. 2006. Digestive physiology and nutrition of ratites. *Avian and Poultry Biology Reviews*. **17**: 41-55.
- Tadjalli, M., Mansouri, S.H. and Poostpasand, A. 2008. Gross anatomy of the oropharyngeal cavity in the ostrich (*Struthio camelus*). *Iranian Journal of Veterinary Research*. **9**: 316-323.
- Tivane, C. 2008. A morphological study of the oropharynx and oesophagus of the ostrich (*Struthio camelus*). M.Sc. thesis, University of Pretoria, South Africa.
- Tivane, C., Soley, J.T. and Groenewald, H.B. 2006. Distribution and structure of Pacinian (Herbst) corpuscles in the non-glandular region of the palate of the ostrich (*Struthio camelus*). *Proceedings of the Microscopy Society of Southern Africa*. **36**: 64.
- Tully, T.N. and Shane, S.M. 1996. Husbandry practices as related to infectious and parasitic diseases of farmed ratites. *Revue Scientifique et Technique, Office International des Épizooties*. **15**: 73-89.
- Wight, P.A.L., Siller, W.G. and Mackenzie, G.M. 1970. The distribution of Herbst corpuscles in the beak of the domestic fowl. *British Poultry Science*. **11**: 165-170.

CHAPTER 2

THE LINGUO-LARYNGEAL APPARATUS

2.1. Introduction

The morphology of the ratite tongue has been addressed in a large body of literature spanning almost two centuries (1829-2012). However, upon closer inspection it becomes evident that the detailed structure of this organ has been neglected. The most comprehensive description detailing the gross morphology, histology and surface morphology of a ratite tongue remains that of the emu (*Dromaius novaehollandiae*) (Crole and Soley, 2009a, b, 2010c) and, more recently, a gross morphological study of the tongue of the greater rhea (*Rhea americana*) (Crole and Soley, 2012). Available information on the ostrich (*Struthio camelus*) tongue is less detailed and appears scattered in the literature (Faraggiana, 1933; Porcescu, 2007; Jackowiak and Ludwig, 2008; Tadjalli *et al.*, 2008, Tivane, 2008; Guimarães *et al.*, 2009; Poost Pasand *et al.*, 2010). Compounding this problem is the existence of a number of publications which contain inaccurate, confusing, conflicting and repetitive information (Jackowiak and Ludwig, 2008; Guimarães *et al.*, 2009; Poost Pasand *et al.*, 2010) and which perpetuate incorrect interpretations, particularly regarding function. However, basic information on the tongue of the ostrich (Meckel, 1829; Owen, 1835; Cuvier, 1836; MacAlister, 1864; Gadow, 1879; Pycraft, 1900; Göppert, 1903; Duerden, 1912; Cho *et al.*, 1984; Bonga Tomlinson, 2000), emu (Faraggiana, 1933; Cho *et al.*, 1984; Bonga Tomlinson, 2000), greater rhea (Owen, 1835; Faraggiana, 1933; Feder, 1972; Cho *et al.*, 1984; Bonga Tomlinson, 2000; Gussekloo and Bout, 2005; Santos *et al.*, 2011), lesser rhea (*Pterocnemia pennata*) (Gadow, 1879; Pycraft, 1900; Cho *et al.*, 1984), cassowary (*Casuarius casuarius*) (Owen, 1835; Gadow, 1879; Pycraft, 1900) and kiwi (*Apteryx australis mantelli*, *Apteryx haastii* and *Apteryx owenii*) (Owen, 1879; Parker, 1891; Roach, 1952; McCann, 1973) exists and seems to point to a certain degree of fascination with this organ in ratites.

There appear to be two specifically unique lingual structures present in ratites, namely, the pocket in the tongue body of the ostrich (Meckel, 1829; Carus, 1835; Cuvier, 1836; Faraggiana, 1933; Bonga Tomlinson, 2000; Porcescu, 2007; Jackowiak and Ludwig, 2008; Tivane, 2008) and the prominent, triangular tongue root of the emu (Faraggiana, 1933; Crole and Soley, 2009a, b, 2010a, b). Despite numerous authors having noted or described a pocket in the base of the ostrich tongue (see below), the function of this anatomical peculiarity has remained unexplained. Carus (1835) suggests that the posterior border of the ostrich tongue may function like an epiglottis; Faraggiana (1933) however, refutes this statement. The pocket is reportedly closed during tongue retraction (Bonga Tomlinson, 2000) and changes shape during intraoral transport of food suggesting a specialisation for an unexplained biological role (Bock and Bühler, 1988, cited by Bonga Tomlinson, 2000). Jackowiak and Ludwig (2008) credit the ostrich tongue with having a far-reaching structural modification yet do not elaborate further. Tivane (2008) reports a secondary fold in the lingual pocket and suggests that an increase in surface area for mucus-producing glands would enhance mucus production and secretion for ingestion of dry food. Owen (1879) described a fold in the base of the kiwi tongue, which, when the tongue is retracted, covers the glottis. Thus it seems that Carus (1835) may originally have been correct regarding the role of the tongue in sealing the glottis and the present study will demonstrate how such an action is possible in the ostrich. In the emu, the extension of the tongue root into the rostral aspect of the laryngeal entrance (Faraggiana, 1933; Crole and Soley, 2009b) represents an interesting modification not observed or illustrated in other ratites (ostrich and greater rhea) (Göppert, 1903; Faraggiana, 1933; Gussekloo and Bout, 2005; Porcescu, 2007; Jackowiak and Ludwig, 2008; Tivane, 2008; Santos *et al.*, 2011; Crole and Soley, 2012). The positioning of the tongue root would appear to assist in sealing off the rostral part of the larynx when the glottis is closed (Crole and Soley, 2009a) almost assuming the role of an epiglottis, which in birds is absent (Kaupp, 1918; Calhoun, 1954; King and McLelland 1984; Nickel *et al.*, 1977). This suggestion regarding the role of the tongue root functioning as an epiglottis in the emu was originally proposed by Gadow (1879) but disputed by Faraggiana (1933). Thus, similar to the situation regarding the lingual pocket of the ostrich, the original suggestion of Gadow (1879) may also be correct and this study will further elaborate on this proposed function.

In mammals the glottis is protected and closed during swallowing mainly by covering it with the epiglottis, as well as the pulling together (adduction) of the cartilages on either side of the glottis. Birds, however, have a slightly different laryngeal cartilage arrangement to mammals, with both the thyroid and epiglottic cartilages being absent. The ostrich and emu, in comparison to neognathous birds, possess a very wide glottis (Pycraft, 1900). The question can therefore be asked (Faraggiana, 1933) (and remains unanswered) as to how it is possible for these large birds to have such a wide glottis, with apparently little protection, and yet avoid inhalation of food particles and fluid. Despite feeding and drinking studies in the domestic chicken (*Gallus gallus*) (Heidweiller *et al.*, 1992) and in palaeognaths (Bonga Tomlinson, 2000; Gussekloo and Bout, 2005) using cinematography and radiography, no attempt has been made to explain or demonstrate how the glottis is protected during swallowing. Unique features necessary to perform this function have been noted; however, their role in protecting or covering the glottis is not mentioned.

This study aims to marry the functional data on living animals and morphological observations on fresh and preserved material to demonstrate how the intricate relationship between the variably structured tongue body, tongue root and laryngeal mound, of the ostrich and emu, functions to close off and stabilize the glottis during swallowing, thus partially fulfilling the role of an epiglottis. Although this study cannot conclusively prove this relationship in the living animal, such perfectly fitting structures cannot merely be explained away as a coincidence. This unique proposed anatomical mechanism has tentatively been named the linguo-laryngeal apparatus.

2.2. Materials and Methods

The heads of 5 adult ostriches (Klein Karoo Ostrich abattoir, Oudtshoorn, Western Cape, South Africa) and 5 adult emus (Oryx Abattoir, Krugersdorp, Gauteng Province, South Africa) of either sex were collected for this study. All the heads were thoroughly rinsed with running tap water to remove mucus, blood and regurgitated food. The tongues and laryngeal mounds were immediately removed by cutting through the arms of the ceratobranchials and the frenulum of the tongue and freeing the structures from the oropharyngeal floor. Manipulations were performed on fresh specimens to mimic

postulated actions during swallowing in the live animal as fixation with formalin does not allow free movement of the structures. Adduction (closure) of the glottis was mimicked by the use of forceps at the base of the arytenoid cartilages (Figs. 2.3e-f) and the tongue body was moved caudally by digital manipulation (Fig. 2.3a) or by using forceps. Two of the specimens for each species was sectioned longitudinally in the midline and manipulated in the same manner. The sequence of movements and interactions were observed for each specimen, described and digitally recorded with a Canon EOS 5D digital camera (Canon, Ōita, Japan) equipped with a Canon Macro 100mm lens. The specimens were subsequently stored in 10% neutral-buffered formalin.

The tongues with attached laryngeal mounds from one 2 week-old ostrich chick (protocol number 36-5-0623, Faculty of Veterinary Science, University of Pretoria) and one 8 week-old emu chick (from the same chick used in Chapter 4.2.3.), which were part of the departmental collection and stored in 10% neutral-buffered formalin, were rinsed in running tap water for 24 hours prior to staining. Both specimens were then treated according to the method of Kelly and Bryden (1983). The specimens were washed in distilled water for 30 minutes (three 10 minute changes) and then placed in Alcian blue solution (10 mg Alcian blue 8GX, 20 ml glacial acetic acid, 80 ml 95% ethanol) for 48 hours to stain the cartilage. The specimens were then rehydrated through a decreasing ethanol series (95%, 95%, 75%, 40%, 15%, distilled water (at least 2 hours per step)). They were then incubated for 72 hours at 37°C in Trypsin enzyme solution (1g trypsin 883600; 30 ml disodium tetraborate, 70 ml distilled water) to which 5 drops of 3% hydrogen peroxide were added to bleach highly pigmented tissues. The specimens were then successively transferred to a 0.5% potassium hydroxide solution, a 3:1 0.5% potassium hydroxide and glycerol solution, a 1:1 0.5% potassium hydroxide and glycerol solution and a 1:3 0.5% potassium hydroxide and glycerol solution for at least 24 hours each. The specimens were finally placed in pure glycerol to which a few thymol crystals had been added to prevent mould growth. Manipulations were also possible in the two stained specimens as the tissues were treated with Trypsin and were rendered soft and moveable. Once stained and cleared, these specimens were used to describe the laryngeal cartilages and hyobranchial apparatus with regards to the functioning of the tongue and laryngeal mound during swallowing (Figs. 2.4 and 2.6) and were digitally recorded with a Canon EOS 5D digital camera (Canon, Ōita, Japan) equipped with a Canon Macro 100mm lens.

2.3. Results

2.3.1. The ostrich

2.3.1.1. Structure of the tongue and laryngeal mound

The tongue body was Ω -shaped with a rounded apex and a concave base (Figs. 2.1 and 2.3a-c). Each lateral margin ended in a small lingual papilla (Figs. 2.3a-c, 2.4 and 2.5a), which was attached from its medial aspect by a fold to the laryngeal mound (Figs. 2.3a, b). The smooth margin of the tongue base (Figs. 2.1 and 2.3b, c) displayed a central papilla in some specimens (Fig. 2.3a). Paired cartilaginous *paraglossalia* were situated ventro-laterally in the tongue body (Fig. 2.4). The tongue root was represented by a folded tract of mucosa positioned between the base of the tongue body and the laryngeal mound (Figs. 2.1 and 2.3a, b). Transverse folds converged medially to form longitudinal folds continuous with the floor of the larynx (Fig. 2.3a). The base of the tongue body was hollowed to form a rostrally directed pocket from the floor of which originated a small caudally directed fold of tissue (Fig. 2.5a). In some specimens (Fig. 2.5a) the floor of the pocket, caudal to the small fold, displayed a structure which was similar in shape and orientation to that of the emu tongue root of (see Figs. 2.3d-f and 2.7). The raised laryngeal mound was a star-shaped structure with a wide, V-shaped glottis (Figs. 2.1 and 2.3a). The lips forming the glottis were slightly raised above the laryngeal mound (Fig. 2.5b), contained many mucous glands below the mucosa (personal observation) and were fleshy structures unsupported internally by the underlying arytenoid cartilages. The laryngeal projections were supported by the arytenoid cartilages (Figs. 2.3a-c and 2.5a).

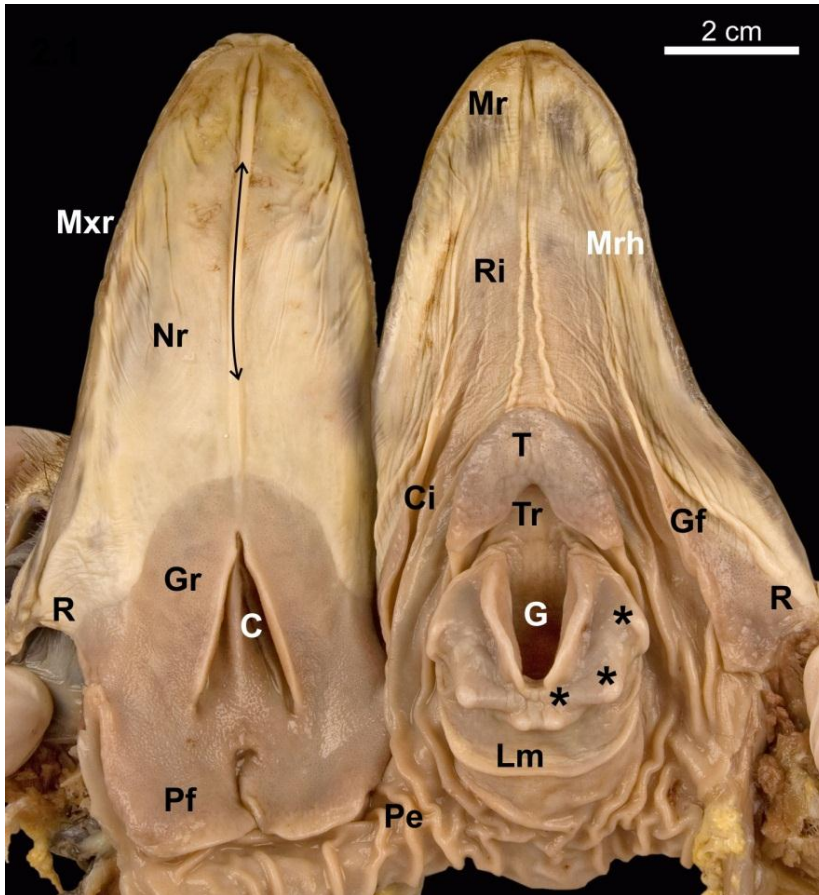


Figure 2.1. Ostrich oropharynx openly displayed to show the salient features. Non-pigmented roof (Nr), median palatine ridge (double-headed arrow), maxillary rhamphotheca (Mxr), rictus (R), glandular roof (Gr), choana (C), pharyngeal folds (Pf), proximal esophagus (Pe), mandibular rostrum (Mr), mandibular rhamphotheca (Mrh), rostral interramal region (Ri), caudal interramal region (Ci), glandular fold (Gf), tongue body (T), tongue root (Tr), laryngeal mound (Lm), glottis (G) and laryngeal papillae (*).

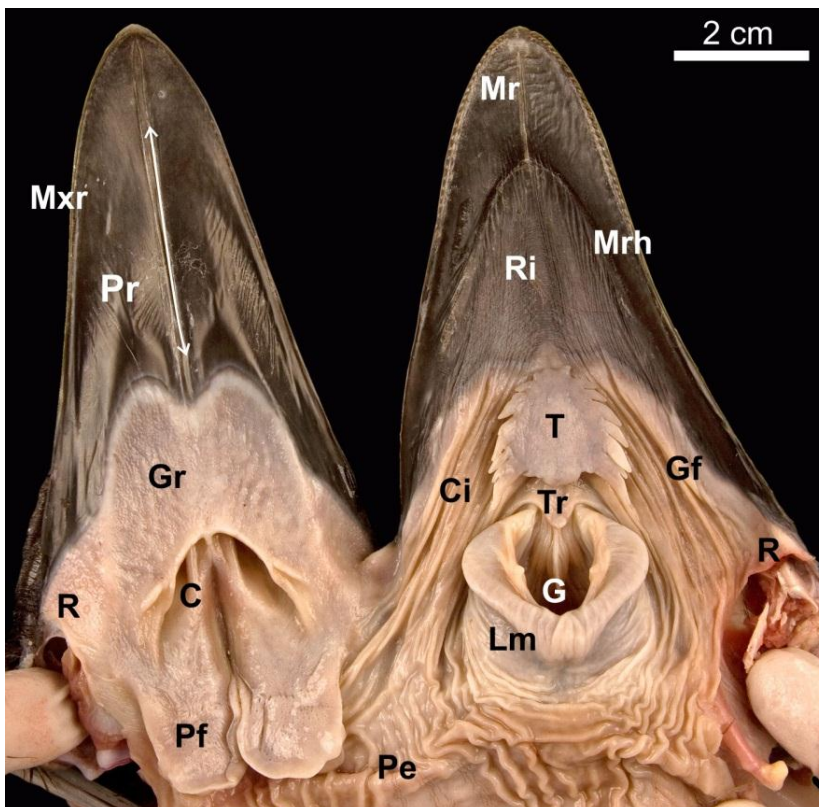


Figure 2.2. Emu oropharynx openly displayed to show the salient features. Pigmented roof (Pr), median palatine ridge (double-headed arrow), maxillary rhamphotheca (Mxr), rictus (R), glandular roof (Gr), choana (C), pharyngeal folds (Pf), proximal esophagus (Pe), mandibular rostrum (Mr), mandibular rhamphotheca (Mrh), rostral interramal region (Ri), caudal interramal region (Ci), glandular fold (Gf), tongue body (T), tongue root (Tr), laryngeal mound (Lm) and glottis (G).

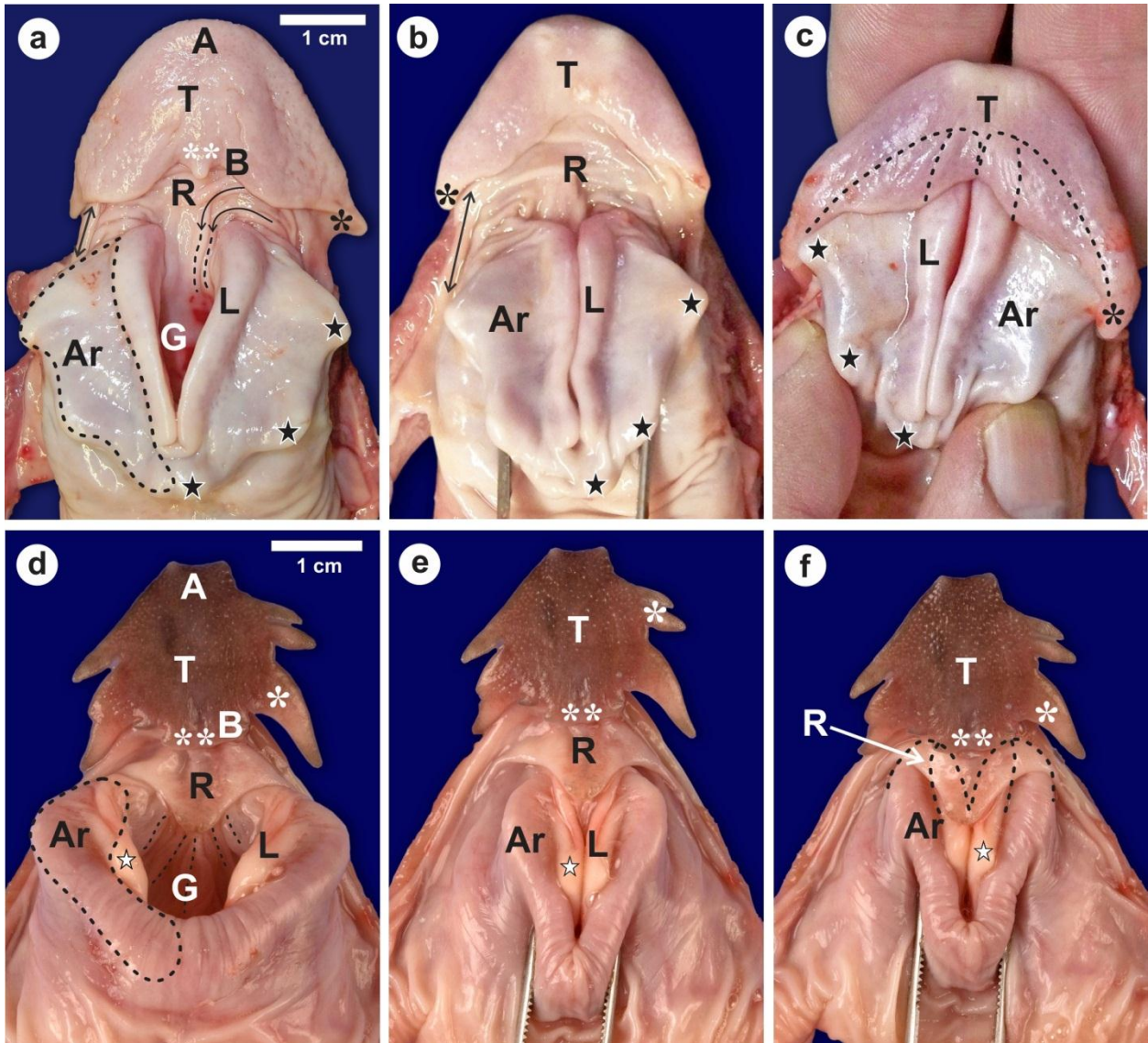


Figure 2.3. Sequence of action of the linguo-laryngeal apparatus.

(a-c). Ostrich. Tongue body (T), apex (A), tongue body base (B), tongue root (R), transverse folds (curved black arrows) and longitudinal folds (dotted lines) of the root, lingual papilla (black *), caudal lingual papilla (white **), fold between tongue and laryngeal mound (\leftrightarrow), glottis (G), laryngeal projections (black stars) and arytenoid cartilage (dotted outline, Ar) which also underlies the lips of the glottis (L).

(a). Resting position of the tongue and laryngeal mound with an open glottis.

(b). The glottis is in the closed position.

(c). The tongue is retracted and covers the rostral portion of the laryngeal mound and lips of the glottis (dotted outline). Note how the lingual papillae hook over the first laryngeal projection.

(d-f). Emu. Tongue body (T), apex (A), tongue body base (B), lateral (white *) and caudal (white **) lingual papillae, tongue root (R), longitudinal folds (dotted lines) on the floor of the larynx, glottis (G), lips of the glottis (L), protrusion of the lips (white star) and arytenoid cartilage (dotted outline, Ar).

(d). Resting position of the tongue and laryngeal mound with an open glottis.

(e). The glottis is in the closed position.

(f). The tongue is retracted and the tongue root covers the rostral portion of the laryngeal mound and lips of the glottis (dotted outline).

2.3.1.2. Closure of the glottis

During closure (adduction) of the glottis the left and right margins were closely apposed (Fig. 2.3b) but did not appear to completely seal the glottis, particularly the rostral (widest) part (Fig. 2.4a). As the tongue was retracted, the smooth tongue root became highly folded and was effectively obliterated (Fig. 2.5b) as the rostral portion of the laryngeal mound was encased by the pocket in the base of the tongue body (Figs. 2.3c and 2.4b). Concurrently, the lingual papillae hooked over the most rostral laryngeal projections (Figs. 2.3c and 2.4b). In this fashion the lingual pocket and lingual papillae effectively encapsulated and stabilized the rostral portion of the laryngeal mound (Figs. 2.3c and 2.4b), which was the weakest point of the adducted glottis. The relatively mobile, paired cartilaginous *paraglossalia* situated within the tongue body (Fig. 2.4) allowed a measure of flexibility and sufficient rigidity to the organ, facilitating its action. The elements of the hyobranchial apparatus have been described (Bonga Tomlinson, 2000; Tivane, 2008), and as seen in a median longitudinal section, the urohyal, body and rostral projection of the basihyal together with the arytenoids and rostral projection of the cricoid cartilage, appeared to form a firm base onto which the lingual pocket could 'clamp' to secure the laryngeal mound and adducted glottis (Fig. 2.5b).

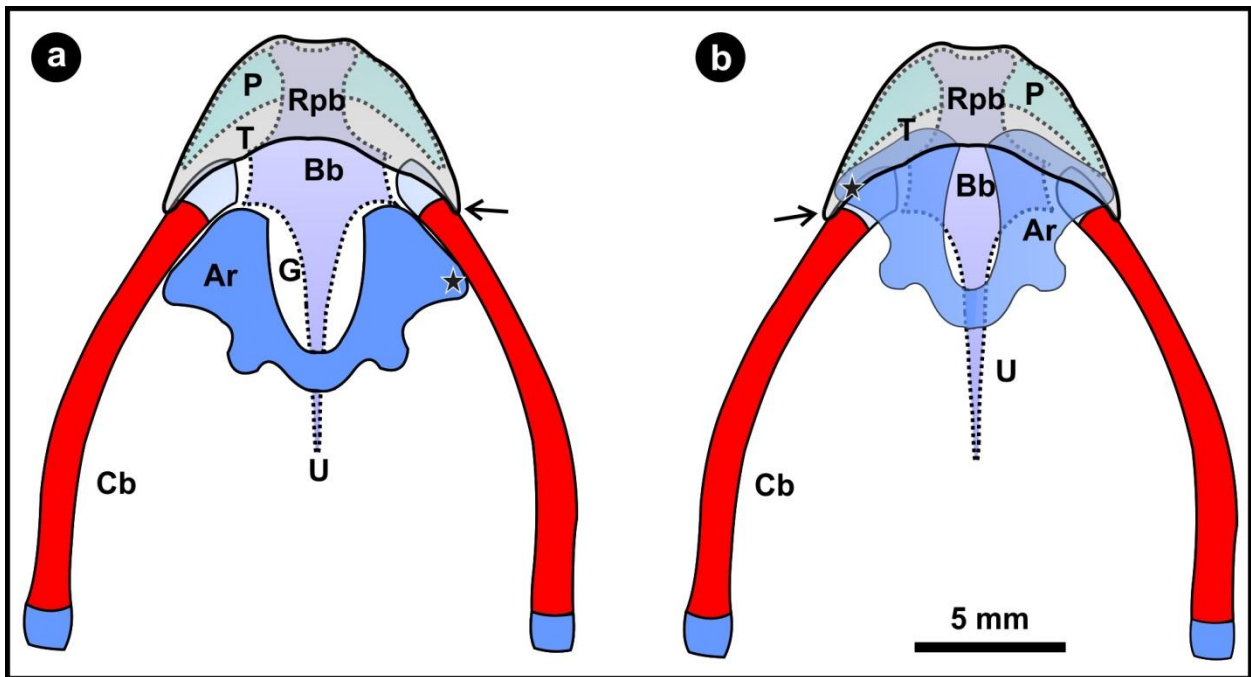


Figure 2.4. Schematic representation of the supporting elements of the linguo-laryngeal apparatus of the ostrich. Dorsal view. The cricoid and procricoid cartilages as well as the tongue root and fleshy lips of the glottis are omitted for clarity. The caudal aspect of the arytenoid cartilages (Ar) are not joined as indicated but separated by the procricoid cartilage (not illustrated). Red indicates bone and blue/purple cartilage as seen in a 2 week-old chick. **(a).** Resting relationship of the arytenoid cartilages, tongue body (T), urohyal (U), body of the basihyal (Bb), rostral projection of the basihyal (Rpb) and *paraglossalia* (P) (see Figure 2.3a). Glottis (G), rostral laryngeal projection (black star), lingual papilla (black arrow) and ceratobranchials (Cb). **(b).** The relationship of the underlying structures following retraction of the tongue (see Figure 2.3c). Note how the rostral portions of the arytenoid cartilages are enclosed in the tongue pocket and how the lingual papillae hook over the rostral laryngeal projections. The glottis appears open as the soft tissue (see Figures 2.3a-c) has not been included in the sketch.

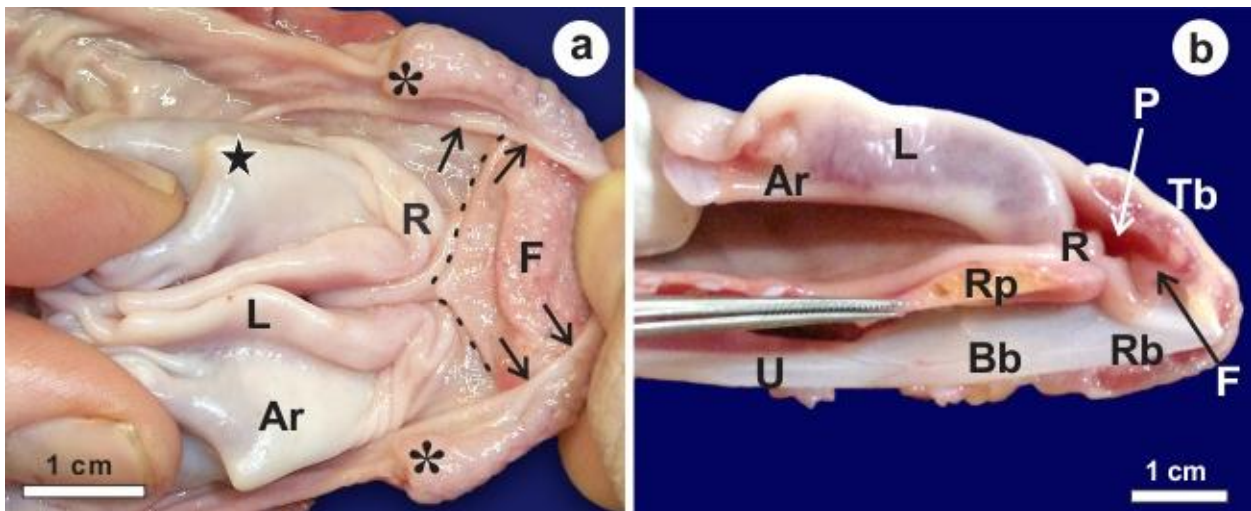


Figure 2.5. The lingual pocket of the linguo-laryngeal apparatus of the ostrich. **(a).** The lingual pocket (caudal margin indicated by arrows) reflected cranially to reveal a secondary fold (F) as well as an additional structure (dotted outline) similar in shape to the emu tongue root (only present in some specimens). Lingual papilla (*), tongue root (R), laryngeal projection (black star), mucosal covered arytenoid cartilage (Ar) and fleshy lips (L) of the glottis. **(b).** Midline longitudinal section of the linguo-laryngeal apparatus as seen in Figure 2.3c. Note how the tongue root concertina's to allow the rostral portion of the laryngeal mound to enter the lingual pocket (P). Tongue body (Tb), rostral process of the cricoid cartilage (Rp), urohyal (U), body of the basihyal (Bb) and rostral projection of the basihyal (Rb).

2.3.2. The emu

2.3.2.1. Structure of the tongue and laryngeal mound

The structure of the tongue (Crole and Soley, 2009a, b, 2010b) and the laryngeal mound (Crole and Soley, 2010a) of the emu have been described in detail. Figures 2.2, 2.3d, 2.6a and 2.7a depict the resting relationship between the tongue body, root and laryngeal mound. In summary, the tongue body was triangular and the lateral margins were adorned with numerous lingual papillae which varied in shape and number (Figs. 2.3d-f and 2.7). The base was rounded caudally due to the presence of one or more caudal papillae. The prominent tongue root was triangular with a round, raised, caudally directed protrusion advancing a short distance into the glottis (Figs. 2.2, 2.3d-f and 2.7). Caudal to the tongue root, on the floor of the larynx, were three to five longitudinal mucosal folds (Fig. 2.3d). The laryngeal mound was rhomboid-shaped and the glottis was widened rostrally, slightly convex medially and narrowed at the caudal end (Figs. 2.3d and 2.7a). As in the ostrich, the lips of the glottis were formed by a mucosa, unsupported internally by the underlying arytenoid cartilages. The glottis was widest rostrally, slightly convex medially and narrowest at the caudal end (Fig. 2.3d). The lips of the glottis were formed by a mucosa, unsupported by the arytenoid cartilages, which sloped dorso-caudally and at the highest point displayed a small, round protrusion. This structure ended in about the middle of the glottis (Figs. 2.3d-f and 2.7).

2.3.2.2. Closure of the glottis

During closure of the glottis (Fig. 2.3e) a small gap was noticeable at the rostral aspect due to the slight concavity of the lips of the glottis. As the tongue was retracted, the tongue root moved caudally together with the tongue body and slid over the rostral portion of the laryngeal mound and adducted glottis (Figs. 2.3f, 2.6b and 2.7b). In this way the rounded caudal protrusion of the tongue root met with the round protrusions of the lips of the glottis (Figs 2.3f, 2.6b and 2.7b), and effectively closed the small gap in the adducted glottis (Fig. 2.3f). Simultaneously, the rostral portion of the laryngeal mound and weakest point of the adducted glottis was enclosed and stabilized by the tongue root and the base of the tongue body, which was stiffened by the presence of the cartilaginous *paraglossum* (Figure 2.6). A shallow recess in the tongue base allowed

the tongue body to slide a short distance caudally over the tongue root, thus stabilizing its position.

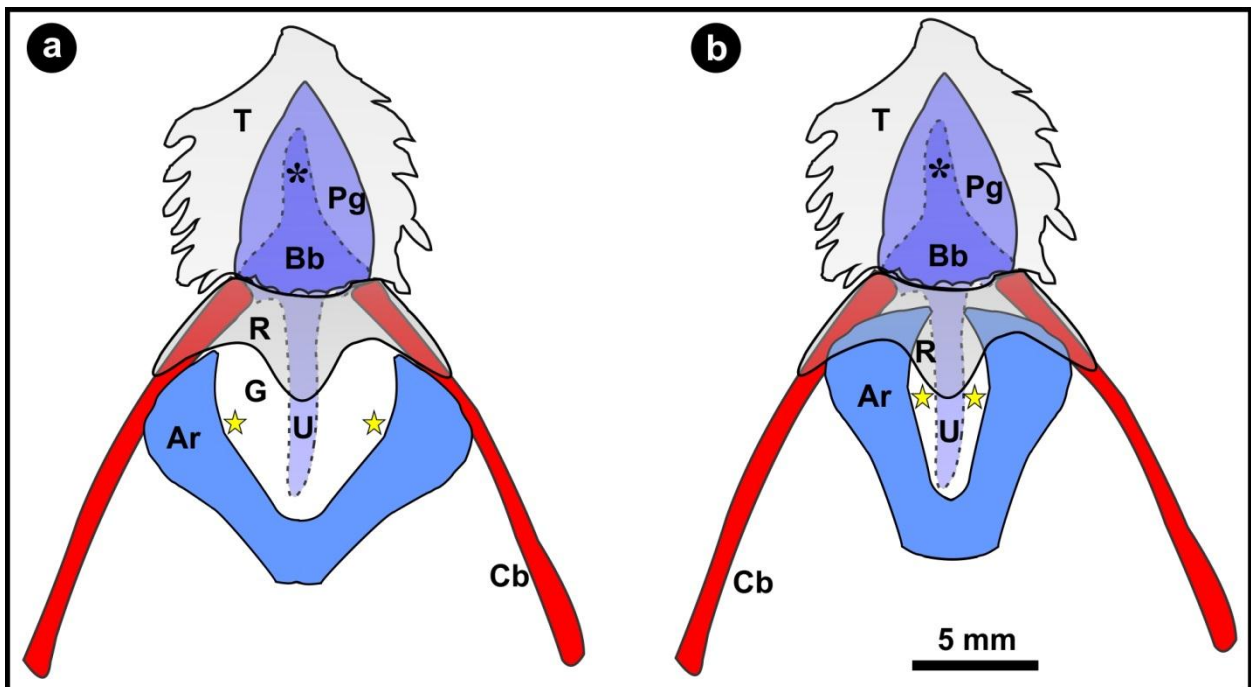


Figure 2.6. Schematic representation of the supporting elements of the linguo-laryngeal apparatus of the emu. Dorsal view. The cricoid and procricoid cartilages as well as the fleshy lips of the glottis are omitted for clarity. The caudal aspect of the arytenoid cartilages (Ar) are not joined as indicated but separated by the procricoid cartilage (not illustrated). However, the relative position of the protrusion of the fleshy lips (yellow star) (see Figures 2.3d-f and 2.7) have been indicated. Red indicates bone and blue/purple cartilage as seen in an 8 week-old chick. **(a).** Resting relationship of the arytenoid cartilages, tongue body (T), tongue root (R), urohyal (U), body of the basihyal (Bb), rostral projection of the basihyal (*) and *paraglossum* (Pg) (see Figure 2.3d). Glottis (G) and ceratobranchials (Cb). **(b).** The relationship of the underlying structures following retraction of the tongue (see Figure 2.3f). Note how the rostral portions of the arytenoid cartilages are enclosed by the tongue root and how the protrusions of the lips of the glottis and the tongue root close off the glottis.

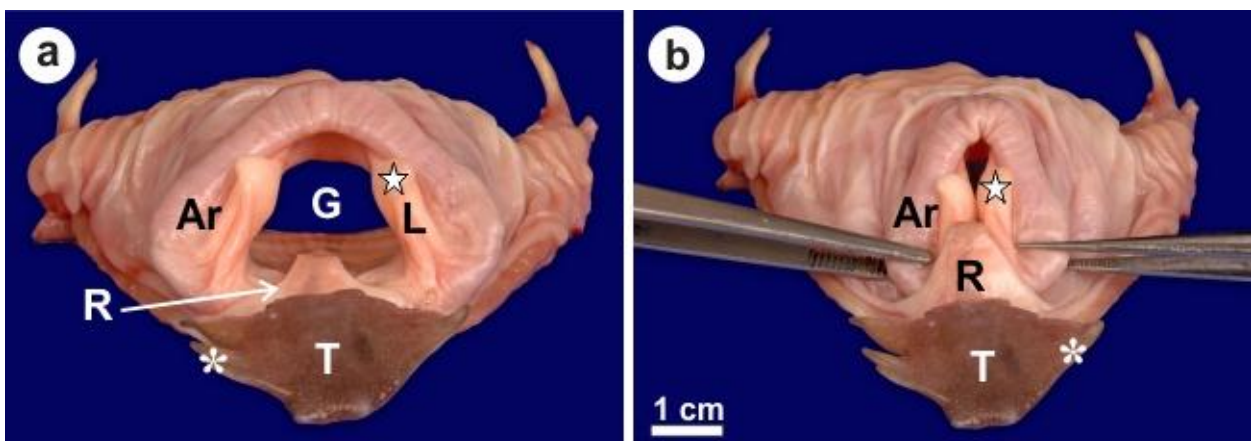


Figure 2.7. Rostral view of the linguo-laryngeal apparatus of the emu. **(a).** The normal resting position of the tongue body (T), root (R) and laryngeal mound. Note the wide glottis (G) and the tongue root which protrudes into the glottis. Mucosal covered arytenoid cartilage (Ar), lips of the glottis (L) and their round protrusion (star) and lateral lingual papilla (*). **(b).** With the linguo-laryngeal apparatus in position note how the caudal protrusion of the tongue root is positioned over the rostral aspect of the laryngeal mound and adducted glottis and approximates the round protrusions of the glottal lips.

2.4. Discussion

Until recently the only reported action of the ratite tongue during feeding was retraction during swallowing (Bonga Tomlinson, 2000) and depression of the mouth floor to allow for the effective intra-oral transfer of food to the proximal oesophagus using the 'catch and throw' method (Gussekkloo and Bout, 2005). The ratite tongue has been classified as rudimentary and of little functional significance during feeding when compared to the tongues of neognaths (Gussekkloo and Bout, 2005). However, recent morphological studies have revealed a number of diverse functions for this organ in ratites (Crole and Soley, 2009a, b, 2010a, b, 2012). Furthermore, as demonstrated here, the ratite tongue potentially plays a far more pivotal role during feeding by closing off the weakest part of the adducted glottis during swallowing and thus preventing the inhalation of food and water (choking). This appears to be achieved, in the ostrich, by folding of the flat tongue root which allows the lingual pocket to encase the adducted glottis, and in the emu, by the specialised structure of the tongue root which slides over the rostral aspect of the adducted glottis. The structural modifications whereby closure of the glottis is assisted and maintained have been termed the linguo-laryngeal apparatus.

Despite the lingual pocket in the ostrich (Cuvier, 1836; Meckel, 1829; Faraggiana, 1933; Bonga Tomlinson, 2000; Porcescu, 2007; Jackowiak and Ludwig, 2008; Tivane, 2008) and triangular tongue root in the emu (Faraggiana, 1933; Crole and Soley, 2009a) having been described, why has such an elegant mechanism eluded discovery for so long? Possible explanations for the prolonged obscurity of this mechanism are, firstly, that most morphological studies are conducted on preserved material. Regardless of the fixative used (commonly formalin or alcohol) the tissues become hardened and the manipulations performed in the present study on fresh specimens are impossible in preserved tissues. Secondly, functional studies (Bonga Tomlinson, 2000; Gussekloo and Bout, 2005) using diagnostic imaging techniques do not detect the soft tissue and cartilage adequately or provide an intra-oral view thus making it impossible to demonstrate or interpret the movements described in this study. Additionally, and only compounding the problem, it was generally accepted that the small ratite tongue was rudimentary, and therefore of little functional significance.

The proposed functioning of the linguo-laryngeal apparatus would rely on muscle action decreasing the distance between the hyobranchial apparatus (and thus the tongue) and the larynx. The detailed study on the musculature of the hyobranchial apparatus of the ostrich and emu (Bonga Tomlinson, 2000) provides supportive evidence in this regard. The muscle groups responsible for decreasing the distance between the two components are the hyolaryngeal and extrinsic hyolingual retractor muscles. The *M. cricohyoideus*, a hyolaryngeal muscle, appears to be a powerful muscle in the ostrich and is partially located in the tongue body which is a situation unknown in other taxa (Bonga Tomlinson, 2000). The *M. ceratocricoideus* is unique to palaeognaths and is considered an unusual hyolaryngeal muscle (Bonga Tomlinson, 2000). The hyolaryngeal muscles contract to decrease the distance between the basiurohyal (and thus the tongue) and the larynx during retraction of the tongue (Bonga Tomlinson, 2000). This muscular action would account for the proposed functioning of the linguo-laryngeal apparatus. Additionally, the extrinsic hyolingual retractors also show some unique features in ratite species. In the ostrich the *M. serpihyoideus* inserts directly on the cricoid cartilage, again a situation unique in known avian taxa (Bonga Tomlinson, 2000). However, in the emu this muscle acts directly on the ceratobranchials and urohyal (Bonga Tomlinson, 2000). The *M. hyomandibularis* acts directly on the ceratobranchials in the ostrich but in the emu shows a unique configuration not reported in other avian taxa and is divided into an *M. hyomandibularis lateralis* (inserting on the mid-ceratobranchial) and *M. hyomandibularis medialis* (inserting on the urohyal) (Bonga Tomlinson, 2000).

In the ostrich it would appear that the main muscle pulling the tongue, and thus the lingual pocket, over the adducted glottis would be the *M. cricohyoideus*, which in the ostrich has a unique conformation. In the emu the main contributors to pulling the tongue root over the adducted glottis would appear to be those muscles attaching to the urohyal, namely the *M. serpihyoideus* and *M. hyomandibularis medialis* of which the latter is again unique to the emu. The existence, conformation and positioning of such unique muscles, coupled with the synergy of the precisely formed anatomical structures reported in this study, further support the proposed functioning of the linguo-laryngeal apparatus and are hard to ignore and explain away as mere coincidence.

There is currently no consensus as to the presence of a structure that functionally replaces the epiglottis in birds. It was originally suggested (Carus, 1835) that the caudal border of the ostrich tongue functioned like an epiglottis; however, this was later refuted (Faraggiana, 1933). To further support this original observation of Carus (1835) in the ostrich, as well as our own conclusions, it was noted that a fold in the base of the tongue of the kiwi (*Apteryx australis*) covers the glottis when the tongue is retracted (Owen, 1879). Other suggestions as to the function of the lingual pocket in the ostrich add further support to our findings on the linguo-laryngeal apparatus. The lingual pocket, observed by high-speed cineradiography, is reported to change shape during intraoral transport of food and is closed during tongue retraction (Bonga Tomlinson, 2000). However, the pocket may have appeared 'closed' due to it being filled by the rostral aspect of the laryngeal mound as the tongue is pulled caudally (see Figures 2.3c, 2.4b and 2.5b). The muscular action of the *M. ceratoglossus* on the *paraglossalia*, thus 'closing' the pocket during swallowing (Bonga Tomlinson, 2000), would no doubt aid in anchoring the pocket over the rostral aspect of the laryngeal mound. A secondary fold is present in the lingual pocket, which would provide an increase in surface area for mucus-producing glands, enhancing mucus production and secretion for the ingestion of dry food (Tivane, 2008). This additional mucus would facilitate a smooth sliding motion of the lingual pocket over the laryngeal mound.

In the emu it was originally proposed that the tongue root functioned like an epiglottis (Gadow, 1879) but, as in the ostrich, this was subsequently refuted (Faraggiana, 1933). However this role for the emu tongue root was again suggested (Crole and Soley, 2009a) and has now been tentatively demonstrated. It may be possible that neognathous birds (the jay and flamingo (Cuvier, 1836) and the chicken and domestic birds (Koch, 1973)) possess similar mechanisms (although less specialised), as has previously been suggested. This mechanism consists of a transverse, semi-lunar fold at the entrance to the glottis (Cuvier, 1836) or folds opposite the base of the tongue (Koch, 1973) that can function as a rudimentary epiglottis. However, the action of these folds was never functionally demonstrated which is most likely why their proposed role as an "epiglottis" has not been accepted and recognised. In the chicken, this mechanism does seem possible where, in the fresh state, the flat, smooth tongue root (which is relatively long) forms a semi-circular fold when the tongue is retracted and which covers the rostral part of the glottis (personal observation). Thus it has been suggested and

debated, but never conclusively stated, that the tongue root in birds may function, albeit partially, as a form of epiglottis.

This study finally proposes a more explicit function for the peculiar lingual structures reported in the ostrich and emu during the past 178 years and may explain why these intriguing birds do not choke. In the absence of an epiglottis, the wide glottis of ratites appears to be protected by the linguo-laryngeal apparatus (which varies in structure between ratite species studied to date) and which may functionally replace the epiglottis. Although the muscles acting on the tongue of the ostrich and emu have been described (Bonga Tomlinson, 2000), further studies on these muscles, in light of this newly described mechanism, could further elaborate, confirm and explain this action. Based on these initial findings on how the glottis is protected in the ostrich and emu it can be proposed that a functional mechanism which protects the glottis does exist in birds. Whereas mammals possess an epiglottis, ratites (and possibly birds in general), possess a multi-component mechanism, the linguo-laryngeal apparatus. The linguo-laryngeal apparatus functions through the synergy created by a number of specialised anatomical components (the tongue body, tongue root, supporting elements of the tongue (bones and cartilage), laryngeal mound and its supporting cartilages). Furthermore, the linguo-laryngeal apparatus represents a newly discovered functional mechanism which should be incorporated into the field of avian biology.

2.5. References

- Bonga Tomlinson, C.A. 2000. *Feeding in Paleognathous Birds*. In: Feeding: Form, Function, and Evolution in Tetrapod Vertebrates. Edited by Schwenk, K. San Diego: Academic Press. pp. 359-394.
- Calhoun, M.L. 1954. *Microscopic Anatomy of the Digestive System of the Chicken*. Ames, Iowa: Iowa State College Press.
- Carus, C.G. 1835. *Traité élémentaire d'anatomie comparée, Suivi de Recherches d'Anatomie Philosophique ou Transcendante sur les parties primaires du système nerveux et du squelette intérieur et extérieur, et Accompagné d'un atlas de 31 planches in-4°, gravées*. Vol. 1. Paris: J.-B. Baillière, librairie de l'académie royale de médecine, Rue de l'Ecole-de-Médecine, no° 13.
- Cho, P., Brown, B. and Anderson, M. 1984. Comparative gross anatomy of ratites. *Zoo Biology*. **3**: 133-144.
- Crole, M.R. and Soley, J.T. 2009a. Morphology of the tongue of the emu (*Dromaius novaehollandiae*). I. Gross anatomical features and topography. *Onderstepoort Journal of Veterinary Research*. **76**: 335-345.
- Crole, M.R. and Soley, J.T. 2009b. Morphology of the tongue of the emu (*Dromaius novaehollandiae*). II. Histological features. *Onderstepoort Journal of Veterinary Research*. **76**: 347-361.
- Crole, M.R. and Soley, J.T. 2010a. Gross morphology of the intra-oral *rhamphotheca*, oropharynx and proximal esophagus of the emu (*Dromaius novaehollandiae*). *Anatomia Histologia Embryologia*. **39**: 207-218.
- Crole, M.R. and Soley, J.T. 2010b. Surface features of the emu (*Dromaius novaehollandiae*) tongue. *Anatomia Histologia Embryologia*. **39**: 355-365.
- Crole, M.R. and Soley, J.T. 2012. Gross anatomical features of the tongue, lingual skeleton and laryngeal mound of *Rhea americana* (Palaeognathae, Aves): morpho-functional considerations. *Zoomorphology*. **131**: 265-273.
- Cuvier, G. 1836. *Leçons d'anatomie comparée*, 3rd edition. Vol. 1 & 2. Edited by M. Duméril. Bruxelles: Dumont.
- Duerden, J.E. 1912. Experiments with ostriches XVIII. The anatomy and physiology of the ostrich. A. The external characters. *Agricultural Journal of the Union of South Africa*. **3**: 1-27.

Faraggiana, R. 1933. Sulla morfologia della lingua e del rialzo laringeo di alcune specie di uccelli Ratiti e Carenati non comuni. *Bollettino dei Musei di Zoologia e Anatomia Comparata*. **43**: 313-323.

Feder, F.-H. 1972. Zur mikroskopischen Anatomie des Verdauungsapparates beim Nandu (*Rhea americana*). *Anatomischer Anzeiger*. **132**: 250-265.

Gadow, H. 1879. Versuch einer vergleichenden Anatomie des Verdauungssystemes der Vögel. *Jenaische Zeitschrift für Medizin und Naturwissenschaft*. **13**: 92-171.

Göppert, E. 1903. Die Bedeutung der Zunge für den sekundären Gaumen und den Ductus nasopharyngeus. *Morphologisches Jahrbuch*. **31**: 311-359.

Guimarães, J.P., Mari, R.B., De Carvalho, H.S. and Watanabe, L. 2009. Fine structure of the dorsal surface of ostrich's (*Struthio camelus*) tongue. *Zoological Science*. **26**: 153-156.

Gusseklou, S.W.S. and Bout, R.G. 2005. The kinematics of feeding and drinking in palaeognathous birds in relation to cranial morphology. *The Journal of Experimental Biology*. **208**: 3395–3407.

Heidweiller, J., van Loon J.A. and Zweers, G.A. 1992. Flexibility of the drinking mechanism in adult chickens (*Gallus gallus*) (Aves). *Zoomorphology*. **111**: 141-159.

Jackowiak, H. and Ludwig, M. 2008. Light and scanning electron microscopic study of the structure of the ostrich (*Strutio camelus*) tongue. *Zoological Science*. **25**: 188-194.

Kaupp, M.S. 1918. *The Anatomy of the Domestic Fowl*. Philadelphia: W.B. Saunders Company.

Kelly, W.L. and Bryden, M.M. 1983. A modified differential stain for cartilage and bone in whole mount preparations of mammalian fetuses and small vertebrates. *Stain Technology*. **58**: 131-134.

King, A.S. and McLelland, J. 1984. *Digestive System*. In: *Birds - Their Structure and Function*. 2nd edition. London: Baillière Tindall. pp. 84-109.

Koch, T. 1973. *Splanchnology*. In: *Anatomy of the Chicken and Domestic Birds*. Edited by B.H. Skold and L. DeVries. Ames, Iowa: Iowa State University Press. pp. 66-100.

MacAlister, A. 1864. On the anatomy of the ostrich (*Struthio camelus*). *Proceedings of the Royal Irish Academy*. **9**: 1-24.

McCann, C. 1973. The tongues of kiwis. *Notornis*. **20**: 123-127.

Meckel, J.F. 1829. *System der vergleichenden Anatomie*. Halle: Der Rehgerschen Buchhandlung.

Nickel, R., Schummer, A. and Seiferle, E. 1977. *Digestive System*. In: *Anatomy of the Domestic Birds*. Berlin: Verlag Paul Parey. pp. 40-61.

Owen, R. 1835. Division I. Organs in plants and animals for the special purposes of the individual. Subdivision VIII. Organs of sense. Series II. Organ of taste. In birds, in *Royal College of Surgeons of England. Museum, Owen R (ed) Descriptive and illustrated catalogue of the physiological series of comparative anatomy contained in the museum of the Royal College of Surgeons in London. Vol. 3. Part 1. Nervous system and organs of sense*. London: Richard Taylor.

Owen, R. 1879. *Memoirs on the extinct and wingless birds of New Zealand; with an appendix of those of England, Australia, Newfoundland, Mauritius and Rodriguez*. Vol. 1. London: John van Voorst.

Parker, T.J. 1891. Observations on the anatomy and development of apteryx. *Philosophical Transactions of the Royal Society of London, B*. **182**: 25-134.

Poost Pasand, A., Tadjalli, M. and Mansouri, H. 2010. Microscopic study on the tongue of male ostrich. *European Journal of Biological Sciences*. **2**: 24-31.

Porcescu, G. 2007. Comparative morphology of the digestive tract of the Black African ostrich, hen and turkey. Ph.D. thesis, Agrarian State University of Moldova, Moldova.

Pycraft, W.P. 1900. On the morphology and phylogeny of the *Palaeognathae* (*Ratitae* and *Crypturi*) and *Neognathae* (*Carinatae*). *Transactions of the Zoological Society of London*. **15**: 149-290.

Roach, R.W. 1952. Notes on the New Zealand kiwis (1). *New Zealand Veterinary Journal*. **1**: 38-39.

Santos, T.C., Fukuda, K.Y., Guimarães, J.P., Oliveira, M.F., Miglino, M.A. and Watanabe, I.-S. 2011. Light and scanning electron microscopy study of the tongue in *Rhea americana*. *Zoological Science*. **28**: 41-46.

Tadjalli, M., Mansouri, S.H. and Poostpasand, A. 2008. Gross anatomy of the oropharyngeal cavity in the ostrich (*Strutio camelus*). *Iranian Journal of Veterinary Research*. **9**: 316-323.

Tivane, C. 2008. A morphological study of the oropharynx and oesophagus of the ostrich (*Struthio camelus*). M.Sc. thesis, University of Pretoria, South Africa.

CHAPTER 3

DISTRIBUTION AND STRUCTURE OF INTRA-ORAL HERBST CORPUSCLES

3.1. Introduction

Herbst corpuscles are lamellated sensory structures found in birds and were originally reported in the avian tongue (Herbst, 1848). They are sensitive to vibratory stimuli (Hörster, 1990; Evans and Martin, 1993) and occur in or on the membranes covering and uniting the leg bones, in the skin near feather roots, the bills of aquatic birds (Quilliam and Armstrong, 1963), the beak (Schildmacher, 1931; Gottschaldt, 1974), oral cavity, tongue, subcutaneous connective tissue (Gottschaldt, 1985), muscles (Cobb and Bennett, 1970), the connective tissue adjacent to joints (Halata and Munger, 1980) and in the lacrimal gland (Dimitrov, 2003). In the deep dermis they are found in the legs, beak and feathered skin (Gottschaldt, 1985). Herbst corpuscles are the avian equivalent of the mammalian Pacinian corpuscle (Iggo and Andres, 1982) and are structurally similar (Schildmacher, 1931; Schwartzkopff, 1949; Quilliam and Armstrong, 1963) but may be sensitive to a greater range of high-frequency vibrations (Schwartzkopff, 1949). Herbst corpuscles have been demonstrated in the avian oropharynx of a number of species (Malinovský and Zemánek, 1969; Ziswiler and Trnka, 1972; Krulis, 1978; Gottschaldt, 1985; Halata and Grim, 1993) including domestic poultry (Schildmacher, 1931; Andersen and Nafstad, 1968; Saxod, 1968; Wight *et al.*, 1970; Hodges, 1974; Berkhoudt, 1980; Gottschaldt *et al.*, 1982; Malinovský and Páč, 1985; Watanabe *et al.*, 1985; Gentle and Breward, 1986). Their presence has also been confirmed in the oropharynx of the ostrich (Palmieri *et al.*, 2002; Tivane *et al.*, 2006; Guimarães *et al.*, 2007; Tivane, 2008; Crole and Soley, 2009a; Crole *et al.*, 2009), emu (Crole, 2009; Crole and Soley, 2009a, b; Crole *et al.*, 2009) and greater rhea (Feder, 1972) as well as in the bill of the kiwi (Cunningham *et al.*, 2007).

The function of lamellated mechanoreceptors is reportedly to supplement the inner ear, which normally only detects airborne vibrations (Quilliam and Armstrong, 1963). Wight *et al.* (1970) suggested that the distribution of Herbst corpuscles may be linked to the structure of the beak which in turn is related to the diet of the bird, and that studying the comparative distribution of Herbst corpuscles in different types of beaks may indicate their function at these specific sites. In this context Berkhoudt (1980) reported that a correlation between mechanoreceptor distribution and feeding habits had been demonstrated in a few granivorous songbirds (Ziswiler, 1965; Ziswiler and Trnka, 1972; Krulis, 1978; Bock and Morony, 1978). Although the feeding strategy of ratites has been documented (Bonga Tomlinson, 2000; Gussekloo and Bout, 2005) future studies on the specific feeding habits of the ostrich and emu may be easier to interpret if the distribution of Herbst corpuscles is known. Significant environmental changes may be communicated to the brain via the simultaneous stimulation of numerous single corpuscles in one location or possibly by clusters of corpuscles at different sites (Quilliam and Armstrong, 1963). In the pigeon it was found that Herbst corpuscles, concentrated in the wing, constituted a functional unit or sense organ with a high specificity to vibrational stimuli, which is likely to be involved in flight control (Hörster, 1990). Similarly, concentrations of Herbst corpuscles in specific regions of the upper digestive tract of the ostrich and emu may constitute previously unknown 'sense organs'.

Studies on Herbst corpuscles have focused mainly on their structure (see below) with only a limited number of investigations describing their distribution in various regions. The distribution of Herbst corpuscles in the upper digestive tract has been documented mainly in domestic poultry, for example, in the beak of the chicken (Wight *et al.*, 1970), beak skin of the Japanese quail (*Cortunix cortunix japonica*) (Halata and Grim, 1993) and bill-skin and tongue of the mallard (Berkhoudt, 1980). In ratites, the relative distribution of Herbst corpuscles in the oropharynx of the ostrich and emu has been briefly documented (Crole and Soley, 2009a). Palmieri *et al.* (2002) and Tivane *et al.* (2006) noted a particular concentration of Herbst corpuscles in the median palatine ridge of the non-glandular region in the oropharyngeal roof of the ostrich. Guimarães *et al.* (2007) reported on the presence of Herbst corpuscles in the caudal third of the ostrich oropharyngeal roof. However, as revealed by other studies in this species (Tivane *et al.*, 2006; Tivane, 2008; Crole and Soley, 2009a), the distribution of these

structures is far more widespread. Additionally, in ratites, Herbst corpuscles have been found in the foot pads (Palmieri *et al.*, 2003), nasal mucosa (Palmieri *et al.*, 2004), male (Pacini-like corpuscles) (Bo Minelli *et al.*, 2006) and female (Palmieri *et al.*, 2006) copulatory organ of the ostrich and in the skin of the emu (Weir and Lunam, 2004).

The description of Herbst corpuscles, as well as their developmental origin (Saxod, 1973; Malinovský and Páč, 1985) and function (Schildmacher, 1931), has been almost exclusively limited to neognathous birds and the earlier literature pertaining to these structures has been summarized by Berkhoudt (1980). Based on these studies the Herbst corpuscles of neognaths demonstrate the following general structural features: a central axon surrounded by an inner core formed by specialised Schwann cells, an outer zone which contains collagen fibres and surrounds the lamellated structure of the inner core, and an outer capsule derived from the perineurium (Gottschaldt, 1985; Malinovský and Páč, 1985). The basic structure of Herbst corpuscles in ratites has been briefly described by light microscopy (LM) in the oropharynx of the ostrich (Palmieri *et al.*, 2002; Tivane *et al.*, 2006; Guimarães *et al.*, 2007; Tivane, 2008), emu (Crole, 2009; Crole and Soley, 2009b) and greater rhea (Feder, 1972) as well as in the bill of the kiwi (Cunningham *et al.*, 2007). Although the presence of Herbst corpuscles appears to be well documented in the ostrich oropharynx, the existing studies are generally superficial and others, such as that of Palmieri *et al.* (2002), are difficult to interpret and contain confusing and unexplained information. At the LM level it appears that Herbst corpuscles in the emu are similar to those of other birds (Crole and Soley, 2009b). However, recent findings from an immunohistochemical investigation into Herbst corpuscles of the emu skin, suggests that the chemical content of Herbst corpuscles may differ between flightless and volant species of birds (Weir and Lunam, 2006).

The complex ultrastructure of Herbst corpuscles has been described in numerous birds including the chicken (Andersen and Nafstad, 1968; Nafstad and Andersen, 1970), Japanese quail (Halata and Grim, 1993), duck (Saxod, 1968; Chouchkov, 1973; Watanabe *et al.*, 1985), pigeon (Halata and Munger, 1980; Malinovský and Páč, 1980), some aquatic birds (Quilliam and Armstrong, 1963; Halata, 1971) and the goose (Gottschaldt *et al.*, 1982). The only documented ultrastructure of Herbst corpuscles in ratites is a preliminary comparative study of these structures in the oropharynx of the ostrich and emu (Crole *et al.*, 2009). A comprehensive ultrastructural study will

determine whether Herbst corpuscles in the ostrich and emu share structural similarities.

A comparative study of the distribution and structure of Herbst corpuscles within the oropharyngeal cavities of the ostrich and emu would aid in determining which regions display the greatest sensitivity to vibratory stimuli as well as whether these corpuscles share morphological features between the two species and with neognathous birds. The brief reports on the distribution (Tivane *et al.*, 2006; Crole and Soley, 2009a) and structure (Palmieri *et al.*, 2002; Tivane *et al.*, 2006; Guimarães *et al.*, 2007; Tivane, 2008; Crole, 2009; Crole and Soley, 2009b; Crole *et al.*, 2009) of Herbst corpuscles in the oropharynx of the ostrich and emu require further examination. Such data may assist in relating the investigatory nature of these birds while foraging/feeding to structures or regions in the oropharynx which display a higher density of mechanoreceptors.

3.2. Materials and Methods

A total of 10 adult ostrich and 10 adult emu heads, from birds of either sex, were collected after slaughter from the Klein Karoo Ostrich Abattoir (Oudtshoorn, Western Cape Province, South Africa), Oryx Abattoir (Krugersdorp, Gauteng Province, South Africa), Emu Ranch (Rustenburg, North-West Province, South Africa) and an emu farm (Krugersdorp, Gauteng Province, South Africa). All the heads were thoroughly rinsed with either distilled water, phosphate buffer or running tap water to remove mucus, blood and regurgitated food.

3.2.1. Light microscopy (LM)

Five ostrich and 5 emu heads were collected as indicated above, immersion-fixed in 10% neutral-buffered formalin and transported to the Faculty of Veterinary Science, University of Pretoria. Care was taken to exclude air from the oropharynx by inserting a small block of wood between the bill tips.

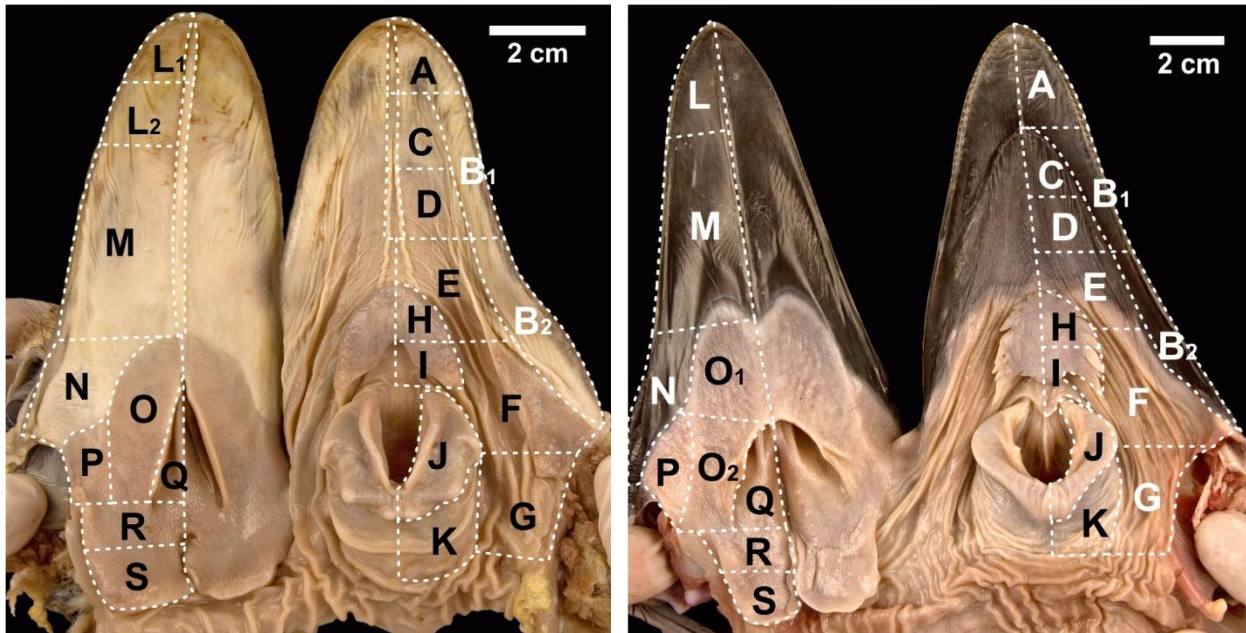


Figure 3.1. Anatomical regions sampled in the ostrich (left) and emu (right). Mandible (A, B₁, B₂), rostral keratinised floor (C, D, E), caudal non-keratinised floor (F, G), tongue body and root (H, I), arytenoid (J) and caudal (K) part of laryngeal mound, keratinised roof (L₁, L₂, M, N), non-keratinised roof (O₁, O₂, P), choana region (Q) and rostral (R) and caudal (S) parts of the pharyngeal folds. In the ostrich the median palatine ridge is outlined and adjacent to L₁, L₂ and M and the median ventral ridge is outlined and adjacent to A, C and D.

The entire oropharynx of the right side (Fig. 3.1) was sampled to determine the distribution of Herbst corpuscles. To achieve sectioning and removal of the mandible the left and right quadratomandibular joints were disarticulated and the esophagus and soft tissue incised to separate the upper and lower parts of the head. Structural features of the oropharynx were described, digitally recorded with a Canon EOS 5D digital camera (Canon, Ōita, Japan) equipped with a Canon Macro 100mm lens, and annotated in Corel Draw X5. The soft interramal region was removed from the bony mandible by sharp incision following the inside mandibular edge. The rostral portions of the maxilla and mandible were removed with a band-saw. These specimens were decalcified (see below). Appropriate segments representing all parts of the oropharynx were removed from the specimens (Fig. 3.1) and their dimensions measured, recorded and used to calculate the area of that specific segment in mm². Each segment was then serially sectioned by hand in the transverse plane at roughly 5 mm intervals. The segments were serially imbedded and this was ensured by cutting a notch on the side not to be imbedded. These samples were processed for light microscopy and stained with H&E (Bancroft and Gamble, 2002) (see below). The number of corpuscles in each anatomical region was counted and the relative percentage calculated for the area of

each region (see below). The median value for each anatomical region was calculated for each species and plotted on a photograph of the oropharynx to depict the relative densities of Herbst corpuscles within the various regions (Fig. 3.2). Additionally, the same histology slides utilised in Chapter 4.2.3 (from 5 ostrich chicks and 1 emu chick) were examined in order to demonstrate the histological location of Herbst corpuscles in the bill tips.

Decalcification of the premaxilla and mandible took place over a period of 6 weeks in an 8% formic acid solution. The samples were placed in a fresh solution fortnightly. All tissue samples were then dehydrated through 70%, 80%, 96%, and 2X 100% ethanol and further processed through 50:50 ethanol: xylol, 2X xylol and 2X paraffin wax (60-120 minutes per step) using a Shandon model 2LE Automatic Tissue Processor (Shandon, Pittsburgh, PA, USA). Tissue samples were then imbedded manually into paraffin wax in plastic moulds. Sections were cut at 4-6 μm and stained with H&E (Bancroft and Gamble, 2002). Histological sections were viewed, features of interest described and digitally recorded using an Olympus BX63 light microscope (Olympus Corporation, Tokyo, Japan) equipped with a DP72 camera and Olympus cellSens imaging software (Olympus Corporation, Tokyo, Japan), and annotated in Corel Draw X5.

3.2.2. Immunohistochemistry (IHC)

The histology slides processed for IHC labelling of neurofilament as described in Chapter 8.2.1 were also utilised for the morphological description of Herbst corpuscles, in particular in respect of their association with neural elements.

3.2.3. Transmission electron microscopy (TEM)

Five ostrich and 5 emu heads were sampled on-site and the tissues immersion-fixed in 2.5% glutaraldehyde in Millonig's phosphate buffer (pH 7.4, 0.13 M) at room temperature for a minimum period of 24 hours. The rostral mandibular *Rhamphotheca* and rostral non-glandular region of the roof of the oropharynx known to contain a high density of Herbst corpuscles were sampled (Regions A and M in both birds and the median palatine ridge in the ostrich, see Fig. 3.1) and routinely processed for TEM to

view the ultrastructure of Herbst corpuscles. The samples were rinsed in Millonig's phosphate buffer for 10 minutes, post-fixed for 1 hour at room temperature in similarly buffered 1% OsO₄ and given two final buffer washes of 10 minutes each. Samples were then rinsed in distilled water for 20 minutes and dehydrated through a graded series of ethanols (50%, 70%, 80%, 96% and 2 X 100% (with added Molecular sieve, Merck, Darmstadt, Germany) for 10 minutes per step. Samples were placed in 2X propylene oxide (PO) for 10 minutes each followed by infiltration in PO: Epoxy resin (2:1) for 30 minutes to 1 hour and PO: Epoxy resin (1:2) for 1 hour to overnight. The tissue blocks were then embedded in 100% Epoxy resin in silicon moulds and cured in an embedding oven at 65°C overnight. Semi-thin sections were cut at 0.3 µm, mounted and stained with 1% toluidine blue and examined with the light microscope to identify areas of interest. The resin blocks were trimmed and ultra-thin sections (50-90 nm) cut using a diamond knife, picked up on copper grids and stained with uranyl acetate and lead citrate. Samples were viewed and images digitally recorded using a Philips CM10 transmission electron microscope (FEI, Eindhoven, The Netherlands) equipped with a Mega View III Soft Imaging System camera and iTEM Soft Imaging System software. Images were digitally enhanced and annotated in Corel Draw X5.

3.2.4. Enumeration of Herbst corpuscles and Statistics

The tissue strips (representing the epithelial lining and underlying connective tissue) from the slides of each region were viewed at an appropriate magnification and the number of Herbst corpuscles (n) recorded. The volumetric concentration of Herbst corpuscles was transformed to a surface concentration to enable it to be related to the surface area of the region sampled. The total surface area (y) of the strips examined for that region was calculated (total length of tissue strips in mm multiplied by the average section thickness (0.005mm) in mm²). To proportionately relate the area of tissue sampled (y – on the microscope slide) to the total area of the region (x – Fig. 3.1) the equation $x \div y$ was used to obtain the factor/value (z) i.e. $x \div y = z$. The number of corpuscles (n) was then multiplied by z ($n(z)$) to obtain a total value for that region (r) ($n(z) = r$). The value of r will not reflect the actual number of Herbst corpuscles present as the calculations assume the length of each corpuscle to be 5 µm (the thickness of the histological sections). This would have resulted in a gross inflation of the actual

numbers of Herbst corpuscles present and the final values were therefore expressed as a percentage and not as a total number. All the regional values (r) were added together to obtain the grand total (t) which represented 100% of the corpuscles counted in each bird. The equation $r(0.01t)$ determined the corpuscular density index (CDI) which was expressed as a percentage of corpuscles in a particular region. The CDI of the pre-defined anatomical regions was determined for each of the 5 ostrich and 5 emu specimens studied. The median CDI values were depicted graphically on a photograph of the oropharynx of each species (Fig. 3.2).

The null hypothesis, that the ostrich and emu are similar (in respect of the aspects studied), was tested by a Student's t test (a 2 sample assuming unequal variances) or the Mann-Whitney Rank Sum Test (where the normality test (Shapiro-Wilk) and/or equal variance test has failed (<0.05)). Values expressed were calculated using SigmaPlot, version 12.0 (Systat Software, San Jose, CA, USA) and comprised the mean, median, standard deviation, standard error of the mean, Mann-Whitney U statistic, significance and power of the test performed with alpha. Significance was set at $p=0.05$. A value of $p<0.05$ rejected the null hypothesis and a value of $p>0.05$ accepted the null hypothesis (Tables 3.1-8).

3.3. Results

3.3.1. Distribution

The distribution of Herbst corpuscles (*Corpusculum lamellosum avium*)¹, in terms of relative percentages, is presented for each region of the oropharynx and is detailed below in Tables 3.1-3.9 and Figure 3.2.

¹ "Synonymy: Herbst corpuscle; *Corpusculum herbsti*. A lamellated, Pacinian-like receptor of birds, showing several specializations of non-nervous elements around afferent nerve fibers." (Evans and Martin, 1993).

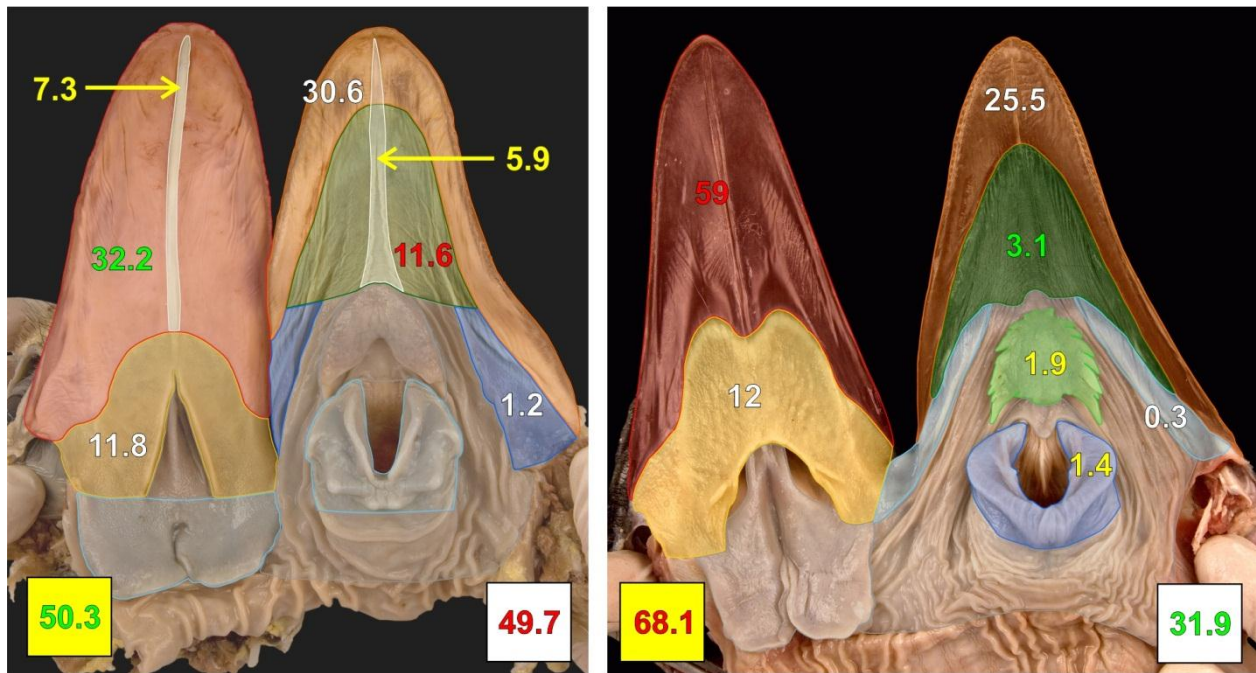


Figure 3.2. Ostrich (left) and emu (right) oropharynx openly displayed. Numbers of Herbst corpuscles are expressed as a relative percentage (median value rounded to the first decimal place of $n=5$, see Tables 3.1-9) and reflect the relative density of Herbst corpuscles in each outlined region proportional to its area (corpussular density index). Numbers in the bottom corners reflect the percentage of the median value of Herbst corpuscles in the roof (yellow block) and floor (white block) of the oropharynx of each species. Non-shaded areas were not sampled and the grey shading represents sampled regions where corpuscles were not observed or occurred in a very low relative percentage. White numbers indicate a similar distribution between the two species for a particular anatomical region, red (higher) and green (lower) numbers show a statistically significant difference between the two species for a particular anatomical region and yellow numbers show a region not statistically compared.

3.3.1.1. The mandible (Regions A, B1 and B2; see Fig. 3.1) (Excluding the median ventral ridge in the ostrich)

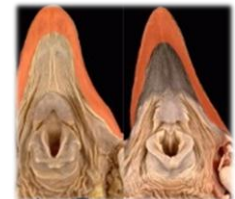


Table 3.1. Comparative distribution of Herbst corpuscles (expressed as a relative percentage) in the mandible of the ostrich (O) and emu (E). Blue highlight indicates the power of the performed test with alpha (P_a) below the desired value of 0.8. Normality Test (Shapiro-Wilk) (NT), Equal Variance Test (EVT), Standard Deviation (SD), Standard Error of the Mean (SEM) and p value (p).

n	1	2	3	4	5	Mean	Median	SD	SEM	NT	EVT	p	P_a
O	27.29	30.56	27.23	34.83	32.45	30.47	30.56	3.30	1.48	Pass	Pass	0.37	0.05
E	19.96	26.16	21.81	25.50	40.8	26.66	25.50	8.24	3.69	Pass	Pass	0.37	0.05

The difference in the mean values of the number of corpuscles in the mandible between the ostrich and emu was not great enough to reject the possibility that the difference was due to random sampling variability. There was no statistically significant difference between the ostrich and emu (Fig. 3.2 and Table 3.1). However, the power of the

performed test (0.05) was below the desired power of 0.8 in this region (Table 3.1). This indicates that, due to the small sample size, a difference is less likely to be detected if one does actually exist. Therefore this result should be interpreted with caution.

At the rostral extremity of the mandibular rostrum the Herbst corpuscles were located within numerous pits in the dentary bone (see Chapters 5 and 7). In the remainder of the rostrum (Region A in Fig. 3.1), the corpuscles formed continuous chains or sheets within the compressed dermis between the dentary bone and epithelium or within or near bony pits (Fig. 3.3) and were closely associated with nerves. A median ventral ridge displaying a high concentration of corpuscles (Figs. 3.4 and 3.12) was present on the mandibular rostrum and non-glandular region of the oropharyngeal floor (see 3.3.1.9. below) in the ostrich but not in the emu. Due to the exclusive nature of the median ventral ridge, both in location and structure, it was considered to represent a regional entity with its own concentration of Herbst corpuscles. In the mandibular arms (Region B in Fig. 3.1) Herbst corpuscles were not as densely packed as in the rostrum and were located in the compressed dermis between the bone and epithelium. In both the ostrich and emu, the Herbst corpuscles in the mandible were concentrated in the rostrum.

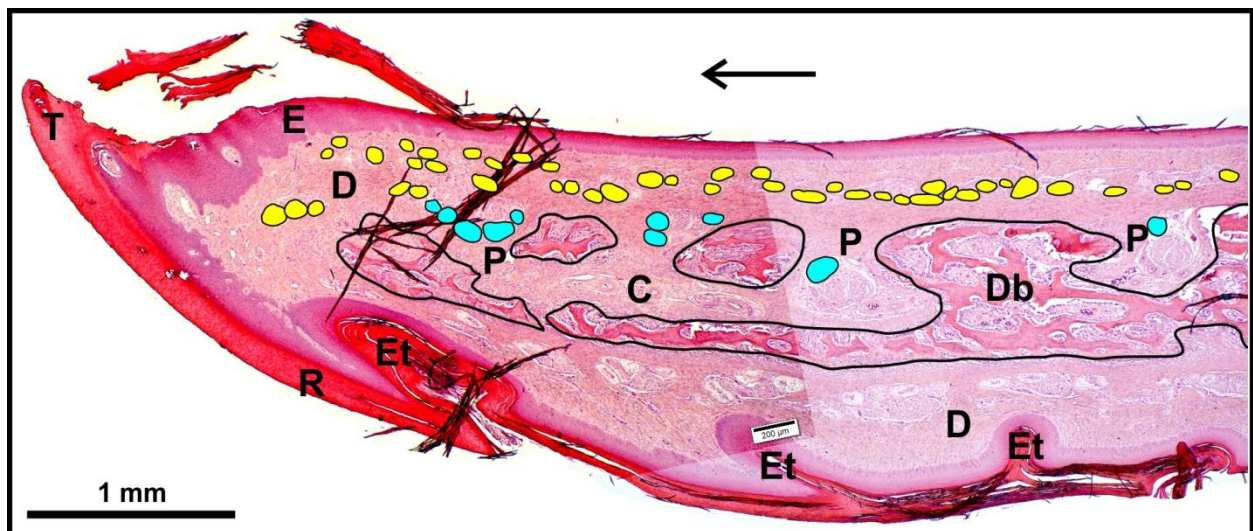


Figure 3.3. Composite micrograph of a longitudinal-section of the mandibular rostrum in an ostrich chick. The arrow indicates rostral and is located on the dorsal (intra-oral) surface. Note the arrangement of Herbst corpuscles (yellow dots) which form a continuous chain in the dermis (D) between the keratinised stratified squamous epithelium (E) (partially lost during processing) and the dentary bone (Db). Herbst corpuscles (blue dots) also occur in cavities (C) within the bone and which open to the dermis via pits (P) (see Chapter 5). Herbst corpuscles (not coloured) also occur on the ventral surface and are associated with the epidermal troughs (Et) (see Chapter 4). *Tomium* (T) and *Rhamphotheca* (R).

3.3.1.2. The rostral keratinised non-glandular oropharyngeal floor (Regions C, D, E; see Fig. 3.1) (Excluding the median ventral ridge in the ostrich)



Table 3.2. Comparative distribution of Herbst corpuscles (expressed as a relative percentage) in the rostral keratinised non-glandular oropharyngeal floor of the ostrich (O) and emu (E). Yellow highlight indicates a significant difference. Normality Test (Shapiro-Wilk) (NT), Equal Variance Test (EVT), Standard Deviation (SD), Standard Error of the Mean (SEM), p value (p) and power of the performed test with alpha (Pa).

n	1	2	3	4	5	Mean	Median	SD	SEM	NT	EVT	p	Pa
O	12.01	11.56	10.79	13.41	10.95	11.74	11.56	1.05	0.47	Pass	Pass	<0,001	1
E	3.12	4.43	5.00	1.86	2.81	3.44	3.12	1.27	0.57				

The difference in the mean value for the number of Herbst corpuscles in the ostrich and emu in the rostral keratinised oropharyngeal floor was greater than what would be expected by chance (Table 3.2). There was a statistically significant difference between this region in the ostrich and emu (Fig. 3.2 and Table 3.2).

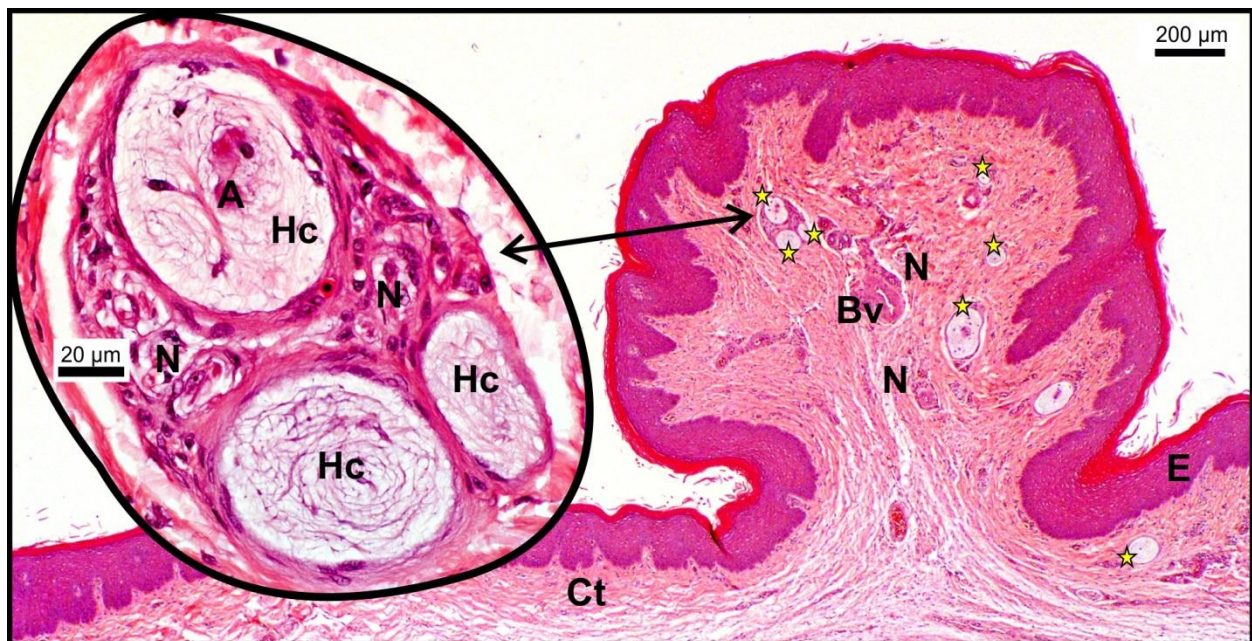


Figure 3.4. Transverse section of the median ventral ridge in the ostrich (adjacent to region D in Fig. 3.1). The Herbst corpuscles (Hc and stars) occur either in groups (see inset) or singly and vary in size. Keratinised stratified squamous epithelium (E), blood vessel (Bv), nerves (N) and connective tissue (Ct).

The Herbst corpuscles in this region were located within the dermis approximately midway between the skeletal muscle layer and the keratinised stratified squamous epithelium (Figs. 3.5 and 3.6). The dermis was not as compact in this region as in the

mandible. In both species, Herbst corpuscles were concentrated within mucosal folds of this region and mostly occurred in groups (Fig. 3.6). A continuation of the median ventral ridge was present in the ostrich (Fig. 3.4); typically displaying a concentration of Herbst corpuscles (see below). However, a comparable ridge was not present in the emu.

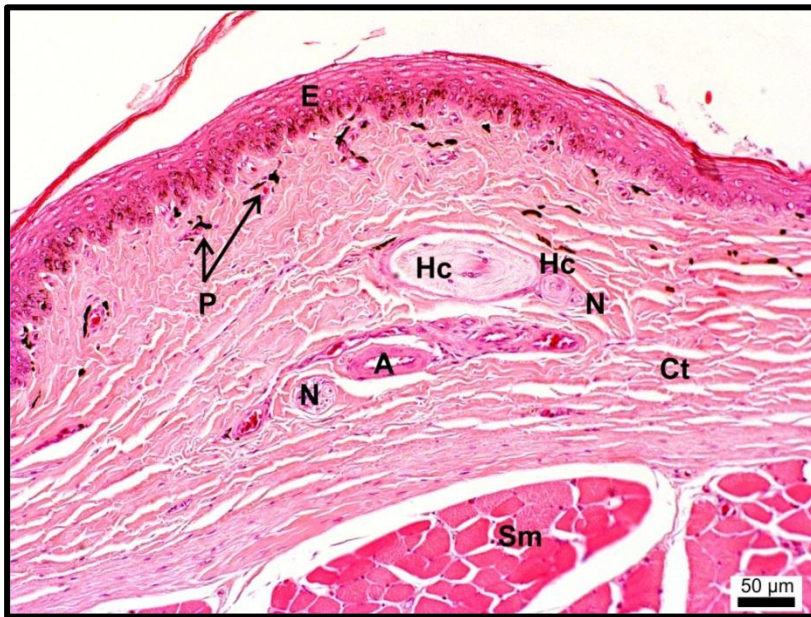


Figure 3.5. Herbst corpuscles (Hc) in the rostral keratinised oropharyngeal floor of the emu (region C in Fig. 3.1). This region is non-glandular and the Herbst corpuscles occur in the connective tissue (Ct) between the keratinised stratified squamous epithelium (E) and the skeletal muscle (Sm). Nerve (N), artery (A) and melanin granules (P).

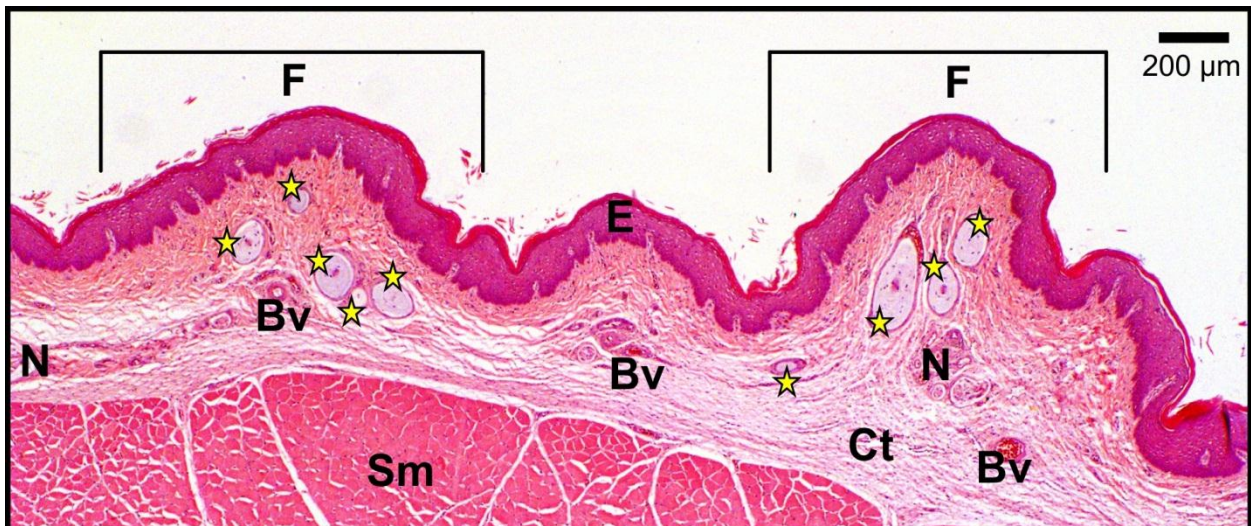


Figure 3.6. Herbst corpuscles (stars) in the rostral keratinised oropharyngeal floor of the ostrich (region D in Fig. 3.1). Herbst corpuscles concentrate in mucosal folds (F) in this region. Keratinised stratified squamous epithelium (E), nerve (N), blood vessels (Bv), connective tissue (Ct) and skeletal muscle (Sm).

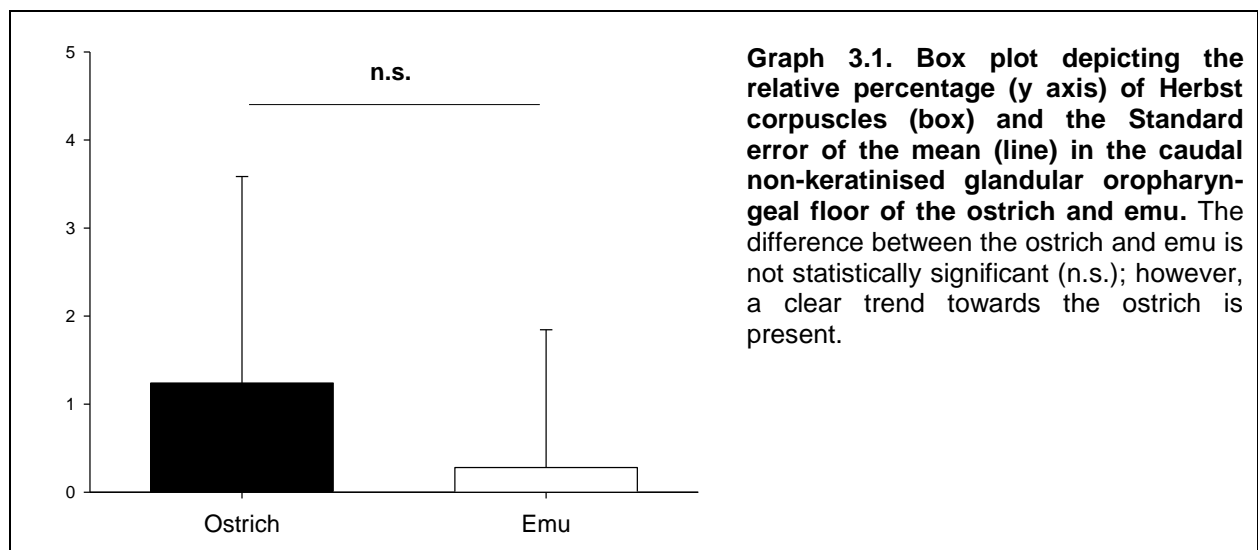


3.3.1.3. The caudal non-keratinised glandular oropharyngeal floor (Regions F, G; see Fig. 3.1)

Table 3.3. Comparative distribution of Herbst corpuscles (expressed as a relative percentage) in the caudal non-keratinised glandular oropharyngeal floor of the ostrich (O) and emu (E). Normality Test (Shapiro-Wilk) (NT), Standard Deviation (SD), p value (p) and Mann-Whitney U Statistic (MUS).

n	1	2	3	4	5	Mean	Median	SD	NT	MUS	p
O	1.15	3.83	3.34	1.24	1.02	2.12	1.24	2.13	Fail	3	0.056
E	0	0	0.63	0.28	3.06	0.82	0.28	0.95			

The difference in the median values of the caudal non-keratinised oropharyngeal floor between the ostrich and emu was not great enough to reject the possibility that the difference was due to random sampling variability. There was no statistically significant difference between the ostrich and emu (Fig. 3.2, Table 3.3 and Graph 3.1). Although there was not a statistically significant difference between this region in the ostrich and emu, there was a clear trend indicating that there are more Herbst corpuscles in this region in the ostrich than in the emu (Graph 3.1).



Herbst corpuscles in this region were located mostly in the fold of mucosa housing the lateral mandibular gland (*Gl. mandibularis lateralis* (Crole and Soley, 2011)) (outlined light blue in Fig. 3.2). The corpuscles were associated with the large, simple branched tubular glands forming the polystomatic glandular field of the lateral mandibular gland. In the caudal region (G in Fig. 3.1), adjacent to the laryngeal mound, Herbst corpuscles were absent or extremely sparse. Where present, they occurred in the connective tissue beneath the simple tubular glands.

3.3.1.4. The tongue body and tongue root (Regions H, I; see Fig. 3.1)

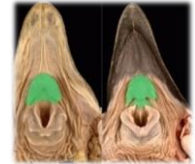


Table 3.4. Comparative distribution of Herbst corpuscles (expressed as a relative percentage) in the tongue of the ostrich (O) and emu (E). Normality Test (Shapiro-Wilk) (NT), p value (p) and Mann-Whitney U Statistic (MUS).

n	1	2	3	4	5	Mean	Median	NT	MUS	p
O	0	0	0	0	0	0	0	Fail	0	0.008
E	4.29	0.92	0.81	1.85	2.37	2.17	1.85			

The difference in the median values of the tongue between the ostrich and emu was greater than what would be expected by chance (Table 3.4). There was a statistically significant difference between this region in the ostrich and emu (Fig. 3.2 and Table 3.4).

Herbst corpuscles only occurred in the tongue body of the emu (Fig. 3.7) and not in the tongue root. No Herbst corpuscles were located in the tongue body or root of the ostrich (Fig. 3.2). Herbst corpuscles in the emu tongue body were mainly associated with the large, simple branched tubular glands (Fig. 3.7). A few Herbst corpuscles were located adjacent to the *Paraglossum* or below the epithelium; both situated within the connective tissue of the tongue. Herbst corpuscles in the tongue body of the emu have previously been described in detail (Crole and Soley, 2009b).

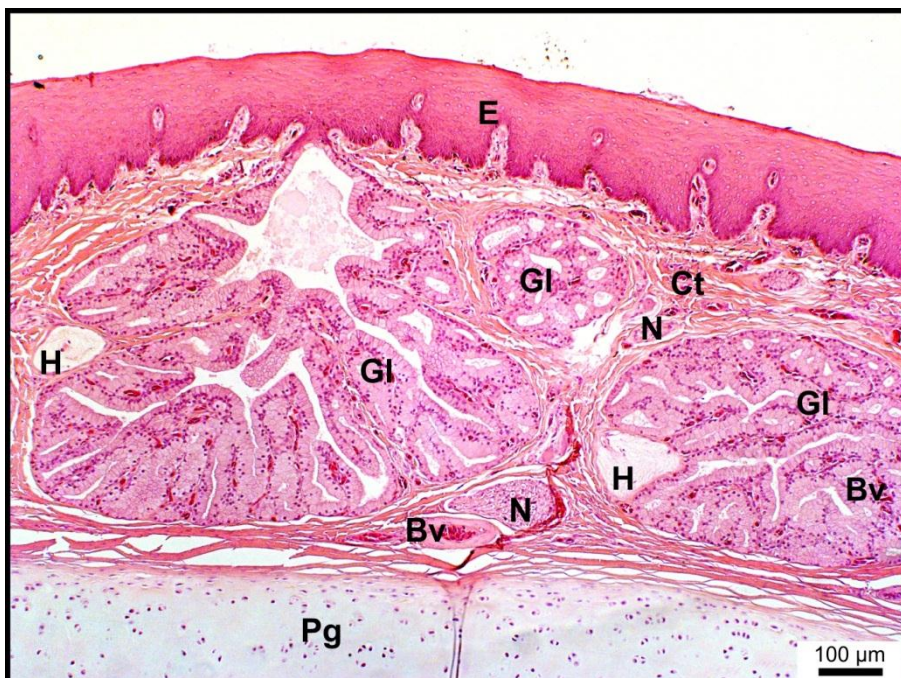


Figure 3.7. Dorsal surface of the emu tongue body. (Region H in Fig. 3.1). Note the close association between the Herbst corpuscles (H) and the large, simple branched tubular glands (Gl). Stratified squamous epithelium (E), connective tissue (Ct), nerves (N), blood vessels (Bv) and *Paraglossum* (Pg).



3.3.1.5. The laryngeal mound (Regions J, K; see Fig. 3.1)

Table 3.5. Comparative distribution of Herbst corpuscles (expressed as a relative percentage) in the laryngeal mound of the ostrich (O) and emu (E). Yellow highlight indicates a significant difference. Normality Test (Shapiro-Wilk) (NT), p value (p) and Mann-Whitney U Statistic (MUS).

	n	1	2	3	4	5	Mean	Median	NT	MUS	p
Arytenoid part	O	0	0.11	0	0	0	0	0	Fail	0	0.008
	E	0.83	1.39	0.53	2.66	1.39	1.36	1.39			
Cricoid part	O	0	0	0	0	0	0	0	Fail	10	0.69
	E	0	0	0	0	0.35	0.07	0			

The difference in the median values of the arytenoid part of the laryngeal mound between the ostrich and emu was greater than what would be expected by chance (Table 3.5). There was a statistically significant difference between this region in the ostrich and emu (Fig. 3.2 and Table 3.5). The difference in the median values of the cricoid part of the laryngeal mound between the ostrich and emu was not great enough to reject the possibility that the difference was due to random sampling variability. There was no statistically significant difference between the ostrich and emu (Fig. 3.2 and Table 3.5).



Figure 3.8. Herbst corpuscle (circled) in the arytenoid part of the laryngeal mound. (Region J in Fig. 3.1). Note the positioning of the corpuscle below the simple tubular glands (GI). Stratified squamous epithelium (E), connective tissue (Ct) and blood vessel (Bv).

Herbst corpuscles only occurred in the lips of the mucosa overlying the arytenoid cartilage in the emu (Fig. 3.2), with the exception of a single Herbst corpuscle in one of the ostrich specimens (Table 3.5). In the emu the Herbst corpuscles were situated within the connective tissue below the *Gl. cricoarytenoidea* (Crole and Soley, 2011) and were not associated with the glands (Fig. 3.8). The single Herbst corpuscle in the ostrich was, however, associated with a large, simple branched tubular gland of the *Gl. cricoarytenoidea*. Herbst corpuscles were only identified in the cricoid part of the laryngeal mound in one emu specimen. They were situated in the connective tissue and not associated with any structures.



3.3.1.6. The keratinised oropharyngeal roof (Regions L, M, N; see Fig. 3.1) (Excluding the median palatine ridge in the ostrich)

Table 3.6. Comparative distribution of Herbst corpuscles (expressed as a relative percentage) in the keratinised oropharyngeal roof of the ostrich (O) and emu (E). Yellow highlight indicates a significant difference. Standard deviation (SD), Normality Test (Shapiro-Wilk) (NT), p value (p) and Mann-Whitney U Statistic (MUS).

n	1	2	3	4	5	Mean	Median	SD	NT	MUS	p
O	29.11	34.03	32.24	32.76	30.61	31.75	32.24	1.90	Fail	0	0.008
E	58.97	61.96	59.11	54.55	38.04	54.50	58.97	9.59			

The difference in the median values of the keratinised oropharyngeal roof between the ostrich and emu was greater than what would be expected by chance (Table 3.6). There was a statistically significant difference between this region in the ostrich and emu (Fig. 3.2 and Table 3.6).

Herbst corpuscles in the maxillary rostrum (Region L in Fig. 3.1) were similarly arranged to those in the mandibular rostrum and were densely packed, forming chains or sheets in the compressed dermis between the premaxilla and epithelium, and also occurred in groups in the pits in the bone (Fig. 3.9) (see Chapter 7). In the caudal parts of the keratinised oropharyngeal roof (Regions M and N in Fig. 3.1) Herbst corpuscles also formed chains in the compressed dermis; however, in these regions not all parts of the mucosa was supported by bone. A median palatine ridge (MPR) was present in both

species (Figs. 3.9 and 3.13) which in the ostrich was more pronounced and contained a concentration of Herbst corpuscles (Fig. 3.13).

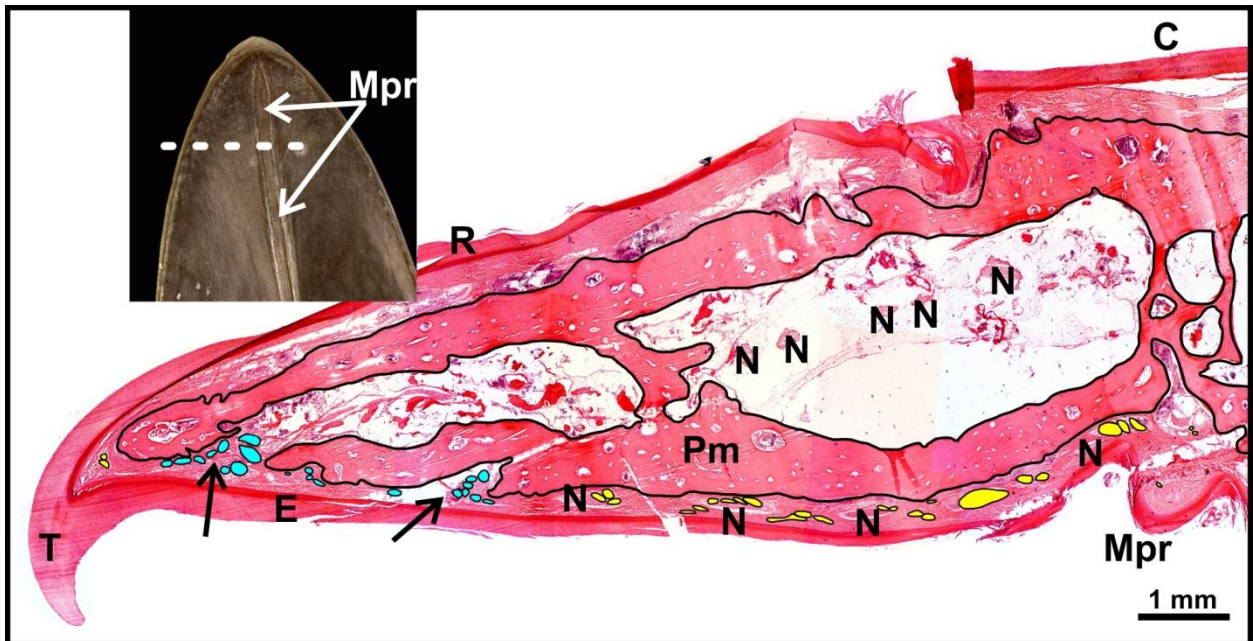


Figure 3.9. A composite micrograph of a transverse section of one half of the premaxilla in the adult emu. (Region L in Fig. 3.1). Inset indicates the approximate level of sectioning. Herbst corpuscles (yellow dots) occur in chains in the connective tissue between the keratinised stratified squamous epithelium (E) and the premaxilla (Pm); they also occur (blue dots) in pits (arrows) in the bone. *Tomium* (T), *Rhamphotheca* (R), nerves (N), median palatine ridge (Mpr) and *Culmen* (C).

3.3.1.7. The non-keratinised oropharyngeal roof (Regions O, P, Q; see Fig. 3.1)



Table 3.7. Comparative distribution of Herbst corpuscles (expressed as a relative percentage) in the non-keratinised oropharyngeal roof of the ostrich (O) and emu (E). Blue highlight indicates the power of the performed test with alpha (Pa) below the desired value of 0.8. Normality Test (Shapiro-Wilk) (NT), Equal Variance Test (EVT), Standard Deviation (SD), Standard Error of the Mean (SEM) and p value (p).

n	1	2	3	4	5	Mean	Median	SD	SEM	NT	EVT	p	Pa
O	14.22	6.93	15.82	9.02	11.78	11.55	11.78	3.65	1.63	Pass	Pass	0.8	0.1
E	12.84	6.16	12.09	13.22	11.18	11.10	12.09	2.87	1.28				

The difference in the mean values of the non-keratinised oropharyngeal roof between the ostrich and emu was not great enough to reject the possibility that the difference was due to random sampling variability. There was no statistically significant difference

between the ostrich and emu (Fig. 3.2 and Table 3.7). However, the power of the performed test (0.1) was below the desired power of 0.8 in this region (Table 3.7). This indicates that, due to the small sample size, a difference is less likely to be detected if one does actually exist. Therefore this result should be interpreted with caution.

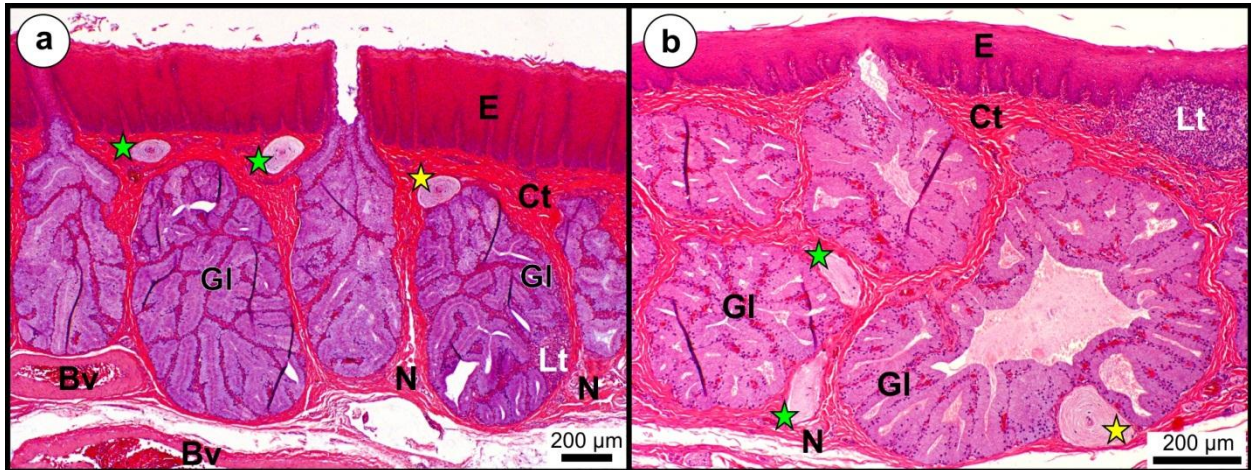


Figure 3.10. Herbst corpuscles (stars) in the non-keratinised oropharyngeal roof in the ostrich (a) and emu (b). (Region O in Fig. 3.1). Herbst corpuscles (yellow stars) are either closely associated with the glands (Gl) or occur more isolated (green stars) within the connective tissue (Ct). Stratified squamous epithelium (E), lymphoid tissue (Lt), nerves (N) and blood vessels (Bv).

Herbst corpuscles in Region O (Fig. 3.1) occurred throughout the connective tissue and were either isolated or closely associated with the large, simple branched tubular glands of the *Gl. palatina* (Crole and Soley, 2011) (Fig. 3.10). When isolated, they occurred anywhere in the connective tissue from below the epithelium to below the glands. In the ostrich, a localised concentration of Herbst corpuscles was present in the mucosa along the free edge of the choana (Fig. 3.11). These Herbst corpuscles were not associated with glands. A localised concentration of Herbst corpuscles was present in the rictus (Region P in Fig. 3.1) of both birds. These corpuscles were also not associated with glands. No Herbst corpuscles were present in the mucosa within the choana (Region Q in Fig. 3.1) in either species.

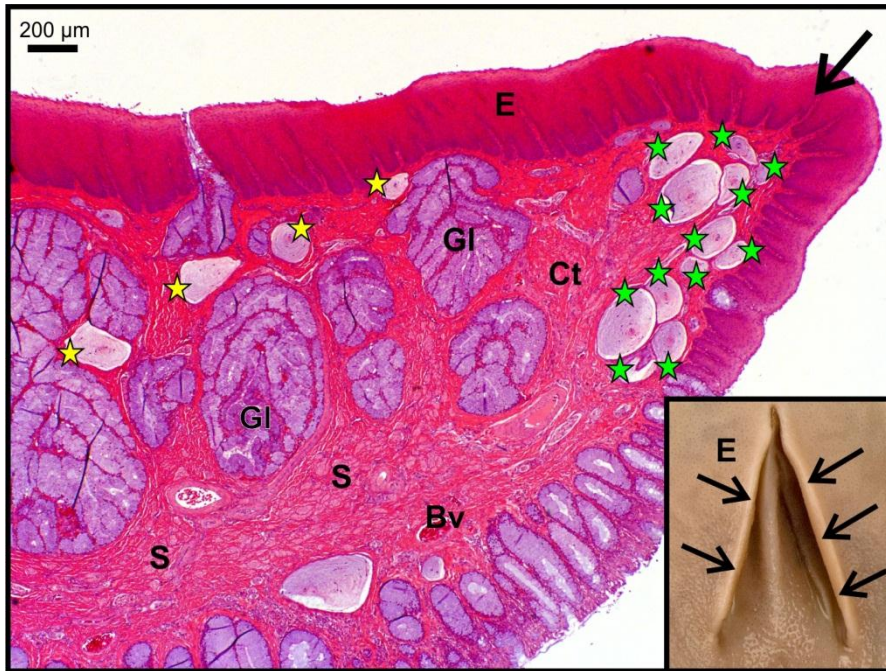


Figure 3.11. Non-keratinised oropharyngeal roof in the ostrich. (Region O in Fig. 3.1). Note the concentration of Herbst corpuscles (green stars) bordering the choana (arrows and inset). Smooth muscle (S) bundles are present in the connective tissue (Ct) of this region. Herbst corpuscles (yellow stars) closely associated with the glands (Gl), stratified squamous epithelium (E) and blood vessel (Bv).

3.3.1.8. The pharyngeal folds (Regions R, S; see Fig. 3.1)

Table 3.8. Comparative distribution of Herbst corpuscles (expressed as a relative percentage) in the pharyngeal folds of the ostrich (O) and emu (E). Normality Test (Shapiro-Wilk) (NT), p value (p) and Mann-Whitney U Statistic (MUS).



n	1	2	3	4	5	Mean	Median	NT	MUS	p
O	0	0	0.13	0	0	0.03	0	Fail	10	0.69
E	0	0	0	0	0	0	0			

The difference in the median values of the pharyngeal folds between the ostrich and emu was not great enough to reject the possibility that the difference was due to random sampling variability. There was no statistically significant difference between the ostrich and emu (Fig. 3.2 and Table 3.8).

Herbst corpuscles were absent from this region in the ostrich and emu. However, in one ostrich specimen (Table 3.8) a Herbst corpuscle was found in the connective tissue at the rostral limit of the region sampled. The pharyngeal folds and associated tonsils have previously been described in both species (Crole and Soley, 2012a).



3.3.1.9. The median ventral ridge and median palatine ridge in the ostrich (Regions A, C, D, L, M; see Fig. 3.1)

Table 3.9. Comparative distribution of Herbst corpuscles (expressed as a relative percentage) in the median ventral ridge (MVR) and median palatine ridge (MPR) of the ostrich. Standard deviation (SD).

n	1	2	3	4	5	Mean	Median	SD
MVR	8.91	7.55	1.41	3.42	5.87	5.43	5.87	3.04
MPR	7.30	5.44	9.03	5.32	7.32	6.88	7.30	1.54

A ridge was present on the ventral midline of the oropharyngeal floor in the ostrich stretching from the mandibular rostrum to the tongue (Fig. 3.2), termed the median ventral ridge (MVR) (Figs. 3.4 and 3.12). In both species a ridge was also present along the midline of the keratinised oropharyngeal roof (Figs. 3.1, 3.9 and 3.13), termed the median palatine ridge (MPR); however, this structure was far more pronounced in the ostrich than the emu. Both the median ventral and palatine ridges in the ostrich contained a large concentration of Herbst corpuscles (Figs. 3.4, 3.12 and 3.13). A large, central artery was present at the base of the MPR and from which finer blood vessels radiated into the ridge. Accompanying the blood vessels were numerous nerves supplying the Herbst corpuscles. Although the emu displayed a small palatine ridge, there was no specific concentration of Herbst corpuscles in this structure and unlike the situation in the ostrich, in which any section displayed numerous Herbst corpuscles, in the emu many sections displayed few or none. The MVR in the ostrich was morphologically similar to the MPR and a large central artery (a branch of the sublingual artery) was also present at the base (Fig. 3.12). However, as the MVR proceeded caudally it divided into two diverging ridges. The concentration of Herbst corpuscles diminished as these ridges neared the region ventral to the apex of the tongue.

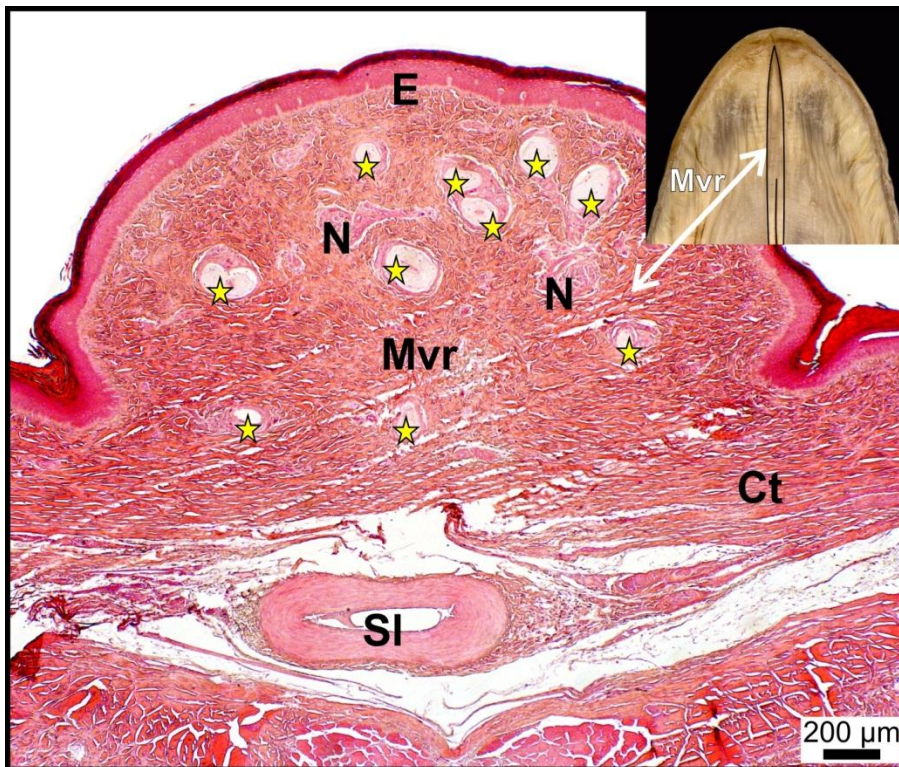


Figure 3.12. Herbst corpuscles (stars) in the median ventral ridge (Mvr) of the rostral keratinised oropharyngeal floor of the ostrich (region C in Fig. 3.1 and outlined on the inset). Note the concentration of Herbst corpuscles (10 in this figure) and nerves (N) in the median ventral ridge. Rostral branch of the sublingual artery (SI), keratinised stratified squamous epithelium (E) and connective tissue (Ct).

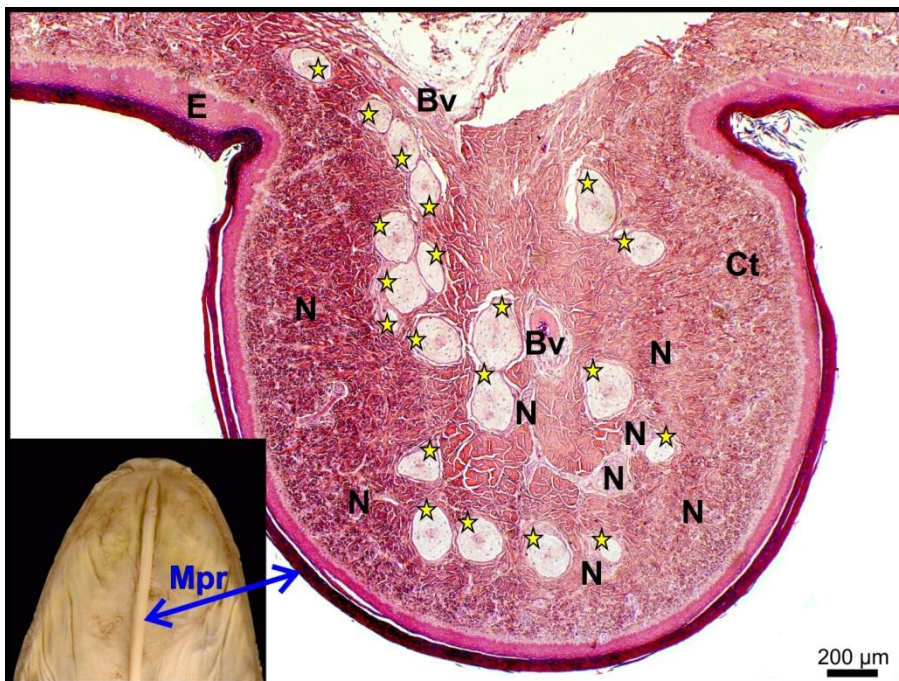


Figure 3.13. Herbst corpuscles (stars) in median palatine ridge (Mpr) of the keratinised oropharyngeal roof of the ostrich (region L and M in Fig. 3.1 and indicated in the inset). Note the concentration of Herbst corpuscles (20 in this figure) and nerves (N) in the median palatine ridge. Connective tissue (Ct), blood vessels (Bv) and keratinised stratified squamous epithelium (E).

Based on the above data it was clear that the ostrich displayed a greater concentration of Herbst corpuscles in the oropharynx (on average 2.5 times higher) than the emu. However, the distribution of the Herbst corpuscles showed a species specific distribution with two thirds of the total number of corpuscles in the emu being located in the oropharyngeal roof and one third on the floor (Fig. 3.2). In contrast the Herbst

corpuscles in the ostrich oropharynx were more evenly distributed with approximately half being present in the roof and the other half on the floor (Fig. 3.2).

3.3.2. Arrangement of Herbst corpuscles

Although the distribution of Herbst corpuscles differed in some regions between the emu and ostrich, the histological location of these mechanoreceptors and their particular arrangement was similar between the two species when viewing comparable regions. In general most Herbst corpuscles were oriented with their long axis in a rostro-caudal direction and were arranged in three specific ways: (1) those concentrated in groups clustered around nerve fibres (see Chapter 7), (2) those occurring singly, or sometimes in groups, and surrounded by connective tissue, and (3) those closely associated with large, simple branched tubular glands. The first arrangement was representative of Herbst corpuscles typically found in the mandibular (Fig. 3.3) and maxillary (Fig. 3.9) rostra (Regions A and L in Fig. 3.1) where they formed the receptors of the intra-oral portion of the bill tip organ (see Chapter 7). The second arrangement was evident at specific locations in the oropharynx reflecting single corpuscles or groups of corpuscles. They were located singly in the rostral keratinised oropharyngeal floor (Figs. 3.5 and 3.6) (Regions C-E), the tongue of the emu (Region H), the arytenoid part of the laryngeal mound in the emu (Fig. 3.8) (Region J) and the non-keratinised oropharyngeal roof (Fig. 3.10 and 3.11) (Region O) (see also Fig. 3.1). Herbst corpuscles were located in groups, but without appearing to be associated with a nerve, in the mandibular arms (Region B), the keratinised oropharyngeal roof (Regions M and N), the rictus (Region P), the edge of the choana in the ostrich (Fig. 3.11) (in Region O) (see Fig. 3.1) and the median palatine (Fig. 3.13) and median ventral (Figs. 3.4 and 3.12) ridges in the ostrich. The third arrangement of Herbst corpuscles was encountered in the following glandular fields (Crole and Soley, 2011) in both species; namely, the palatine gland (Figs. 3.10 and 3.11) (Region O), the oral angular gland (Region P), the lateral mandibular gland (Region F) and, in the emu only, the lingual glands (Fig. 3.7) (Region H).

3.3.3. Structure

3.3.3.1. Light microscopy (LM)

The Herbst corpuscles displayed a wide variety of shapes and sizes in the ostrich and emu throughout the oropharynx (Fig. 3.14). Herbst corpuscles occurring in the compressed connective tissue layer underlying the keratinised epithelium of the mandible and rostral oropharyngeal roof were more consistent in their shape and size than those associated with the glands. The Herbst corpuscles were ovoid structures that, depending on the plane of sectioning, appeared either round (transverse section) (Figs. 3.14h and j) or elongated (longitudinal section) (Fig. 3.14j). The corpuscles, on average, appeared larger in the ostrich than in the emu, specifically those corpuscles associated with the glands. Each corpuscle was composed of an outer capsule, an outer zone, inner core and axon which were clearly demonstrated with H&E staining (Figs. 3.14a-j), toluidine blue staining (Figs. 3.14k and 3.17a) and immunohistochemical labelling for neurofilament protein (Figs. 3.15 and 3.16 b, d). The capsule appeared thicker in the ostrich than the emu (see also TEM below). Positive IHC labelling demonstrated nerve fibres running directly outside the capsule (Fig. 3.15). The outer zone was composed of rings of collagen fibres and intervening fibroblasts (generally identified only by their nuclei) arranged concentrically around the inner core (Figs. 3.16a, c). Some corpuscles displayed a double (Figs. 3.14a, b, g) or branched (Fig. 3.14i) axon, each surrounded by an inner core and outer zone but contained within a common capsule (Figs. 3.14a, b, g, i). In the ostrich and emu chick specimens (Figs. 3.14i, j) the inner core of the Herbst corpuscles appeared thicker relative to the outer zone and more cellular in nature than that observed in the adults.

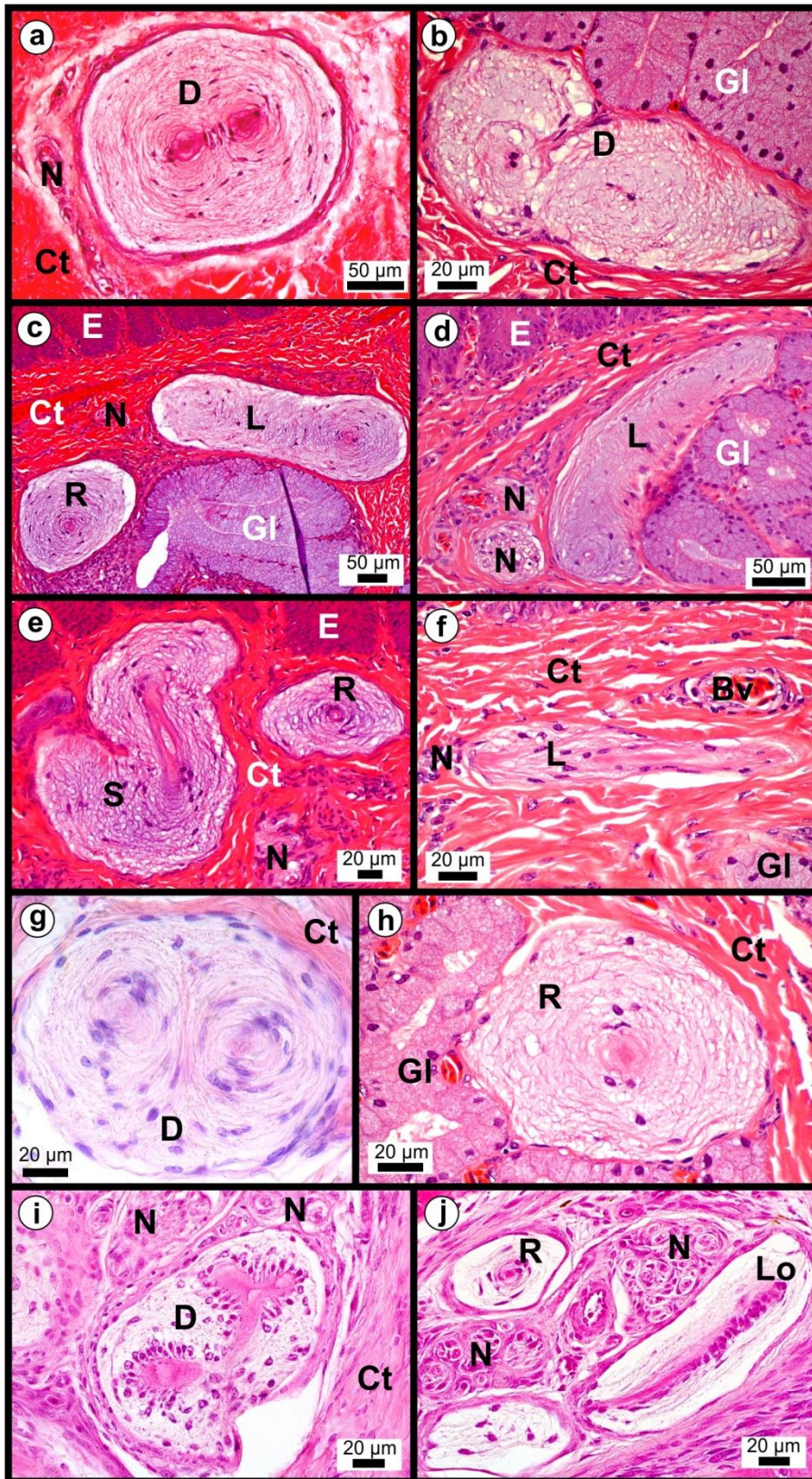
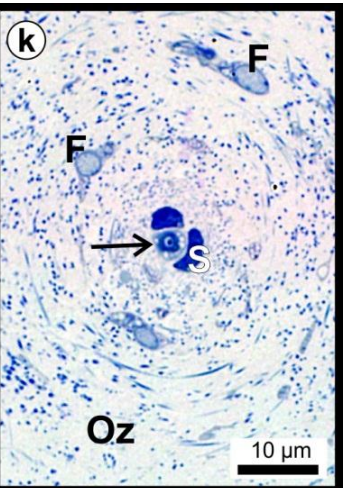


Figure 3.14. Morphology of Herbst corpuscles in the ostrich (left) and emu (right) oropharynx. Some Herbst corpuscles display double (D) axons (a, b, g and i), long, oval profiles (L) with an eccentric axon in transverse section (c and d), oddly-shaped profiles such as an S-shape (S) (e), round profiles (R) in transverse section (a, c, e, g, h and j) and oval profiles (Lo) in longitudinal section (f and j). Note that the Herbst corpuscles in chicks (i and j) display a more cellular region around the central pink axon compared to that of adults (a-h). Connective tissue (Ct), nerve (N), gland (Gl), stratified squamous epithelium (E) and blood vessel (Bv).



k. Myelinated axon (arrow) in an ostrich Herbst corpuscle. Note that the axon is surrounded by a myelin sheath and not by an inner core. Outer zone (Oz), fibroblast nucleus (F) and Schwann cell nucleus (S). Toluidine blue stained section.

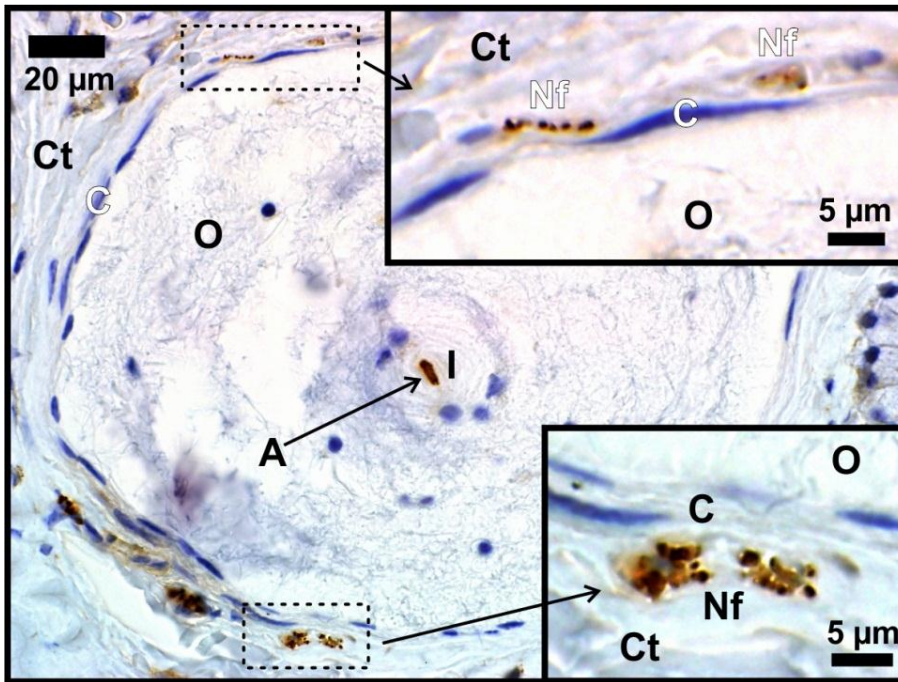


Figure 3.15. Positive IHC labelling for neurofilament (Nf) in a Herbst corpuscle in the emu. The relationship of nerve fibres with the capsule (C) is clearly demonstrated on light microscopy with IHC labelling. Connective tissue (Ct), outer zone (O), inner core (I) and axon (A).

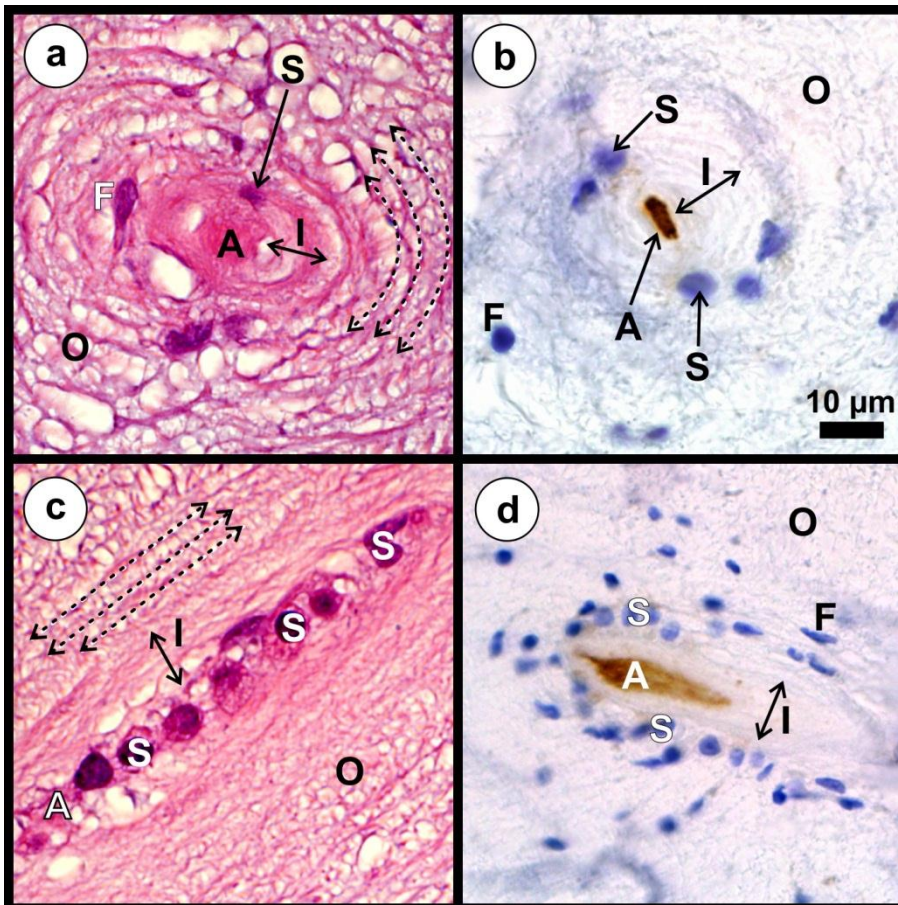


Figure 3.16. Light micrographs of the outer zone (O) and inner core (I) of Herbst corpuscles in the emu. Transverse sections (a and b) and longitudinal sections (c and d). H&E stained sections (a and c) and positive IHC labelling (A) for neurofilament (b and d). Note the concentric arrangement (dotted double-headed arrows) of elements of the outer zone which is more obvious with H&E staining whereas the same region appears more homogeneous in b and d. The inner core is formed by Schwann cells (S) surrounding the axon (A). Fibroblast nucleus (F). All images are to the same scale.

3.3.3.2. Transmission electron microscopy (TEM)

As noted by light microscopy, Herbst corpuscles in both the ostrich and emu were composed of a fibrous outer connective tissue capsule, an outer zone (subcapsular space), a lamellated inner core (formed by specialised Schwann cells) and a receptor axon (Fig. 3.17).

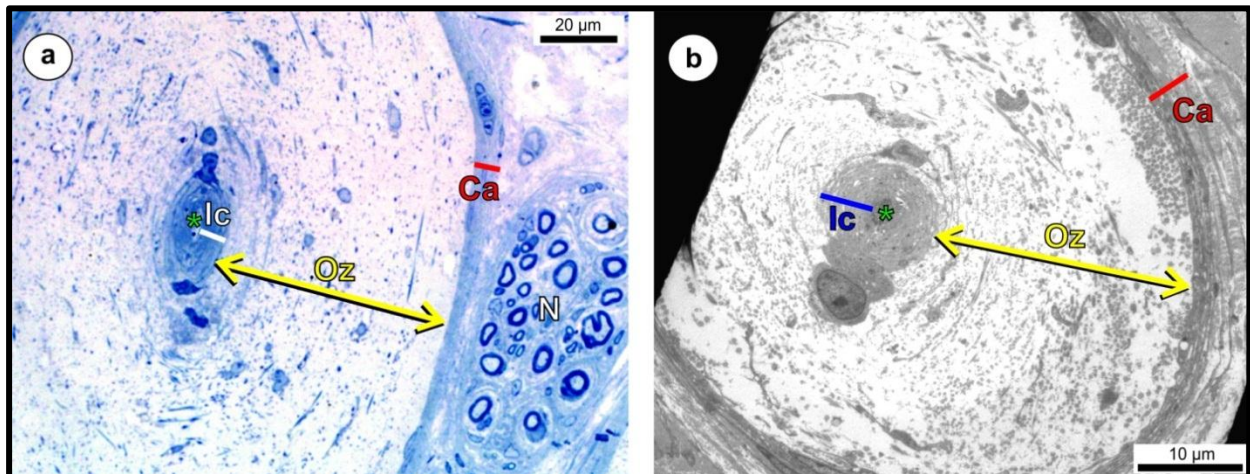


Figure 3.17. Low magnification of an ostrich (a – toluidine blue) and emu (b - TEM) Herbst corpuscle from the oropharynx in transverse section. The four basic components of the Herbst corpuscle are, from without inwards, the capsule (Ca), the outer zone (Oz), inner core (Ic) and axon (*). Note the concentric arrangement of the elements in the wide outer zone and the closely associated nerve (N) in the ostrich.

3.3.3.2.1. Capsule

The capsule consisted of concentrically arranged alternating layers of cellular and acellular lamellae (Figs. 3.20-23) and was continuous with the perineurium of the accompanying nerve fibre/s (Figs. 3.17a and 3.19). The capsule in both species shared similar basic features although in the emu it appeared thinner and more compact in nature. The average thickness of the capsule was $7.63 \pm 2.48 \mu\text{m}$ (n=13) in the ostrich and $6.32 \pm 1.89 \mu\text{m}$ (n=13) in the emu. In the emu some Herbst corpuscles displayed an ill-defined capsule which was composed of loosely arranged acellular lamellae only (Fig. 3.18)

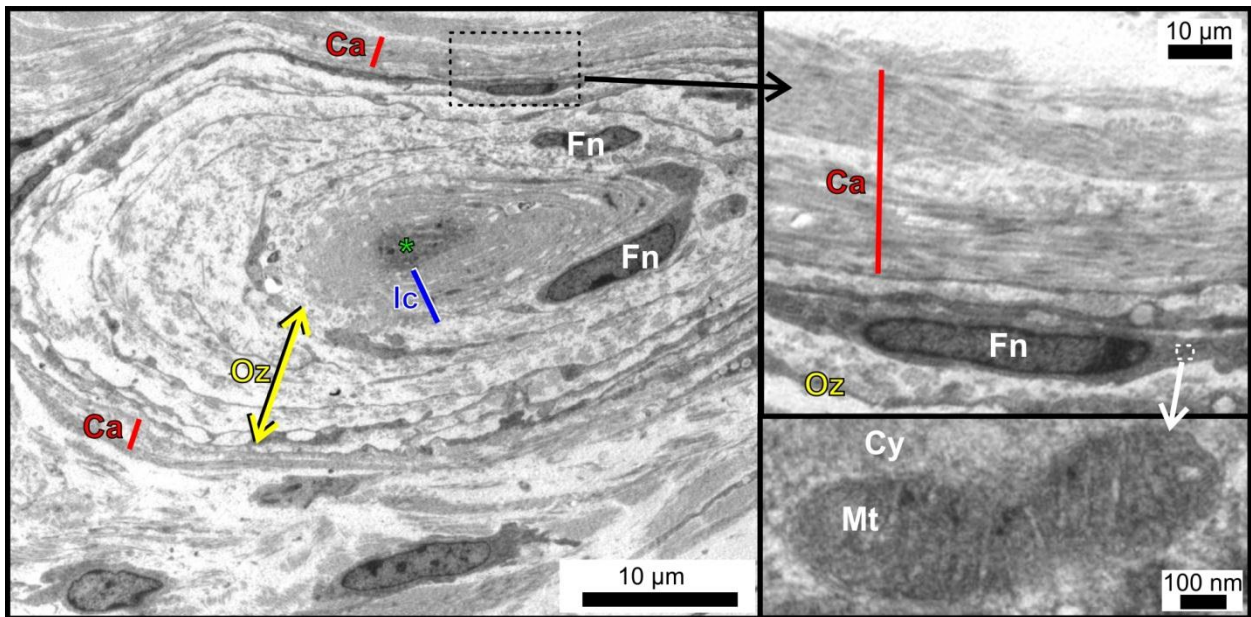


Figure 3.18. Low magnification of an emu (Left) Herbst corpuscle in transverse-section from the mandibular rostrum. The four basic components of the Herbst corpuscle are, from without inwards, the capsule (Ca), the outer zone (Oz), inner core (Ic) and axon (*). Note the concentric arrangement of the elements in the outer zone. The capsule of this Herbst corpuscle is ill-defined (top right) and is composed of acellular lamellae only. Fibroblasts (Fn) appear to form a boundary between the ill-defined capsule and the outer zone. A section of the fibroblast cytoplasm (Cy) has been enlarged (bottom right) to demonstrate a mitochondrion (Mt).

Based on obvious morphological characteristics the capsule could be divided into two parts. The outermost part typically displayed a series of relatively wide acellular lamellae (containing collagen microfibrils) separated by equally wide alternating cellular lamellae (Figs. 3.20 and 3.21). This region formed approximately three quarters of the width of the capsule in the ostrich but only half the width in the emu (Fig. 3.20).

The wide acellular lamellae were packed with similarly sized collagen microfibrils that were generally oriented either horizontally or longitudinally within a particular lamellum, although variable microfibril orientation within a given lamellum was occasionally observed (Figs. 3.21 and 3.22). In some areas the orientation of the microfibrils alternated between neighbouring acellular lamellae although most of the microfibrils lay parallel to the long axis of the corpuscle. Giant collagen microfibrils (up to 10 times larger in diameter) were occasionally present between the normal sized microfibrils.

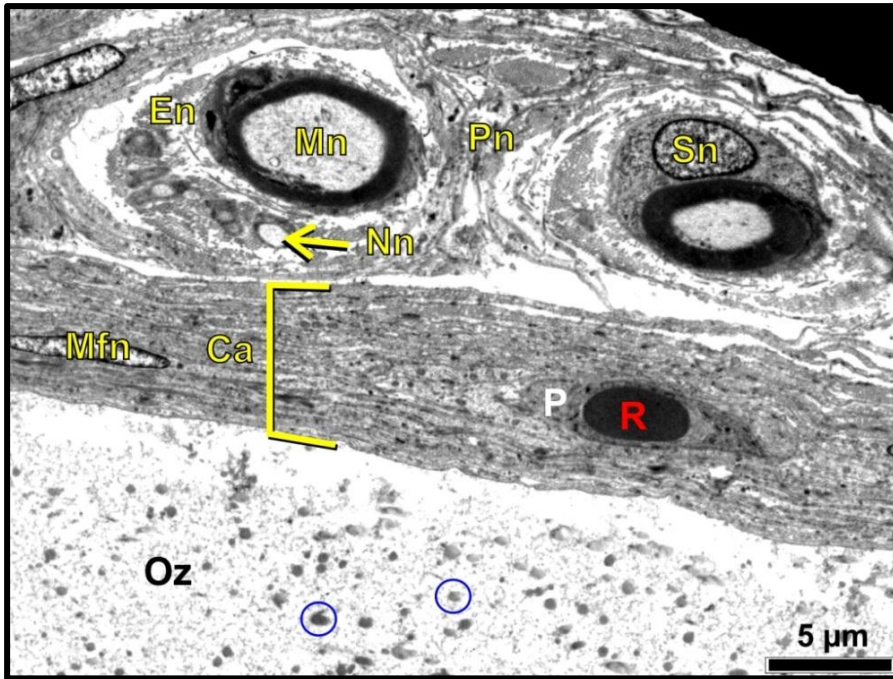


Figure 3.19. Low magnification micrograph illustrating the relationship between a Herbst corpuscle and a peripheral nerve in the ostrich. The capsule of the Herbst corpuscle (Ca) is continuous with the perineurium of the adjacent nerve. A capillary (P) with a red blood cell (R) lies in the middle third of the capsule. Perineurium (Pn), endoneurium (En), Schwann cell nucleus (Sn), myelinated nerve (Mn), non-myelinated nerve (Nn), myofibroblast nucleus (Mfn), outer zone (Oz) and collagen microfibrils (blue circles).

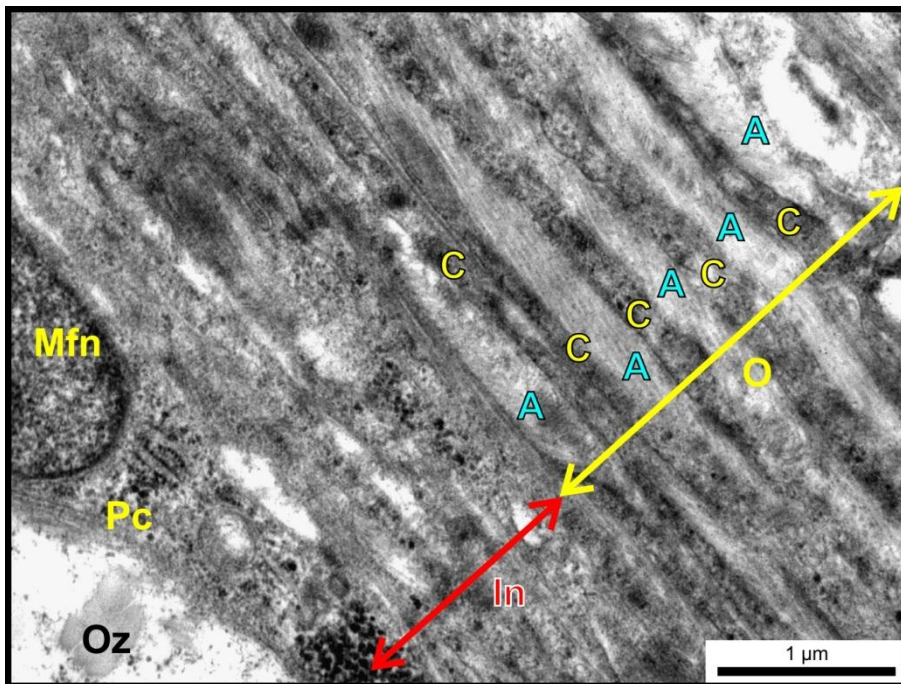


Figure 3.20. High magnification of the lamellae in the capsule in the emu. The capsule is formed by alternating wider acellular (A) and cellular (C) lamellae in the outer layers (O) and by thinner lamellae, with cellular lamellae more predominant, in the inner layers (In). Myofibroblast nucleus (Mfn), perinuclear cytoplasm (Pc) and outer zone (Oz).

The cellular lamellae were formed by the cytoplasmic extensions of numerous myofibroblasts (Figs. 3.20-23). The long, cigar shaped nuclei of these cells were vesicular in appearance and displayed a layer of dense marginal chromatin (Figs. 3.18 and 3.23). The cytoplasm was composed of a fine, homogenous matrix containing numerous micro-pinocytotic vesicles, mitochondria (Fig. 3.18), swollen profiles of RER, microtubules and bundles of myofilaments (Figs. 3.21-23). Accumulations of small

electron dense granules of similar dimensions to glycogen granules were also commonly observed (Fig. 3.23b). Isolated structures resembling lysosomes were also present (Fig. 3.21). The cell membrane displayed numerous marginal densities and in places was bordered by an incomplete layer of basal lamina-like material (Fig. 3.21). Adjoining cytoplasmic processes of the myofibroblasts either overlapped or interdigitated (Fig. 3.22) and were connected by small adhering junctions. The outer part of the capsule was vascularised by a system of small arterioles located at the periphery of the capsule and by a bed of deeper lying capillaries sandwiched between the cellular lamellae (Fig. 3.19).

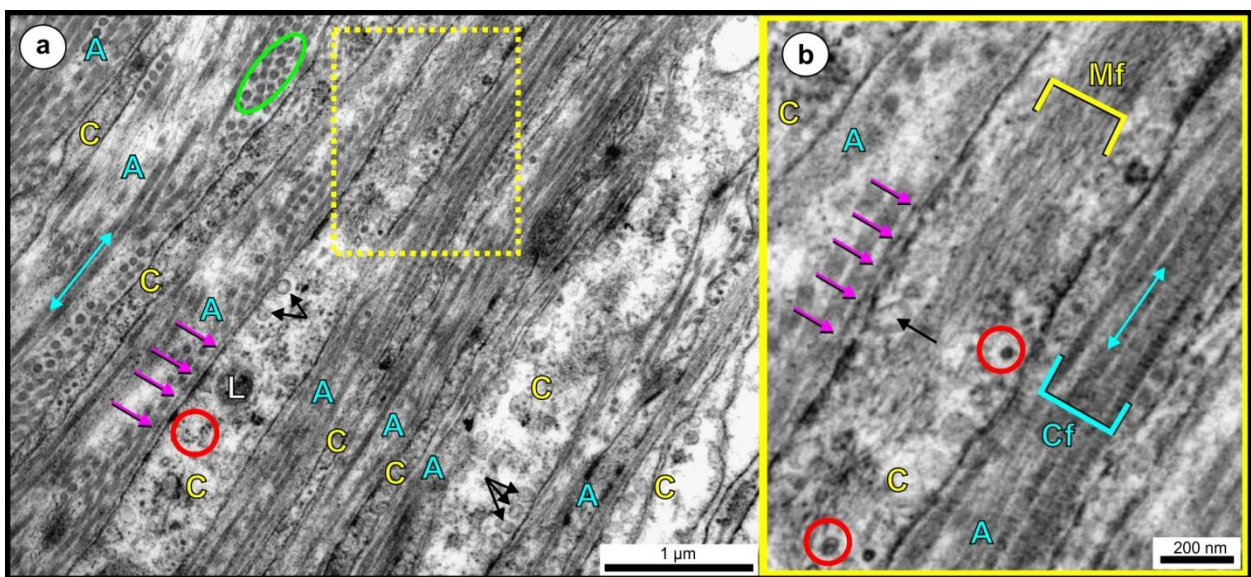


Figure 3.21. (a). Outer region of the capsule in the ostrich with the yellow square enlarged in (b). The acellular lamellae (A) with collagen fibrils (Cf) oriented in both longitudinal (double-headed blue arrow) and transverse (green circle) profile, and the cytoplasmic lamellae (C) formed by the myofibroblasts are clearly seen alternating with one another. The broad cellular lamellae display numerous micro-pinocytotic vesicles (black arrows), microtubules (red circles), isolated lysosome-like structures (L) and occasional bundles of myofilaments (Mf). In places the plasmalemma rests on a discontinuous layer of basal lamina-like material (pink arrows).

The inner part of the capsule was more compact in nature with the acellular component forming narrow bands between the wider, predominant cellular lamellae (Fig. 3.23). However, the ultrastructural features of both types of lamellae were similar to those observed in the outer part of the capsule (Fig. 3.23). The nuclei of the myofibroblasts bordering the inner margin of the capsule and the outer zone were more rounded in appearance, often bulging into the substance of the outer zone. In some of the marginal myofibroblasts a single sensory cilium was observed in the vicinity of the nucleus and partially embedded within the cell (Fig. 3.23). The core of the cilium displayed a 9 X 2 +

0 arrangement of microtubules and was surrounded by an intracellular canal (Fig. 3.23b).

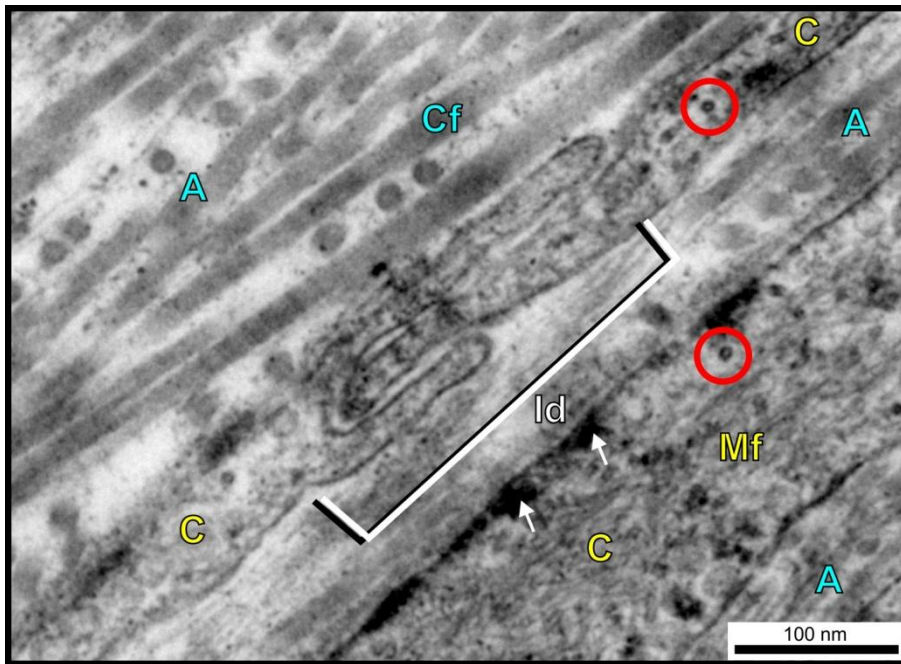


Figure 3.22. Interdigitation (ld) between two myofibroblast cytoplasmic lamellae (C) in the ostrich. Acellular (A) lamellae with collagen fibrils (Cf), marginal densities (white arrows), myofilaments (Mf) and microtubules (red circles). Note the mixed orientation of collagen fibrils in the acellular lamellum.

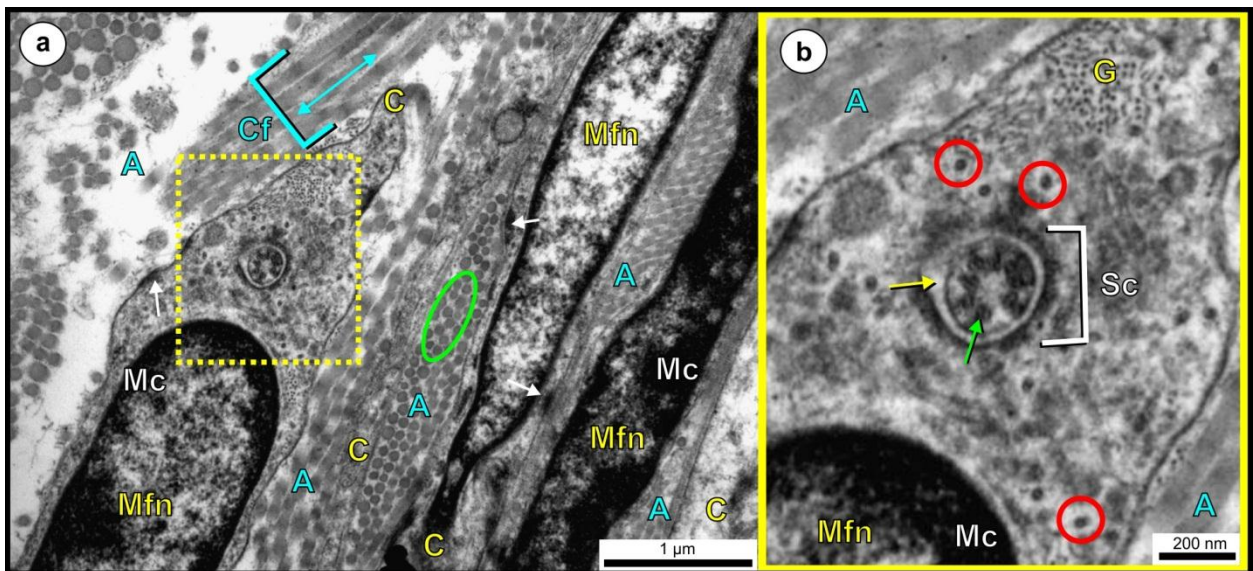


Figure 3.23. (a). Innermost region of the capsule in the ostrich. Note the narrow acellular lamellae (A) with collagen microfibrils (Cf) orientated in longitudinal (blue double-headed arrow) and transverse (green circle) profile alternating with cellular lamellae (C). The cigar-shaped myofibroblast nuclei (Mfn) display a layer of dense marginal chromatin (Mc). Marginal densities (white arrows) and a sensory cilium (yellow square – enlarged in b) are also apparent.

(b). The sensory cilium (Sc) displays a 9 x 2 + 0 arrangement of microtubules (green arrow) and is surrounded by an intracellular canal (yellow arrow). Microtubules (red circles) and presumptive glycogen granules (G) are also present. Acellular lamellae (A).

3.3.3.2.2. Outer zone (subcapsular space)

The bulk of the corpuscle was formed by the outer zone which was composed of scattered stellate fibroblasts and numerous randomly scattered collagen fibrils (Figs. 3.17, 3.24-26 and 3.29). Although widely dispersed, the elements of the outer zone, at low magnification, were observed to adopt a concentric arrangement (Figs. 3.17, 3.25 and 3.29), forming ill-defined cellular (fibroblasts) and acellular (matrix and collagen microfibrils) lamellae. The acellular component formed the bulk of the outer zone. The collagen microfibrils were mostly oriented along the long axis of the corpuscle and displayed two sizes, those of similar dimension to the microfibrils seen in the capsule (Fig. 3.23) and giant microfibrils that were up to 10 times larger in diameter (Fig. 3.24a). The fibrils were imbedded in a matrix of interconnected flocculent material and variably sized, intervening clear spaces (Fig. 3.24). Fibroblasts were sparse, although they increased in number (as did the density of the collagen microfibrils) towards the inner core (Fig. 3.25). These cells were typically mesenchymal in appearance and the nuclei were more rounded than those of the myofibroblasts in the capsule. The cytoplasm contained conspicuous collections of granular endoplasmic reticulum, scattered mitochondria, numerous small vesicles, Golgi fields and an occasional sensory cilium (Fig. 3.24). When present, the cilium, with its 9 X 2 + 0 microtubular arrangement, emerged from a typical basal body and was partly enclosed within an intracellular canal (Fig. 3.24b). The patchy basal lamina-like material and marginal cytoplasmic densities typical of the capsular myofibroblasts were not observed in the fibroblasts of the outer zone. The attenuated cytoplasmic extensions of the fibroblasts were sparsely scattered throughout the matrix. The morphological characteristics outlined above were similar in both the ostrich and emu.

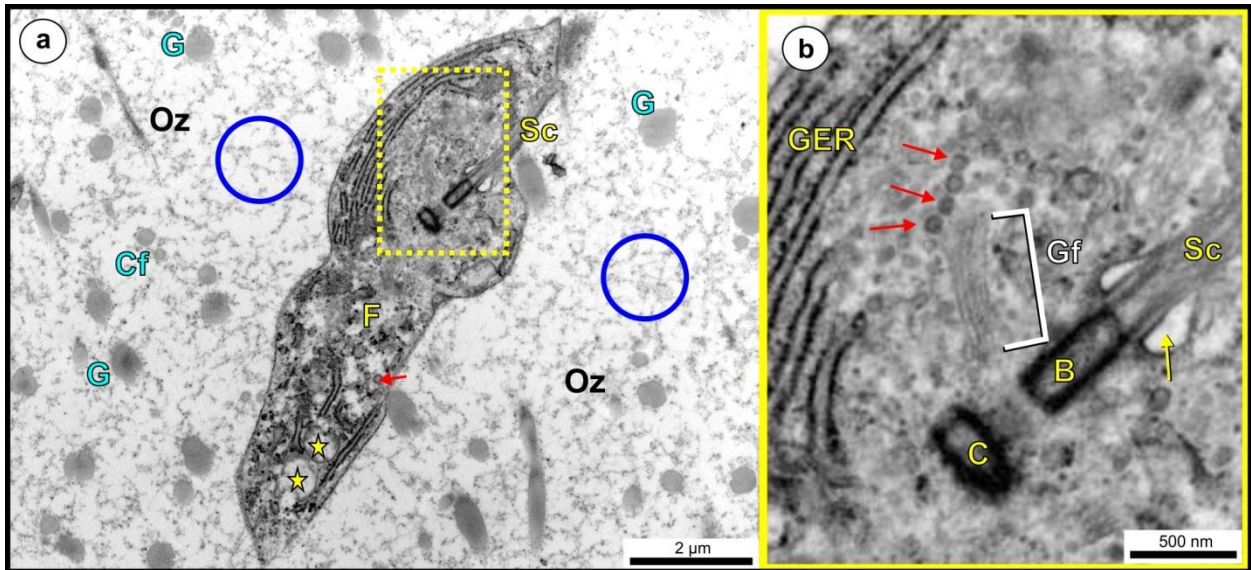


Figure 3.24. A fibroblast (F) located in the outer zone (Oz) of an ostrich Herbst corpuscle (a) with the yellow square enlarged in (b). The outer zone demonstrates a matrix of flocculent material (blue circles), and normal (Cf) and giant sized (G) collagen fibrils. The fibroblast cytoplasm displays strands of granular endoplasmic reticulum (GER), Golgi fields (Gf), mitochondria (stars), small vesicles (red arrows) and a sensory cilium (Sc). The basal body (B) and an underlying centriole (C) appear to form a typical diplosome. Intracellular canal (yellow arrow).

3.3.3.2.3. Inner core

The inner core, which was similar in the ostrich and emu, occupied the centre of the Herbst corpuscle (Fig. 3.17) and was formed by two sets of closely opposed, interdigitating, semi-circular cytoplasmic lamellae (Figs. 3.25-28) emanating from terminal Schwann cells situated on either side (opposite poles) of the afferent nerve fibre (central axon) (Figs. 3.25 and 3.26). Oblique sections of Herbst corpuscles revealed a row of Schwann cell bodies indicating that individual Schwann cells only formed a short segment of the inner core along the length of the corpuscle. A number of relatively large fibroblasts were sometimes observed in close proximity to the inner core (Fig. 3.25). The location of the Schwann cell bodies, the particular radiation of the cytoplasmic processes (lamellae) and the central positioning of the axon resulted in the inner core being subdivided into two semi-circular units by intervening clefts devoid of cytoplasmic material (Fig. 3.25). The outer lamellae were more loosely arranged than those closer to the axon (Fig. 3.27). Scattered collagen fibrils were randomly situated in the inter-lamellar spaces (Figs. 3.27 and 3.28) and appeared to be concentrated towards the poles of the inner core in the vicinity of Schwann cell bodies. The collagen fibrils were oriented with their long axis parallel to the long axis of the corpuscle. The

more compactly arranged inner lamellae lay closely apposed with only a thin intervening layer of extracellular matrix between them (Figs. 3.26 and 3.27).

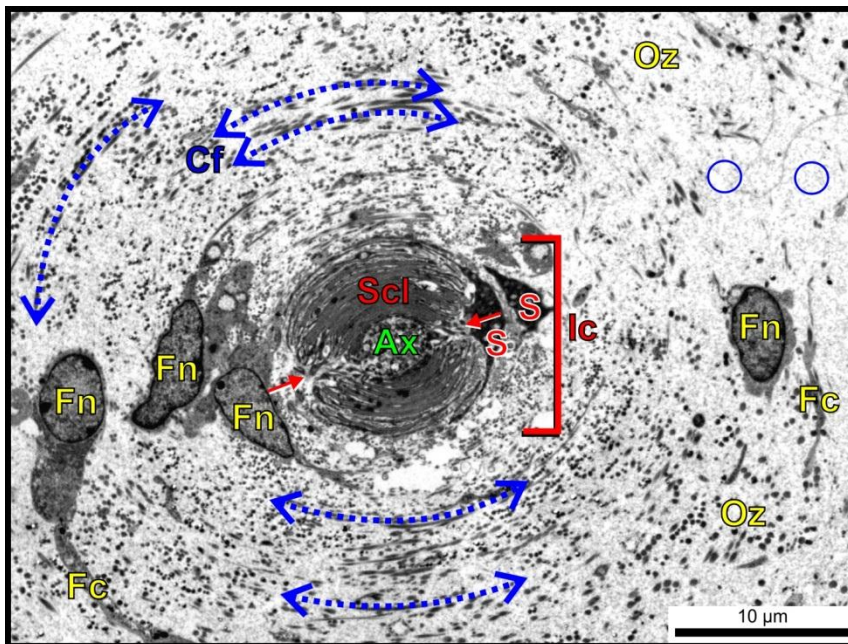


Figure 3.25. An orientation micrograph showing the outer zone (Oz) and inner core (Ic) of a Herbst corpuscle in the ostrich. Note the concentric arrangement (dotted blue double-headed arrows) of elements of the outer zone; collagen fibrils (Cf), cytoplasmic processes of fibroblasts (Fc) and flocculent (blue circles) matrix. The inner core is formed by Schwann cells (S) located at the poles which form cytoplasmic lamellae (Scl), separated by clefts (red arrows), surrounding the axon (Ax). (Fn) Fibroblast nucleus.

The large round nucleus of the Schwann cells displayed nuclear clefts and contained aggregations of mostly peripherally situated heterochromatin (Fig. 3.26). A prominent nucleolus was also evident (Fig. 3.26). The cytoplasm of the Schwann cell body, compared to the adjacent fibroblasts, was relatively electron-dense and surrounded by a discontinuous basal lamina (Fig. 3.26). The most conspicuous organelles were mitochondria, micro-pinocytotic vesicles and lysosome-like structures (dense bodies). Also present were collections of rough endoplasmic reticulum (normal and swollen profiles), scattered free and polyribosomes, elements of the Golgi apparatus and numerous microtubules. The cytoplasmic lamellae were composed of a featureless, moderately electron-dense matrix containing microtubules and micro-pinocytotic vesicles (many of which were coated). Mitochondria were also occasionally observed (Figs. 3.26-28) and were frequently situated at the termination of the lamellum giving it a club-shaped appearance (Fig. 3.28). The presence of mitochondria was generally indicated by a localized thickening of the lamellum (Fig. 3.27). Basal lamina-like material appeared sporadically on the surface of the loosely arranged outer lamellae (Fig. 3.26) but was not observed on the inner, tightly-packed lamellae. Prominent hemidesmosomes were present between the inner lamellae and axolemma (Fig. 3.31) and occasional desmosome-like adhering junctions connected adjacent lamellae.

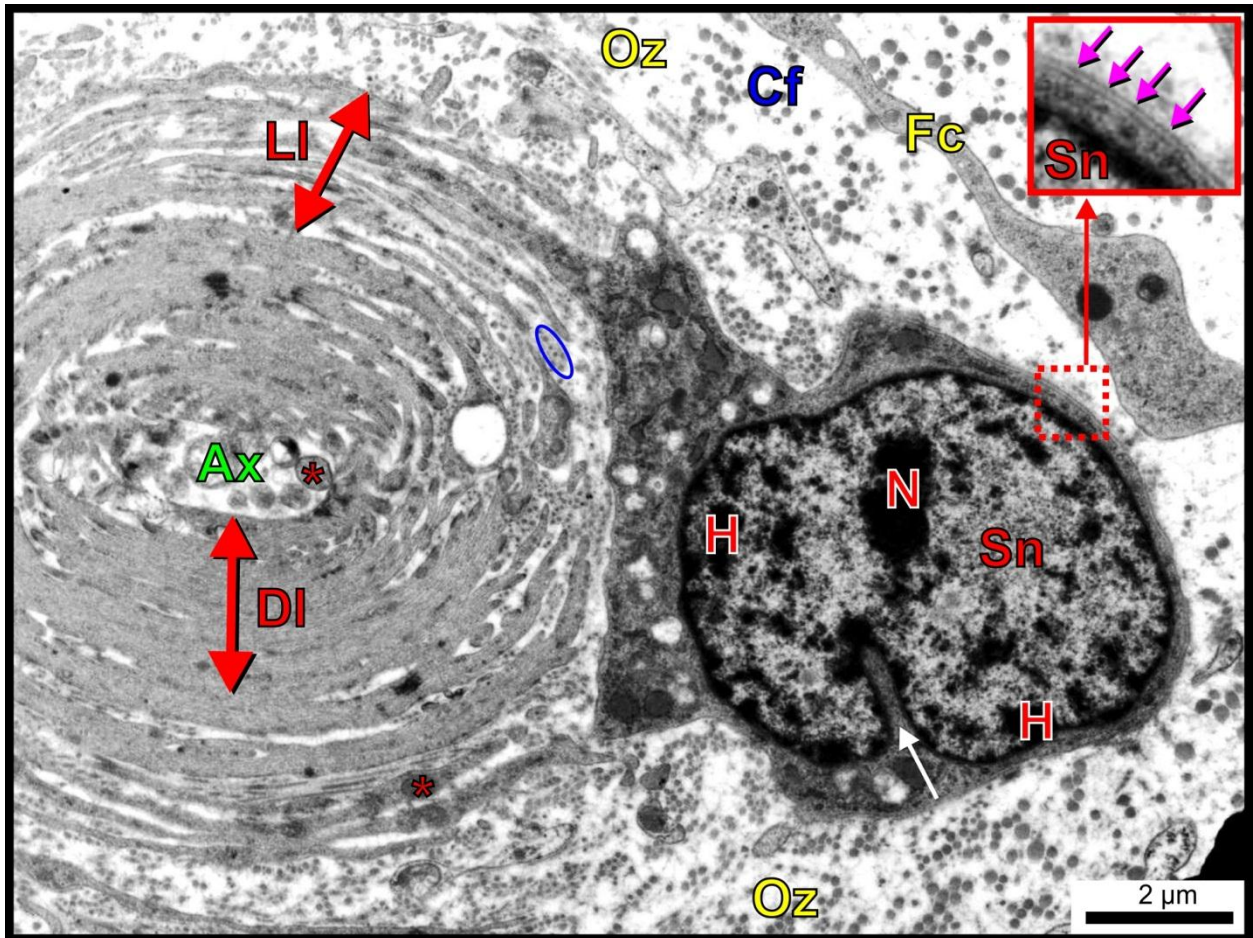


Figure 3.26. Inner core of a Herbst corpuscle in the ostrich. Note the large, indented (white arrow) Schwann cell nucleus (Sn) with a prominent nucleolus (N) and clumps of heterochromatin (H). The outer layers of cytoplasmic lamellae are loosely arranged (LI) whereas the inner lamellae are more densely packed (DI). The outer lamellae are interspersed with collagen fibrils (blue circle). Fibroblast cell processes (Fc), collagen fibrils (Cf), outer zone (Oz), mitochondria (red *) and axon (Ax). The enlargement shows a short section (continuous) region of the Schwann cell basal lamina (pink arrows).

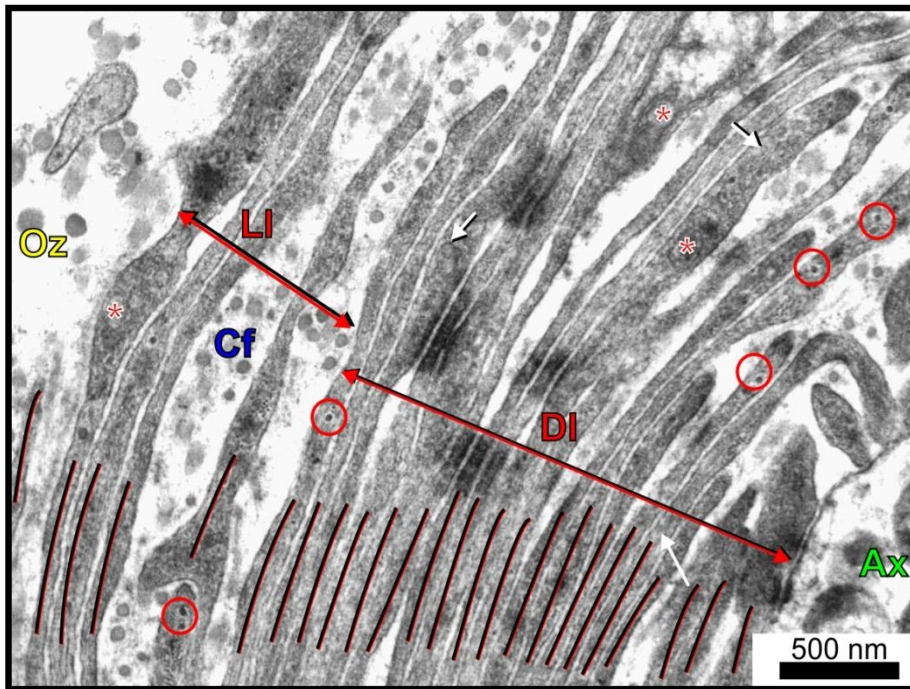


Figure 3.27. Cytoplasmic lamellae of the inner core in the ostrich. A total of 24 lamellae (red lines) form loosely arranged (LI) and densely packed lamellae (DI) closer to the axon (Ax). Mitochondria (red *), microtubules (red circles) and micro-pinocytotic vesicles (white arrows). Collagen microfibrils (Cf) mainly oriented with their long axis parallel to the long axis of the Herbst corpuscle occur between the looser lamellae. Outer zone (Oz).

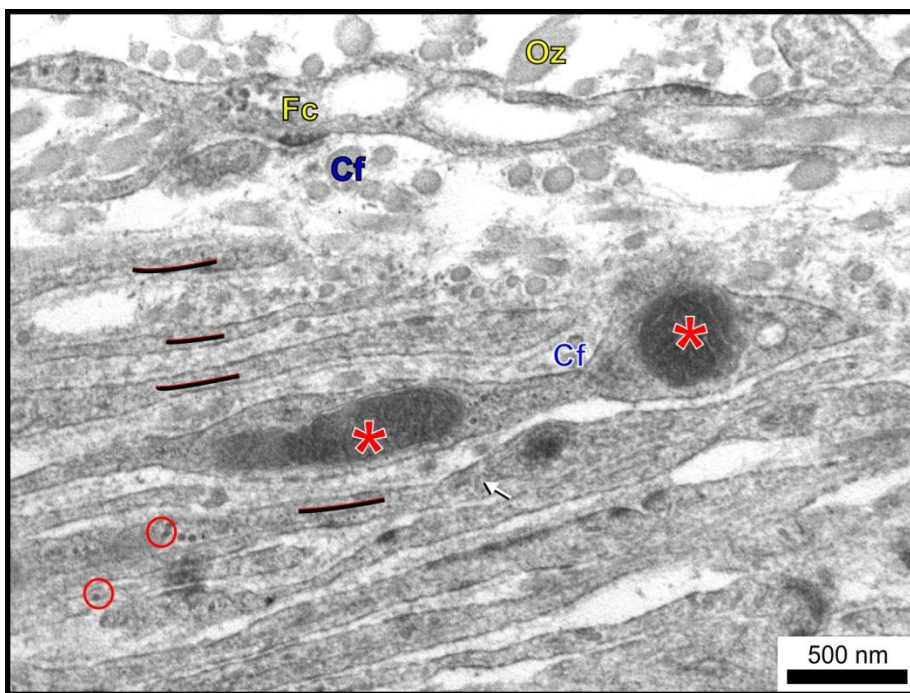


Figure 3.28. Cytoplasmic lamellae of the inner core in the emu. Cellular lamellae (black lines) are more loosely arranged nearer the outer zone (Oz). Intervening collagen fibrils (Cf) are not present between lamellae closer to the axon. Mitochondria (red *), fibroblast cytoplasmic process (Fc), microtubules (red circles) and micro-pinocytotic vesicle (white arrow).

3.3.3.2.4. Receptor axon

The receptor axon of the Herbst corpuscles displayed similar features in both species and typically contained many mitochondria, microtubules and neurofilament (Figs. 3.30 and 3.31). The axon could be morphologically divided into two components, namely the myelinated part (Figs. 3.29 and 3.30) and the non-myelinated part (Figs. 3.25-27 and

3.31). The non-myelinated part represented the greatest length of the axon within the corpuscle. The axon appeared slightly larger in diameter (across the shortest length in oval-shaped axons) in the ostrich $3.33 \pm 1.09 \mu\text{m}$ ($n=5$) than in the emu $2.60 \pm 0.71 \mu\text{m}$ ($n=5$). In both species the profile varied from round to oval; however, the myelinated portion always displayed a round profile.

The axon, as it entered the Herbst corpuscle, was surrounded by a myelin sheath (Figs. 3.14k, 3.29 and 3.30) which was soon replaced by the cytoplasmic lamellae of the inner core (see above) (Figs. 3.25-28 and 3.31). The myelinated axon displayed the typical features of peripheral myelinated nerves (see also Chapter 6), namely, a Schwann cell with a basal lamina displaying an outer collar of cytoplasm, an outer mesaxon, a myelin sheath, an inner mesaxon and an inner collar of cytoplasm surrounding the axon (Figs. 3.29 and 3.30). The axoplasm displayed numerous mitochondria, longitudinally arranged microtubules and neurofilaments (Fig. 3.31). Transducer sites (Fig. 3.31) were marked by slender axon processes projecting into the cellular lamellae of the inner core, in some instances invaginating them (Fig. 3.31). The axoplasm at the base of the processes was devoid of mitochondria and contained clear vesicles and neurofilaments (Fig. 3.31).

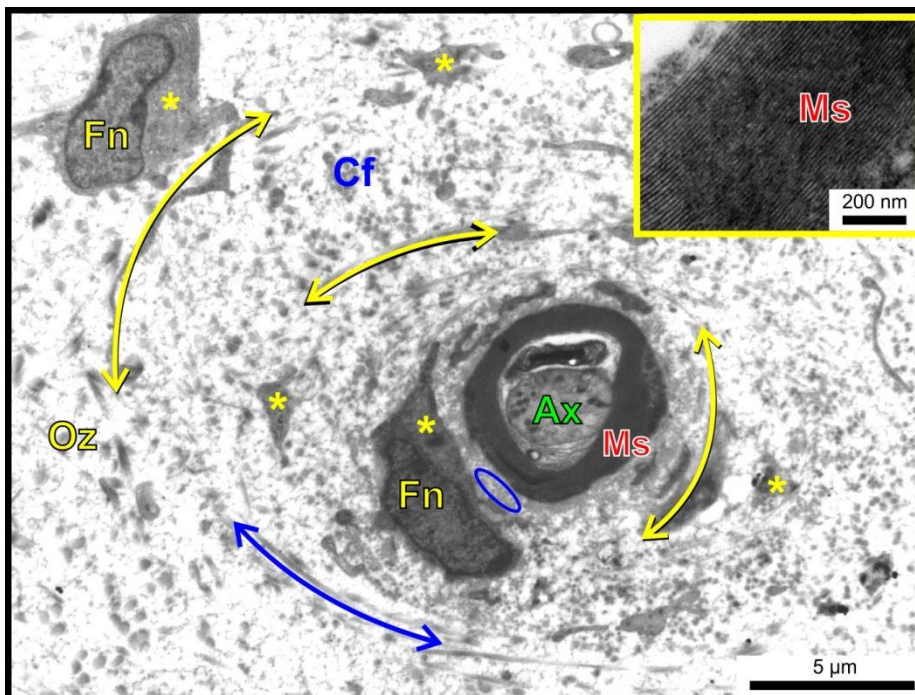


Figure 3.29. Myelinated axon (Ax) in the emu. The cytoplasmic lamellae (curved yellow arrows) and the collagen fibrils (Cf and blue curved arrow) of the outer zone (Oz) are concentrically arranged around the myelinated axon. A distinct endoneurium of tightly packed collagen fibrils (blue circle) is present. Fibroblast nucleus (Fn), fibroblast cytoplasm (*), myelin sheath (Ms).

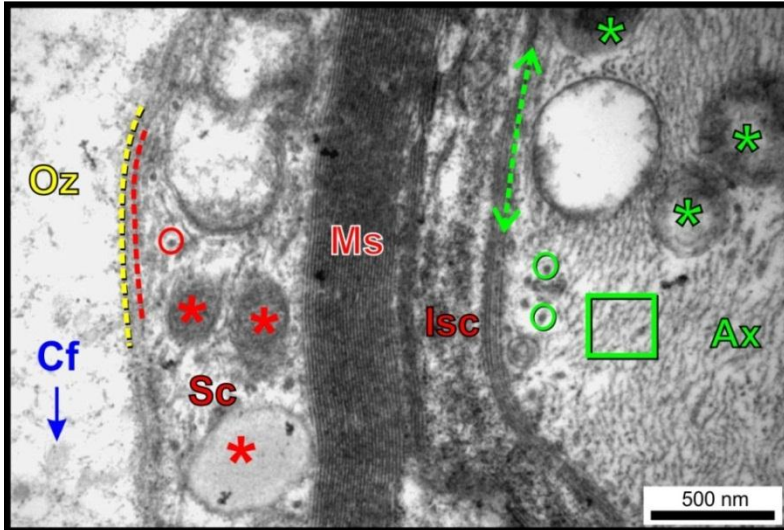


Figure 3.30. Myelinated axon in the ostrich. The Schwann cell cytoplasm (Sc) displays many mitochondria (red *) and microtubules (red circle) in the cytoplasm. A typical myelin sheath (Ms) surrounds the axon (Ax). The cell membrane (red dotted line) displays a clear basal lamina (yellow dotted line). The axon contains many neurofilaments (green square), microtubules (green circles) and mitochondria (green *). Axolemma (green dotted line), Inner Schwann cell collar (Isc), outer zone (Oz) and collagen fibril (Cf). Mitochondrial ultrastructure was not adequately preserved.

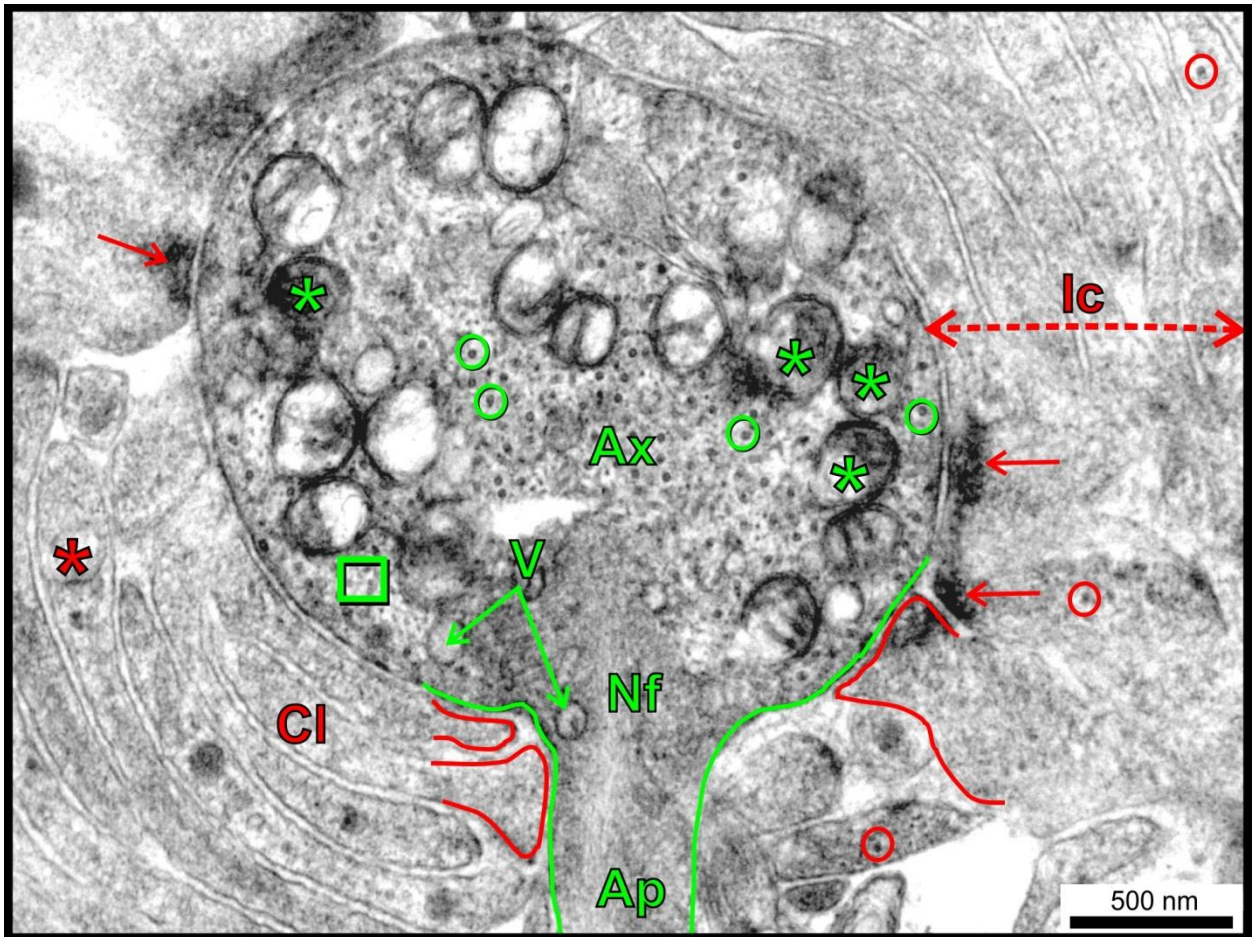


Figure 3.31. Transducer site of the receptor axon (Ax) in the emu. Note the finger-like axon process (Ap) emanating from the axon and the lack of mitochondria but presence of clear vesicles (V) and neurofilament (Nf) at the point of origin. Both the axon and the process are surrounded by cytoplasmic lamellae (Cl) of the inner core (Ic) which display hemi-desmosomes (red arrows). Some lamellae have been invaginated by the axon and the process (red lines). Mitochondria (green *), axolemma (green lines) microtubules (green circles) and microfilaments (green square) are the main features of the axon. Mitochondria (red star) and microtubules (red circles) in the cytoplasmic lamellae. Mitochondrial ultrastructure was not adequately preserved.

3.4. Discussion

3.4.1. Distribution of Herbst Corpuscles

3.4.1.1. Comparison between the ostrich and emu oropharynx

In the present study the total number of Herbst corpuscles in the oropharynx of both species could only be estimated. As noted by Gottschaldt and Lausmann (1974) an error results from examining serial sections as the same receptor can be counted several times. In the present study an error would occur by each corpuscle assuming an infinite length. Without an accurate estimate of the mean length of the corpuscles, a factor cannot be derived with which to divide the total number of Herbst corpuscles. As discussed below, there was a large variability in the shape and size of Herbst corpuscles throughout the oropharynx and obtaining a mean length for each region was not practical. It should also be noted that the median palatine and ventral ridges in the ostrich were treated as separate entities. As they occupied part of the mandibular rostrum, rostral oropharyngeal floor and rostral oropharyngeal roof, this may have skewed the data for these regions. However, the only part affected would have been the mandibular rostrum, which if counted as part of the rostrum would have made the corpuscle count in this region significantly higher in the ostrich than the emu.

This study represents the first report detailing the distribution of Herbst corpuscles throughout the entire avian oropharynx. Previous studies have noted the abundance of Herbst corpuscles in the oropharynx of the ostrich (Tivane, 2008) and emu (Crole, 2009); however, their specific distribution was not described. Other studies have noted the presence of Herbst corpuscles in limited regions of the oropharynx such as the median palatine ridge (Tivane *et al.*, 2006) and the oropharyngeal roof (Palmieri *et al.*, 2002; Guimarães *et al.*, 2007) of the ostrich and the tongue (Crole and Soley, 2009b) of the emu. In total, the ostrich displayed an even distribution of Herbst corpuscles between the oropharyngeal roof and floor, whereas two thirds of the Herbst corpuscles were present in the oropharyngeal roof and one third on the oropharyngeal floor of the emu. The present study revealed that the relative distribution of Herbst corpuscles was similar between both birds in respect of the mandible, caudal oropharyngeal floor and

caudal oropharyngeal roof, whereas the ostrich displayed a higher relative distribution of Herbst corpuscles on the rostral oropharyngeal floor, and the emu a higher relative distribution in the rostral oropharyngeal roof. These results indicate that the main contributing factor to the overall difference in relative distribution of Herbst corpuscles noted in the oropharyngeal roof and floor between the ostrich (50:50) and emu (68:32) is the significantly higher relative percentage of Herbst corpuscles present on the rostral oropharyngeal floor (including the median ventral ridge) in the ostrich. This would suggest that the rostral oropharyngeal floor is of a greater tactile importance in the ostrich than the emu, as detailed below. The apparent concentration of corpuscles at the rostral aspect of the oropharyngeal roof is supported by Palmieri *et al.* (2002) who noted that more Herbst corpuscles were present in the rostral portion of the palate (presumably the keratinised oropharyngeal roof) of the ostrich than the caudal parts. The greater rhea also displays more Herbst corpuscles in the rostral keratinised part than the caudal, non-keratinised, glandular part of the oropharyngeal roof (Feder, 1972). This would appear to be a general pattern in ratites.

Important differences were noted regarding the distribution of Herbst corpuscles in the tongue, laryngeal mound, choana and median palatine and ventral ridges in the ostrich and emu which appeared to be linked to the specific feeding method of these birds. The ostrich and emu only use the tongue during feeding to protect the glottis (Chapter 2; Crole and Soley, 2012c) and to scrape the oropharyngeal roof clear of food particles (Bonga Tomlinson, 2000). It is thus unusual that the emu tongue displays such a high relative percentage of Herbst corpuscles and the ostrich tongue none. Another peculiar point of difference between the ostrich and emu is the restricted presence of Herbst corpuscles to the arytenoid part of the laryngeal mound in the emu and only along the edge of the choana in the ostrich. Herbst corpuscles were absent from the pharyngeal folds of both species.

As noted above, the ratite tongue is used to scrape the oropharyngeal roof after swallowing (Bonga Tomlinson, 2000), which appears to be an essential process for removing any possible food items which may adhere to the region in and around the choana. The glottis of both these birds is large (Pycraft, 1900; Crole and Soley, 2012c) and any food items not removed from the vicinity of the choana could be inhaled directly into the large glottis and eventually result in an inhalation pneumonia. The tongue and

laryngeal mound of the emu (Crole and Soley, 2010, 2012c), ostrich (Crole and Soley, 2012c) and greater rhea (Crole and Soley, 2012b) all display their own unique adaptations for engaging with, and cleaning the choana, which would occur while the linguo-laryngeal apparatus (Crole and Soley, 2012c; Chapter 2) is functionally in place. It has been proposed that the tongue in the greater rhea is able to be manipulated in such a manner during its retraction as to allow the two caudal lingual papillae to scrape out the heart-shaped choana (Crole and Soley, 2012b). Likewise, in the emu the centrally positioned tongue root and the small protuberances of the arytenoid part of the laryngeal mound would clean out the central groove in the choana and the infundibular cleft, and the lingual papillae of the tongue body would clean the internal nares (Crole and Soley, 2010). Additionally, in the ostrich, it would appear that the internal nares would be cleaned by the caudal laryngeal projections (personal observation). The proposed contribution of different structures in cleaning the choana in the ostrich and emu is supported by the distribution of Herbst corpuscles. In the emu, the tongue body and arytenoid part of the laryngeal mound contain Herbst corpuscles; this would provide the tactile acuity for the emu to 'feel' whether the relevant structures were correctly positioned to scrape the choana clean. In contrast, in the ostrich, which has no corpuscles in the tongue, the Herbst corpuscles were present at the edge of the choana, but again, affording the tactile acuity to 'feel' if the choana had been cleaned. It is noteworthy that Herbst corpuscles in the tongue of the mallard, although sparse, appear to be associated with the parts of the tongue involved in feeding and straining food (Berkhoudt, 1980). The mallard actively uses its tongue during feeding by assisting in straining and by transporting food (Zweers *et al.*, 1977). In the greater rhea it would be of interest to note the specific concentration of Herbst corpuscles in respect of the tongue and choana to determine whether they are appropriately located to assist in proprioception during cleaning of the choana. Although Feder (1972) did not find Herbst corpuscles in the greater rhea tongue, the author admitted that their presence could not be excluded. In light of the above information, if present, they would most likely be situated in the vicinity of the caudal lingual papillae.

3.4.1.2. Comparison to the oropharynx of other birds

The distribution of Herbst corpuscles in ratites appears to differ significantly from the situation in other birds, such as the chicken, where they are absent from the soft palate

(caudal oropharyngeal roof), tongue and floor of the oropharynx (Winkelmann and Myers, 1961). It is difficult to draw overall comparisons between the ostrich and emu to other birds, as only portions of the oropharynx have been documented in other species, such as the rostral portion of the bill (see Chapter 7), the beak and/or tongue (Leitner and Roumy, 1974; Toyoshima *et al.*, 1992), the beak and/or bill skin (Malinovský and Zemánek, 1969; Wight *et al.*, 1970; Halata and Grim, 1993) or the oropharyngeal roof rostral to the choana (Ziswiler and Trnka, 1972). However, the distribution of Herbst corpuscles (and Grandry corpuscles) was determined in the oropharynx and bill of the mallard (Berkhoudt, 1980), although the pharyngeal folds were not included in this study. When added together, the number of Herbst corpuscles in the oropharyngeal roof was similar to that of the oropharyngeal floor in this species (Berkhoudt, 1980) as in the ostrich (see above). In common with the emu, the mallard displayed Herbst corpuscles in the tongue (Berkhoudt, 1980) and is discussed above.

In the chicken (Wight *et al.*, 1970) and mallard (Berkhoudt, 1980), the intra-oral surfaces of the upper bill only contained Herbst corpuscles in the soft tissue supported by bone. The distribution of corpuscles also appeared to follow the presence of underlying bony structures of the oropharyngeal roof in buntings, the pigeon, finches and swift (Ziswiler and Trnka, 1972) as well as a number of other bird species (Schildmacher, 1931). The close association of the Herbst corpuscles with the premaxilla indicates that the presence of hard bone may increase the sensitivity of the Herbst corpuscles to vibrations (Wight *et al.*, 1970). This contrasts sharply to the situation in the ostrich and emu where Herbst corpuscles, in addition to those overlying bone, were also abundant in regions of the oropharynx unsupported by bone, indicating that either the Herbst corpuscles are more sensitive than those of the chicken and mallard, or that the tissue unsupported by bone is firm enough to transmit vibrations sufficiently.

3.4.1.3. Orientation of Herbst corpuscles

Most of the Herbst corpuscles observed in the present study were oriented with their long axis positioned rostro-caudally, which appears to be similar to that noted in the greater rhea (Feder, 1972). This preferential orientation was also noted in the beak skin of a number of bird species (Schildmacher, 1931) including the goose (Gottschaldt and Lausmann, 1974). Although no explanation was offered for this preferential

arrangement in the goose, it can only be assumed that it relates to the function of these receptors. Herbst corpuscles are optimally stimulated by vibrations which are received perpendicular to the surface (Berkhoudt, 1980). Interpreted in this manner, the Herbst corpuscles in the oropharynx of the ostrich and emu would be optimally stimulated by objects moving across the surface of the oropharynx, causing vibrations perpendicular to the rostro-caudal plane, and not during the action of pecking which would transmit vibrations parallel to the long axis of the corpuscles. The orientation of the Herbst corpuscles thus seems appropriate to avoid signals generated during the forceful act of pecking, which would provide little useful tactile information. Preferential orientations of Herbst corpuscles were also noted in the wing of the pigeon, with the long axis placed either parallel or perpendicular to the feather follicle (Hörster, 1990). The preferential orientation of Herbst corpuscles would seem to indicate a directional sensitivity for these structures (Hörster, 1990), similar to that suggested above for the ostrich and emu oropharynx. The shape of the axon also plays a role in determining the direction of the impulse and is discussed below.

3.4.1.4. Arrangement / grouping of Herbst corpuscles

It was noted in the present study that Herbst corpuscles in the oropharynx were arranged in three ways. These groupings can be placed in two broad categories; those associated with receiving tactile information (groups of corpuscles associated/not associated with a nerve as seen in arrangements 1 and 2) and those which receive stimuli from associated structures such as the mucous glands (arrangement 3). The first two arrangements have been reported in the oropharyngeal roof of the ostrich (Palmieri *et al.*, 2002) as well as in other birds where they have been described in the beak skin of the quail (Halata and Grim, 1993), in the wing of the pigeon (Hörster, 1990) and in the beak and hard palate of the chicken (Wight *et al.*, 1970) and finches (Genbrugge *et al.*, 2012). The Herbst corpuscles involved in the 1st arrangement were densely packed and would function in detecting vibrational stimuli and afford a high tactile acuity; their role in receiving tactile information as part of the bill tip organ is discussed in Chapter 7. The corpuscles in the 2nd arrangement would act similarly to those above; however, the tactile acuity would depend on the density of the corpuscles (whether the corpuscles are arranged singly or in groups). Therefore, other than the bill tips (arrangement 1) (see Chapter 7), specific regions of tactile acuity would be present in the median palatine and

ventral ridges in the ostrich (arrangement 1), the rictus (arrangement 2) of both species and the edges of the choana (arrangement 2) in the ostrich.

There have been many reports of Herbst corpuscles being associated with specific structures, such as feather follicles (Weir and Lunam, 2004), smooth muscle (Cobb and Bennett, 1970), the articular capsule (Halata and Munger, 1980), the crus (Zelená *et al.*, 1997) and the bill tip organ (Bolze, 1968; Gentle and Breward, 1986; Berkhoudt, 1976; see also Chapter 7). However, the association between Herbst corpuscles and glands has received little mention in the literature and has only been documented in the lacrimal gland of the chicken (Dimitrov, 2003), the salivary glands of the mallard (although sparse) (Berkhoudt, 1980) and in glands in the tongue of the emu (Crole and Soley, 2009b) and caudal oropharyngeal roof of the ostrich (Palmieri *et al.*, 2002; Guimarães *et al.*, 2007; Tivane, 2008). It is not clear what signals the Pacinian corpuscles in the deep viscera of mammals detect; however, they may respond to pulsations of blood pressure (Hunt, 1974). The presence of Herbst corpuscles along blood vessels further suggests that these mechanoreceptors do not necessarily always serve a tactile function (Gottschaldt, 1985). Although the Herbst corpuscles associated with glands would conceivably also function in detecting tactile stimuli, their primary function may be to provide feedback on the status of the mucous salivary glands. The relationship between location and the structure and function of Herbst corpuscles has been emphasised by Gottschaldt and Lausmann (1974) who note the knowledge of the distribution of Herbst corpuscles is necessary for the interpretation and understanding of the electrophysiology and ultrastructure of these mechanoreceptors. Future functional studies will determine whether the Herbst corpuscles associated with glands serve a different function to the other Herbst corpuscles present in the oropharynx.

3.4.1.5. Functional implications during feeding

A concentration of Herbst corpuscles in the median palatine ridge (MPR) (Palmieri *et al.*, 2002; Tivane *et al.*, 2006; Tivane, 2008) and median ventral ridge (MVR) (Tivane, 2008) has previously been reported in the ostrich. The emu also displays a less prominent MPR (Crole and Soley, 2010), and although Herbst corpuscles were present, they did not reveal a particular concentration or pattern. Additionally, the emu does not possess a corresponding MVR. A median palatine ridge has also been reported in the

mallard (Berkhoudt, 1980) and concentrations of Herbst corpuscles have been identified at locations in the oropharynx important during the discrimination and transport of food (Zweers *et al.*, 1977; Berkhoudt, 1980), including the above ridge. It is clear that the ostrich must use these structures in a manner relating to the discrimination and positioning of food items, a hypothesis also forwarded by Palmieri *et al.* (2002). The feeding method of catch-and-throw (Gussekkloo and Bout, 2005) or cranio-inertial feeding (Bonga Tomlinson, 2000) in ratites involves only the bill tip initially holding the food. The bill tips are then opened, and the head is accelerated over the food causing the item to land in the proximal esophagus. The mandibular rostrum is larger in the emu than in the ostrich (see also Chapters 4 and 5) and is richly supplied with Herbst corpuscles. In the emu the food is most likely discriminated, held, and positioned adequately between the mandibular and maxillary rostra. In the ostrich, however, the small size of the mandibular rostrum may exclude the above actions for large food items. The presence of two ridges, richly supplied with Herbst corpuscles and which extend along the intra-oral surface of the maxillary and mandibular rostra and beyond, would implicate the involvement of these structures in the discrimination and positioning of food items before they are accelerated through the oropharynx. Thus in the ostrich, the regions caudal to the bill tip (Regions C, D, E and M in Fig. 3.1) may also be indirectly involved in feeding. The positioning and potential function of these corpuscle-rich median palatine and median ventral ridges in the ostrich defines them as important sensory organs; the palatal and interramal organs, respectively.

3.4.2. Structure

3.4.2.1. Light microscopy

The intra-oral Herbst corpuscles assumed a variety of shapes in both the ostrich and emu, although the round to elliptical form was the most prominent. Unusually shaped Herbst corpuscles have previously been noted (Malinovský, 1996) including observations in other regions in the ostrich such as the copulatory organ (Palmieri *et al.*, 2006). Halata and Grim (1993) identified some ultrastructural differences between small and large Herbst corpuscles found in the beak of the Japanese quail and hypothesized that this reflected functional differences. Although different sized corpuscles were observed with light and electron microscopy in the present study, they were not

differentiated between and future studies will be necessary to determine whether variably sized Herbst corpuscles demonstrate subtle structural differences that may translate into functional specialisation.

Despite a number of reports on the occurrence of both Herbst and Grandry corpuscles in the bill skin of geese (Gottschaldt and Lausmann, 1974) and ducks (Saxod, 1968; Berkhoudt, 1980; Watanabe *et al.*, 1985), only Herbst corpuscles were identified in the bill skin (*Rhamphotheca*) and oropharynx of the ostrich and emu, thus leading to the conclusion that Grandry corpuscles do not occur in this specific location in the ratites studied. Although Grandry corpuscle-like structures were identified in the kiwi, and termed terminal cell receptors (Cunningham *et al.*, 2007), these structures appeared similar to the myelinated afferent nerve fibres observed in the ostrich and emu and which were associated with clusters of Herbst corpuscles (arrangement 1) (see Chapter 7).

3.4.2.2. Ultrastructure

Although Herbst corpuscles in the ostrich and emu display the same basic structure to that described in avian Herbst corpuscles in general (the capsule, outer zone, inner core and axon; see Berkhoudt (1980) for a summary of the earlier literature) there appear to be some differences in the organisation of these components. As Herbst corpuscles display such varied shapes, sizes and locations, and have been well-described in birds (see Berkhoudt, 1980; Gottschaldt, 1985), an attempt will be made to limit the comparison to those corpuscles found in comparable regions in other birds.

3.4.2.2.1. Capsule

Herbst corpuscles are less bulky than Pacinian corpuscles, although the capsule is better developed, being two to three times thicker and more rigid than that of Pacinian corpuscles (Quilliam and Armstrong, 1963). The structure of the avian Herbst corpuscle capsule has received little attention and the most in-depth description is that of Halata (1971) in the Canada goose (*Branta canadensis*) and mute swan (*Cygnus olor*). The capsule of Herbst corpuscles is composed of alternating cytoplasmic cellular lamellae and acellular lamellae (collagen fibrils) (Quilliam and Armstrong, 1963). The collagen

fibrils mechanically strengthen the capsule and form a network between which the slender cellular lamellae are found (Halata, 1971). This arrangement was noted in the Canada goose and mute swan (Halata, 1971) as well as in the ostrich and emu (present study). Halata (1971) further notes that the cellular lamellae formed by fibroblasts within the collagen fibril network increases the sensitivity of the Herbst corpuscles to vibratory signals. More weakly developed capsules, which consist of acellular lamellae only, have also been reported in the skin of pigeons and domestic fowl (Malinovský and Páč, 1978) and were found sparingly in the emu; however, their presence in the ostrich was not confirmed. The cytoplasm of the cellular lamellae in both ratites, as well as their basic structure, was similar to that described in the Canada goose, mute swan (Halata, 1971), duck (Watanabe *et al.*, 1985) and Japanese quail (Halata and Grim, 1993). In the former two species fibroblasts were presumed to form the cellular lamellae and the presence of many micro-pinocytotic vesicles was taken as an indication of the cell's high level of activity (Halata, 1971). Additionally, in the ostrich and emu, myofilaments, a discontinuous basal lamina, marginal densities and presumptive glycogen granules in the cytoplasm of the cellular lamellae were indicative of myoid properties, thus making these cells myofibroblasts. This is in sharp contrast to the fibroblasts or fibroblast-like cells reported in the capsule of the chicken (Wight *et al.*, 1970) and other birds (Halata, 1971; Watanabe *et al.*, 1985; Halata and Grim, 1993). Filaments and microtubules have been identified in the fibroblasts of the capsule in the duck but a basal lamina was absent (Watanabe *et al.*, 1985); however, the authors did not elaborate on these findings. The observation of components such as filaments (Watanabe *et al.*, 1985) and basal lamina-like material (Halata, 1971; Halata and Grim, 1993) associated with the cellular component of the capsule of other birds may suggest the more widespread occurrence of contractile elements in the avian Herbst corpuscle capsule.

Sensory cilia, which were present in the capsule of the ostrich, were not found in the emu, although the presence of these structures could not be excluded. The capsule in the chicken reacted faintly with elastic tissue stains (Winkelmann and Myers, 1961) and in conjunction with a thicker capsule (in comparison to Pacinian corpuscles), which exhibits both strengthening and contractile properties (present study), it would seem that the capsule of the Herbst corpuscle in the ostrich and emu may be able to alter the frequency to which the corpuscle responds by tightening (response to higher frequencies) or relaxing (response to lower frequencies) the capsule. This proposed

property of the ratite Herbst corpuscle capsule may compensate for the less organised outer zone reportedly present in the ostrich and emu compared to other birds (see below), and which itself is less organised than in the Pacinian corpuscle. The manner in which the myofibroblasts in the capsule are signalled to vary the tension of the capsule may be related to the presence of sensory cilia in the myofibroblasts in the capsule bordering the outer zone and the fibroblasts located in the outer zone (see below) of the Herbst corpuscle. Sensory cilia in the mammalian kidney have been shown to function in sensory transduction, where the cilium may be bent by the flow of fluid (see Pazour and Witman, 2003). It has also been proposed that sensory cilia possess chemical receptors (Pazour and Witman, 2003); however, in a specialised mechanoreceptor such as the Herbst corpuscle, sensory cilia would more likely react to mechanical signals than to chemical signals. If the sensory cilia in the ratite Herbst corpuscle do react to mechanical displacements, they may regulate and coordinate the contraction of the myofibroblasts, thus controlling the tensioning of the capsule for optimum signal enhancement and transduction. Herbst corpuscles from the wing skin of 3-13 day-old emu chicks display axons which are immunoreactive to calcitonin gene-related peptide or neuropeptide Y (Weir and Lunam, 2006). In contrast calbindin D-28k immunoreactivity is found in the Herbst corpuscle axons of many volant birds (see Weir and Lunam, 2006) suggesting that Herbst corpuscles of volant birds display a different chemical content to that of non-volant birds (Weir and Lunam, 2006). This difference in chemical composition of a ratite Herbst corpuscle (Weir and Lunam, 2006), linked with the subtle ultrastructural differences noted between the ostrich and emu and volant birds (see elsewhere in the discussion), strengthens the possibility that the Herbst corpuscles of palaeognaths and neognaths are perhaps functionally different. These observations will need further investigation and may open up a new field of study into the functional response of these mechanoreceptors.

3.4.2.2.2. Outer zone

The outer zone is reportedly an enlargement of the endoneural space (Halata, 1971; Gottschaldt, 1985) and is characterised by a content of collagen microfibrils and sparse fibrocytes, a feature also apparent in the ostrich and emu. Halata (1971) refers to the outer zone as the subcapsular space and states that it is functionally part of the capsule. The collagen microfibre system forms incomplete lamellae (Quilliam and

Armstrong, 1963; Halata, 1971; Berkhoudt, 1980) which exists in the form of a two-dimensional coiled network of fibres emanating from flattened fibrocytes (Gottschaldt, 1985). This particular arrangement was not confirmed in the present study, and the elements of this zone were not as regular and concentrically arranged as in domestic poultry (Saxod, 1968; Cobb and Bennett, 1970; Wight *et al.*, 1970; Halata and Munger, 1980; Gottschaldt *et al.*, 1982; Gottschaldt, 1985; Watanabe *et al.*, 1985; Zelená *et al.*, 1997) and other birds (Schildmacher, 1931; Halata, 1971; Ziswiler and Trnka, 1972; Halata and Grim, 1993; Genbrugge *et al.*, 2012). In general, the outer zone of the Herbst corpuscle is less highly organised than that of the Pacinian corpuscle (Quilliam and Armstrong, 1963; Halata, 1971) and has been graphically demonstrated in comparative SEM illustrations of a transverse-fractured Herbst corpuscle in the duck and Pacinian corpuscle in the cat (Malinovský, 1996). The more regular organisation of the outer zone in the Pacinian corpuscle is clearly demonstrated in these images. In the ostrich and emu the outer zone was much larger in proportion to the inner core and axon in the majority of the Herbst corpuscles. This differs from the Herbst corpuscles depicted in the bill tip organ in the kiwi (Cunningham *et al.*, 2007) and in other birds (Bolze, 1968; Cobb and Bennett, 1970; Watanabe *et al.*, 1985; Toyoshima *et al.*, 1992; Halata and Grim, 1993) where the outer zone is relatively narrow and the inner core forms a considerable component of the corpuscle. This feature of a larger outer zone and smaller inner core was also briefly noted by Guimarães *et al.* (2007) when comparing the Herbst corpuscles in the ostrich palate to those in the chicken. As in the capsule of the ostrich, a fibroblast displaying a sensory cilium was identified in the outer zone, a phenomenon not previously reported in avian Herbst corpuscles. Although similar structures have not been noted in fibroblasts of the emu corpuscle, their presence cannot be excluded. The relative scarcity of cells displaying single cilia in both the ostrich and emu can be ascribed to the limited chance of sectioning the region of the cell from where the cilium emerges. Sensory cilia of the fibroblasts in the Herbst corpuscle outer zone may be a unique feature to ratites.

3.4.2.2.3. Inner core

The inner core in birds is formed by 8-30 pairs of Schwann cells (Gottschaldt, 1985), and 30-40 in the greater rhea (Feder, 1972), but were not counted in the in the present study in ostrich and emu due to the scarcity of appropriate longitudinal sections. The

bilateral, symmetrical rows of Schwann cell nuclei are another feature which distinguishes Herbst corpuscles from Pacinian corpuscles (Quilliam and Armstrong, 1963). There is reportedly great variation between Herbst corpuscles of different species and from different regions regarding the number, thickness and distance between the lamellae of the inner core (Gottschaldt, 1985). However, the structure of the inner core in the ostrich and emu was generally similar to that collectively described in other birds (Andersen and Nafstad, 1968; Halata, 1971; Gottschaldt, 1985; Watanabe *et al.*, 1985; Halata and Grim, 1993). The non-myelinated nerve fibres present in the outer zone and inner core of the chicken Herbst corpuscle (Anderson and Nafstad, 1969; Nafstad and Anderson, 1970) were not confirmed in the ostrich or emu with either IHC labelling for neurofilament protein or by TEM. These intra-corporal non-myelinated nerve fibres were also not present in the goose (Gottschaldt *et al.*, 1982). Why these fibres would appear in one species and not in others remains unexplained. The inner core appeared more cellular and relatively larger in the ostrich and emu chicks than in the adults (present study). This observation is explained by the fact that the inner core grows in length as the bird matures and results in the lamellar system wrapping more tightly around the axon with a concomitant decrease in diameter (Gottschaldt, 1985).

3.4.2.2.4. Receptor axon

The axon of the Herbst corpuscle displays three parts, the initial myelinated part (not surrounded by an inner core), the non-myelinated part, and the dilated, terminal end-bulb (also non-myelinated) (both surrounded by the inner core) (Andersen and Nafstad, 1968; Saxod, 1968; Halata, 1971; Halata and Munger, 1980; Gottschaldt, 1985; Toyoshima *et al.*, 1992; Halata and Grim, 1993). This was the typical pattern observed in both the ostrich and emu. The ostrich displayed a higher frequency of corpuscles with double axons. This could either be a result of axonal branching or a 180 degree bending of the axon, both of which have been demonstrated in the ostrich (Palmieri *et al.*, 2002, 2006). Double or multiple axons are not common but have been reported in other birds (Winkelmann and Myers, 1961; Wight *et al.*, 1970; Ziswiler and Trnka, 1972; Halata and Munger, 1980; Gottschaldt, 1985). Although the axon in the ostrich and emu sometimes appeared more round in transverse section (also described in the small Herbst corpuscles in the beak of the Japanese quail (Halata and Grim, 1993)) oval shaped

axons were also observed as described in other birds (Andersen and Nafstad, 1968; Halata, 1971; Gottschaldt *et al.*, 1982; Gottschaldt, 1985, Halata and Grim, 1993). In Pacinian corpuscles the oval shape of the axon reflects the ability of the corpuscle to detect direction (Ilyinsky *et al.*, 1976). Depolarization occurs with an increase in surface membrane area (deformed along the shorter axis) and hyperpolarization occurs with a decrease in surface membrane area (deformed along the longer axis) (Ilyinsky *et al.*, 1976). Thus the Herbst corpuscles in the ostrich and emu with round axons are most likely not direction sensitive. This seems plausible in light of the fact that the majority of the Herbst corpuscles in the oropharynx are situated in a very thin layer of dense, irregular connective tissue and can only be stimulated from a dorso-ventral plane (between the upper and lower bills), negating the need for a directional sensitivity. However, Herbst corpuscles present in the median palatine and ventral ridges, which project into the oropharynx, would be able to detect vibrations from a variety of directions and may display oval-shaped axons. The non-myelinated axons in the present study displayed the same basic ultrastructural features and attachments to the inner lamellae of the inner core as noted in other birds (Halata, 1971; Chouchkov, 1973; Halata and Munger, 1980; Gottschaldt, 1985; Watanabe *et al.*, 1985; Halata and Grim, 1993). However, the smooth endoplasmic reticulum described in the duck (Watanabe *et al.*, 1985) was not observed in the ostrich and emu. The terminal end-bulb of the axon was not demonstrated in the present study in the ostrich and emu; however, it is likely that it is present. More careful orientation of the blocks for TEM to ensure longitudinal sections through the axon will be required to establish the presence of the end-bulb. The transducer sites in the ostrich and emu displayed attachment to the inner core lamellae via hemi-desmosomes junctions, but no synapses as described by Saxod (1968) and Halata (1971) were found. This may simply reflect differences in the preparation of material for electron microscopy. The highest frequency of transducer sites is present in the terminal end-bulb (Gottschaldt, 1985) indicating that this part of the axon is the most 'reactive' to vibrational stimuli.

3.4.2.2.5. Morpho-functional properties

The specific structure of Herbst corpuscles determines the response properties displayed by these receptors and the discussion that follows is summarised from Gottschaldt (1985). The outer zone and inner core (auxiliary structures) attenuate the

velocity and amplitude of mechanical stimuli. However, higher frequencies are transmitted more easily through the auxiliary structures. The mucous fluid in the outer zone and between the inner core lamellae may play a role in the particular mechanical filtering characteristics of the auxiliary structures. A receptor potential is generated when the axon processes become deflected by displacements of the inner core lamellae. The deflection of the axon process is facilitated by fixing of the base, by desmosome-like attachments, to the inner core lamellae, while the inherent elasticity of the microfilaments return the axon process to its original position when the deformation of the inner core lamellae ceases. The structure of the Herbst corpuscles in the ostrich and emu supports the functioning of the corpuscles as described above (present study). However, the physical effect of a contractile capsule on the response properties of Herbst corpuscles in these two species remains to be determined.

3.5. References

- Andersen, A.E. and Nafstad, P.H.J. 1968. An electron microscopic investigation of the sensory organs in the hard palate region of the hen (*Gallus domesticus*). *Zeitschrift für Zellforschung und Mikroskopische Anatomie*. **91**: 391-401.
- Bancroft, J.D. and Gamble, M. 2002. *Theory and Practice of Histological Techniques. Fifth edition*. China: Churchill Livingstone Elsevier.
- Berkhoudt, H. 1976. The epidermal structure of the bill tip organ in ducks. *Netherlands Journal of Zoology*. **26**: 561-566.
- Berkhoudt, H. 1980. The morphology and distribution of cutaneous mechanoreceptors (Herbst and Grandry corpuscles) in bill and tongue of the mallard (*Anas platyrhynchos* L.). *Netherlands Journal of Zoology*. **30**: 1-34.
- Bock, W.J. and Morony, I. 1978. The preglossale of Passer (Aves: Passeriformes). A skeletal neomorph. *Journal of Morphology*. **155**: 99-109.
- Bolze, G. 1968. Anordnung und Bau der Herbstchen Körperchen in Limicolenschnäbeln im Zusammenhang mit der Nahrungsfindung. *Zoologischer Anzeiger*. **181**: 313-355.

- Bo Minelli, L., Botti, M., Antonio Dessole, A., Palmieri, G. and Acone, F. 2006. The autonomic and sensitive innervation of the ostrich copulatory organ. *Annali della Facoltà di Medicina Veterinaria di Parma*. **26**: 67-78.
- Bonga Tomlinson, C.A. 2000. *Feeding in Paleognathous Birds*. In: Feeding: Form, Function, and Evolution in Tetrapod Vertebrates. Edited by K. Schwenk. San Diego: Academic Press. pp. 359-394.
- Chouchkov, C. 1973. On the ultrastructure of the Herbst corpuscles in the bill skin of the Pekin duck. *Comptes Rendus de Academie Bulgare des Sciences*. **26**:1705–1708.
- Cobb, J.L.S. and Bennett, T. 1970. Herbst corpuscles in the smooth muscles in the wings of chicks. *Experientia* **26**: 768–769.
- Crole, M.R. 2009. A gross anatomical and histological study of the oropharynx and proximal oesophagus of the emu (*Dromaius novaehollandiae*). MSc dissertation, University of Pretoria, South Africa.
- Crole, M.R. and Soley, J.T. 2009a. Comparative distribution of Herbst corpuscles within the oropharyngeal cavity of the ostrich (*Struthio camelus*) and emu (*Dromaius novaehollandiae*). *17th Congress of the International Federation of Associations of Anatomists*, Cape Town, South Africa. p. 361.
- Crole, M.R. and Soley, J.T. 2009b. Morphology of the tongue of the emu (*Dromaius novaehollandiae*). II. Histological features. *Onderstepoort Journal of Veterinary Research*. **76**: 347-361.
- Crole, M.R. and Soley, J.T. 2010. Gross morphology of the intra-oral *rhamphotheca*, oropharynx and proximal esophagus of the emu (*Dromaius novaehollandiae*). *Anatomia Histologia Embryologia*. **39**: 207-218.
- Crole, M.R. and Soley, J.T. 2011. Gland distribution and structure in the oropharynx and proximal oesophagus of the emu (*Dromaius novaehollandiae*). *Acta Zoologica* (Stockholm). **92**: 206-215.
- Crole, M.R. and Soley, J.T. 2012a. Evidence of a true pharyngeal tonsil in birds: A novel lymphoid organ in *Dromaius novaehollandiae* and *Struthio camelus* (Palaeognathae). *Frontiers in Zoology*. **9**: 21.
- Crole, M.R. and Soley, J.T. 2012b. Gross anatomical features of the tongue, lingual skeleton and laryngeal mound of *Rhea americana* (Palaeognathae, Aves): morpho-functional considerations. *Zoomorphology*. **131**: 265-273.
- Crole, M.R. and Soley, J.T. 2012c. What prevents *Struthio camelus* and *Dromaius novaehollandiae* (Palaeognathae) from choking? A novel anatomical mechanism in ratites, the linguo-laryngeal apparatus. *Frontiers in Zoology*. **9**: 11.

Crole, M.R., Soley, J.T. and du Plessis, L. 2009. The ultrastructure of Herbst corpuscles in the oropharynx of the emu (*Dromaius novaehollandiae*) and ostrich (*Struthio camelus*). *Proceedings of the Microscopy Society of Southern Africa*. **39**: 27.

Cunningham, S., Castro, I. and Alley, M. 2007. A new prey-detection mechanism for kiwi (*Apteryx* spp.) suggests convergent evolution between paleognathous and neognathous birds. *Journal of Anatomy*. **211**: 493-502.

Dimitrov, D. 2003. Encapsulated nerve endings in the lachrymal glands of broiler chickens – A light microscopy study. *Trakia Journal of Sciences*. **1**: 38-41.

Evans, H.E. and Martin, G.R. 1993. *Organa Sensuum [Organa Sensoria]*. In: Handbook of Avian Anatomy: Nomina Anatomica Avium, 2nd edition. Edited by Baumel, J.J., King, A.S., Breazile, J.E., Evans, H.E. and Vanden Berge, C. Cambridge, Massachusetts: The Nuttall Ornithological Club, No. 23. pp. 585-611.

Feder, F.-H. 1972. Zur mikroskopischen Anatomie des Verdauungsapparates beim Nandu (*Rhea americana*). *Anatomischer Anzeiger*. **132**: 250-265.

Genbrugge, A., Adriaens, D., De Kegel, B., Brabant, L., Van Hoorebeke, L., Podos, J., Dirckx, J., Aerts, P and Herrel, A. 2012. Structural tissue organization in the beak of Java and Darwin's finches. *Journal of Anatomy*. **221**: 383-393.

Gentle, M.J. and Breward, J. 1986. The bill tip organ of the chicken (*Gallus gallus* var. *domesticus*). *Journal of Anatomy*. **145**: 79-85.

Gottschaldt, K.-M. 1974. *Mechanoreceptors in the Beaks of Birds*. In: Mechanoreception. Edited by Schwartzkopf, J. Germany: Düsseldorf: Westdeutscher Verlag. pp. 109–113.

Gottschaldt, K.-M. 1985. *Structure and Function of Avian Somatosensory Receptors*. In: Form and function in birds. Vol. 3. Edited by King, A.S. and McLelland, J. London: Academic Press. pp. 375-462.

Gottschaldt, K.-M. and Lausmann, S. 1974. The peripheral morphological basis of tactile sensitivity in the beak of geese. *Cell and Tissue Research*. **153**: 477-496.

Gottschaldt, K.-M., Fruhstorfer, H., Schmidt, W. and Kräft, I. 1982. Thermosensitivity and its possible fine-structural basis in mechanoreceptors in the beak skin of geese. *Journal of Comparative Neurology*. **205**: 219-245.

- Guimarães, J.P., Mari, R.B., Miglino, M.A., Hernandez-Blasquez, F.J. and Watanabe, I. 2007. Mecanorreceptores da mucosa palatine de avestruz (*Struthio camelus*): estudo ao microscópio luz. *Pesquisa Veterinária Brasileira*. **27**: 491-494.
- Gussekkloo, S.W.S. and Bout, R.G. 2005. The kinematics of feeding and drinking in palaeognathous birds in relation to cranial morphology. *The Journal of Experimental Biology*. **208**: 3395–3407.
- Halata, Z. 1971. Die Ultrastruktur der Lamellenkörperchen bei Wasservögeln (Herbstsche Endigungen). *Acta Anatomica*. **80**: 362-376.
- Halata, Z. and Munger, B.L. 1980. The ultrastructure of Ruffini and Herbst corpuscles in the articular capsule of domestic pigeon. *The Anatomical Record*. **198**: 681-692.
- Halata, Z. and Grim, M. 1993. Sensory nerve endings in the beak skin of Japanese quail. *Anatomy and Embryology*. **187**: 131-138.
- Herbst, G. 1848. *Die Pacinischen Körper und ihre Bedeutung. Ein Beitrag zur Kenntnis der Nervenprimitivfasern*. Göttingen: Vandenhoeck & Ruprecht.
- Hodges, R.D. 1974. *The Digestive System*. In: *The Histology of the Fowl*. London: Academic Press. pp. 35-47.
- Hörster, W. 1990. Histological and electrophysiological investigations on the vibration-sensitive receptors (Herbst corpuscles) in the wing of the pigeon (*Columba livia*). *Journal of Comparative Physiology A*. **166**: 663-673.
- Hunt, C.C. 1974. *Chapter 13. The Pacinian Corpuscle*. In: *The Peripheral Nervous System*. Edited by Hubbard, J.I. New York: Plenum Press. pp. 405-420.
- Iggo, A. and Andres, K.H. 1982. Morphology of cutaneous receptors. *Annual Review of Neuroscience*. **5**: 1-31.
- Ilyinsky, O.B., Volkova, N.K., Cherepnov, V.L. and Krylov, B.V. 1976. Morphofunctional properties of Pacinian corpuscles. *Progress in Brain Research*. **43**: 173-186.
- Krulis, V. 1978. Struktur und Verteilung von Tastrezeptoren im Schnabel-Zungenbereich von Singvögeln im besonderen der Fringillidae. *Revue Suisse Zoologie*. **85**: 385-447.
- Leitner, L.-M. and Roumy, M. 1974. Mechanosensitive units in the upper bill and in the tongue of the domestic duck. *Pflügers Archiv - European Journal of Physiology*. **345**: 141-150.

- Malinovský, L. 1996. Sensory nerve formations in the skin and their classification. *Microscopy Research and Technique*. **34**: 283-301.
- Malinovský, L. and Páč, L. 1978. Ultrastructure of simple sensory corpuscles in the domestic pigeon. *Folia Morphologica, Prague*. **26**: 170-171.
- Malinovský, L. and Páč, L. 1980. Ultrastructure of Herbst corpuscle from beak skin of pigeon. *Zeitschrift für Mikroskopisch-Anatomische Forschung, Leipzig*. **94**: 292-304.
- Malinovský, L. and Páč, L. 1985. Ultrastructural development of the Herbst corpuscles in the skin of the beak of the domestic duck (*Anas platyrhynchos*, f. *domestica*). *Folia Morphologica*. **33**: 150-155.
- Malinovský, L. and Zemánek, R. 1969. Sensory corpuscles in the beak skin of the domestic pigeon. *Folia Morphologica*. **17**: 241-250.
- Nafstad, P.H.J. and Andersen, A.E. 1970. Ultrastructural investigation on the innervation of the Herbst corpuscle. *Zeitschrift für Zellforschung und Mikroskopische Anatomie*. **103**: 109-114.
- Palmieri, G., Acone, F., Sanna, M., Bo Minelli, L., Botti, M., Maxia, M., Corriero, A., De Metrio, G. 2002. On the sensitive and vegetative innervation of the ostrich's palate. *Italian Journal of Anatomy and Embryology*. **107**: 5-18.
- Palmieri, G., Cappai, M.G., Costa, G., Bo Minelli, L., Botti, M., Desantis, S., Corriero, A. and Acone, F. 2006. Sensory innervation of the copulatory organ in *Struthio camelus*: comparison to the corresponding district in female proctodeum. *Italian Journal of Anatomy and Embryology*. **111**: 31-44.
- Palmieri, G., Dessole, A.A., Bo Minelli, L., Botti, M., Gazza, F., Corriero, A., Desantis, S. and Acone, F. 2004. The sensitive innervation of the ostrich nasal mucosa. *Italian Journal of Anatomy and Embryology*. **109**: 239-248.
- Palmieri, G., Sanna, M., Bo Minelli, L., Botti, M., Gazza, F., Di Summa, A., Santamaria, N., Passantino, L., Maxia, M. and Acone, F. 2003. On the sensitive innervation of the ostrich's foot pads. *Italian Journal of Anatomy and Embryology*. **108**: 25-37.
- Pazour, G.J. and Witmer, G.B. 2003. The vertebrate primary cilium is a sensory organelle. *Current Opinion in Cell Biology*. **15**: 105-110.
- Pycraft, W.P. 1900. On the morphology and phylogeny of the palaeognathae (*Ratitae and Crypturi*) and neognathae (*Carinatae*). *Transactions of the Zoological Society of London*. **15**: 149-290.

Quilliam, T.A. and Armstrong, J. 1963. Mechanoreceptors. *Endeavour*. **22**: 55-60.

Saxod, R. 1968. Ultrastructure des corpuscules sensoriels cutanés de Herbst et Grandry chez le canard. *Archives d'anatomie microscopique et de morphologie expérimentale*. **57**: 379-400.

Saxod, R. 1973. Developmental origin of the Herbst cutaneous sensory corpuscle. Experimental analysis using cellular markers. *Developmental Biology*. **32**: 167-178.

Schildmacher, H. 1931. Untersuchungen über die Funktion der Herbstschen Körperchen. *Journal für Ornithologie*. **79**: 374-415.

Schwartzkopff, J. 1949. Über Sitz und Leistung von Gehör und Vibrationssinn bei Vögeln. *Zeitschrift für Vergleichende Physiologie*. **31**: 527-608.

Tivane, C. 2008. A morphological study of the oropharynx and oesophagus of the ostrich (*Struthio camelus*). M.Sc. thesis, University of Pretoria, South Africa.

Tivane, C., Soley, J.T. and Groenewald, H.B. 2006. Distribution and structure of Pacinian (Herbst) corpuscles in the non-glandular region of the palate of the ostrich (*Struthio camelus*). *Proceedings of the Microscopy Society of Southern Africa*. **36**: 64.

Toyoshima, K., Seta, Y. and Shimamura, A. 1992. Fine structure of the Herbst corpuscles in the lingual mucosa of the finch, *Lonchura striata*. *Archives of Histology and Cytology*. **55**: 321–331.

Watanabe, I., Ususkura, J. and Yamada, E. 1985. Electron microscope study of the Grandry and Herbst corpuscles in the palatine mucosa, gingival mucosa and beak skin of the duck. *Archivum histologicum Japonicum*. **48**: 89-108.

Weir, K.A. and Lunam, C.A. 2004. A histological study of emu (*Dromaius novaehollandiae*) skin. *Journal of Zoology*. **264**: 259–266.

Weir, K.A. and Lunam, C.A. 2006. Immunohistochemical study of cutaneous nerves in the emu. *Cell and Tissue Research*. **326**: 697–705.

Wight, P.A.L., Siller, W.G. and Mackenzie, G.M. 1970. The distribution of Herbst corpuscles in the beak of the domestic fowl. *British Poultry Science*. **11**: 165-170.

Winkelmann, R.K. and Myers, T.T. 1961. The histochemistry and morphology of the cutaneous sensory end-organs of the chicken. *Journal of Comparative Neurology*. **117**: 27-31.

Zelená, J., Halata, Z., Szeder, V. and Grim, M. 1997. Crural Herbst corpuscles in chicken and quail: numbers and structure. *Anatomy and Embryology*. **196**: 323–333.

Ziswiler, V. 1965. Zur Kenntnis des Samenöffnens und die Struktur des hörnernen Gaumens bei körnerfressenden Oscines. *Journal für Ornithologie, Leipzig*. **106**: 1-48.

Ziswiler, V., and Trnka, V. 1972. Tastkörperchen im Schlundbereich der Vögel. *Revue Suisse Zoologie*. **79**: 307-318.

Zweers, G.A., Gerritsen, A.F.C. and Van Kranenburg-voogd, P.J. 1977. *Mechanics of Feeding in the Mallard (Anas platyrhynchos L.; Aves, Anseriformes)*. In: Contributions to Vertebrate Evolution. Vol. 3. Edited by Hecht, M.K. and Szalay, F.S. Karger: A.G. Basel. pp. 1-109.

CHAPTER 4

MORPHOLOGY AND SENSORY SPECIALISATIONS OF THE BILL.

I. EPIDERMIS AND DERMIS

4.1. Introduction

The bill can be described as a highly specialised sensory organ which has the ability to discriminate between edible and non-edible items (Widowski, 2010), the morphology of which can be linked to foraging behaviour, diet and habitat selection (see Nebel *et al.*, 2005; Widowski, 2010). The bill is covered by a tough, keratinized epithelium (rhamphotheca) and is supported by the premaxillary and mandibular bones (Widowski, 2010). The dermis, situated between the epithelium and bone, is richly supplied with blood vessels, nerves and sensory receptors (Widowski, 2010). The bill has been studied extensively in domestic poultry (Gottschaldt and Lausmann, 1974; Gentle and Breward, 1986; Berkhoudt, 1976, 1980; Halata and Grim, 1993) and, more recently, in non-domestic species such as the Java finch (*Padda oryzivora*) and Darwin's finches (12 species) (Genbrugge *et al.*, 2012), and the black-capped chickadee (*Pocile atricapillus*) (Van Hemert *et al.*, 2012).

In contrast, relatively little information is currently available on the rhamphotheca in ratites. Parkes and Clark (1966) documented the external features of the bill (rhamphotheca) in several ratite and tinamou natal downs (recently hatched chicks), including the ostrich and emu. The main aim of this study was to provide additional evidence supporting the monophyletic theory of origin of the palaeognaths (Parkes and Clark, 1966) and consequently focused more on similarities between the species rather than on a thorough description of the external features of the bill. In the ostrich the distal maxillary tip of the hatchling has been briefly studied by scanning electron microscopy (Richardson *et al.*, 1998). Additionally, serrations (*Lamellae rostri*) have been described in the rostral third of the mandibular tomium in the emu (Crole and Soley, 2010) and fine serrations have been noted in a comparable region in the ostrich (Tivane, 2008). These

findings (Crole and Soley, 2010) challenge the assumption that the bill of ratites is relatively less adapted and specialised (Gussekklo and Bout, 2005) or requires little strength (Davies, 1978), and future in-depth studies of the serrations in the emu bill may reveal a more specialised function for these structures.

Both the ostrich and emu display a segmented rhamphotheca (Parkes and Clark, 1966) and Herbst corpuscles are numerous in the dermis of the bill between the epidermis and underlying bone (see Chapters 3 and 5). The keratinised rhamphotheca is reported to play an important role in the dissipation of stress during biting (Soons *et al.*, 2012). Thus the rhamphotheca needs to be durable enough to withstand the foraging behaviour and diet of the ostrich and emu. Conversely, the rhamphotheca cannot be too tough or thick as this would impede the myriad of underlying Herbst corpuscles from receiving stimuli. The bill of the chicken is hard due to the high degree of keratinisation; however, dermal papillae (with associated Herbst corpuscles) extend a substantial distance into the surrounding rhamphotheca and therefore have a thinner covering of keratin (Gentle and Breward, 1986). It was suggested that in the presence of a hard bill, the thinner keratin layer overlying the dermal papilla may enhance sensitivity by allowing a greater deformation of soft tissues (Gentle and Breward, 1986). To allow a bill with a tough covering of keratin to be both strong and afford a high degree of sensitivity, it would seem that modifications of the dermis and epidermis would be necessary. This chapter characterises and compares the rhamphotheca of the ostrich and emu in order to identify whether specific modifications exist which would facilitate a tough outer covering of the beak but still afford a high degree of sensitivity. Consideration will also be given to the contribution such modifications may make to the structure and functioning of the bill tip organ (see Chapter 7).

4.2. Materials and Methods

A total of 5 adult ostrich and 10 adult emu heads, from birds of either sex, were collected after slaughter from the Klein Karoo Ostrich abattoir (Oudtshoorn, Western Cape Province, South Africa), Oryx Abattoir (Krugersdorp, Gauteng Province, South Africa) and Emu Ranch (Rustenburg, North-West Province, South Africa). All heads were thoroughly rinsed with either distilled water or running tap water to remove mucus,

blood and regurgitated food. Additionally, 5 ostrich chick heads (2-4 weeks-old) and 1 emu chick head (8 weeks-old) were collected for histology of the bill. Chicks were used as the entire bill could be viewed histologically on one slide. Ostrich chicks had been euthanized for a separate, unrelated study (protocol number 36-5-0623, Faculty of Veterinary Science, University of Pretoria) and the emu chick was euthanized due to health reasons.

4.2.1. Preparation of osseous elements of the mandible in the emu

Five fresh adult emu heads were collected and prepared for osteological examination of the bony elements relevant to the structure of the mandible (Fig. 4.5b). The rhamphotheca was partially and sequentially stripped in these specimens to allow the description of the rhamphothecal serrations (see below). The heads were left at room temperature for a few days to facilitate softening of material and the removal of as much soft tissue as possible. Each head was then individually secured in a muslin cloth bag and boiled in water for 24 hours in a stainless steel catering pot after which any remaining soft tissues, muscle and skin were removed from the bones. The bones, in their individual muslin cloth bags, were then placed in a degreasing plant (Proctor Industrial Cleaning Systems, Johannesburg, South Africa) and boiled in stabilized trichloroethylene for 48 hours to de-fatten the bones. The mandibles were described, digitally recorded with a Canon EOS 5D digital camera (Canon, Ōita, Japan) equipped with a Canon Macro 100mm lens, and annotated in Corel Draw X5. They were also viewed with an Olympus SZX16 stereomicroscope (Olympus Corporation, Tokyo, Japan) equipped with a DP72 camera and Olympus cellSens imaging software (Olympus Corporation, Tokyo, Japan), described and annotated in Corel Draw X5.

4.2.2. Gross description

Five adult ostrich and 5 adult emu heads were collected (see above) and fixed in 10% neutral-buffered formalin and transported to the Faculty of Veterinary Science, University of Pretoria. Care was taken to exclude air from the oropharynx by inserting a small block of wood between the bill tips. The external rhamphotheca was described, digitally recorded with a Canon EOS 5D digital camera (Canon, Ōita, Japan) equipped with a Canon Macro 100mm lens, and annotated in Corel Draw X5. To reveal the

keratinised pegs in the emu and their relationship to the rhamphothecal serrations, the rhamphotheca was partially and sequentially stripped (Figs. 4.4d and 4.5a) by gradually scraping it away with a scalpel blade. The tomium was also forcibly removed (Figs. 4.4a and b) by using a pair of bone-cutting pliers which cut through the rhamphotheca and allowed a portion of the serrations and pegs to be freed from the surrounding tissues (Fig. 4.4c). The rhamphotheca in the 5 ostrich specimens was partially and sequentially stripped as for the emu specimens. The epidermis was scraped away on either side (externally and internally) of the maxillary and mandibular tomium in the ostrich (Figs. 4.12a, d). The tomium was then gently manipulated until it separated from the dermis. This allowed visualisation of the dermal papillae (Fig. 4.12b). Dermal papillae (in the ostrich) and rhamphothecal serrations and keratinised pegs (in the emu) were viewed with an Olympus SZX16 stereomicroscope (Olympus Corporation, Tokyo, Japan) equipped with a DP72 camera and Olympus cellSens imaging software (Olympus Corporation, Tokyo, Japan), described and annotated in Corel Draw X5.

4.2.3. Light microscopy

The microscopic features of the rhamphothecal modifications in the 5 adult ostriches and 5 adult emus were studied using the same histology slides prepared in Chapter 3.2.3. The upper and lower bills of the 5 ostrich and 1 emu chick were removed and decalcified (see below). The upper bill was cut into transverse-sections at approximately 5 mm intervals and the lower bill was divided into left and right halves. The right halves were transversely sectioned and the left halves longitudinally sectioned.

Decalcification took place over a period of 6 weeks in an 8% formic acid solution. The samples were placed in a fresh solution fortnightly. Tissue samples were dehydrated through 70%, 80%, 96%, and 2X 100% ethanol and further processed through 50:50 ethanol: xylol, 2X xylol and 2X paraffin wax (60-120 minutes per step) using a Shandon model 2LE Automatic Tissue Processor (Shandon, Pittsburgh, PA, USA). Tissue samples were then imbedded manually into paraffin wax in plastic moulds. Sections were cut at 4-6 μm and stained with H&E (Bancroft and Gamble, 2002). Samples of a rhamphothecal serration and keratinised peg were processed for light microscopy and as follows for resin embedding. The samples were rinsed in Millonig's phosphate buffer (pH 7.4, 0.13 M at room temperature) for 10 minutes, post-fixed for 1 hour at room

temperature in similarly buffered 1% OsO₄ and given two final buffer washes of 10 minutes each. Samples were then rinsed in distilled water for 20 minutes and dehydrated through a graded series of ethanols (50%, 70%, 80%, 96% and 2 X 100% (with added Molecular sieve, Merck, Darmstadt, Germany)) for 10 minutes per step. Samples were placed in 2X propylene oxide (PO) for 10 minutes each followed by infiltration in PO: Epoxy resin (2:1) for 30 minutes to 1 hour and PO: Epoxy resin (1:2) for 1 hour to overnight. The blocks were orientated using a stereo microscope to ensure that the tissue samples were placed in both longitudinal and transverse profile, embedded in 100% Epoxy resin in silicone moulds and cured in an embedding oven at 65°C overnight. Semi-thin sections were cut at 0.3 µm using a diamond knife, mounted and stained with 1% Toluidine blue. Histological sections were viewed, features of interest described and digitally recorded using an Olympus BX63 light microscope (Olympus Corporation, Tokyo, Japan) equipped with a DP72 camera and Olympus cellSens imaging software (Olympus Corporation, Tokyo, Japan), and annotated in Corel Draw X5.

4.3. Results

4.3.1. External features of the bill (Figs. 4.1-3)

The bill was U-shaped in the ostrich and V-shaped in the emu in both dorsal and ventral view. Thus the emu displayed a pointed bill tip whereas in the ostrich it was more rounded and blunt (Figs. 4.1-3). In formalin-fixed specimens the rhamphotheca¹ (the keratinised *Str. corneum* covering the bill) was a light cream/tan to brown colour in the ostrich and a dark brown/black colour in the emu (Fig. 4.3). In the ostrich the rhamphotheca of the bill tips was textured with fine lines running obliquely from the *Culmen*² and *Gonys*³ towards the maxillary and mandibular tomia, respectively. The rhamphotheca was hard to the touch in the ostrich but softer and more rubbery in consistency in the emu.

¹ “The horny covering of the beak, both inside and outside surfaces of the bones of the jaws. The rhamphotheca is hard in most birds, but leathery, for example, at the tip (nail) in flamingos and anatids. The shape of the rhamphotheca is basically that of the underlying bone, but modified by outgrowths and local thickenings.” (Clark, 1993a).

² “The middorsal ridge of the Rostrum maxillare extending from the tip of the bill to the base of the feathers on the forehead at or near the craniofacial angle.” (Clark, 1993a).

³ “The midventral ridge of rhamphotheca lying superficial to the Rostrum [Symphysis] mandibulae.” (Clark, 1993a).

4.3.1.1. The upper bill

The upper bill was segmented in both species and comprised a number of components. The *Culmen* occupied the dorsal midline, was both broader and longer in the ostrich than in the emu, and in both species did not extend the full length of the bill (Figs. 4.1 and 4.3a, c). Caudal to the *Culmen*, in both species, was a portion of rhamphotheca which formed the dorsal and caudo-lateral extremity of the upper bill and which abutted the feathered skin of the forehead (*Frons*)⁴ (Fig. 4.3). In the ostrich the origin (caudal border) of the *Culmen* was covered by the rhamphotheca bordering the feathered skin, forming a small pocket (Figs. 4.1 and 4.3). In both species the craniofacial angle (*Angulus craniofacialis*)⁵ was not formed at the base of the *Culmen* (Fig. 4.3). The rostral extremity of the *Culmen* in both species ended as the prominent maxillary nail (*Unguis maxillaris*)⁶ (Figs. 4.1, 4.3a, c, 4.4a, d, 4.8 and 4.12a). As previously described in the emu (Crole and Soley, 2010) the maxillary nail was considerably more pointed or hooked than that of the ostrich.

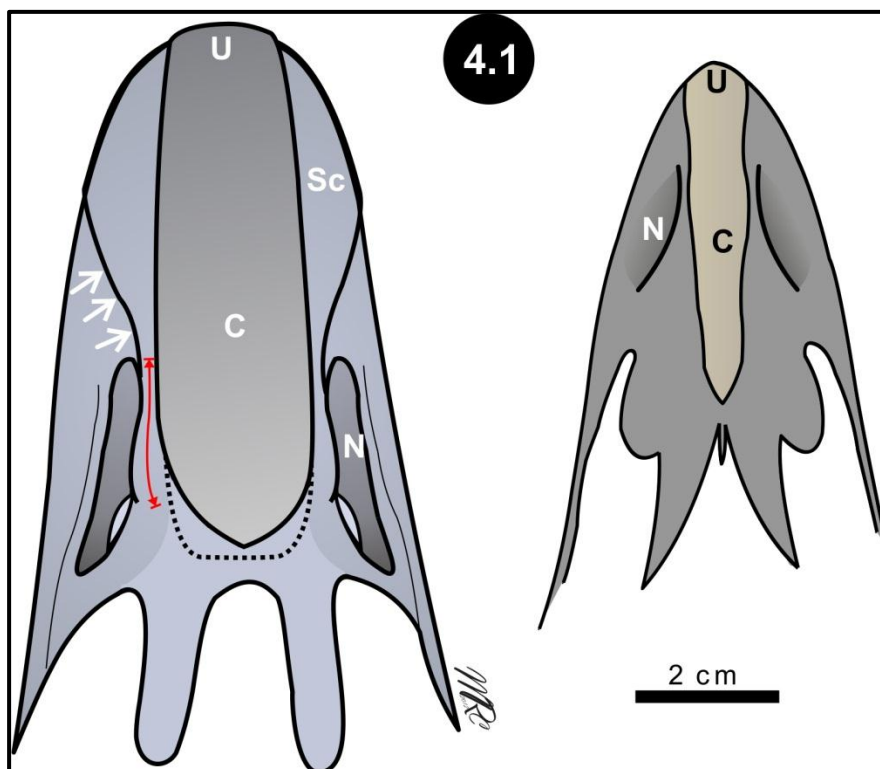


Figure 4.1. Schematic dorsal view of the external features of the maxillary rhamphotheca of the ostrich (left) and emu (right). See also Figs 4.3.a and c. Note the massive bill in the ostrich and the more slender and pointed bill in the emu. The *Culmen* (C) is wider in the ostrich and the nostrils (N) are situated more caudally. The maxillary *unguis* (U) is sharper in the emu. Rhamphothecal ridge (red arrow) and its continuation delineating (white arrows) the sensory cap (Sc). The caudal extent of the *Culmen* in the ostrich is indicated by the dotted line.

⁴ "The forehead extends from the bill to about the transverse level of the nasal (rostral) margin of the eye." (Clark, 1993a).

⁵ "The angle at the junction of the culmen with the slope of the frontal region." (Clark, 1993a).

⁶ "The thickened areas of rhamphotheca "nails", at the tips of the maxillary and mandibular rostra and delimited by a difference in color or by a groove in procellariform, most pelecaniform, and anseriform birds." (Clark, 1993b).

In the ostrich the nostrils (*Naris*)⁷ were visible in both dorsal and lateral view, their rostral extent coinciding with the caudal third to quarter of the *Culmen* and projecting a short distance caudally beyond the caudal termination of the *Culmen* (Figs. 4.1 and 4.3). In lateral profile they were elliptical in shape and positioned more or less parallel to the *Tomium maxillare*⁸. The ventral border of the nostril was delineated by a thickening of the rhamphotheca and the dorso-medial border was separated from the *Culmen* by a rhamphothecal ridge (Fig. 4.1). This ridge continued rostrally and obliquely towards the maxillary tomium becoming progressively less pronounced and delineated a raised portion of rhamphotheca on the upper bill tip flanking the *Culmen* (Fig. 4.1). Fine lines were visible below the surface running obliquely from the *Culmen* towards the maxillary tomium (Figs. 4.3 and 4.12a). This region was termed the sensory cap and externally demarcated the underlying bill tip organ in the upper bill of the ostrich (Figs. 4.1, 4.3 and 4.8) (see Chapter 7). The tomium of the sensory cap region was sharp and hard and projected further ventrally than that of the tomium caudal to the sensory cap (Fig. 4.12a). In the emu the nostril was only clearly visible in lateral view. In this view the portion of the rhamphotheca covering the dorsal border of the nostril effectively formed an operculum (*Operculum nasale*)⁹ which sloped from the *Culmen*, caudo-ventrally. The ventral border of the nostril was continuous with the surrounding rhamphotheca. Relative to the length of the bill (from the bill tip to the angle of the mouth (*Rictus*)) the nostrils in the emu were situated more rostrally than those of the ostrich. In the emu they occupied the caudal part of the rostral third of the bill, whereas in the ostrich they occupied the rostral portion of the middle third of the bill (Fig. 4.3).

⁷ "Synonymy: nostril or external nasal aperture. The nares, commonly round or elongate in shape, penetrate the bone and rhamphotheca of the maxilla usually near its caudal end." (Clark, 1993a).

⁸ "The cutting edge of the rhamphotheca on each ramus of the upper and lower jaws. The tomia form the borders of the forward part of the opening of the mouth (**Rima oris**)." (Clark, 1993a).

⁹ "A projecting shelf termed the **Operculum nasale** (operculum, L. lid or cover) partially or completely covers the naris in some birds including chickens, pigeons, and starlings (*Sturnus vulgaris*)." (Clark, 1993a).

4.3.1.2. The lower bill

The *Gonys* was similar in width to that of the corresponding *Culmen* and as a result was broader in the ostrich than in the emu. However, they were of similar length in both birds. The edges of the *Gonys* ran parallel in the ostrich but in the emu diverged rostrally to widen as the *Gonys* ended in the mandibular nail (*Unguis mandibularis*) (Fig. 4.2). Caudo-laterally, the rhamphotheca covering the mandibular arms was split horizontally into dorsal and ventral components separated by feathered skin. The ventral component ended rostral to the dorsal component, which continued to the angle of the mouth. This division was more pronounced in the emu where the intervening strip of feathered skin appeared indented. The dorsal part of the mandibular arm carried the *Tomium mandibulare* which was blunt and rounded caudally but on the rostral third (overlying the dentary bone (see below and Chapter 5)) was modified. In the ostrich it was sharp and hard whereas in the emu rhamphothecal serrations were present (see below). These serrations have previously been described (Crole and Soley, 2010, 2012) and referred to as *Lamellae rostri*¹⁰.

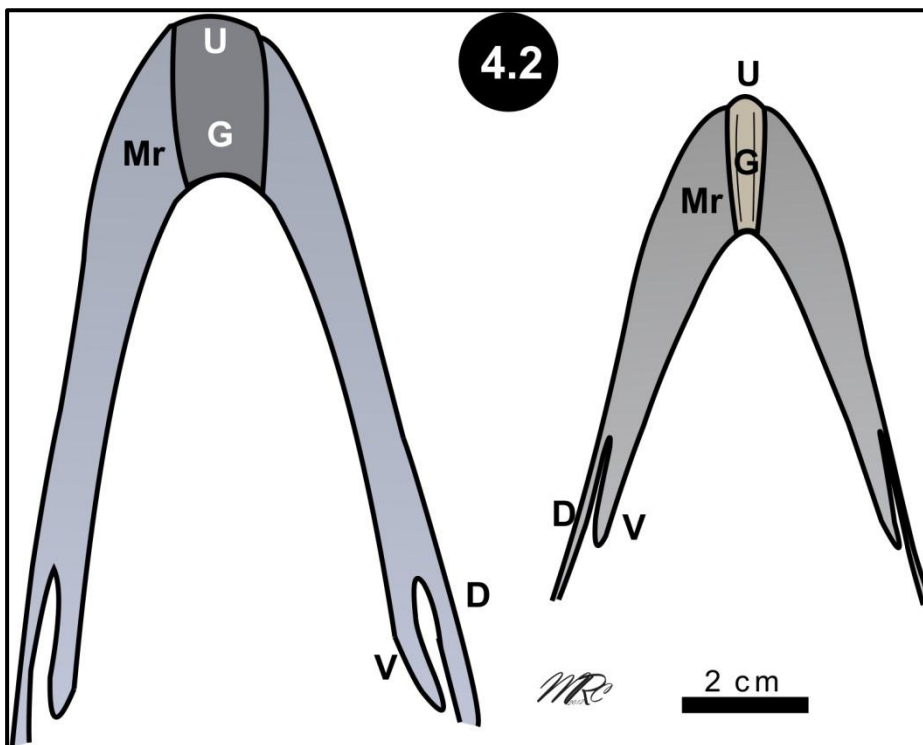


Figure 4.2. Schematic ventral view of the external features of the mandibular rhamphotheca of the ostrich (left) and emu (right). Note the robust nature of the ostrich mandible and the more slender and pointed form in the emu. The *Gonys* (G) is relatively wider in the ostrich and widens rostrally in the emu. The mandibular *unguis* (U) is sharper in the emu. Mandibular rostrum (Mr). The caudal split in the rhamphotheca forms dorsal (D) and ventral (V) components.

¹⁰ "A series of small, closely set vertical ridges of rhamphotheca along the outer margin of the lower tomia and/or the inner margin of the upper tomia used for straining or grasping food as in the phoenicopterids (flamingos) and anatids." (Clark, 1993a).

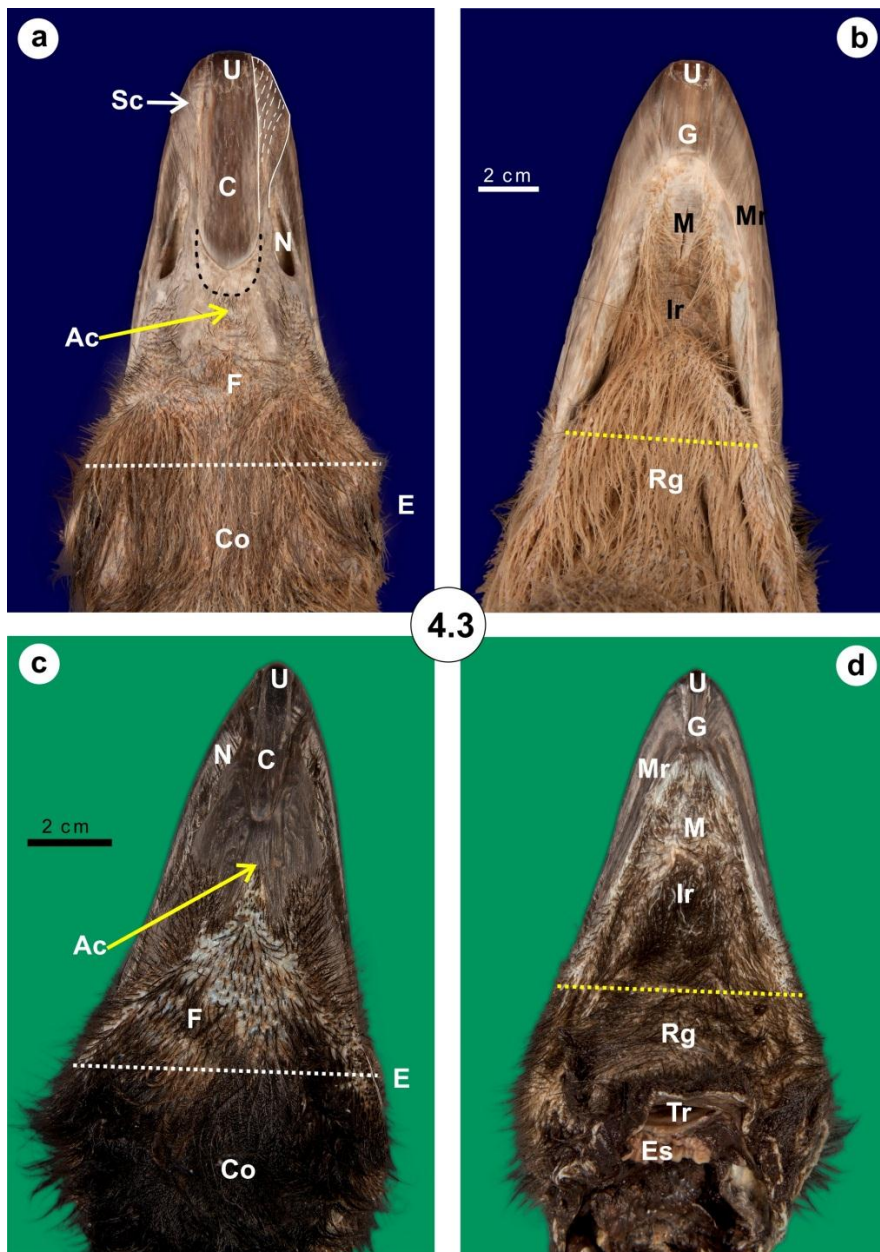


Figure 4.3. Comparative dorsal (a and c) and ventral (b and d) views of the head of the ostrich (a and b) and the emu (c and d) indicating the extent of the rhamphotheca. The sensory cap (Sc) in the ostrich has been outlined in figure 4.3a for clarity and the orientation of the fine lines indicated by white dotted lines. Maxillary (a and c) and mandibular (b and d) *unguis* (U), mandibular ramus (Mr), *Culmen* (C) and *Gonys* (G). The craniofacial angle (Ac) is situated just caudal to the termination of the *Culmen*. The dotted white line in (a) and (c) shows the approximate boundary between the *Frons* (F) and the *Corona*¹¹ (Co) dorsally and the dotted yellow line in (b) and (d) the approximate boundary between the interramal region¹² (Ir) and the gular region¹³ (Rg) ventrally. Approximate position of the eye (E), *Mentum*¹⁴ (M), trachea (cut) (Tr) and esophagus (cut) (Es). The caudal extent of the *Culmen* in the ostrich is shown by the dotted line.

(Some feathers on the *Frons* and lateral side of the bill have been cut to allow better visualisation of the rhamphotheca).

¹¹ "The crown extends over the top of the head (Caput) from the *Frons* to the *Occiput*. A boundary between the crown and occiput is sometimes distinguishable by feather coloration, but is more often indefinite." (Clark, 1993a).

¹² "**Regio interramalis**. Synonymy: *Regio intermandibularis*. This triangular area lies between the two mandibular rami caudal to the *Rostrum* [Symphysis] mandibulae (gonys)." (Clark, 1993a).

¹³ "**Regio gularis** [R. submalaris]. The gular region, the caudal part of the interramal region, forms the throat and extends from the *mentum* caudally to an imaginary line between the caudal ends of the mandibles." (Clark, 1993a).

¹⁴ "The *Mentum* is the soft rostral part of the interramal region caudal to the *Gonys* and hard interramal space. The *Mentum* is caudally continuous with the gular (submalar) region. The *Mentum* is thus the area, usually feathered between the exposed mandibular rami, i.e., the rostral part of the interramal region in the fork on the underside of the bill." (Clark, 1993a).

4.3.2. Modifications of the epidermis and dermis

Specialised structures of dermal and epidermal origin were present in the mandibular rostrum in the emu and in the mandibular and maxillary rostra of the ostrich. The features described below were unique to each species.

4.3.2.1. Mandibular rhamphothecal serrations and keratinised pegs in the emu (Figs. 4.4-7)

As previously described (Crole and Soley, 2010, 2012) and confirmed in the present study, the serrations of the mandibular rhamphotheca were located on the rostral third of the mandibular tomia. The average number of serrations present on each half of the mandible was 44.6 with a slightly higher number always present on the right mandible (Crole and Soley, 2010). The serrations were more prominent in some birds than others but fairly uniform for each bird (Crole and Soley, 2010). Each rhamphothecal serration corresponded to a small raised region of the lateral edge of the dentary bone (Fig. 4.5b). Sequential and partial stripping of the rhamphotheca from the rostral mandibular tomium revealed the presence of pale, tapered cylindrical structures located in the underlying connective tissue between the rhamphothecal serrations (Figs. 4.4c, d and 4.5a). Based on histological observations (see light microscopy below) these structures were termed keratinised pegs. The pegs were located in cylindrical hollows (Figs. 4.4a, b) formed by the dermis which were in turn situated in bony grooves (Fig. 4.5). The keratinized pegs were slanted caudo-ventrally and were positioned on the lateral edge of the dentary bone (Figs. 4.4d and 4.5a). Each shallow bony groove led to a small foramen or pit, above which the tapered point of the keratinized peg was situated (Figs. 4.4d and 4.5b). The location of the pegs was occasionally visible on the surface of the rhamphotheca in the valleys formed between adjacent rhamphothecal serrations in the form of tubular openings where the trapped keratinised cells had flaked away (Fig. 4.4c).

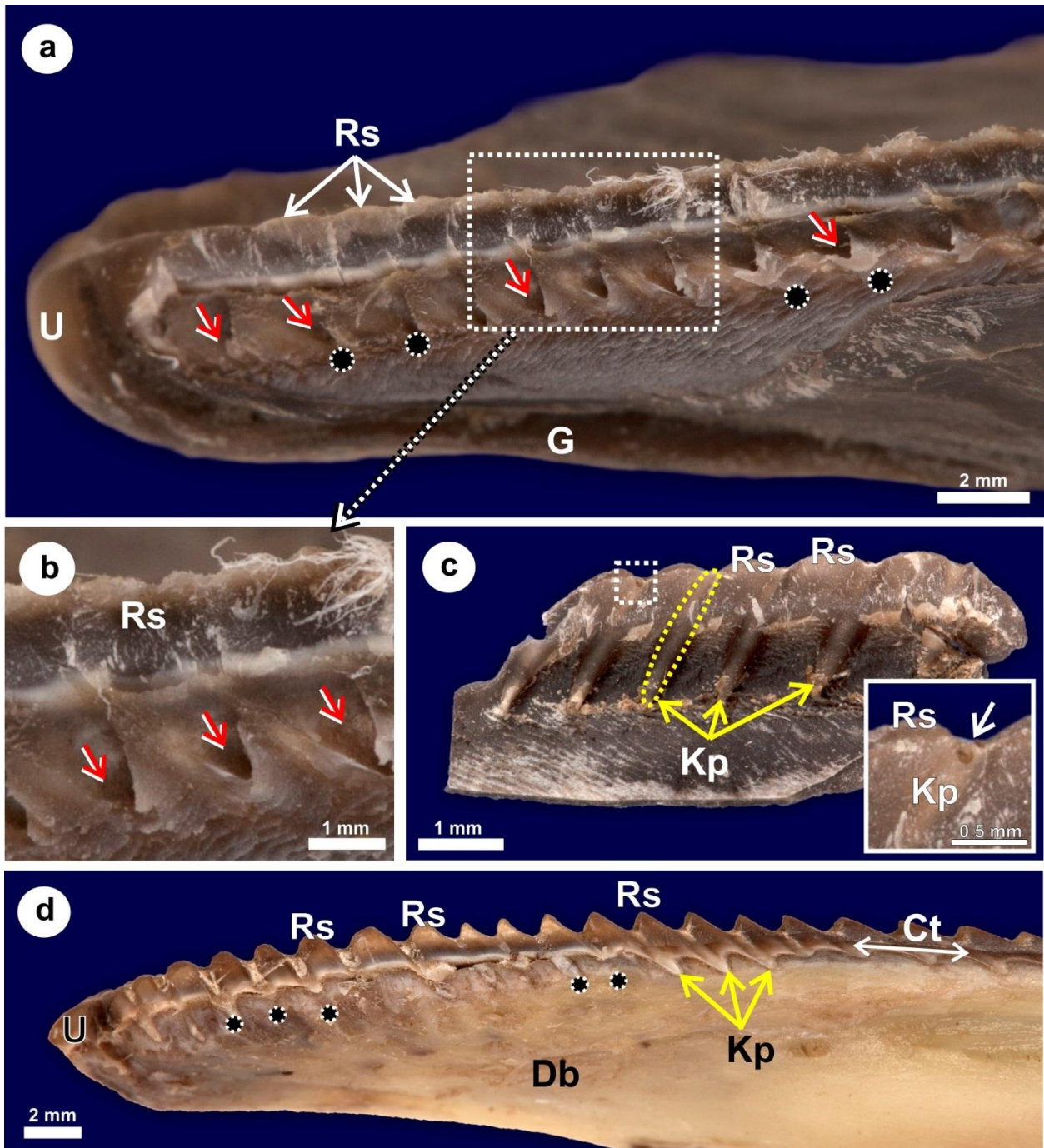


Figure 4.4. A series of photographs showing progressive stripping of the rhamphotheca to reveal the keratinised pegs (Kp).

(a-b). Lateral view of the mandibular rostrum. A section of the rhamphotheca was removed (seen in c) to reveal the cylindrical dermal hollows (red arrows) in which the keratinised pegs are housed. Each rhamphothecal serration (Rs) is separated by a keratinised peg, the point of which terminates near a small pit/hole in the underlying bone (approximate position indicated by circles). An area (white square) is enlarged in figure 4.4b for better clarity. Mandibular *Unguis* (U) and *Gonys* (G).

(c). Portion of stripped epidermis viewed from the medial aspect. Note the keratinised pegs (one outlined in yellow) positioned between each rhamphothecal serration (Rs) and slanting caudo-ventrally. The enlarged area (dotted square) shows the surface location of a keratinised peg as it merges with the surrounding *Str. corneum* (white arrow). The inner layers have desquamated leaving a hollow.

(d). Epidermis and dermis stripped to the dentary bone (Db). The keratinised pegs lie in shallow dermis-lined grooves in the underlying bone and end near small pits/holes (approximate position indicated by black circles). *Crista tomialis* (Ct).

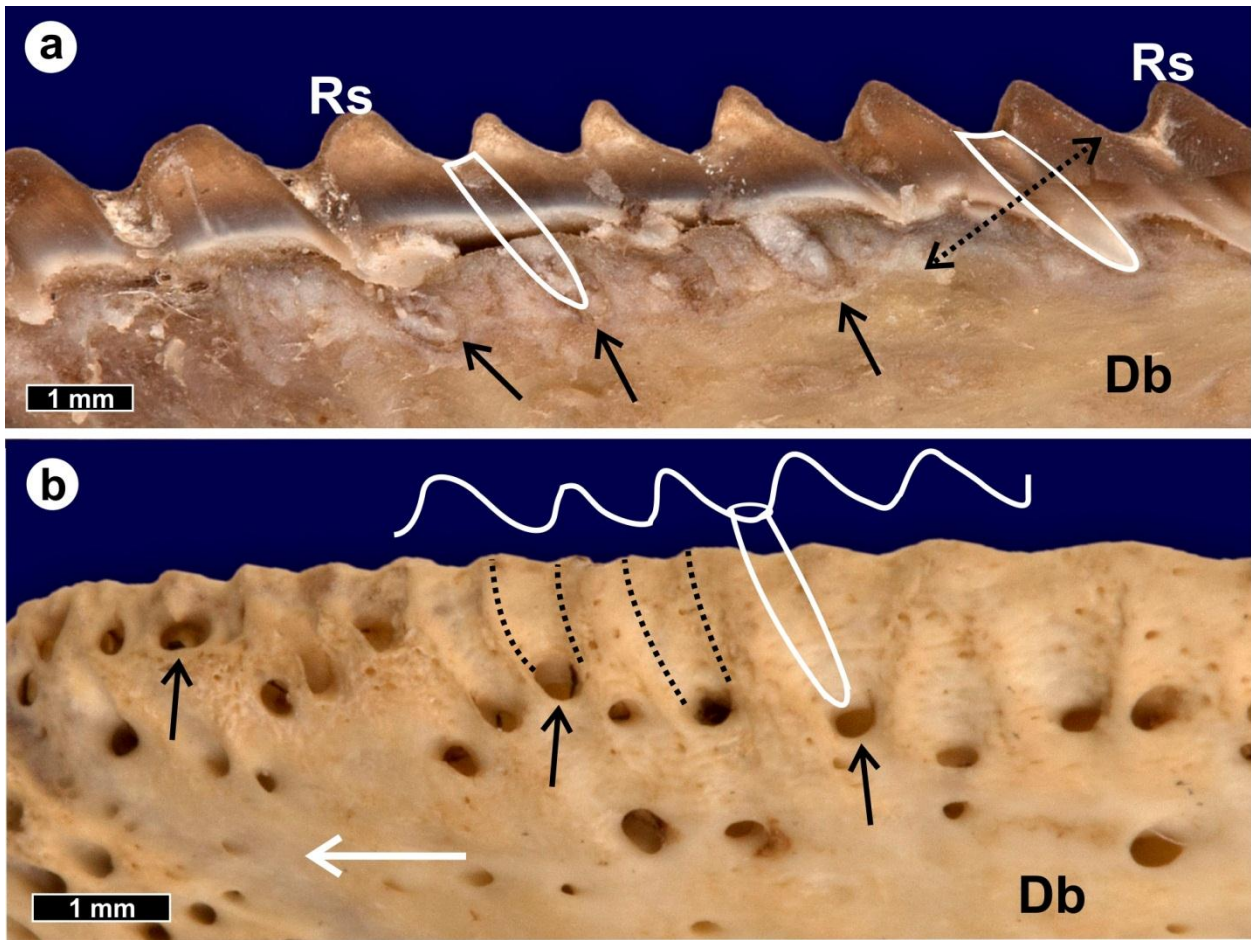


Figure 4.5. (a). Lateral dentary bone (Db) forming the mandibular rostrum with the epidermis and dermis partially stripped. A keratinised peg (white outline) lies in a bony groove which ends in a pit (black arrows). Note the rhamphothecal serrations (Rs) flanking each keratinised peg (white cylinder). The double-headed dotted arrow indicates the plane of sectioning of the keratinised peg illustrated in Figure 4.7d.

(b). Lateral view of the dentary bone (Db) illustrating the bony grooves (black dotted lines) and pits (black arrows). The relationship of the rhamphothecal serrations is schematically indicated (white wavy line) as well as a keratinised peg (white cylinder). Rostral is indicated by the horizontal white arrow.

Light microscopy revealed that the rhamphothecal serrations were formed by localised thickenings of the *Str. corneum* of the keratinized, pigmented, stratified squamous epithelium (Figs. 4.6 and 4.7d) and thus represented rhamphothecal modifications. The underlying *Str. germinativum* and the supporting dermis formed a small, raised point from which the *Str. corneum* proliferated, forming the rhamphothecal serrations (Fig. 4.6). The *Str. corneum* of the keratinized pegs was non-pigmented (Fig. 4.6) and arranged in concentric cell layers, presenting a lamellated appearance in cross-section (Fig. 4.7d). This arrangement was particularly clear in the deeper regions of the pegs (Fig. 4.7d) but less obvious where the material of the pegs merged with the surrounding rhamphotheca (Figs. 4.7a, b), particularly in longitudinal section (Fig. 4.6). The

underlying *Str. germinativum* and supporting dermis formed a tapered, cylindrical shell from which the keratinized peg originated (Figs. 4.6 and 4.7d).

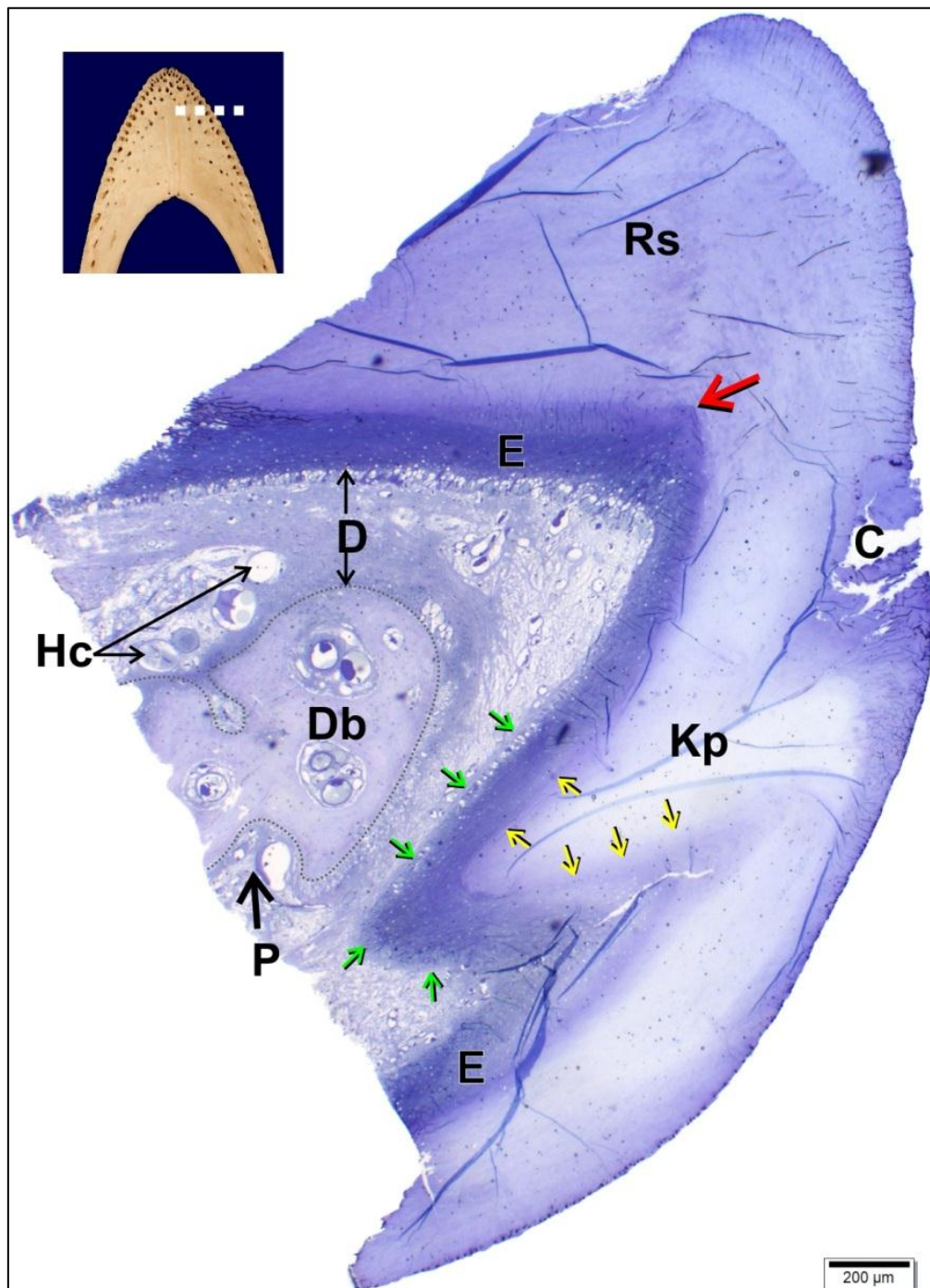


Figure 4.6. Transverse section of the lateral edge of the mandibular rostrum (see inset) showing a rhamphothecal serration (Rs) and a keratinised peg (Kp) in longitudinal section. The dentary bone (Db) (dotted outline) contains numerous pits (P) leading into the bone and which house Herbst corpuscles (Hc), fat cells, blood vessels and nerves. The dermis (D) and germinal layers of the epidermis (E) form a point (red arrow) which shapes the overlying rhamphothecal serration. The *Str. germinativum* of the epidermis forms a tapered shell (green arrows) which produces the *Str. corneum* (yellow arrows) in a concentric manner forming the poorly pigmented (lighter colour) keratinised peg. Note how at the surface the *Str. corneum* emanating from the peg appears to desquamate (C) (also see inset in Figure 4.4c). Toluidine blue staining.

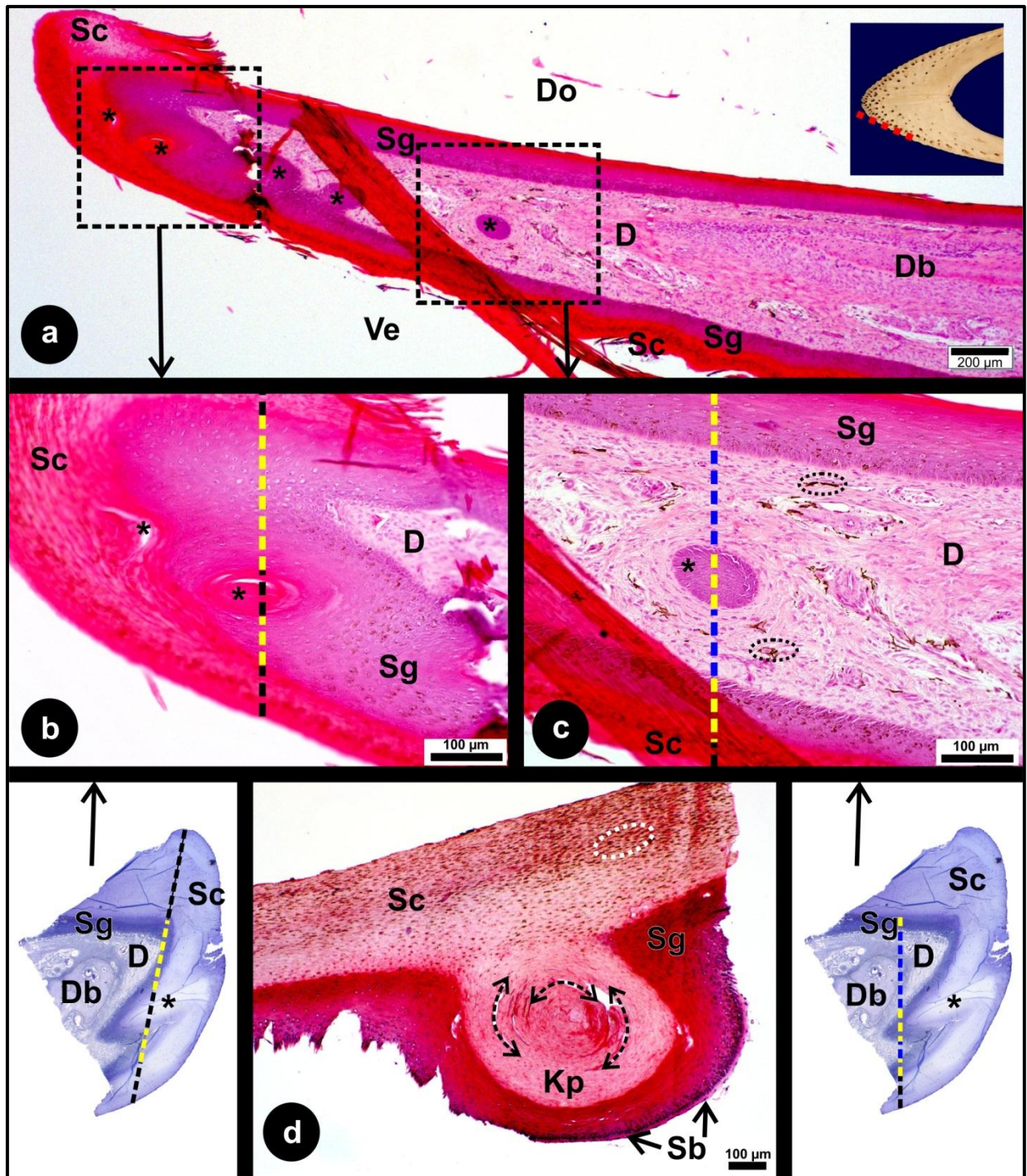


Figure 4.7. (a-c). Longitudinal sections along the edge of the mandibular rostrum (inset in a) of a 2 month-old emu. (a). Numerous keratinised pegs (*) are seen sectioned at different points along their length. Dorsal (Do), Ventral (Ve), *Str. corneum* (Sc), *Str. germinativum* (Sg), dermis (D), dentary bone (B). The squares are enlarged in figures b-c.

(b-c). The toluidine blue-stained sections show the keratinised peg in longitudinal section and the coloured lines indicate the corresponding parts seen in transverse section in figures b and c. *Str. corneum* (black line), *Str. germinativum* (yellow line), dermis, (blue line). Figure b illustrates the distal aspect and figure c the proximal aspect of a keratinised peg. Note the pigment in figure c (black circles).

(d). Transverse section of the epidermis and a keratinised peg (Kp) stripped from the mandible of an adult emu. The *Str. corneum* of the epidermis is pigmented (white circle) and forms the rhamphotheca. Note the concentric, lamellated structure of the keratinised peg (double-headed arrows) which is non-pigmented. *Str. germinativum* (Sg) and *Str. basale* (Sb).

4.3.2.2. Epidermal troughs and modification of the rostral tomia in the ostrich

Light microscopy revealed two specialisations of the rhamphotheca of the upper and lower bills, namely epidermal troughs and modifications of the rostral tomia in the form of tubular and inter-tubular horn. The epidermal troughs appeared macroscopically as oblique striations both in the sensory cap (upper bill) (Figs. 4.1, 4.3a, 4.8 and 4.12a) and the mandibular rostrum (Fig. 4.9a). Deep epidermal troughs also bordered the *Culmen* and *Gonys* (Fig. 4.9d) in the ostrich as well as in the emu.

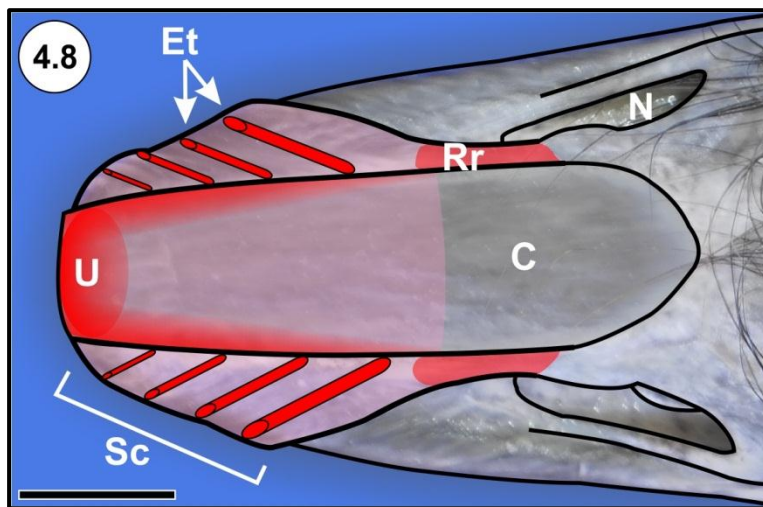


Figure 4.8. Semi-schematic illustration of the sensory cap (Sc) in the ostrich upper bill. Structures have been outlined for clarity. The pink shaded regions indicate the distribution of underlying Herbst corpuscles (see Chapter 7) with the darker shaded areas showing specific concentrations of Herbst corpuscles such as the maxillary unguis (U), the edges of the *Culmen* (C), and the rhamphothecal ridges (Rr) in the sensory cap (Sc). The specialised epidermal troughs (Et) are shown schematically. External nare (N). Bar = 1 cm.

The epidermal troughs ran obliquely and followed a line from the rhamphothecal ridge between the *Culmen* and external nare to the maxillary tomium (Fig. 4.12a) or from the *Gonys* to the mandibular tomium. These structures were visible macroscopically as pigmented stripes. The troughs were formed by gutter-like depressions of the epidermis, which varied from U-shaped (Fig. 4.9c) to teardrop-shaped (Fig. 4.9b), and were filled with layers of keratinised cells. The depressions were lined by a continuation of the *Str. germinativum* from which the *Str. corneum* originated, forming a plug of keratinised cells that filled the trough (Figs. 4.9a, b). These cells merged on the surface of the rhamphotheca with the surrounding cells resulting in a smooth surface profile. The *Str. germinativum* was thinnest near the base of the troughs (Fig. 4.9b). The rhamphothecal troughs were deep at their origin from the *Culmen* or *Gonys* but became shallower as they reached the tomia.

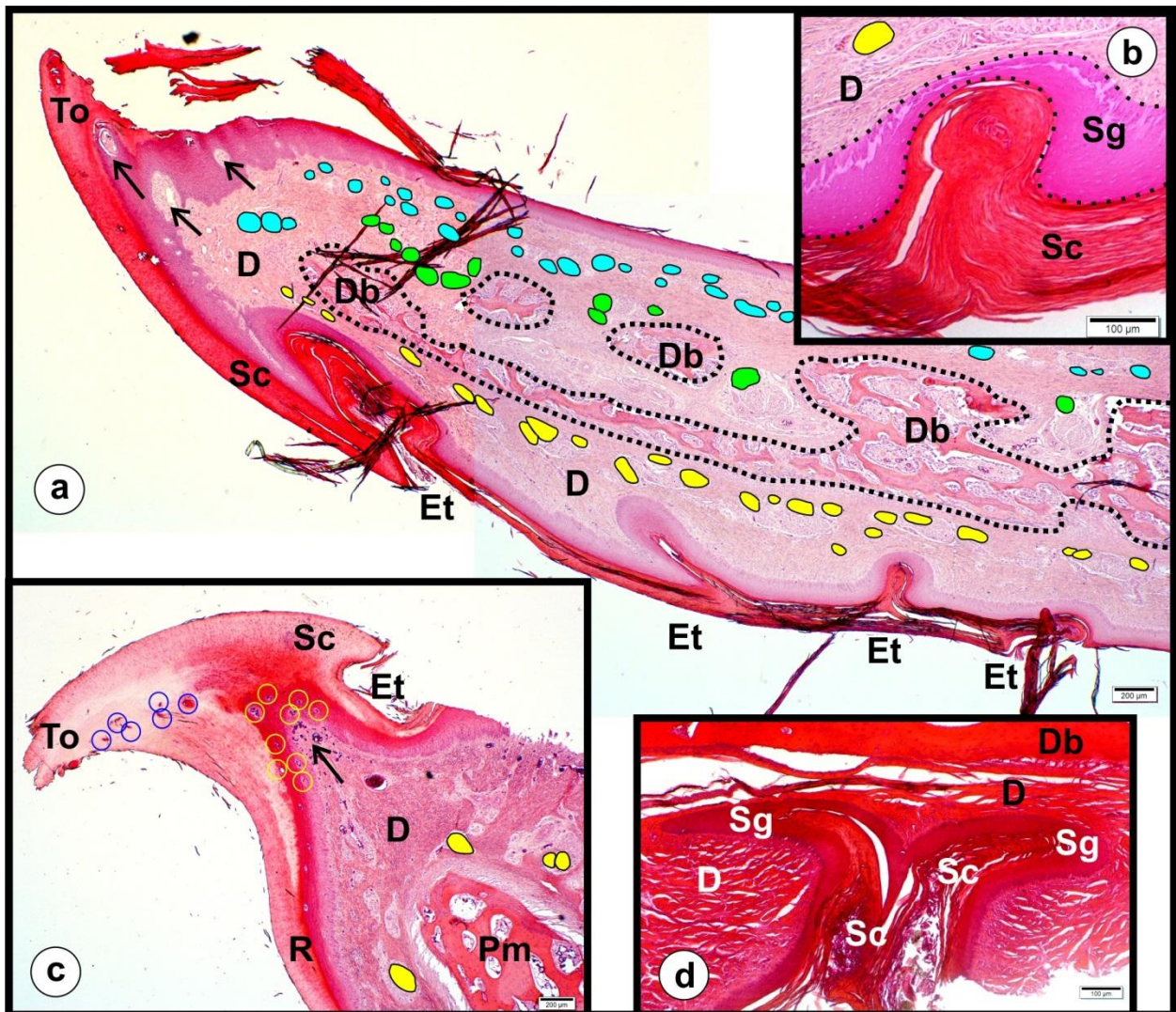


Figure 4.9. (a). Longitudinal section of the mandibular rostrum in an ostrich chick. The epidermal troughs (Et) are clearly visible on the ventral surface. Note the proximity of the base of the troughs to the sheet of Herbst corpuscles (yellow dots) which are situated in the dermis (D) close to the dentary bone (Db, outlined for clarity). Cells of the *Str. corneum* (Sc) fill the troughs in concentric layers (see b) and merge smoothly with the adjacent rhamphotheca. Herbst corpuscles are also present in the bone and bony pits (green dots) and in sheets dorsally (blue dots). Tomium (To) and dermal papillae in longitudinal section (black arrows).

(b). Transverse section of an epidermal trough in an ostrich chick. The *Str. germinativum* (Sg, shaded pink) narrows near the base of the trough and a Herbst corpuscle (yellow dot) lies in the dermis (D) near the trough. *Str. corneum* (Sc)

(c). Maxillary tomium (To) in the sensory cap of an adult ostrich. A shallow epidermal trough (Et) is visible near the tomium (the keratinised elements of the *Str. corneum* have been lost during sample processing). Tubular (blue circles) horn is present in the rhamphotheca (R) of the tomium and originates from vascularised dermal papillae (yellow circles, cross section) (black arrow, longitudinal section) which project into the generative layers of the epidermis. Dermis (D), Herbst corpuscles (yellow dots), premaxillary bone (Pm).

(d). Epidermal invagination of the Gonys in an adult ostrich. Note how the invaginated *Str. germinativum* (Sg) flares and lies close to the dentary bone (Db), compressing the dermis (D). Keratinised cells of the *Str. corneum* (Sc) fill the invagination.

Occasional epidermal troughs were present intra-orally (Fig. 4.10) and displayed similar morphological features and relationships to adjacent structures as the external troughs. In the ostrich and emu the junctions demarcating the edges of the *Culmen* and *Gonys* were clearly visible macroscopically and were seen microscopically to extend deep into the dermis, in similar fashion to the epidermal troughs, and lie close to the underlying bone (Fig. 4.9d). The grooves were lined by *Str. germinativum* and filled with keratinised cells of the *Str. corneum* (Fig. 4.9d). Clusters of Herbst corpuscles, within the dermis and exiting from sensory pits, were often concentrated near the base of the troughs (Figs. 4.9a, b and 4.10).

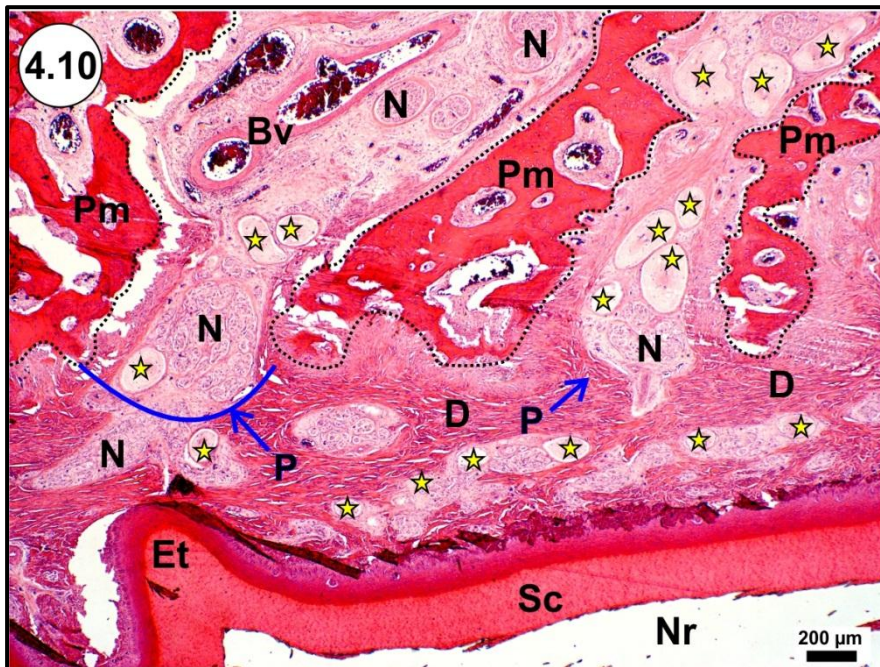


Figure 4.10. An intra-oral epidermal trough (Et) in the keratinised non-pigmented roof (Nr) of an adult ostrich. Note how the base of the trough abuts a pit (P) in the premaxillary bone (Pm) through which nerves (N) and associated Herbst corpuscles (yellow stars) communicate with the dermis. The premaxilla forms bony trabeculae (outlined) and the dermis (D) is composed of dense irregular connective tissue. The dermis is compact but richly supplied with nerves, blood vessels and Herbst corpuscles. *Str. corneum* (Sc).

On all epidermal surfaces the tall columnar cells of the *Str. basale* of the epidermis appeared to interdigitate with bundles of collagen fibres emanating from the superficial layer of the underlying dermis (Fig. 4.11). The cells of the *Str. intermedium* lay parallel to the surface and were approximately 8-12 cell layers thick (Fig. 4.11). The proximal layers displayed rounded nuclei and angular cell profiles with the characteristic spinous processes clearly visible in the intercellular space (Fig. 4.11). The more distal layers progressively flattened horizontally (including the nucleus) to eventually form a superficial layer of the *Str. intermedium* which was 1-2 cell-layers thick and was distinguished by flattened cells with a granular cytoplasm (Fig. 4.11). The *Str. corneum* consisted of multiple layers of horizontally positioned keratinised cells which became

more compressed towards the surface where desquamation occurred (Fig. 4.11). Very few obvious dermal papillae were present in these regions. Melanocytes were present in the pigmented regions of the bill and were situated in the *Str. basale* and *intermedium* (Fig. 4.11). Collections of melanin granules were observed in the overlying flattened cells of the *Str. corneum*. Towards the tomia, the tall columnar cells of the *Str. basale* were seen to angle towards the tomial edge. The interface with the underlying dermis was smooth; however, numerous well-developed dermal papillae stretched deep within the epidermis in the direction of the tomial edge (Figs. 4.9a, c, 4.12 and 4.13). These papillae were obliquely oriented, richly vascularised and lined by cuboidal cells of the *Str. basale* (Figs. 4.13b and c).

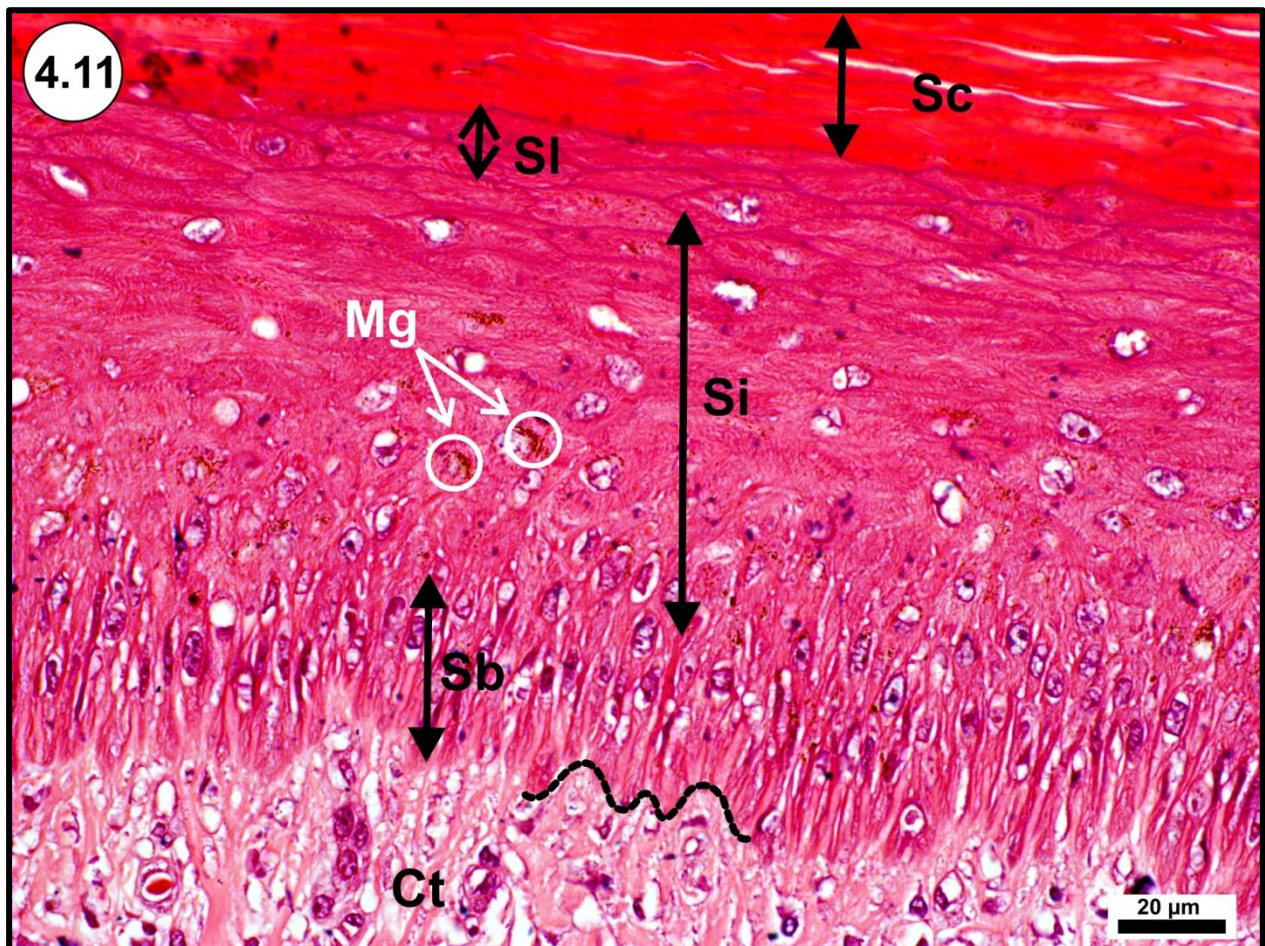


Figure 4.11. Epidermis of the mandibular arm in an adult ostrich. The typical layers forming the epidermis are demonstrated; the *Str. basale* (Sb), *Str. intermedium* (Si), superficial layer of the *Str. intermedium* (SI) and *Str. corneum* (Sc). Note how the base of the *Str. basale* cells interdigitate (black dotted line) with the underlying connective tissue (Ct). Melanin granules (Mg) present in the *Str. intermedium*.

The tomium (Fig. 4.12a) of the maxillary and mandibular rostra was a specialised region emanating from the dermis and overlying *Str. germinativum* (termed here the tomial bed). This part of the tomium was sharp, tough and projected beyond the level of the oropharyngeal roof and floor (Figs. 4.9 and 4.13). The dermal component of the tomial bed displayed numerous richly vascularised dermal papillae (Figs. 4.12a-d and 4.13) composed of finer connective tissue than that of the underlying dermis. In transverse section the tomium was a tapered structure (Fig. 4.13a) and displayed three structurally distinct layers. The internal and external layers were similar and could be likened to a *Str. externum* (of the equine hoof), each being composed of a typical *Str. corneum* as described above but not displaying tubular and inter-tubular horn (Fig. 4.13a). The internal layer (intra-orally) was non-pigmented and concave and the external layer was convex and pigmented (Fig. 4.13a). Sandwiched between these two layers was a thick core of typical tubular and inter-tubular horn (Figs. 4.12c, e and 4.13a, d), resembling a *Str. medium*, as seen in the equine hoof. Tubular horn was produced from the surface of the dermal papillae and appeared as concentric layers of flattened, keratinised cells which were strongly eosinophilic (Figs. 4.12c, e and 4.13a, d). The inter-tubular horn was formed by the *Str. corneum* originating from the surface of the dermis between the dermal papillae and was markedly less eosinophilic than the tubular horn (Figs. 4.12c-e and 4.13a, d).

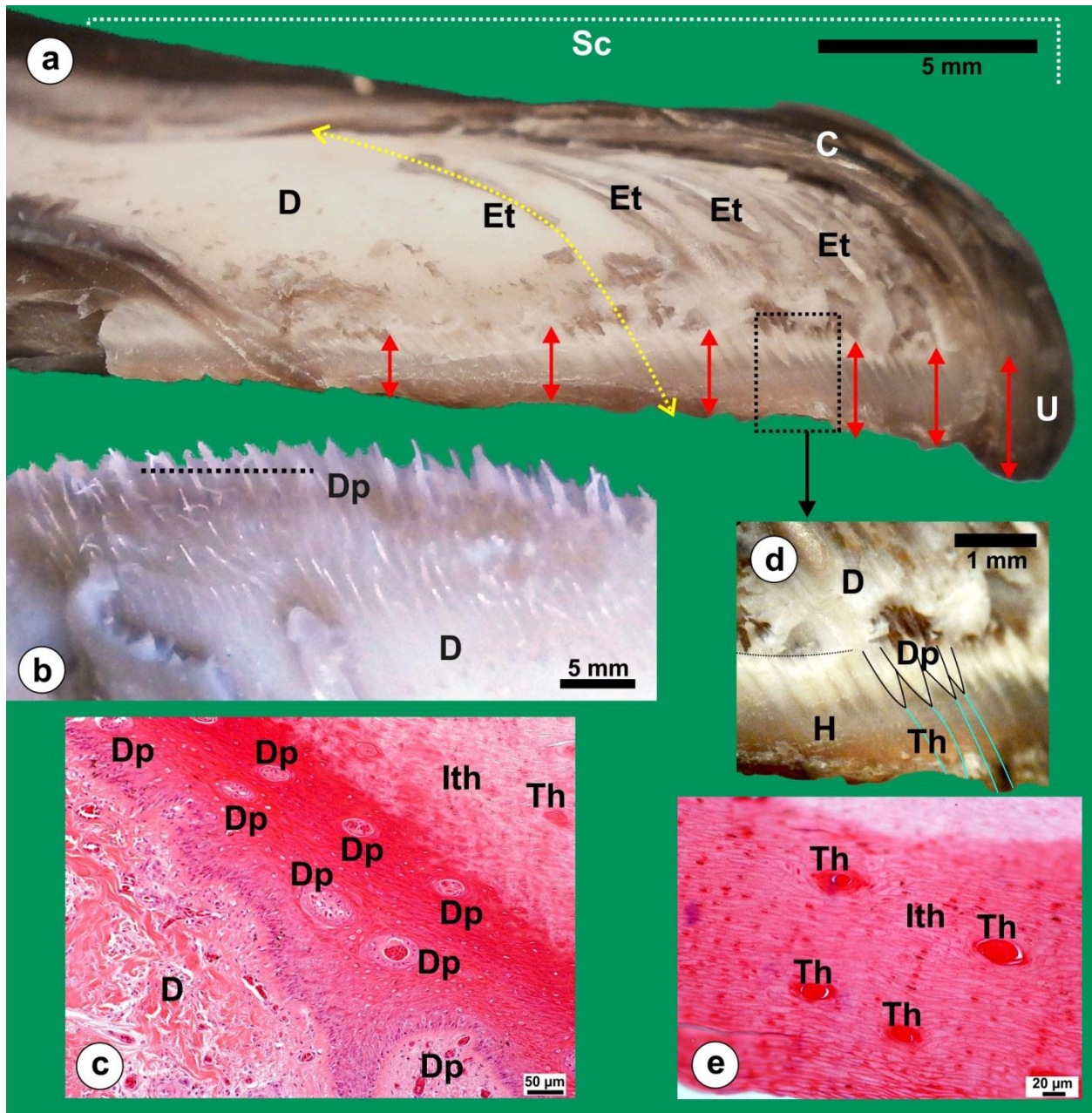


Figure 4.12. (a). Lateral view of the maxillary rostrum of an adult ostrich with the rhamphotheca of the sensory cap (Sc) partially stripped. The dermis (D) is visible as a white layer and the epidermal troughs (Et and yellow dotted line) are seen as stripes of pigmented rhamphotheca imbedded deep within the dermis. A layer of hard horn forms the tomium (Red arrows) and is longest at the *Unguis* (U). *Culmen* (C). **(b).** Lateral view of the mandibular rostrum of an adult ostrich with the epidermis stripped to reveal the underlying dermis (D). Note the myriad of fine dermal papillae (Dp) which project obliquely from the dermis in the direction of the tomium. The papillae are more robust at the tomial edge. The dotted line indicates a group of dermal papillae similar to those which appear in cross section in figure 4.12c. **(c).** Richly vascularised dermal papillae (Dp) in transverse section in the *Str. germinativum* of the tomium in an adult ostrich. Tubular (Th) and inter-tubular horn (lth) form the *Str. corneum*. Dermis (D). **(d).** Enlargement of the black square in figure 4.12a. The dermal papillae (Dp and some outlined in black) are conspicuous as white projections at the base of the horn (H). Tubular horn (Th and outlined in blue) can be seen as feint white lines projecting off the tips of the dermal papillae. Base of the horn (dotted black line) and dermis (D). **(e).** Cross section of the tomial horn in an adult ostrich. The region in figure 4.12d with tubular horn (Th) is shown here histologically. The spaces between the tubular horn is filled by inter-tubular horn, representing the *Str. corneum* of the epidermis.

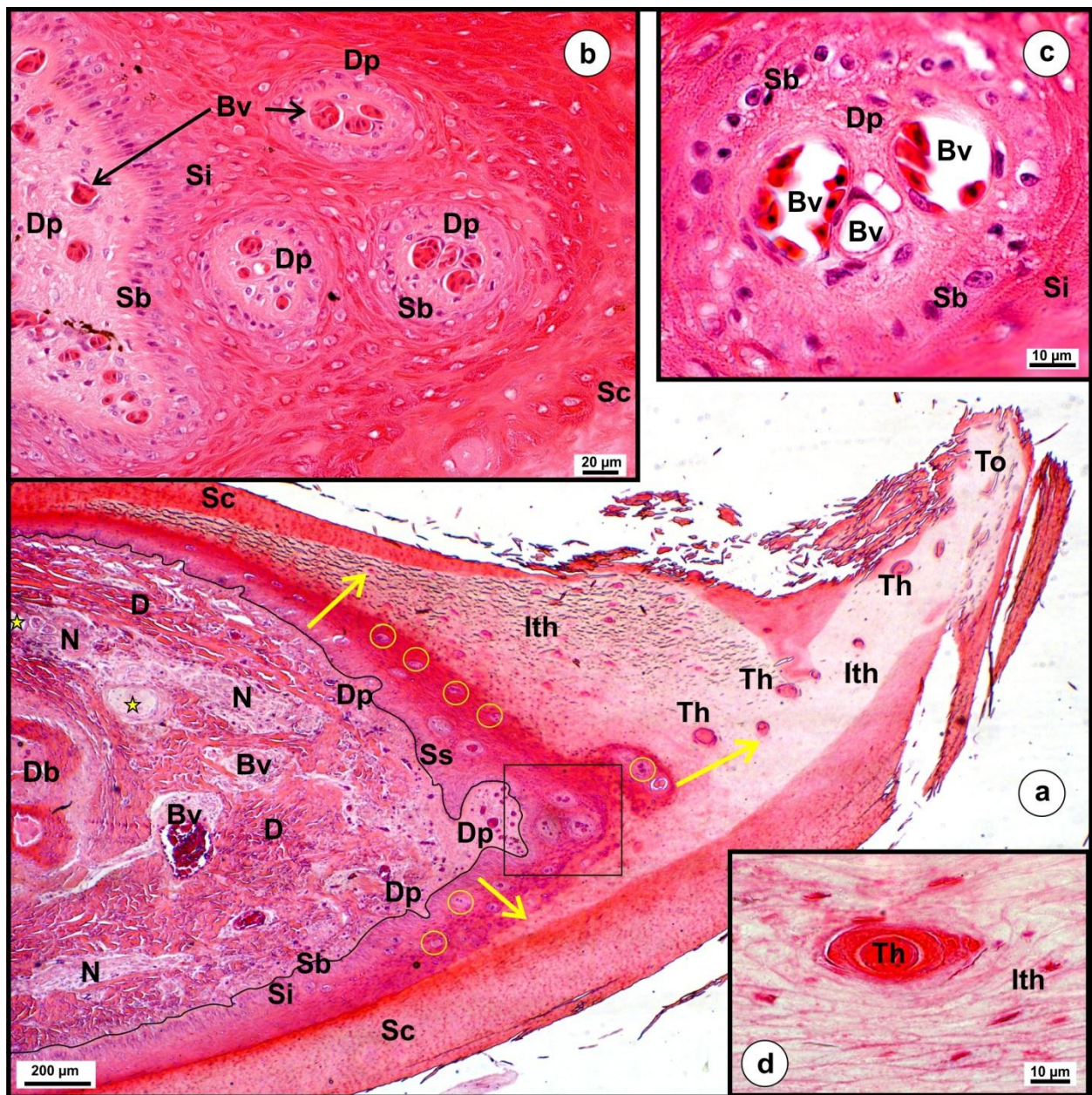


Figure 4.13. (a). Transverse section of the mandibular rostrum detailing the tomium (To) in an adult ostrich. The dermal papillae (Dp and yellow circles) are seen in cross section. The underlying dermis (D) consists of dense irregular connective tissue which houses many nerves (N), Herbst corpuscles (yellow stars) and blood vessels (Bv). The dermis in the dermal papillae is richly vascularised and is composed of loosely arranged connective tissue. The *Str. germinativum* lining the dermal papillae forms tubular horn (Th) which grows in a dorso-ventral direction in a matrix of inter-tubular horn (Ith). The base of the *Str. basale* (Sb) is outlined in black for clarity. Vascularised dermal papillae are present in the *Str. intermedium* (Si) and non-keratinised layers of the epidermis (yellow circles). *Str. corneum* (Sc) and Dentary bone (Db).

(b). Enlargement of the black square in figure 4.13a. Note the various dermal papillae (Dp) containing numerous blood vessels (Bv). *Str. basale* (Sb), *Str. intermedium* (Si) and *Str. corneum* (Sc).

(c). High magnification of a single dermal papilla (Dp). Three blood vessels (Bv) are present in a fine connective tissue matrix. *Str. basale* (Sb) and *Str. intermedium* (Si).

(d). High magnification of the horn forming the tomium. The tubular horn (Th) is concentrically arranged and is imbedded in a matrix of inter-tubular horn (Ith).

4.4. Discussion

4.4.1. External features of the bill

The findings of this study generally agree with the earlier work of Parkes and Clark (1966) in downy ratite and tinamou chicks. The rhamphotheca of the ostrich and emu is segmented and the particular pattern of segmentation appears to be unique amongst the ratites and tinamous (Parkes and Clark, 1966). In the kiwi, these segmentations or junctions were found to correspond to discrete morphological areas in the underlying bone (Cunningham *et al.* 2007), a characteristic also observed in the ostrich and emu (see Chapter 5). The morphology of the external features of the bill in the ostrich and emu, although sharing similar basic structural features such as the *Culmen*, *Gonys* and mandibular and maxillary nails (Parkes and Clark, 1966; present study), are distinct enough to allow easy differentiation between the two species based on the colour (ostrich tan and emu brown/black) and shape of the bill (ostrich U-shaped, emu V-shaped), and position of the nostrils (ostrich caudal, emu rostral). Additionally, the ostrich displays a defined region on the maxillary rostrum, named in this study the sensory cap. The demarcation of this structure, although not identified as such, is depicted in the sketch of an ostrich chick by Parkes and Clark (1966).

The *Culmen* in birds extends to the base of the feathers of the forehead and corresponds to the craniofacial angle (Clark, 1993a) which in turn corresponds to the *Zona flexoria craniofacialis*¹⁵ (Baumel and Raikow, 1993). However, the *Culmen* in the ostrich and emu differs from that described in other birds as it terminates before the craniofacial angle. The resulting strip of rhamphotheca between the *Culmen* and the *Frons* has been likened to a cere-like structure by Parkes and Clark (1966); however, this region remains unnamed in the ratites. The maxillary and mandibular nails have been discussed in the emu and reportedly assist in the tearing of food, prehension and pecking (Crole and Soley, 2010). Although the nails in the emu are sharper than those in the ostrich, they would conceivably perform a similar function in both species. The

¹⁵ "...In birds the bending zone between neurocranium and the facial skeleton is a transverse band of limited rostrocaudal extent consisting of thinned parts of the Proc. premaxillaris of Os nasale and the Proc. frontalis of Os premaxillare at their junction with the rostral ends of Os frontale and Lamina dorsalis of Os mesethmoidale. The cranio-facial connection occurs only rarely as a syndesmosis or as a synovial joint...". (Baumel and Raikow, 1993).

only observable functional difference, in respect of the external features of the bill between the ostrich and emu, is the positioning of the nostrils (which possibly relates to the relative importance of olfaction during foraging in these two species), the presence of a sensory cap in the upper bill of the ostrich (see below) and the rhamphothecal serrations in the lower bill of the emu (see below). The olfactory bulb to cerebral hemisphere ratio (expressed as a percentage) is greater in the emu (26.3) than in the ostrich (19.2) and indicates that the emu has a better developed sense of smell than the ostrich (Zelenitsky *et al.*, 2011). This is supported by the morphology and positioning of the nostrils which in the emu are situated near the tip of the bill and open rostrally, whereas in the ostrich they are more caudally located on the upper bill and open dorsally. However, the basic similarities in gross bill structure identified in these species would appear to further support the conclusion of Parkes and Clark (1966) that the ostrich and emu (and other ratites and tinamous) share a monophyletic origin.

4.4.2. Modifications of the epidermis and dermis

4.4.2.1. Mandibular rhamphothecal serrations and keratinised pegs in the emu

Extant birds do not possess teeth (King and King, 1979) and true teeth are known only from a few fossil birds such as *Ichthyornis* (Gingerich, 1972), *Archaeopteryx*, *Parahesperornis* and *Hesperornis* (Martin, 1984) and Enantiornithines, for example, *Sulcavis geeorum* (O'Connor *et al.*, 2013). Pseudo-teeth, rhamphothecal-covered bony projections from the jaw, have been identified in *Osteodontornis* and its relatives (Howard, 1957). However, it has been proposed that avians maintain the potential for tooth development (Harris *et al.*, 2006). Serrations of the rhamphotheca on the rostral third of the mandibular tomia in the emu have been identified by gross observation and referred to as *Lamellae rostri* (Crole and Soley, 2010), which is the term used to define the vertical ridges of rhamphotheca in flamingos and anatids used for grasping or straining food (Clark, 1993a). However, closer inspection has revealed that these structures in the emu may be more likened to vestigial 'pseudo-teeth' rather than to lamellae as they are supported by underlying bony projections, although greatly reduced, in comparison to those in *Osteodontornis* species (Howard, 1957).

The keratinised epidermal pegs located between the rhamphothecal serrations in the emu appear to be a unique morphological feature of this species. These structures may serve to anchor the rhamphothecal serrations as well as conduct vibrational stimuli from the rhamphothecal surface to the Herbst corpuscles situated within the dermis (see Chapter 3) and within the pits in the dentary bone (see Chapter 5 and 7). Thus the 'teeth' of the emu may be modified during early development to form part of an intricate sensory system.

However, the keratinised pegs also display some features of initial, but arrested, tooth development (inward growth of ectodermal cell cords reminiscent of dental lamina formation and an ensuing ectoderm/mesoderm interaction) which results in the formation of complex keratinised structures instead of typical teeth. Additional morphological evidence is further suggestive of arrested tooth formation in the emu. The keratinised pegs are closely associated with a bony groove. Both *Ichthyornis* and *Hesperornis*, in the juvenile state, have teeth set in a constricted groove, similar to that reported in young crocodylians (Martin *et al.*, 1980). Adding to this argument is the observation that when comparing tooth formation in the *talpid²* chicken mutant to that in the alligator, it was apparent that the first generation teeth in the avian embryo were markedly archosaurian (crocodylian) (Harris *et al.*, 2006). During development initial teeth are termed first generation teeth and these are the first teeth of the dentition to grow in a given position and become functional (Sire *et al.*, 2002). Studies on emu embryos may help determine whether the cylindrical keratinised pegs unique to this species share a similar origin to that of first generation crocodylian teeth, although it seems apparent that they never reach a stage which could be classified as first generation teeth.

Conflicting opinions exist regarding the potential for tooth formation in birds. The gene expression patterns in the jaw primordia of birds and mammals, up to a certain stage, are similarly expressed and development of orofacial structures involves the same genes in mammals (teeth, cartilage and bone) and birds (cartilage and bone but no teeth) (McCollum and Sharpe, 2001). This similarity in gene expression can be explained by the fact that tooth morphogenesis shares many key genes with that of jaw skeletal morphogenesis (McCollum and Sharpe, 2001). Whereas it is tempting to suggest that the emu may display the potential for tooth development, it has conversely

been stated (based on a study using the chicken genome) that the ability for birds to form teeth was lost in the ancestor of all modern birds (Sire *et al.*, 2008). This conclusion was reached by performing a search for dental protein genes in the chicken genome using BLASTN (Sire *et al.*, 2008). Although the emu genome is not yet available for study, a similar search in the future may help to determine whether this species possesses the genes for tooth development but which are not fully expressed.

4.4.2.2. Epidermal troughs and modification of the rostral tomia in the ostrich

The epidermal troughs identified in the sensory cap of the upper bill and the mandibular rostrum represents a sensory specialisation of the rhamphotheca, whereas the tomia of the maxillary and mandibular rostra represent a mechanical specialisation.

4.4.2.2.1. Epidermal troughs

The rows of epidermal troughs were a unique feature of the bill of the ostrich. These structures were located in a clearly demarcated region of the upper bill which by virtue of their close association to clusters of Herbst corpuscles, both within the dermis and sensory pits, was termed the sensory cap. The role of the sensory cap in the functioning of the bill tip organ is discussed fully in Chapter 7. The concentrations of hard keratin within the troughs may be a more suitable conductor than the dermis to deliver vibrational stimuli to the underlying clusters of Herbst corpuscles. A similar situation is seen in the mandible of the emu (see above) where keratinised pegs are associated with Herbst corpuscles and may also be a better conductor of vibrational stimuli. In contrast, in the chicken a thinner layer of keratinised tissue overlies numerous dermal papillae (with Herbst corpuscles at their base) that extend a substantial distance into the surrounding rhamphotheca (Gentle and Breward, 1986). These dermal papillae are present in the bill tip organ of the chicken which displays a hard bill due to the high degree of keratinisation (Gentle and Breward, 1986). It was thus suggested that in the presence of a hard bill, the thinner keratin layer overlying the dermal papilla may enhance sensitivity by allowing a greater deformation of soft tissues (Gentle and Breward, 1986).

4.2.2.3. The rostral tomia

In comparison to the emu (Crole and Soley, 2010; present study), the tomia in the rostral part the ostrich bill were more robust and prominent. Histologically, this part of the tomium consisted of a core of horn-like tissue sandwiched between the rhamphotheca (externally) and the *Str. corneum* of the intra-oral epithelial lining (internally). This tissue in the ostrich was associated with long dermal papillae and morphologically resembled the horn typically found in the hooves of ungulates and *Cornu* (horns) of ruminants (such as in the bovine) (Monteiro-Riviere, 2006). Horn is a specialisation of the integument, is hard and contains tubular (growing from the *Stratum germinativum* lining the dermal papillae) and inter-tubular horn, which are both keratinised components (Monteiro-Riviere, 2006). Although horn or horny tissue has been referred to in the beaks of birds (Lüdicke, 1940; Menzel and Lüdicke, 1974; Berkhoudt, 1980; Genbrugge *et al.*, 2012, van Hemert *et al.*, 2012), it would appear from these reports that the tissue described simply represents a well-developed *Stratum corneum* and not true horn composed of tubular and inter-tubular elements as seen in the ostrich. Round packets of uncornified cells have been observed in the *Stratum corneum* of the tomium in finches (Genbrugge *et al.*, 2012) but these elements differ markedly from the concentrically arranged collections of flattened cells present in the *Stratum corneum* of the tomium in the ostrich. These uncornified cells possibly represent part of the *Stratum basale* surrounding the dermal projections that push into the *Stratum corneum* (Genbrugge *et al.*, 2012). It would thus appear that the presence of true horn in the tomium of the ostrich is a unique feature amongst birds.

The dermal (corium) papillae involved in tubular horn formation in the ostrich are also present in other birds but not associated with true horn formation. Dermal papillae (projections) have been described at different locations in the bill in a number of birds (Lüdicke, 1940), including the tomium of Java and Darwin's finches (Genbrugge *et al.*, 2012), in the bill tip organ of the duck (Berkhoudt, 1976), mallard (Berkhoudt, 1980), goose (Gottschildt and Lausmann, 1974) and chicken (Gentle and Breward, 1986) and in the skin at the base of the beak in the black-capped chickadee (Van Hemert *et al.*, 2012). Contrary to the situation in the ostrich tomium, the dermal papillae associated with the bill tip organ in the duck, goose and chicken contain Herbst corpuscles (see Chapter 7) and it has been questioned whether their primary role is that of horn

(*Stratum corneum*) formation or tactile perception (Berkhoudt, 1980). Interestingly, a comparison has been drawn in earlier studies between the dermal papillae in the avian bill tip and those found in hoofs (Lüdicke, 1940; see Berkhoudt, 1980) although no indication is given to show that the avian dermal papillae produce true horn.

Based on the absence of Herbst corpuscles in the underlying dermal papillae, the horn-like tissue in the ostrich does not appear to be related to any form of sensory function and its occurrence in the tomia and maxillary and mandibular nails would presumably act to further strengthen these parts of the bill. This would suggest that, in addition to the general organisational adaptations of the bill tissues for dissipating mechanical stress (Genbrugge *et al.*, 2012), the tomium of the ostrich requires additional structural support. This may be an adaptation to the diet of the ostrich reflecting the need for strong cutting edges which functionally replace teeth and allow the ostrich to cut through tough plant material. A reduction of the postorbital ligament and the lateral bar of the upper bill in palaeognaths may be the cause of a relatively unstable configuration of the upper bill (Gussekkloo and Bout, 2005). It is thus possible that, together with a more rigid pterygoid-palatinum complex (Gussekkloo and Bout, 2005), the hard, horny tomium provides additional reinforcement of the upper bill in the ostrich. This is especially important as the palatal processes present in the emu are absent in the ostrich (see Chapter 5). The tomium of the emu (present study) and greater rhea (personal observation) does not display this structural modification (true horn). This again may be related to the specific diet of the emu (Davies, 1978) and greater rhea (Raikow, 1968) which reportedly consists of softer plant material and insects. A point of practical importance to note is that due to the highly vascularised nature and length of the dermal papillae projecting into the epidermis in the tomium of the ostrich, superficial trauma in this region, for example, pecking at sharp objects resulting in partial tearing or breaking of the tomium, will result in mild bleeding.

4.5. References

Bancroft, J.D. and Gamble, M. 2002. *Theory and Practice of Histological Techniques. Fifth edition.* China: Churchill Livingstone Elsevier.

Baumel, J.J. and Raikow, R.J. 1993. *Arthrologia*. In: Handbook of Avian Anatomy: Nomina Anatomica Avium, 2nd edition. Edited by Baumel, J.J., King, A.S., Breazile, J.E., Evans, H.E. and Vanden Berge, C. Cambridge, Massachusetts: The Nuttall Ornithological Club, No. 23. pp. 133-187.

Berkhoudt, H. 1976. The epidermal structure of the bill tip organ in ducks. *Netherlands Journal of Zoology*. **26**: 561-566.

Berkhoudt, H. 1980. The morphology and distribution of cutaneous mechanoreceptors (Herbst and Grandry corpuscles) in bill and tongue of the mallard (*Anas platyrhynchos* L.). *Netherlands Journal of Zoology*. **30**: 1-34.

Clark, G.A. Jr. 1993a. *Anatomia Topographica Externa*. In: Handbook of Avian Anatomy: Nomina Anatomica Avium, 2nd edition. Edited by Baumel, J.J., King, A.S., Breazile, J.E., Evans, H.E. and Vanden Berge, C. Cambridge, Massachusetts: The Nuttall Ornithological Club, No. 23. pp. 7-16.

Clark, G.A. Jr. 1993b. *Integumentum Commune*. In: Handbook of avian anatomy: Nomina Anatomica Avium, 2nd edition. Edited by Baumel, J.J., King, A.S., Breazile, J.E., Evans, H.E. and Vanden Berge, C. Cambridge, Massachusetts: The Nuttall Ornithological Club, No. 23. pp. 17-44.

Crole, M.R. and Soley, J.T. 2010. Gross morphology of the intra-oral *rhamphotheca*, oropharynx and proximal esophagus of the emu (*Dromaius novaehollandiae*). *Anatomia Histologia Embryologia*. **39**: 207-218.

Crole, M.R. and Soley, J.T. 2012. As rare as “emu” teeth. *Proceedings of the Microscopy Society of Southern Africa*. **42**: 18.

Cunningham, S., Castro, I. and Alley, M. 2007. A new prey-detection mechanism for kiwi (*Apteryx* spp.) suggests convergent evolution between paleognathous and neognathous birds. *Journal of Anatomy*. **211**: 493-502.

Davies, S. J. J. F., 1978. The food of emus. *Australian Journal of Ecology*. **3**: 411–422.

Genbrugge, A., Adriaens, D., De Kegel, B., Brabant, L., Van Hoorebeke, L., Podos, J., Dirckx, J., Aerts, P and Herrel, A. 2012. Structural tissue organization in the beak of Java and Darwin’s finches. *Journal of Anatomy*. **221**: 383-393.

Gentle, M.J. and Breward, J. 1986. The bill tip organ of the chicken (*Gallus gallus* var. *domesticus*). *Journal of Anatomy*. **145**: 79-85.

Gingerich, P.D. 1972. A new partial mandible of *Ichthyornis*. *The Condor*. **74**: 471-473.

- Gusseklou, S.W.S. and Bout, R.G. 2005. The kinematics of feeding and drinking in palaeognathous birds in relation to cranial morphology. *The Journal of Experimental Biology*. **208**: 3395–3407.
- Gottschaldt, K.-M. and Lausmann, S. 1974. The peripheral morphological basis of tactile sensitivity in the beak of geese. *Cell and Tissue Research*. **153**: 477-496.
- Halata, Z. and Grim, M. 1993. Sensory nerve endings in the beak skin of Japanese quail. *Anatomy and Embryology*. **187**: 131-138.
- Harris, M.P., Hasso, S.M., Ferguson, M.W.J. and Fallon, J.F. 2006. The development of archosaurian first-generation teeth in a chicken mutant. *Current Biology*. **16**: 371–377.
- Howard, H. 1957. A gigantic 'toothed' marine bird from the Miocene of California. *Santa Barbara Museum of Natural History Department of Geology Bulletin*. **1**: 1–23.
- King, A.S. and King, D.Z. 1979. *Avian Morphology: General Principles*. In: Form and Function in Birds. Vol. 1. Edited by King, A.S. and McLelland, J. London, Academic Press. pp. 1-38.
- Lüdicke, M. 1940. Aufbau und Abnutzung der Hornzähne und Hornwülste des Vogelschnabels. *Zeitschrift für Morphologie und Ökologie der Tiere*. **37**: 155-201.
- Martin, L.D. 1984. A new Hesperornithid and the relationships of the Mesozoic birds. *Transactions of the Kansas Academy of Science*. **87**: 141-150.
- Martin, L.D., Stewart, J.D. and Whetstone, K.N. 1980. The origin of birds: structure of the tarsus and teeth. *The Auk*. **97**: 86-93.
- McCollum, M. and Sharpe, P.T. 2001. Evolution and development of teeth. *Journal of Anatomy*. **199**: 153-159.
- Menzel, R. and Lüdicke, M. 1974. Funktionell-anatomische und autoradiographische Untersuchungen am Schnabelhorn von Papageien (Psittaci). *Zoologische Jahrbücher. Abteilung für Anatomie und Ontogenie der Tiere*. **93**: 175-218.
- Monteiro-Riviere, N.A. 2006. *Integument*. In: Dellmann's Textbook of Veterinary Histology. 6th edition. Edited by Eurell, J.-A., Frappier, B.L. Ames, Iowa: Blackwell Publishing. pp. 320-349.
- Nebel, S., Jackson, D.L. and Elner, R.W. 2005. Functional association of bill morphology and foraging behaviour in calidrid sandpipers. *Animal Biology*. **55**: 235-243.

- O'Connor, J.K., Zhang, Y., Chiappe, L.M., Meng, Q., Quangua, L. and Di, L. 2013. A new enantiornithine from the Yixian formation with the first recognized avian enamel specialization. *Journal of Vertebrate Paleontology*. **33**: 1-12.
- Parkes, K.C. and Clark, G.A. 1966. An additional character linking ratites and tinamous, and an interpretation of their monophyly. *The Condor*. **68**: 459-471.
- Raikow, R.J. 1968. Maintenance behavior of the common rhea. *The Wilson Bulletin*. **80**: 312-319.
- Richardson, M.K., Deeming, D.C. and Cope, C. 1998. Morphology of the distal tip of the upper mandible of the ostrich (*Struthio camelus*) embryo during hatching. *British Poultry Science*. **39**: 575–578.
- Sire, J.-V., Davit-Beal, T., Delgado, S., Van Der Heyden, C. and Huysseune, A. 2002. First-generation teeth in nonmammalian lineages: evidence for a conserved ancestral character? *Microscopy Research and Technique*. **59**: 408–434.
- Sire, J.-Y., Delgado, S.C. and Girondot, M. 2008. Hen's teeth with enamel cap: from dream to impossibility. *BMC Evolutionary Biology*. **8**: 246.
- Soons, J., Herrel, A., Genbrugge, A., Adriaens, D., Aerts, P. and Dirckx, J. 2012. Multi layered bird beaks: a finite-element approach towards the role of keratin in stress dissipation. *Journal of the Royal Society Interface*. **9**: 1787-1796.
- Tivane, C. 2008. A morphological study of the oropharynx and oesophagus of the ostrich (*Struthio camelus*). M.Sc. thesis, University of Pretoria, South Africa.
- Van Hemert, C., Handel, C.M., Blake, J.E., Swor, R.M. and O'Hara, T.M. 2012. Microanatomy of passerine hard-cornified tissues: beak and claw structure of the black-capped chickadee (*Poecile atricapillus*). *Journal of Morphology*. **273**: 226-240.
- Widowski, T. 2010. *The Physical Environment and its Effect on Welfare*. In: *The Welfare of Domestic Fowl and Other Captive Birds*. Edited by Duncan I.J.H. and Hawkins, P. Dordrecht, Heidelberg, London, New York: Springer. pp. 137-164.
- Zelenitsky, D., Therrien, F., Ridgely, R.C., McGee, A.R. and Witmer, L.M. 2011. Evolution of olfaction in non-avian theropod dinosaurs and birds. *Proceedings of the Royal Society B. Biological Sciences*. **278**: 3625–3634.

CHAPTER 5

MORPHOLOGY AND SENSORY SPECIALISATIONS OF THE BILL.

II. THE OSSEOUS COMPONENT OF THE BILL TIP

5.1. Introduction

Although the bony palatal structure of ratites has been widely studied (Müller, 1963; Webb, 1957; Bock, 1963; Dzerzhinsky, 1999; Gussekloo and Bout, 2002, 2005; Maxwell, 2009; Johnston, 2011), the morphology of the maxillary and mandibular rostra has been largely neglected. Studies on the structure of the ratite palate have generally been aimed at determining the phylogeny of this superorder (Palaeognathae) and have not focused on descriptions of anatomical structures *per se*. In ratites, studies of the skull and mandible have largely been restricted to their embryological development (Parker, 1866; Parker, 1891; Müller, 1963; Webb, 1957) with the result that the equivalent structures in adult birds are not well documented. The embryological development of the bony part of the kiwi bill has been described (Parker, 1891) and the rostral portion investigated in relation to the bill tip organ (Cunningham *et al.*, 2007). Parker (1866) described the early development of the skull in various ratite species, namely the ostrich (*Struthio camelus*), greater rhea (*Rhea americana*), emu (*Dromaeus Novae-Hollandiae* and *Dromaeus irroratus*) and dwarf cassowary (*Casuarius bennettii*); however, this study was restricted to embryological and chick specimens. The development of the cranium of the greater rhea has been described in detail (Müller, 1963). Whereas the distal maxillary tip of the hatchling ostrich has been briefly studied by scanning electron microscopy (Richardson *et al.*, 1998), no significant contribution to the morphology of the ostrich bill tip has been made. Although the mandible of the ostrich was used as a model which aimed at validating specimen-specific finite elemental models (Rayfield, 2011) this study did not address the basic descriptive anatomy of the mandible.

A specialised region of the bill tip characterised by a complex arrangement of mechanoreceptors and referred to as a bill tip organ, has been identified in numerous avian species including the woodcock and snipe (Goglia, 1964), *Limicolae* (sandpipers) (Bolze, 1968), goose (Gottschaldt and Lausmann, 1974), *Fringillidae* (finches) (Krulis, 1978), duck (Berkhoudt, 1976), mallard (Berkhoudt, 1980), chicken (Gentle and Breward, 1986), Japanese quail (Halata and Grim, 1993) and ibises (Cunningham *et al.*, 2010a, b). A bill tip organ was identified in the kiwi by the presence of numerous, obvious bony pits in the rostrum of the bill (Cunningham *et al.*, 2007), termed *Foveae corpusculorum nervosorum* (Baumel and Witmer, 1993). The sketches of Parker (1866) and digital images available on the internet (Dodd, 2013; Franzosa, 2013) of the ostrich and emu skull similarly reveal numerous small, bony pits in the bill tip. Additionally, Herbst corpuscles have been identified in the same region of both species (Crole and Soley, 2009). It is thus likely that the emu and ostrich possess a bill tip organ. In order to fully elaborate on this complex organ, this chapter describes the structure of the bony bill tip as well as enumerating and comparing the number and distribution of pits present in this region in the ostrich and emu.

5.2. Materials and Methods

A total of 13 adult ostrich and 8 adult emu heads, from birds of either sex, were collected after slaughter from the Klein Karoo Ostrich abattoir (Oudtshoorn, Western Cape Province, South Africa), Oryx Abattoir (Krugersdorp, Gauteng Province, South Africa), Emu Ranch (Rustenburg, North-West Province, South Africa) and an emu farm (Krugersdorp, Gauteng Province, South Africa). All heads were thoroughly rinsed with either distilled water or running tap water to remove mucus, blood and regurgitated food.

5.2.1. Preparation of osseous elements of the upper and lower bill

Ten fresh adult ostrich and 5 emu heads were collected and prepared for osteological examination of the bony elements relevant to the structure of the mandible and premaxilla (Figs. 5.1, 5.5-7 and 5.15-18). The heads were left at room temperature for a few days to facilitate the softening and removal of as much soft tissue as possible. Each

head was then individually secured in a muslin cloth bag and boiled in water for 24 hours in a stainless steel catering pot. This process loosened the remaining soft tissues, muscles and skin which were then manually removed from the bones. The bones, in their individual muslin cloth bags, were then placed in a degreasing plant (Proctor Industrial Cleaning Systems, Johannesburg, South Africa) and boiled in stabilized trichloroethylene for 48 hours to de-fat the bones. Two additional skulls and mandibles from previous studies on the ostrich (protocol number V023/06, Faculty of Veterinary Science, University of Pretoria) and emu (protocol number V040/08, Faculty of Veterinary Science, University of Pretoria) were also used to investigate the bony structures. The literature distinguishes between *Foveae corpusculorum nervosorum* (sensory pits) and *Foramina [Pori] neurovascularia* (neurovascular pits) in the bill tips (Baumel and Witmer, 1993). As it was not possible in the boiled specimens to determine exactly which pits carried Herbst corpuscles (sensory), blood vessels and nerves (neurovascular) or both, all the pits in the premaxilla and mandibular rostrum were studied by stereomicroscopy, counted and averaged for each head (Figs. 5.17 and 5.18). The premaxilla and mandibular rostrum were described, digitally recorded with a Canon EOS 5D digital camera (Canon, Ōita, Japan) equipped with a Canon Macro 100mm lens and annotated in Corel Draw X5. They were also viewed with an Olympus SZX16 stereomicroscope (Olympus Corporation, Tokyo, Japan) equipped with a DP72 camera and Olympus cellSens imaging software (Olympus Corporation, Tokyo, Japan) and digital images annotated in Corel Draw X5.

5.2.2. Modified differential staining of the mandibles for cartilage

The mandibles from 3 fresh ostrich and 3 fresh emu heads were disarticulated by incising through the left and right quadratomandibular joints and the esophagus to separate the upper and lower parts of the head. The soft interramal region was removed from the bony mandible by sharp incision along the inside mandibular edge. As much rhamphotheca and soft tissue as possible was removed from the underlying bone. The ostrich and emu mandibles were subsequently fixed in a solution of formalin (40%): acetic acid: alcohol (70%) (1:1:8) for 2 hours. Both sets of specimens were then treated according to the method of Kelly and Bryden (1983). Each step of this technique was followed except that alizarin red S was not applied to stain the bone. The specimens were washed in distilled water for 30 minutes (three 10 minute changes) and then

placed in Alcian blue solution (10 mg Alcian blue 8GX, 20 ml glacial acetic acid, 80 ml 95% ethanol) for 48 hours to 2 months (in the emu) to stain the cartilage. The specimens were then rehydrated through a decreasing ethanol series (95%, 95%, 75%, 40%, 15%, distilled water (at least 2 hours for each step)). They were then incubated for 72 hours at 37 °C in Trypsin enzyme solution (1g trypsin 883600; 30 ml disodium tetraborate, 70 ml distilled water) to which 5 drops of 3% hydrogen peroxide were added to bleach highly pigmented tissues. The specimens were then successively transferred to a 0.5% potassium hydroxide solution, a 3:1 0.5% potassium hydroxide and glycerol solution, a 1:1 0.5% potassium hydroxide and glycerol solution and a 1:3 0.5% potassium hydroxide and glycerol solution for at least 24 hours each (Figs. 5.2-4). The specimens were finally placed in pure glycerol to which a few thymol crystals had been added to prevent mould growth. Once stained and cleared, these specimens were used to describe the intramandibular cartilage (Meckel's cartilage) running in the mandibular neurovascular canal. They were digitally recorded with a Canon EOS 5D digital camera (Canon, Ōita, Japan) equipped with a Canon Macro 100mm lens and annotated in Corel Draw X5.

5.2.3. Light microscopy

For this part of the study the same histology slides utilised in Chapter 3.2.3 (from 5 adult ostrich and 5 adult emu) and Chapter 4.2.3 (from 5 ostrich chicks and 1 emu chick) were examined in order to describe the microscopic features of the bony bill tip. Histological sections were viewed, features of interest described and digitally recorded using an Olympus BX63 light microscope (Olympus Corporation, Tokyo, Japan) equipped with a DP72 camera and Olympus cellSens imaging software (Olympus Corporation, Tokyo, Japan), and annotated in Corel Draw X5.

5.2.4. Statistics

The null hypothesis, that the ostrich and emu are similar (in respect of the aspects studied), will be tested by a Student's *t* test (a 2 sample assuming unequal variances) or a Mann-Whitney Rank Sum Test (where the normality test (Shapiro-Wilk) and/or equal variance test has failed). Values expressed were calculated using SigmaPlot, version 12.0 (Systat Software, San Jose, CA, USA) and comprised the mean, median, standard

deviation, standard error of the mean, Mann-Whitney U statistic, significance and power of the test performed with alpha. Significance was set at $p=0.05$. A value of $p<0.05$ rejected the null hypothesis and a value of $p>0.05$ accepted the null hypothesis (Tables 5.1 and 5.2).

5.3. Results

5.3.1. Gross morphology

5.3.1.1. The mandibular rostrum

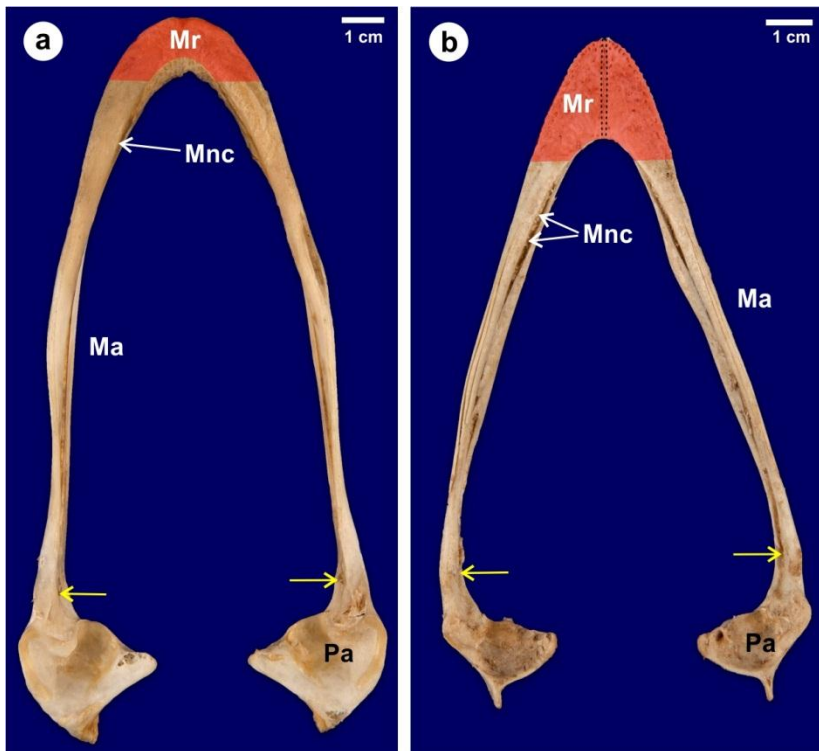


Figure 5.1. Dorsal view of the ostrich (a) and emu (b) mandible. The mandibular rostrum (Mr and shaded red) covers a larger surface area in the emu compared to the ostrich. Note the shallow dorsal groove (black dotted lines) in the emu. Mandibular arm (Ma), *Pars articularis* (Pa), point of entry of the intramandibular nerve (yellow arrows) into the mandibular neurovascular canal (Mnc).

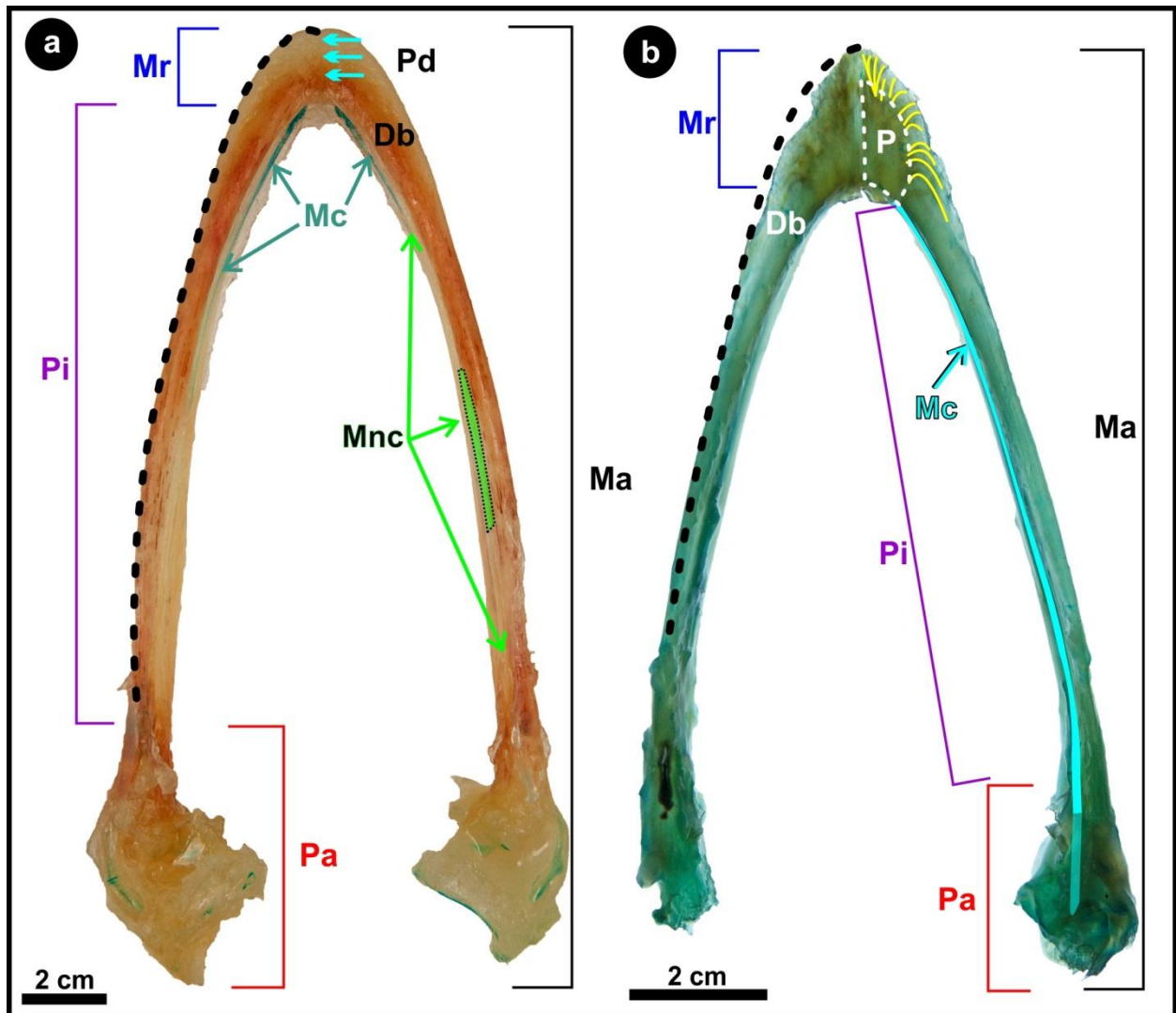


Figure 5.2. Dorsal view of the ostrich (a) and emu (b) mandible. The mandible is formed by left and right mandibular arms (Ma) which unite rostrally at the mandibular symphysis (turquoise arrows, not indicated in b). The mandibular arm comprises three components, the *Pars articularis* (Pa), *Pars intermedia* (Pi) and the mandibular rostrum (Mr). Two components of the dentary bone (Db) are visible, namely the *Pars dorsalis* (Pd, indicated in a) and the *Pars symphysialis* (turquoise arrows indicated in a). The tomial crest (dotted black line) is located dorso-laterally on the mandibular rostrum and intermediate part of the mandible. The mandibular neurovascular canal (Mnc, indicated in a) is situated medially and Meckel's cartilage (Mc), stained with alcian blue, runs within the canal. Stained and cleared specimens (Kelly and Bryden, 1983).

(b). The plexus (P) of nerves and their lateral branches (yellow outline) (see Chapter 6) are visible within the fat body (outlined in white on the right). The specimen appears blue as it was left in the alcian blue solution for 2 months to allow the cartilage to stain.

The mandible of the ostrich and emu was similarly sized; however, in the ostrich it was U-shaped and in the emu it was V-shaped (Figs. 5.1 and 5.2). The mandible was formed by a number of bones in both the ostrich and emu (Figs. 5.3 and 5.4). The dentary bone (*Os dentale*)¹ was the most rostral component and was responsible for

¹ "Synonymy: dentary; dentosplenic; mentomandibular. This is the principal element of each mandibular ramus; it articulates with the supra-angular and splenic elements by squamous sutures at the junction of intermediate and caudal segments of the ramus." (Baumel and Witmer, 1993).

forming the mandibular rostrum (*Rostrum mandibulae*)² and a portion of the distal arm of the mandible (*Ramus mandibulae*) (Figs. 5.2-4). The splenial bone (*Os spleniale*)³ was situated immediately caudal to the dentary bone and contributed to the intermediate part (*Pars intermedia*) of the mandibular arm (Figs. 5.2-4 and 5.11). The dentary and splenial bones were united by the *Sutura dentosplenialis* (Fig. 5.11). The comparative positioning of the remaining bones forming the mandible is indicated in figures 5.3-4 based on the embryological studies of Webb (1957) and Parker (1866).

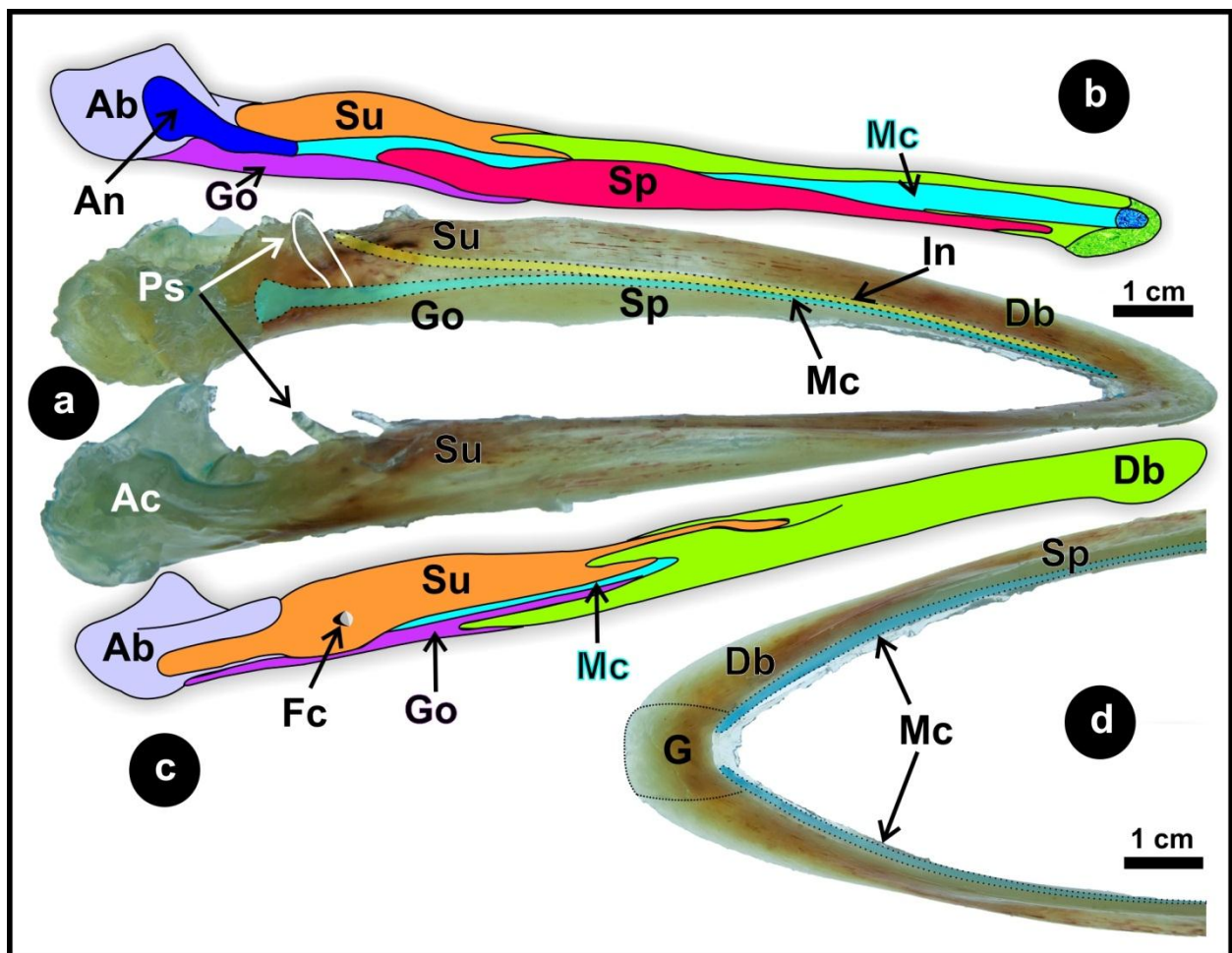


Figure 5.3. Ostrich mandible. (a) (dorso-lateral view) and (d) (ventral view): Sub-adult specimen stained with alcian blue for cartilage and the tissues cleared. (b and c). Medial (b) and lateral (c) sketch of the components forming the mandible of a 27 day-old ostrich embryo (adapted from original sketch by Webb, 1957). Meckel's cartilage (Mc, outlined in a and d for clarity) is still clearly visible in this 12-14 month old ostrich, the rostral ends of which terminate at the bony region underlying the Gonys (G), without fusing. The intramandibular nerve (In, outlined and coloured yellow for clarity) is closely associated with Meckel's cartilage. Dentary bone (Db), splenial bone (Sp), supra-angular bone (Su), gonial bone (Go), angular bone (An), articular cartilage (Ac), articular bone (Ar), *Fenestra mandibularis caudalis* (Fc) and tendinous insertion of *M. pseudotemporalis superficialis* onto the caudo-dorsal aspect of Meckel' cartilage.

² "The rostrum is the pointed, apical region of the mandible formed by the union of the symphyseal segments of the right and left mandibular rami." (Baumel and Witmer, 1993).

³ "Synonymy: *Os operculare*" (Baumel and Witmer, 1993).

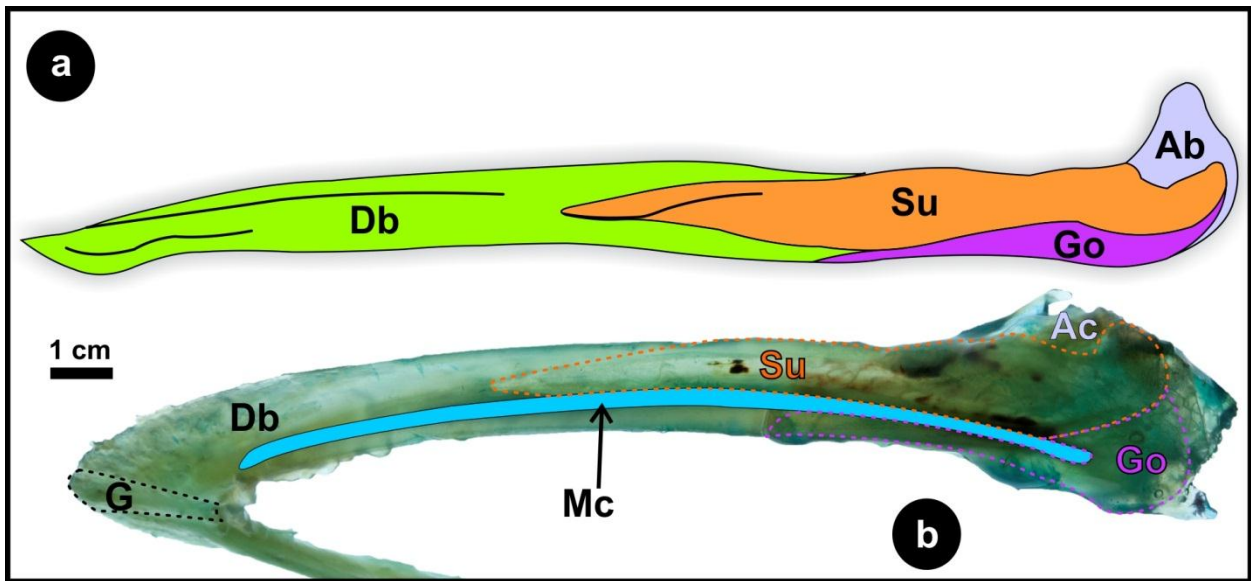


Figure 5.4. Emu mandible. (a) (lateral view) and (b) (ventro-lateral view): Sub-adult specimen stained with alcian blue for cartilage and the tissues cleared. (a). Sketch of the components forming the mandible of a 6 week-old emu chick (adapted from original sketch by Parker, 1866). Meckel's cartilage (Mc, outlined and shaded blue in b for clarity) is clearly visible in this 12-14 month old emu and in this view obscures the intramandibular nerve. Dentary bone (Db), supra-angular bone (Su), gonial bone (Go) and articular cartilage (Ac) overlying the retroarticular process (Rp). The specimen in (b) appears blue as it was left in the alcian blue solution for 2 months to allow the cartilage to stain.

Three parts of the dentary bone could be identified, the dorsal part (*Pars dorsalis*), the ventral part (*Pars ventralis*) and the symphyisial part (*Pars symphyisialis*)⁴ (Fig. 5.2). The tomial crest (*Crista tomialis*)⁵ was situated on the dorso-lateral edge of the dentary bone and continued caudally along the mandibular arm (Fig. 5.2). The intramandibular nerve (see Chapter 6) entered the mandibular neurovascular canal at the canal's origin, at approximately the junction of the articular and intermediate part of the mandibular arm (Figs. 5.1 and 5.3a). There was no obvious bony structure indicating the opening of the mandibular neurovascular canal in either of the birds. The mandibular neurovascular canal (*Canalis neurovascularis mandibulae*)⁶ was not an entirely closed canal in either the ostrich or emu (Fig. 5.11). The canal was formed by all the bones of the mandible except for the articular bone and was wide caudally and narrowed rostrally. The canal was more open in the ostrich than in the emu and resembled a shallow groove. Located in the above canal or groove was a bar of cartilage, which was considered to represent Meckel's cartilage (Figs. 5.2-4 and 5.11). This cartilage was positioned deep within the canal/groove and for the caudal two-thirds lay ventro-lateral to the closely associated

⁴ "The symphyisial part of the mandibular ramus is the rostral segment which unites with the opposite ramus at the Symphysis mandibularis..." (Baumel and Witmer, 1993).

⁵ "Synonymy: tomial shelf. The paired sharp edges of the upper and lower jaws." (Baumel and Witmer, 1993).

⁶ "The canal conducts vessels and the intramandibular ramus of the mandibular nerve from the region of the coronoid process to the symphyisial region of the Ramus mandibulae." (Baumel and Witmer, 1993).

intramandibular nerve. In the rostral third of the canal Meckel's cartilage was situated ventral and medial to the intramandibular nerve (Fig. 5.11). The proximal end of Meckel's cartilage was ossified in the region of the articular bone of the mandible. At the point of entry of the mandibular nerve into the mandibular neurovascular canal, in the ostrich, the long, narrow tendon of insertion of *M. pseudotemporalis superficialis* was attached to the medial aspect of the supra-angular bone and the caudo-dorsal aspect of Meckel's cartilage via the perichondrium (Fig. 5.3a). In the emu a small portion of the tendon was attached to the dorso-medial aspect of the supra-angular bone and the main part to the caudo-dorsal aspect of Meckel's cartilage via the perichondrium, as in the ostrich. The distal end of Meckel's cartilage was ossified in some specimens, and where this occurred, the ossified portion fused with the caudal part of the mandibular rostrum (Figs. 5.15c, e). The cartilage was more robust in the emu than in the ostrich (Figs. 5.2-4 and 5.11). At the caudal border of the mandibular rostrum were 2 (ostrich) (Fig. 5.15a) or 2-3 (emu) (Fig. 5.15b) openings (unnamed) which led into the mandibular rostrum and allowed the passage of nerves (*N. intramandibularis* see Chapter 6) and blood vessels (*A. intramandibularis* and a branch of the *A. sublingualis*).

The mandibular rostrum presented a larger surface area in the emu than in the ostrich (Fig. 5.1). In the emu it was triangular or V-shaped and in the ostrich it was U-shaped (Fig. 5.1). This resulted in the tip of the mandible being rounded in the ostrich and pointed in the emu (see Chapter 4). The tomial crest was sharper in the emu and more rounded/blunt in the ostrich (Figs. 5.15c, d). On the dorsal aspect of the rostrum the site of the mandibular symphysis was clearly marked in the emu by a shallow groove whereas in the ostrich the symphysis was not demarcated (Fig. 5.1). On the ventral aspect a raised rectangular bony prominence was present overlying the region of the mandibular symphysis. This prominence was considerably wider in the ostrich than in the emu and supported the overlying, raised thickening of rhamphotheca, the *Gonys* (Figs. 5.3-4, 5.7c, 5.15e, f, 5.16a, b and 5.17-18). Numerous openings, presumably both neurovascular foramina (*Foramina [Pori] neurovascularia*)⁷ as well as sensory pits (*Fovea corpusculorum nervosorum*)⁸, were present on the dorsal and ventral surfaces

⁷ "The ramifications of the branches of the ophthalmic and nasopalatine nerves (and companion vessels) leave their neurovascular canals via smaller Canaliculi neurovasculares that open on the surface of the bone of the upper jaw via foramina (pores) deep to the rhamphotheca (especially in the Rostrum maxillae). The foramina often open into Foveae corpusculorum nervosorum, pits or hollows beneath the rhamphotheca which house sensory corpuscles; the foveae are remarkably abundant in *Capella*." (Baumel and Witmer, 1993).

⁸ "In the bones of the maxilla and mandible these small pits deep to the rhamphotheca house sensory corpuscles;..." (Baumel and Witmer, 1993).

of the mandibular rostrum and formed specific patterns in both the ostrich and emu (see below) (Figs. 5.15 and 5.16a, b).

5.3.1.2. The premaxilla

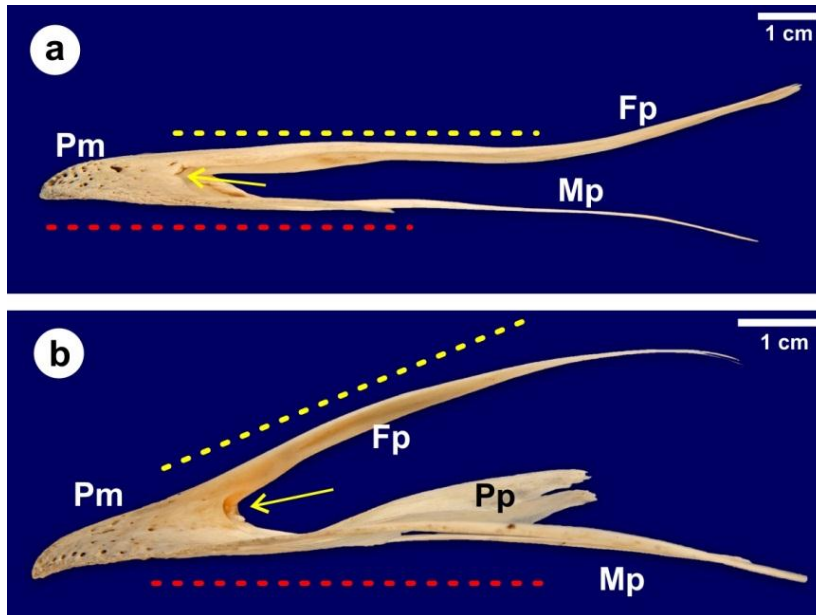


Figure 5.5. Lateral view of the ostrich (a) and emu (b) premaxilla. Note the flatter profile of the rostrum in the ostrich where the frontal process (Fp) and maxillary processes (Mp) run parallel (dotted lines) compared to the emu where an acute angle is formed between the two processes (dotted lines). Maxillary neurovascular canal (yellow arrow), premaxillary body (Pm) and palatal processes (Pp).

The rostral portion of the upper bill was supported by the premaxillary bone (Figs. 5.5, 5.6 and 5.12-14). The premaxilla was composed of a rostral body (*Corpus ossis premaxillare*) which formed the maxillary rostrum (Fig. 5.6a-b) and three (in the ostrich) (Fig. 5.6c) or five (in the emu) (Figs. 5.6d and 5.7a, b) caudally directed processes. The maxillary rostrum (*Rostrum maxillare*)⁹ was U-shaped in the ostrich and V-shaped in the emu (Fig. 5.6). In both birds the ventral (intra-oral) surface of the rostrum was concave. In lateral profile the premaxilla in the ostrich was dorso-ventrally flattened (frontal and maxillary processes positioned parallel) (Fig. 5.5a) whereas in the emu the frontal process sloped upwards relative to the maxillary processes (Fig. 5.5b). The medially positioned frontal process (*Processus frontalis*) was 3 to 4 times wider in the ostrich than in the emu (Figs. 5.6c, d). In both species the frontal process merged with the body of the premaxilla forming a raised area which, together with the frontal process, constituted the underlying bony support of the *Culmen* (Fig. 5.6c-d, 5.12-14 and 5.16a-d). The paired maxillary processes (*Processus maxillaris*) in both birds diverged laterally, tapering caudally towards their termination which lay approximately in line with

⁹ "This is the pointed, apical region of the upper jaw formed by the ankylosis of the bodies of right and left premaxillary bones that corresponds to the *Rostrum mandibulae*." (Baumel and Witmer, 1993).

the termination of the frontal process (Figs. 5.5 and 5.6c-d). Situated between the frontal process and each maxillary process in the emu were paired palatal processes (*Processus palatinus*) (Figs. 5.5, 5.6b, d, 5.7a, b and 5.14d). These processes were attached to the maxillary processes along their rostral half from where they tapered medially to end in a point (Figs. 5.6b and d). The palatal processes did not meet in the midline (Figs. 5.6b and 5.7b). Palatal processes were absent in the ostrich and this resulted in a large region being devoid of bone (Fig. 5.6a). A tomial crest (*Crista tomialis*) was present along the lateral edges of the premaxillary body and the maxillary process (Fig. 5.16c-e). The paired maxillary neurovascular canals (*Canalis neurovascularis maxillae*)¹⁰ were represented by 1-3 foramina (Figs. 5.5 and 5.15a-b). The canals could be viewed from the caudal aspect and in the ostrich were situated at the junction of the frontal and maxillary processes with the premaxillary body (Fig. 5.15a), whereas in the emu they were located at the junction of the ventral surface of the frontal process and the rostro-medial part of the palatal processes (Fig. 5.15b). As in the mandibular rostrum numerous openings, presumably both neurovascular foramina (*Foramina [Pori] neurovascularia*) as well as sensory pits (*Fovea corpusculorum nervosorum*) (Figs. 5.7a, b, c and 5.16), were present on the dorsal and ventral surfaces of the premaxillary body and formed specific patterns (Figs. 5.16c-f and 5.19) in both the ostrich and emu (see below).

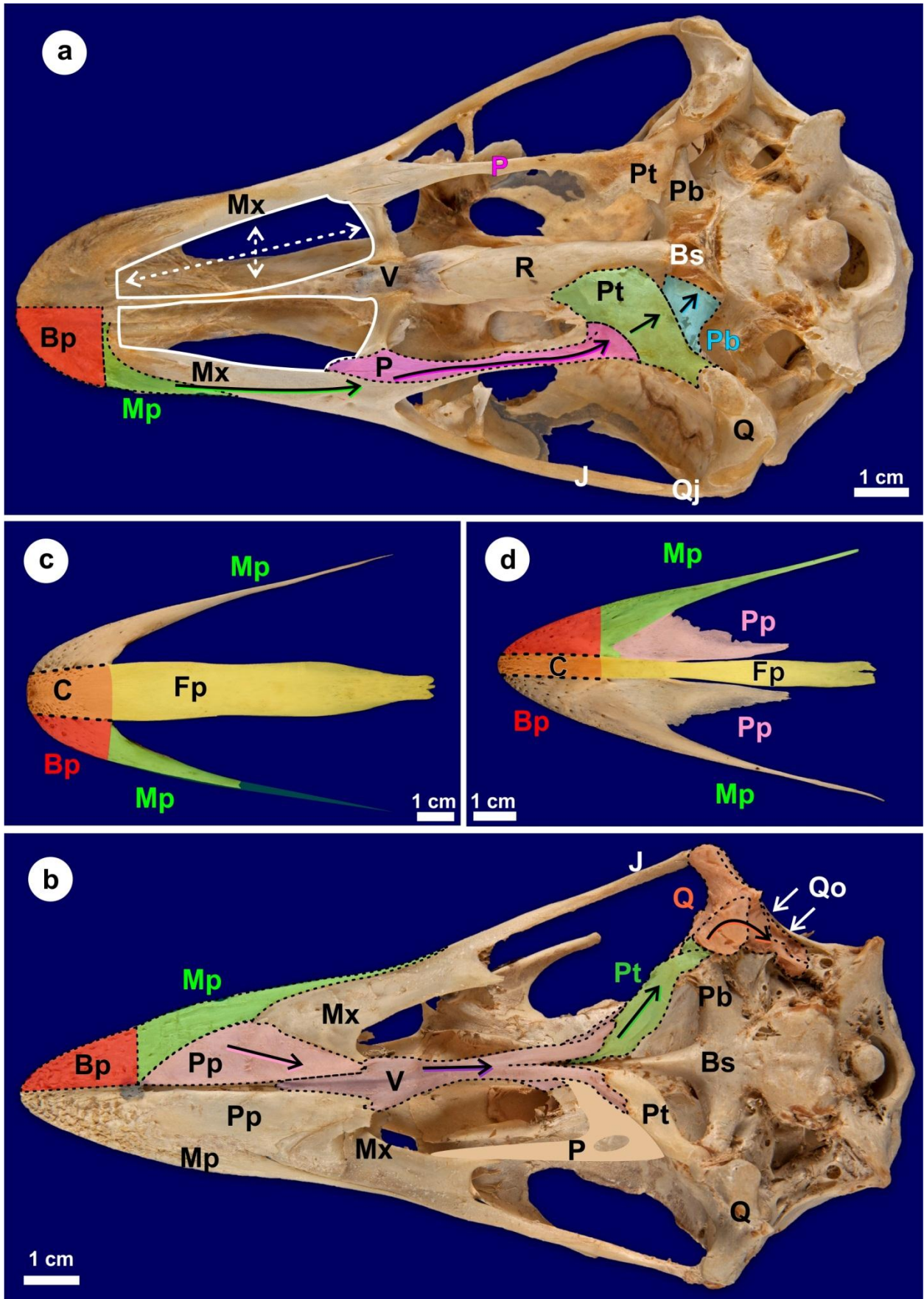
The premaxilla represented the most rostral portion of the skull in the ostrich and emu. Its relation to the surrounding bones (maxilla, palatal, vomer, rostrum, jugal, quadratojugal, quadrate, pterygoid and basisphenoid) (as depicted by Webb, 1957 and confirmed in this study) of the ventral aspect of the skull is shown in Figure 5.6a and b.

Figure 5.6. Ventral view of the ostrich (a) and emu (b) skull and dorsal view of the ostrich (c) and emu (d) premaxilla.

(a and b). The premaxilla is shown in relation to the skull. Dried rhamphotheca covers the premaxilla in the ostrich. Note the large gaps (white outline and dotted arrows) enclosed by the body of the premaxilla (Bp), maxillary process (Mp), maxilla (Mx) and vomer (V) in the ostrich. The corresponding region in the emu is filled by the palatal process (Pp). Arrows demonstrate the path followed by the force from the premaxilla to the braincase during pecking according to Dzerzhinsky (1999). The palatal bone (P) is not shown in the emu skull as it was lost during boiling, but has been schematically drawn in on the right side. Pterygoid (Pt), basisphenoid (Bs), rostrum (R), basiptyergoid process (Pb), quadrate (Q), otic process of the quadrate (Qo), quadratojugal (Qj) and jugal (J).

(c and d). Note the wider region of the premaxilla underlying the *Culmen* (C) in the ostrich compared to the emu. The body of the premaxilla (Bp) is U-shaped in the ostrich and V-shaped in the emu. Frontal process (Fp), maxillary process (Mp) and palatal process (Pp).

¹⁰ "Paired longitudinal canal that conducts the terminal branch of N. ophthalmicus and accompanying vessels from the rostral end of the nasal cavity into the Rostrum maxillae of the upper jaw (mainly in Os premaxillae). The canal is relatively long, e.g., in a heron or duck, quite short in a gull or vulture...." (Baumel and Witmer, 1993).



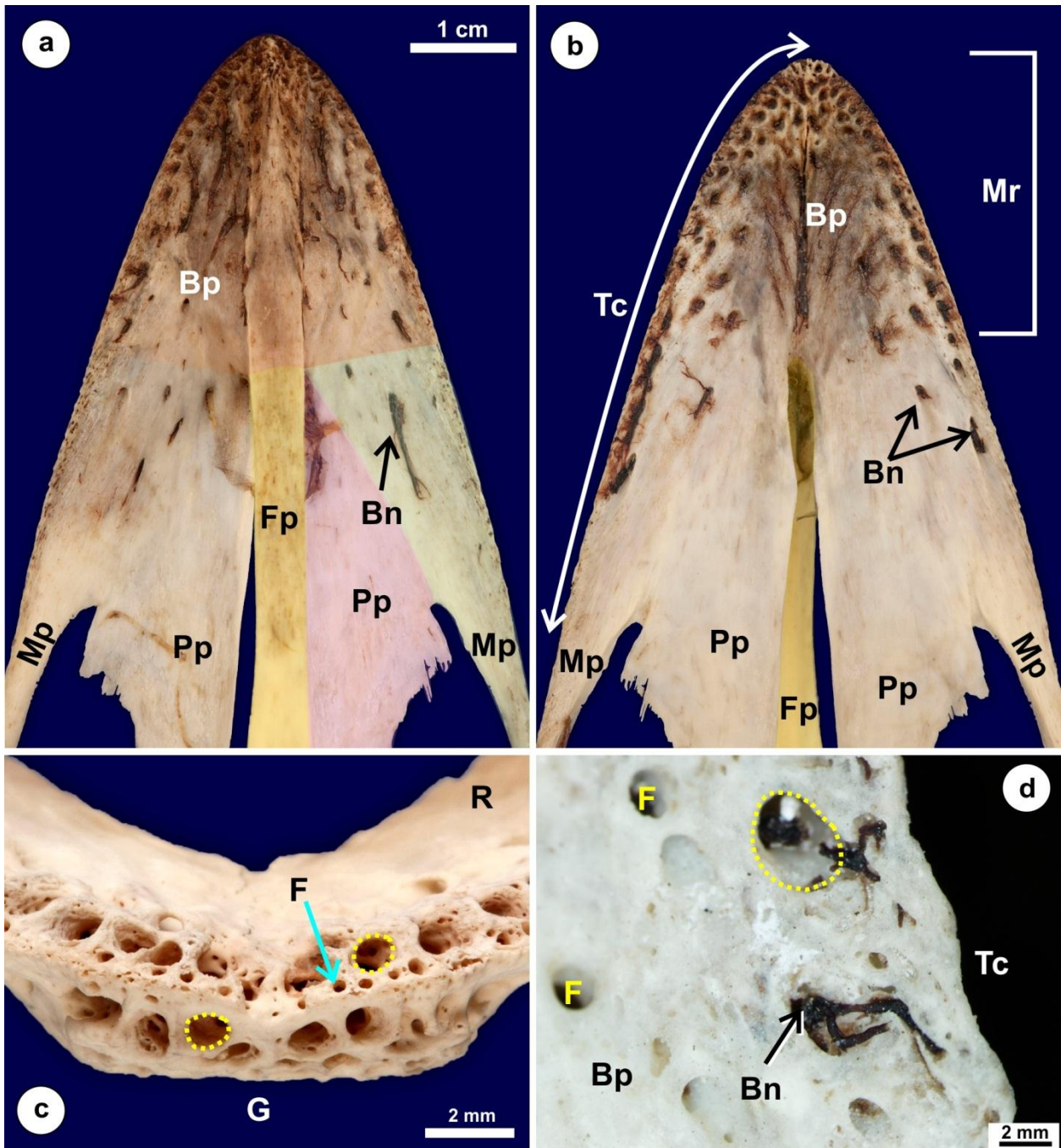


Figure 5.7. Dorsal (a) and ventral (b) views of the emu premaxilla. The tomial crest (Tc) is present on the lateral edge of the body of the premaxilla (Bp) and maxillary process (Mp, shaded green). Note the numerous blood vessels and nerves (Bn) which exit through the foramina. Maxillary rostrum (Mr), frontal process (Fp, shaded yellow) and palatal process (Pp, shaded pink).

(c). Rostral view of the mandibular rostrum in the ostrich. Note the honeycomb appearance due to the presence of numerous small foramina (F) and larger foramina (yellow circles). Mandibular arm (R) and bony region underlying the Gonys (G).

(d). High magnification of the body of the premaxilla (Bp) in the emu. Blood vessels and nerve (Bn) can be seen exiting from the large foramina (yellow circle). Smaller sized foramina (F) and tomial crest (Tc).

5.3.2. General microscopic features of the osseous bill tips

5.3.2.1. The mandibular rostrum

The dentary bone forming the mandibular rostrum was composed of dorsal and ventral parts interconnected by bony trabeculae (Figs. 5.8, 5.9 and 5.10b). The bone presented an irregular outline (Figs. 5.8 and 5.9) due to the numerous pits present in the mandibular rostrum (Figs. 5.7c, 5,15c-f and 5.16a, b). The tissue forming the dentary bone was aerated compact bone (Figs. 5.8-11) which consisted of multiple layers of lamellae with osteocytes in lacunae. In some areas typical Haversian systems (osteons) could be discerned with the lamellae concentrically arranged around a central Haversian canal. Thin-walled blood vessels were present in the canals. Many osteons were arranged parallel to the long axis of the mandibular rostrum although others were variably oriented. The interconnecting trabeculae, which appeared more concentrated at the lateral edges and rostral tip of the mandibular rostrum, enclosed numerous cavities of varying size (Figs. 5.9, 5,10b and 5.11a). The contents of the cavities differed in composition. Some cavities contained a cellular stroma similar in composition to the connective tissue/periosteum surrounding the bone, the continuity between the two presumably being facilitated by the numerous pits in the bone, while other cavities were filled with adipose tissue. Favourable sections through the pits demonstrated nerves and blood vessels traversing the space between the bony cavity and the dermis located between the dentary bone and the epidermis (Fig. 5.9). Herbst corpuscles were often visible in these openings and occasionally within the cavities, especially towards the rostral and lateral extremities of the rostrum. All cavities displayed blood vessels as well as a peripheral layer of osteoblasts indicating that bone-forming elements were present. In addition, the bigger cavities contained large arteries, veins and terminal branches of the intramandibular nerve (see Chapter 6) (Figs. 5.8, 5.9 and 5.10a). A single, large fat body, enclosed by the dorsal and ventral surfaces of the dentary bone, was present in the centre of the mandibular rostrum in the emu (Figs. 5.8, 5.9 and 5.10a) whereas in the ostrich a series of smaller cavities, which diminished in size from medial to lateral, was apparent (Figs. 5.10b and 5.11a). Meckel's cartilage (hyaline cartilage) and its close association with the intramandibular nerve was readily identified at the border of the mandibular arms and the rostrum in both species (Fig. 5.11).

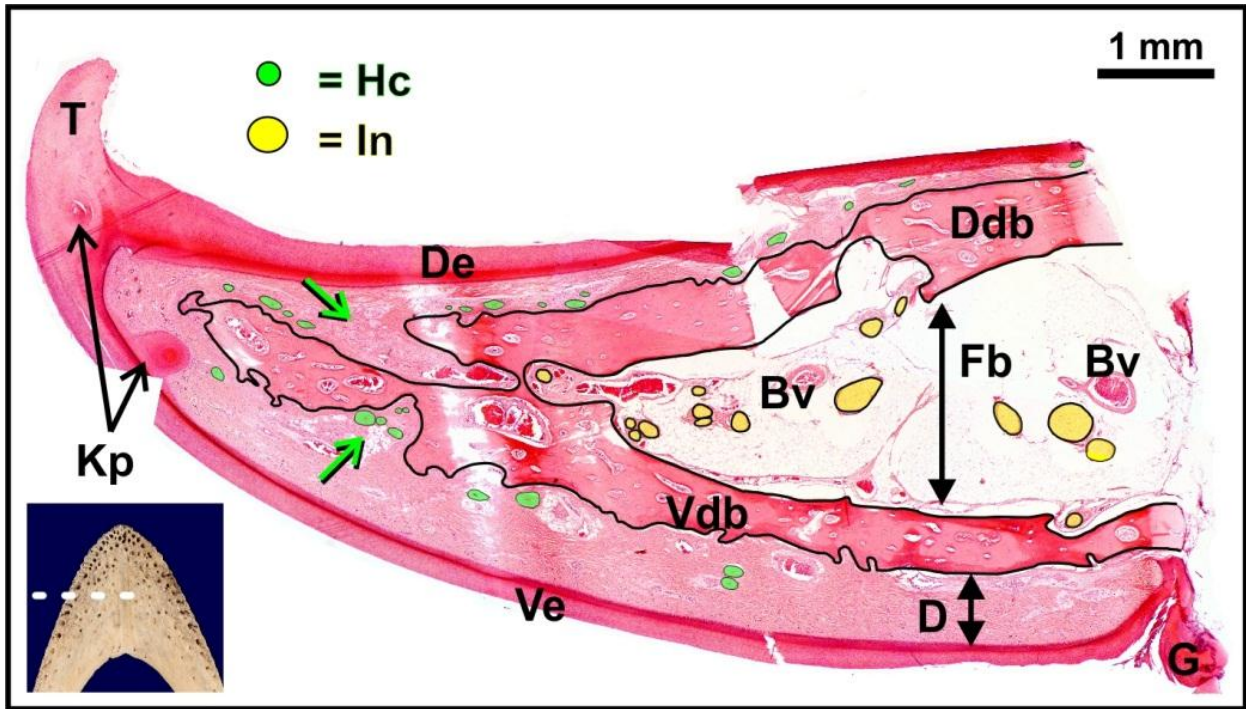


Figure 5.8. A composite micrograph illustrating one half of the emu mandibular rostrum in transverse section. A large fat body (Fb) separates the dentary bone (black outline) into a dorsal (Ddb) and ventral (Vdb) part. The fat body carries many terminal branches of the intramandibular nerve (yellow circles) as well as blood vessels (Bv). The bone displays an irregular profile reflecting the numerous pits present (green arrows), some of which house groups of Herbst corpuscles (green circles). Dorsal (De) and ventral (Ve) epithelium, dermis (D), tomium (T), keratinised pegs (Kp) and Gonys (G). **Inset:** Dorsal view of the bony mandibular rostrum indicating the plane of sectioning.

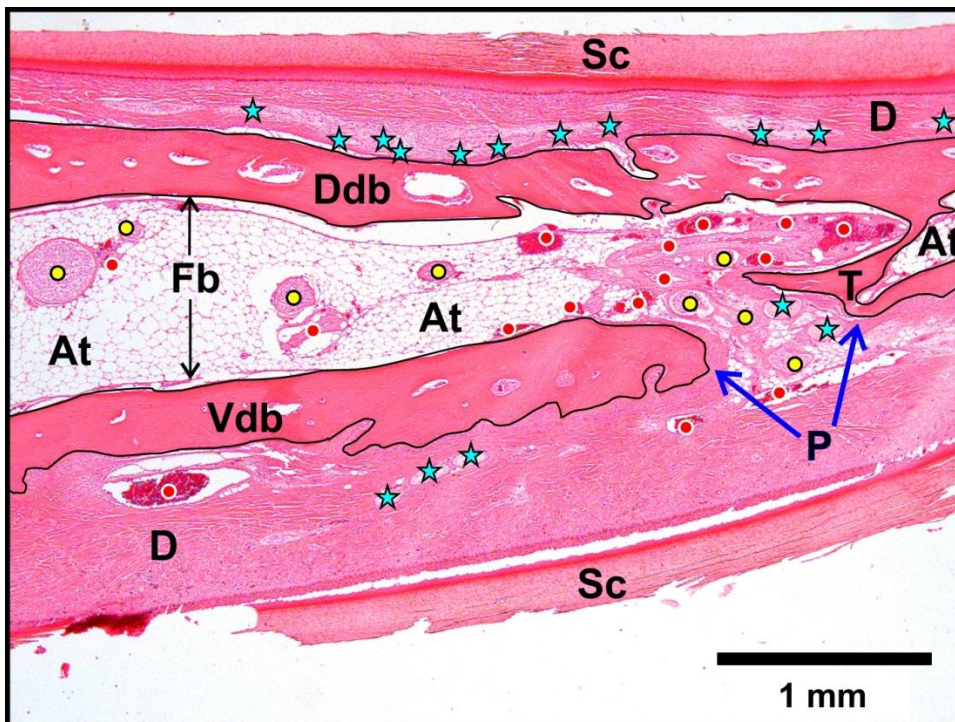


Figure 5.9. Median longitudinal section of the emu mandibular rostrum. A sensory pit (P) has been sectioned and clearly shows the continuity of blood vessels (red dots), nerves (yellow dots) and Herbst corpuscles (blue stars) between the fat body (Fb) and dermis (D). The dorsal (Ddb) and ventral (Vdb) parts of the dentary bone enclose numerous smaller cavities, separated by bony trabeculae (T). *Str. corneum* (Sc) and bone outlined in black for clarity. Adipose tissue (At).

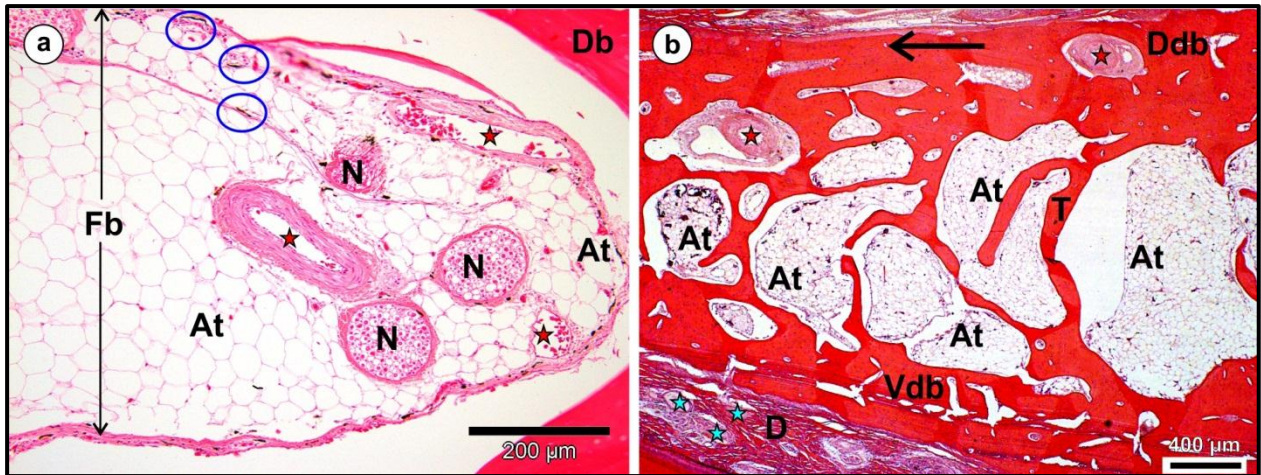


Figure 5.10. (a). Fat body (Fb) in the emu dentary bone (Db). Numerous nerves (N) and blood vessels (red stars) are present in the adipose tissue (At) as well as melanin granules (blue circles).

(b). The series of cavities present in the dentary bone in the ostrich. The dorsal (Ddb) and ventral (Vdb) parts of the dentary bone are connected by trabeculae (T). Adipose tissue (At) fills some of the cavities and occasional blood vessels (red stars) are present. Herbst corpuscles (blue stars) and dermis (D). Lateral is indicated by the arrow.

5.3.2.2. The premaxilla

The rostral extremity of the premaxilla was similar in the ostrich and emu and in both birds was composed of aerated compact bone with similar morphological properties to that of the dentary bone in the mandibular rostrum. The bone throughout the premaxilla had an irregular profile due to the many pits present in this region (Figs. 5.13b, c and 5.14b, c). Based on transverse sections of the premaxilla in ostrich and emu chicks, variations in the cavitation of the bone were noted. Present in the rostral aspect of the premaxilla were numerous smaller cavities enclosed by bony trabeculae and which contained connective tissue, numerous Herbst-corpuscles, blood vessels and terminal branches of the ventral premaxillary nerve (see Chapter 6) (Figs. 5.13a and 5.14a). Further caudally two separate cavities became apparent. Each cavity was present in the left and right body of the premaxilla, on either side of the central, raised bony region underlying the *Culmen* (Figs. 5.12, 5.13b and 5.14b) and carried the larger blood vessels and nerves. The cavities were smaller in size in the ostrich and dorso-ventrally flattened in comparison to those in the emu. In the emu they were mainly filled with adipose tissue (Fig. 5.14b) whereas in the ostrich they mostly contained a connective tissue stroma (Fig. 5.12 and 5.13b). Pigment was present throughout the cavities in the emu.

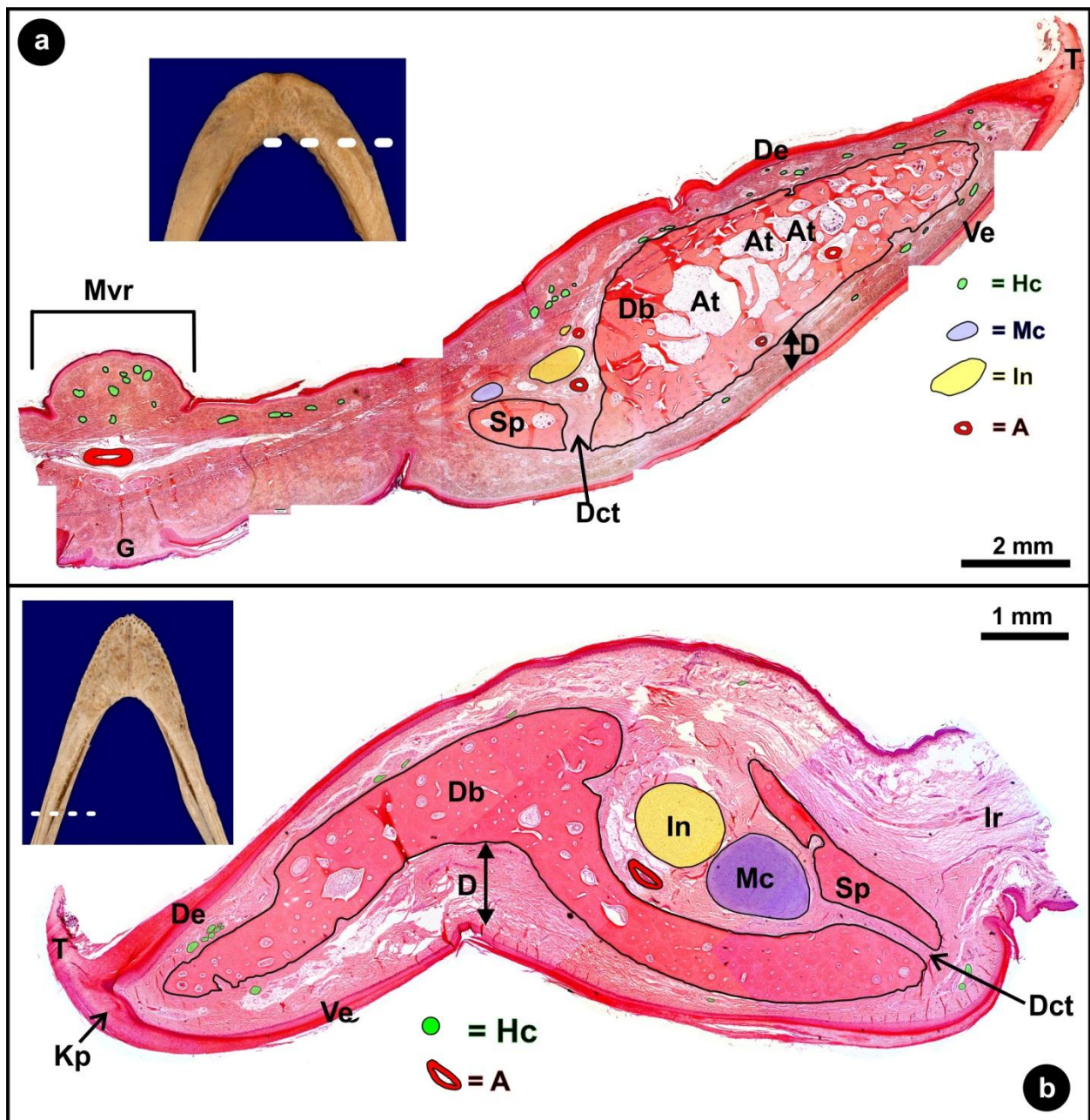


Figure 5.11. Composite micrographs showing a transverse section just caudal to the mandibular rostrum in the ostrich (a) and the mandibular arm in the emu (b). Note that Meckel's cartilage (Mc) is situated medial to the intramandibular nerve (In) and is more robust in the emu. The ventro-medial aspects of the dentary (Db) and splenial (Sp) bones are joined by dense, irregular connective tissue (Dct); the *Sutura dentosplenialis*. The dentary bone in the ostrich at this level still contains small cavities filled with mainly adipose tissue (At). Herbst corpuscles (green dots), dermis (D), tomium (T), dorsal (De) and ventral (Ve) epithelium and artery (A). Insets indicate the approximate level of sectioning.

(a). Gonys (G), median ventral ridge (Mvr).

(b). Keratinised peg (Kp) and interramal region (Ir). The tissue has been slightly distorted during processing. Insets show the approximate level of sectioning.

Heavily aerated compact bone made up the central part (underlying the *Culmen*) of this segment of the premaxilla, effectively separating the two main cavities (Figs. 5.12, 5.13b, c and 5.14b, c). Proceeding caudally, each cavity in the ostrich split into a smaller dorsal and a larger ventral part, each filled with adipose tissue, blood vessels and nerves (Fig. 5.13c). The corresponding region of the premaxilla in the emu differed in that only a single cavity was present bilaterally. These cavities were larger (Fig. 5.14c) than in the more rostral region described above. In both species, the enclosed bony cavities were not present caudally where the frontal process, maxillary processes and palatal processes (emu) of the premaxilla arose (Figs. 5.13d and 5.14d). These processes were composed of aerated compact bone.

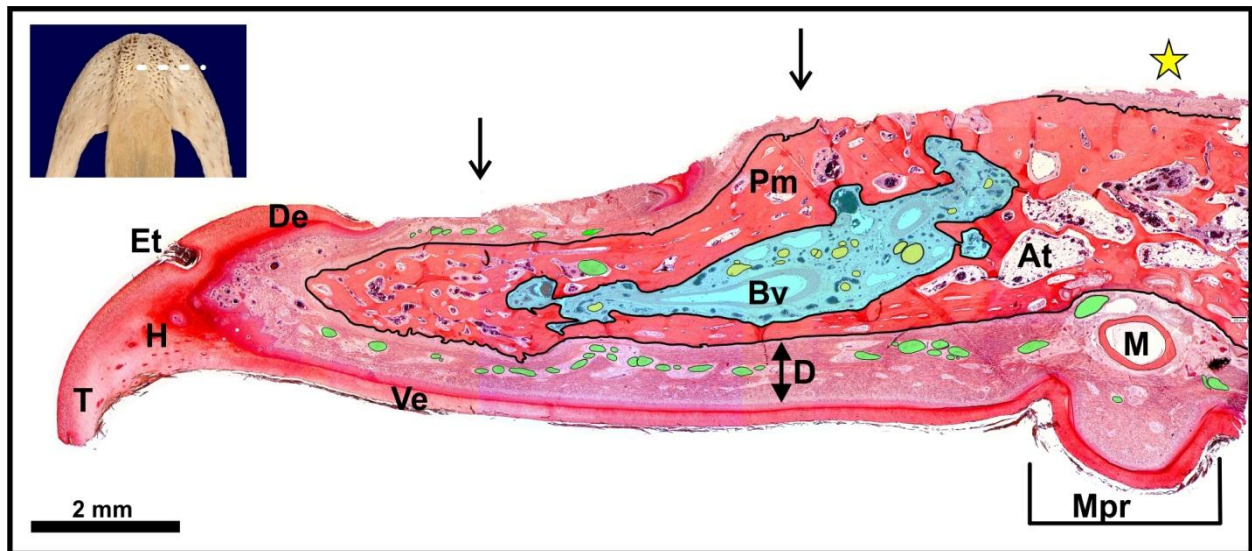


Figure 5.12. A composite micrograph of the premaxilla in the adult ostrich. Most of the dorsal epithelium has been removed (arrows) to facilitate processing. A single cavity (shaded in blue) is present in this portion of the rostrum (see Fig. 5.13b) and is filled with adipose tissue (At), blood vessels (Bv) and nerves (yellow dots). Dorsal (De) and ventral (Ve) epithelium, tomium (T), epidermal trough (Et), horn (H), dermis (D), Herbst corpuscles (green dots), median palatine artery (M), median palatine ridge (Mpr), premaxilla (Pm) and the region of the *Culmen* (star). Inset indicates the approximate level of sectioning.

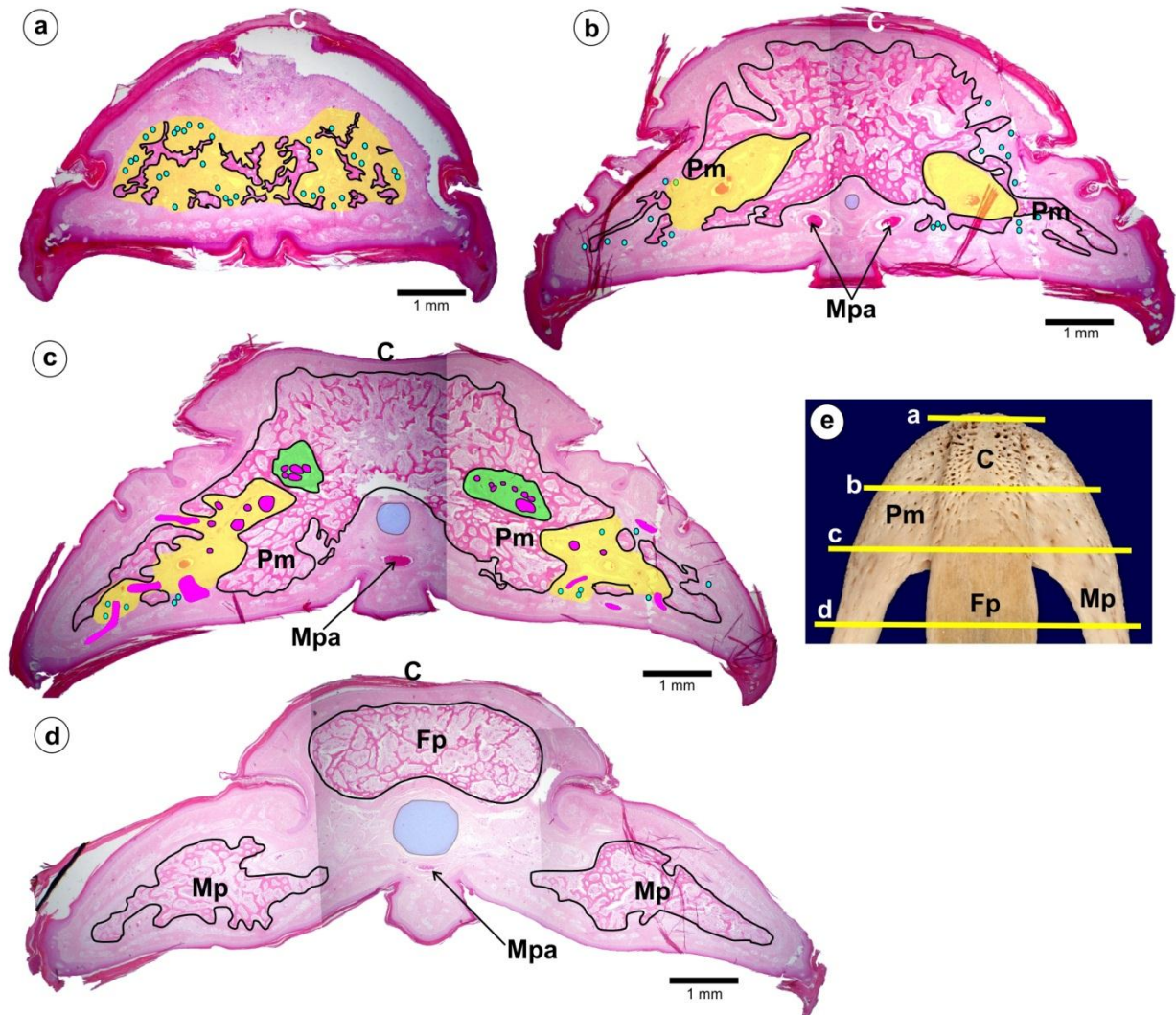


Figure 5.13. Composite micrographs of serial transverse-sections of the premaxilla (Pm) in an ostrich chick (a-d) with the location of each section indicated on an adult ostrich premaxilla (e).

(a). The bone has an irregular profile and encloses numerous ill-defined cavities (shaded yellow) with Herbst corpuscles (blue dots). *Culmen* (C).

(b). The premaxilla (Pm) displays two main cavities (shaded yellow), one on either side of the midline (see also Fig. 5.12). The median palatine artery (Mpa) has split into two vessels.

(c). The premaxilla at this level displays paired dorsal (green) and ventral (yellow) cavities on either side of the midline. Note the continuity between the bony region underlying the *Culmen* (C) and the rest of the premaxilla. Median palatine artery (Mpa) and nerves (pink dots).

(d). The frontal process (Fp) and the maxillary processes (Mp) are formed by aerated compact bone. Median palatine artery (Mpa). The distal portion of the cartilaginous nasal septum is outlined and shaded light blue in b-d.

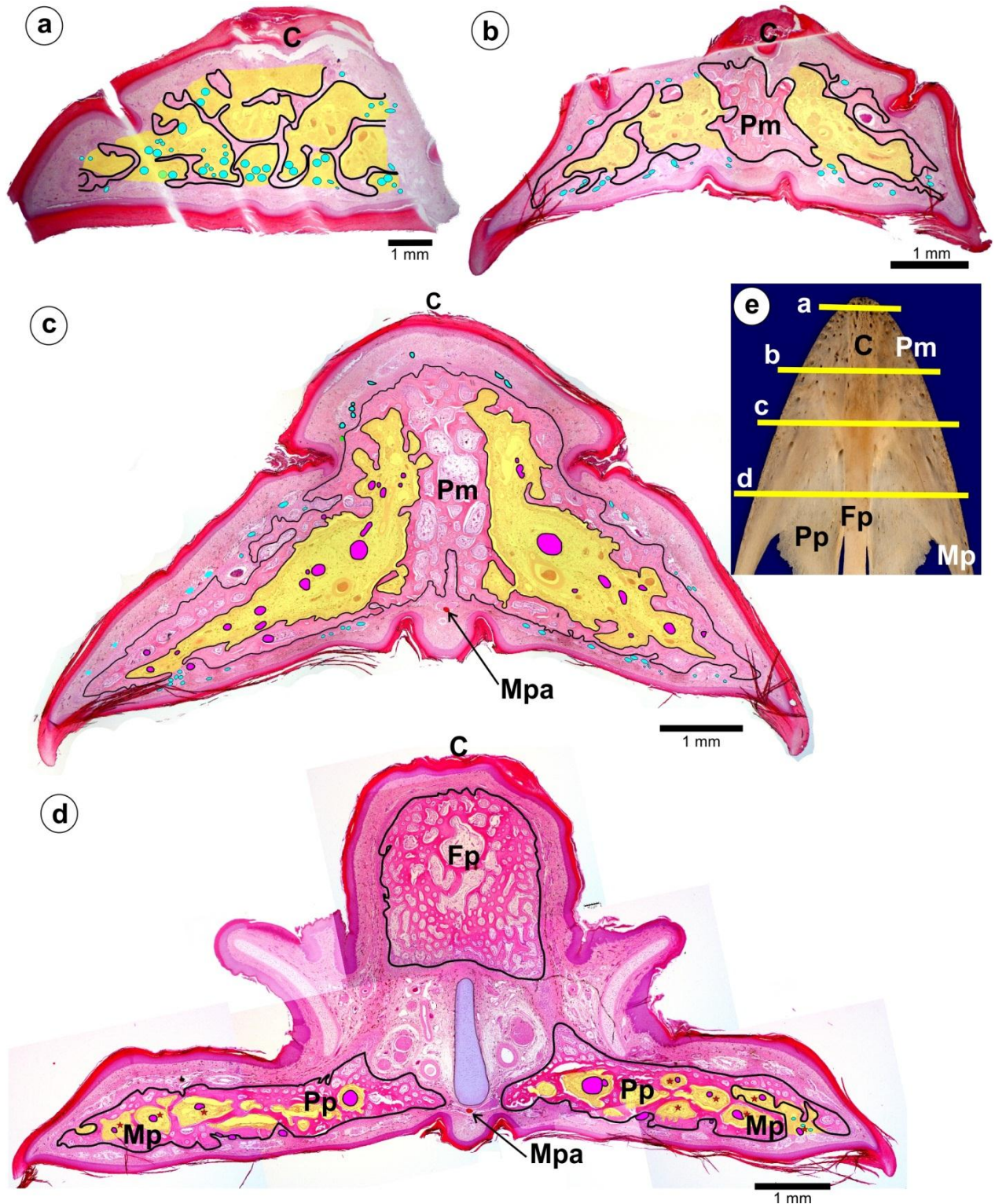


Figure 5.14. Composite micrographs of serial transverse-sections of the premaxilla (Pm) in an emu chick (a-d) with the location of each section indicated on an adult emu premaxilla (e). (a). The bone has an irregular profile and encloses numerous ill-defined cavities (shaded light yellow) with Herbst corpuscles (blue dots). *Culmen* (C). **(b).** The premaxilla (Pm) displays single main cavities (shaded yellow) on either side of the midline. **(c).** The premaxilla at this level displays larger paired cavities (shaded yellow) on either side of the midline. Note the continuity between the bony region underlying the *Culmen* (C) and the premaxilla. Median palatine artery (Mpa) and nerves (pink dots). **(d).** The frontal process (Fp) and the maxillary (Mp) and palatal (Pp) processes are formed by aerated compact bone. At this level the maxillary and palatal processes contain numerous fat-filled cavities (shaded yellow) carrying nerves (pink dots) and blood vessels (red stars). Median palatine artery (Mpa) and the distal portion of the cartilaginous nasal septum (outlined and shaded light blue).

5.3.3. The distribution and number of pits in the bill tip

5.3.3.1. Distribution of pits

Numerous neurovascular openings and sensory pits were present on the dorsal and ventral surfaces of the mandibular and maxillary rostra and extended a short distance onto the distal region of the intermediate part of the mandibular arms. The pits were round to oval in shape and slightly larger in the ostrich than in the emu. The majority of the pits opened directly to the surface; however, some of the pits displayed a slightly slanted opening which corresponded to the location of the pits (rostral pits slanted rostrally, lateral pits slanted laterally and caudal pits slanted caudo-laterally). The pits displayed a discernible pattern of distribution which was basically similar between the two species (Figs. 5.15 and 5.16).

The most rostral extremity of the bill tip in the ostrich and emu was densely packed with pits resulting in this region adopting a honey-comb appearance (Figs. 5.16a, b). Viewed rostrally this concentration of pits was mostly in the bony regions underlying the *Culmen* and *Gonys* in both species (Figs. 5.16a, b) although in the emu the immediate surrounding bone was also heavily pitted (Fig. 5.16b). Large holes were visible in caudal view (Figs. 5.15a, b) but were not considered to represent bill tip pits. These cavities allowed the entry of large blood vessels and nerves such as the *R. medialis N. ophthalmicus*, the *N. intramandibularis*, the median palatine artery and a branch of the sublingual artery into the mandibular rostrum and premaxilla (Figs. 5.15a, b and 5.15c, d, e).

In both species three main rows of pits were present on the dorsal surface of the mandibular rostrum (Figs. 5.15c, d). Row 1 lay adjacent to the *Crista tomialis* and rows 2-3 were situated medial and parallel to row 1 (Figs. 5.15c, d). In the ostrich the pits in row 1 were smaller than those in rows 2-3, which were similarly sized (Fig. 5.15c), whereas in the emu all the pits in rows 1-3 were similarly sized (Fig. 5.15d). The more peripheral 1st and 2nd rows extended further onto the mandibular arms than the inner 3rd row (Figs. 5.15c, d). The pits were most concentrated at the rostral tip of the rostrum (Figs. 5.15c, d). The ventral surface of the mandibular rostrum differed slightly between the ostrich and emu. On the raised bony region underlying the *Gonys* in the ostrich were

4 rows of pits, on either side of the midline (Fig. 5.15e), and only 2 rows of pits in the emu (Fig. 5.15f). In both species, 3 rows of pits were present on the *Ramus mandibulae* (Figs. 5.15e, f). Similar to that seen on the dorsal surface, in the ostrich the pits in row 1 were smaller than those in rows 2-3 and not as well-defined (Fig. 5.15e), whereas in the emu the pits in rows 1-3 were similarly sized (Fig. 5.15f). Row 3 in both species was ill-defined (Figs. 5.15e, f). Similar to the pattern observed on the dorsal surface, the pits were concentrated at the rostral tip of the rostrum (Figs. 5.15e, f).

In the premaxilla the bony region underlying the *Culmen* was wider in the ostrich than in the emu (Figs. 5.16a-d). In both species the midline of this region was free of pits whereas on the lateral edges were 4 rows of pits in the ostrich (Fig. 5.16c) and 2 rows in the emu (Fig. 5.16d). As in the lower bill the pits were most heavily concentrated at the rostral tip of the rostrum, both dorsally and ventrally (Fig. 5.16). In the ostrich, the lateral parts of the dorsal premaxillary rostrum did not display a discernible pattern of pits (Fig. 5.16c), whereas in the emu, 2 ill-defined rows of pits were present (Fig. 5.16d). Three to four rows of pits were present on the ventral surface of the premaxillary rostrum in both species (Figs. 5.16e, f). Row 1, adjacent to the tomial crest, was formed by small pits and rows 2-3 in both species were ill-defined (Figs. 5.16e, f). The pits on the ventral surface in the ostrich were larger than those in the emu (Figs. 5.16e, f).

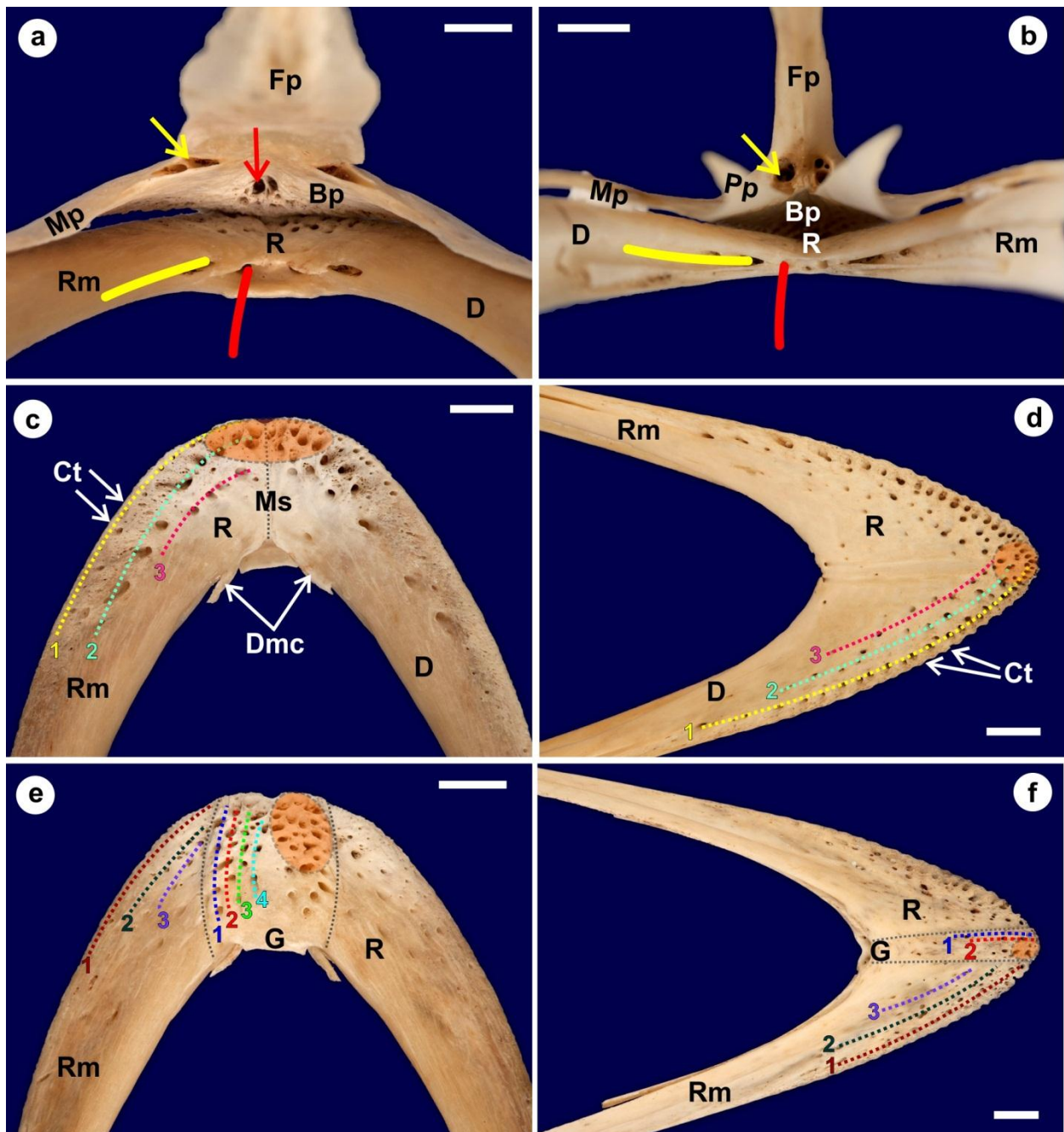


Figure 5.15. Distribution of pits in the bill tip of the ostrich (a, c, e) and emu (b, d, f). (a and b). Caudal (intra-oral) view of the bill tip. Note the body (Bp), frontal process (Fp), maxillary processes (Mp) and palatal processes (emu only) (Pp) of the premaxilla and the mandibular rostrum (R), *Ramus mandibulae* (Rm) and dentary bone (D) of the lower bill. *Canalis neurovascularis maxillae* (yellow arrow), *N. intramandibularis* (yellow line), branch of the sublingual artery (red line) and foramen for the median palatine artery (red arrow).
(c and d). Dorsal view of the mandibular rostrum (R) formed by the dentary bone (D). The distal ossified ends of Meckel's cartilage (Dmc) are obvious in the ostrich. Three main rows of pits (numbers 1-3 and dotted lines) are present in both species. Concentration of pits at the rostral tip (orange-shaded region), mandibular symphysis (Ms), *Ramus mandibulae* (Rm) and *Crista tomialis* (Ct).
(e and f). Ventral (external) view of the mandibular rostrum (R). The raised portion of the rostrum which corresponds to the external *Gonys* (G) is outlined in grey for clarity and which in the ostrich displays 4 rows and in the emu 2 rows of pits (numbers and dotted lines) on either side of the midline. In both species 3 rows of pits (numbers 1-3 and dotted lines) are present on the *Ramus mandibulae* (Rm). Concentration of pits at the rostral tip (orange-shaded region). Scale bars = 5 mm.

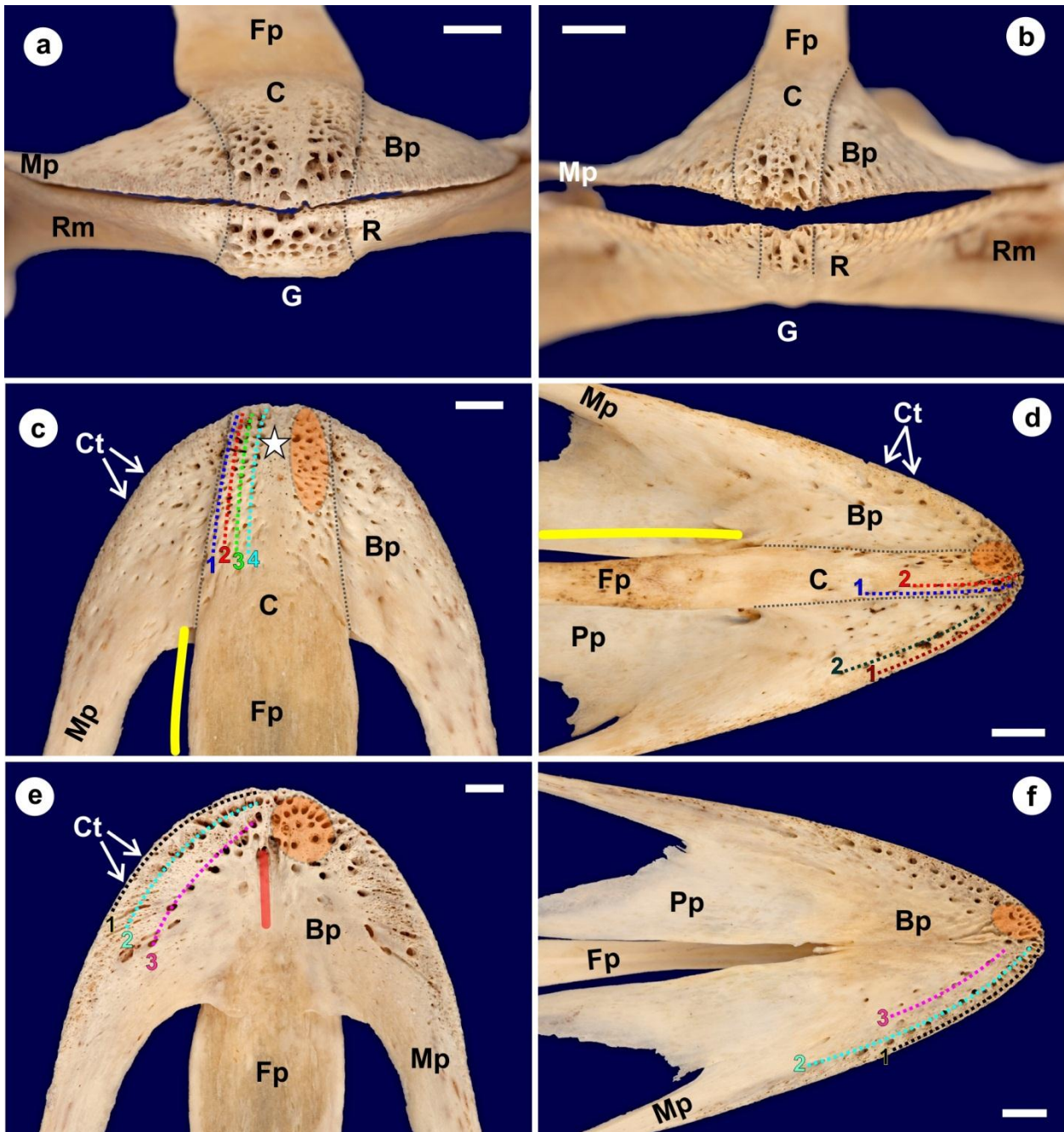


Figure 5.16. Distribution of pits in the bill tip of the ostrich (a, c, e) and emu (b, d, f). (a and b). Rostral (external) view of the bill tips. Note the body (Bp), frontal process (Fp), maxillary processes (Mp) and palatal processes (emu only) (Pp) of the premaxilla, and the mandibular rostrum (R) and *Ramus mandibulae* (Rm) of the lower bill. The part of the premaxilla (C) and mandibular rostrum (G) supporting the overlying *Culmen* and *Gonys*, respectively, are outlined in grey. Note the honey-comb appearance of the rostral bill tip due to the concentration of pits in this region.

(c and d). Dorsal view of the premaxilla. Rows of pits (numbers and dotted lines) occur on the bony region underlying the *Culmen* (C). Pits on the lateral parts of the body of the premaxilla (Bp) form rows (numbers and dotted lines) in the emu but are randomly dispersed in the ostrich. Concentration of pits at the rostral tip (orange-shaded region), region of tiny pits not counted in the ostrich (star), *Crista tomialis* (Ct), *R. medialis N. ophthalmicus* (yellow line) and palatal process (emu only) (Pp) of the premaxilla.

(e and f). Ventral (internal) view of the premaxilla. Three to four rows of pits (numbers and dotted lines) are present in both species. Median palatine artery (red line). Concentration of pits at the rostral tip of the rostrum (orange-shaded region). Scale bars = 5 mm.

5.3.3.2. Number of pits

The number of pits on the dorsal and ventral surfaces of the premaxilla and mandibular rostrum of the ostrich (Fig. 5.17) and emu (Fig. 5.18) were counted and the values compared between the different regions for the two species (Tables 5.1 and 5.2).

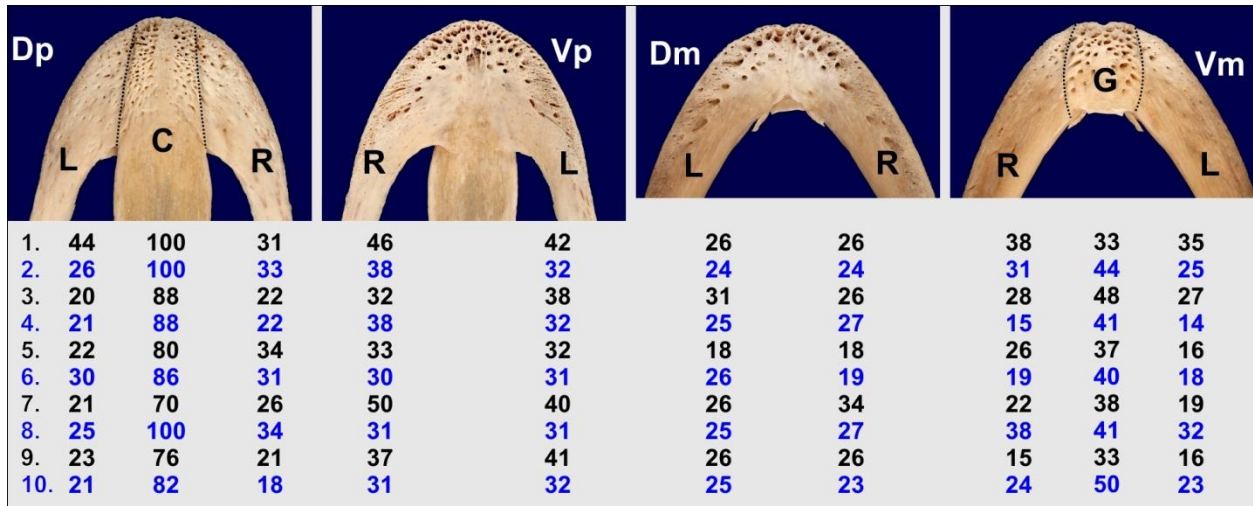


Figure 5.17. The number of pits in the premaxilla and mandibular rostrum of the ostrich. The rostral portions of the dorsal (Dp) and ventral (Vp) premaxilla and the dorsal (Dm) and ventral (Vm) mandibular rostrum are depicted. The pits were counted on the left (L) and right (R) side of each surface of the bill tips. Additionally, the pits on the bony regions underlying the *Culmen* (C) and *Gonys* (G), which are both outlined for clarity, were counted. The values reflected in each column indicate the number of pits counted in that specific region for each of the 10 specimens.

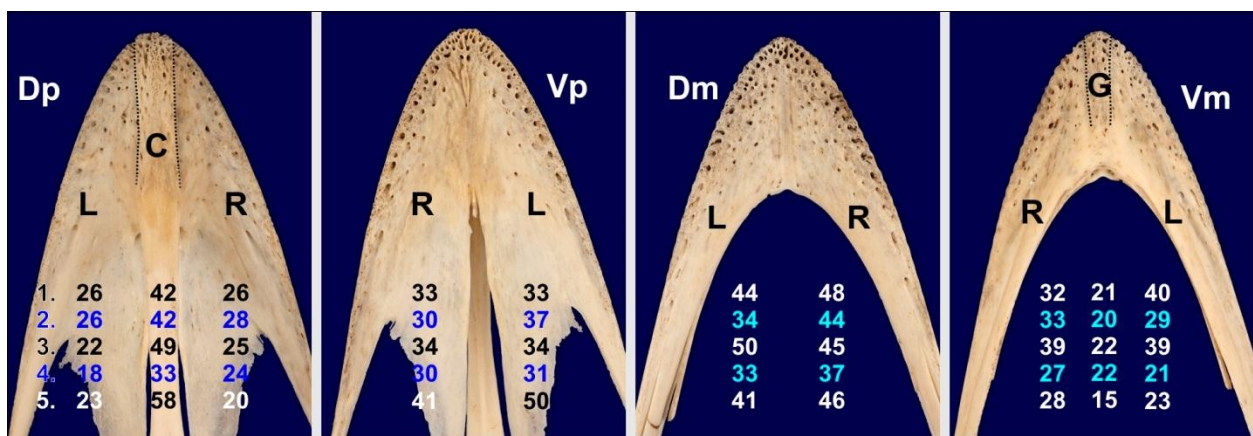




Figure 5.18. The number of pits in the premaxilla and mandibular rostrum of the emu. The rostral portions of the dorsal (Dp) and ventral (Vp) premaxilla and the dorsal (Dm) and ventral (Vm) mandibular rostrum are depicted. The pits were counted on the left (L) and right (R) side of each surface of the bill tips. Additionally, the pits on the bony region underlying the *Culmen* (C) and *Gonys* (G), which are both outlined for clarity, were counted. The values reflected in each column indicate the number of pits counted in that specific region for each of the five specimens.

Table 5.1. Comparative values for the number of pits present in the mandibular rostrum of the ostrich and emu. Yellow highlights indicate a significant difference and blue highlights indicate the power of the performed test with alpha (Pa) below the desired value of 0.8. Mandibular rostrum (MR), Normality Test (Shapiro-Wilk) (NT), Equal Variance Test (EVT), Standard Deviation (SD), Standard Error of the Mean (SEM) and Mann-Whitney U Statistic (MUS).

	n	Ventral MR			MR Ventral Total	Dorsal MR		MR Dorsal Total	MR Total
		Left	Gonys	Right		Left	Right		
Ostrich 	1	35	33	38	106	26	26	52	158
	2	25	44	31	100	24	24	48	148
	3	27	48	28	103	31	26	57	160
	4	14	41	15	70	25	27	52	122
	5	16	37	26	79	18	18	36	115
	6	18	40	19	77	26	19	45	122
	7	19	38	22	79	26	34	60	139
	8	32	41	38	111	25	27	52	163
	9	16	33	15	64	26	26	52	116
	10	23	50	24	97	25	23	48	145
Mean		22.50	40.50	25.60	88.60	25.20	25.00	50.20	138.80
Median		21	40.5	25	88	25.50	26	52	142
SD		7.17	5.68	8.34	16.61	3.16	4.50	6.61	18.79
SEM		2.27	1.80	2.64	5.25	-	1.42	2.09	5.94
Emu 	1	40	21	32	93	44	48	92	185
	2	29	20	33	82	34	44	78	160
	3	39	22	39	100	50	45	95	195
	4	21	22	27	70	33	37	70	140
	5	23	15	28	66	41	46	87	153
Mean		30.40	20.00	31.8	82.20	40.40	44.00	84.40	166.60
Median		29	21	32	82	41	45	81	160
SD		8.82	2.92	4.76	14.53	-	4.18	10.31	22.81
SEM		3.95	1.30	2.12	6.50	-	1.87	4.61	10.20
NT		Pass	Pass	Pass	Pass	Pass	Pass	Pass	Pass
EVT		Pass	Pass	Pass	Pass	Fail	Pass	Pass	Pass
MUS		-	-	-	-	0	-	-	-
p value		0.08	<0.001	0.15	0.48	0.002	<0.001	<0.001	0.03
Pa 0.05:		0.30	1	0.18	0.05	-	1	1	0.57



The differences in the mean values of the left ventral mandibular rostrum (MR), the right ventral MR and the combined left and right ventral MR between the ostrich and emu were not great enough to reject the possibility that the differences were due to random sampling variability (Table 5.1). There was no statistically significant difference between

these three regions in the ostrich and emu (Table 5.1). However, the power of the performed tests (0.3, 0.18 and 0.05 respectively) was below the desired power of 0.8 in these three regions (Table 5.1). This indicates that, due to the small sample size, a difference is less likely to be detected if one does actually exist. Therefore these results should be interpreted with caution.

The difference in the mean values of the *Gonys*, right dorsal MR, the combined left and right dorsal MR and combined dorsal and ventral MR and the difference in the median value between the left dorsal MR between the ostrich and the emu was greater than what would be expected by chance (Table 5.1). There was a statistically significant difference between these regions in the ostrich and the emu (Table 5.1). However, the power of the performed test (0.57) for the total MR was below the desired power of 0.8 (Table 5.1). This indicates that, due to the small sample size, a difference is more likely to be detected when one does not actually exist. Therefore this result should be interpreted with caution.

In summary the emu displayed more pits in the mandibular rostrum than in the ostrich (Figs. 5.17-18 and Table 5.1). This difference was due to the greater number of pits on the dorsal (intra-oral) surface of the MR in the emu compared to the ostrich (Figs. 5.17-18 and Table 5.1). Although the number of pits on the ventral surface of the MR was similar between the two species, the bony region underlying the *Gonys* in the ostrich contained twice as many pits as the comparable region in the emu (Figs. 5.17-18 and Table 5.1). Thus on the ventral MR the ostrich displayed a regional concentration of pits whereas in the emu the pits were more evenly distributed over the entire ventral surface.

Table 5.2. Comparative values for the number of pits present in the premaxilla of the ostrich and the emu. Yellow highlights indicate a significant difference and the blue highlight indicates the power of the performed test with alpha (Pa) below the desired value of 0.8. Mandibular Rostrum (MR), Normality Test (Shapiro-Wilk) (NT), Equal Variance Test (EVT), Standard Deviation (SD), Standard Error of Mean (SEM) and Mann-Whitney U Statistic (MUS).

	n	Dorsal Pm			Pm dorsal Total	Ventral Pm		Pm ventral Total	Pm Total
		Left	Culmen	Right		Left	Right		
Ostrich 	1	44	100	31	175	42	46	88	263
	2	26	100	33	159	32	38	70	229
	3	20	88	22	130	38	32	70	200
	4	21	88	22	131	32	38	70	201
	5	22	80	34	136	32	33	65	201
	6	30	86	31	147	31	30	61	208
	7	21	70	26	117	40	50	90	207
	8	25	100	34	159	31	31	62	221
	9	23	76	21	120	41	37	78	198
	10	21	82	18	121	32	31	63	184
Mean		25.30	87.00	27.20	139.50	35.10	36.60	71.70	211.20
Median		22.50	87	28.5	133.5	32	35	70	204
SD		7.24	10.51	6.09	19.67	4.56	6.77	10.42	22.04
SEM		-	3.23	1.93	6.22	-	-	-	6.97
Emu 	1	26	42	26	94	33	33	66	160
	2	26	42	28	96	37	30	67	163
	3	22	49	25	96	34	34	68	164
	4	18	33	24	75	31	30	61	136
	5	23	58	20	101	50	41	91	192
Mean		23.00	44.80	24.60	92.40	37.00	33.60	70.60	163.00
Median		23	42	25	96	34	33	67	163
SD		3.32	9.31	2.97	10.07	7.58	4.51	11.72	19.88
SEM		-	4.16	1.33	4.50	-	-	-	8.89
NT		Fail	Pass	Pass	Pass	Fail	Fail	Fail	Pass
EVT		-	Pass	Pass	Pass	-	-	-	Pass
MUS		25	-	-	-	21	18.5	22.5	-
p value		1	<0.001	0.39	<0.001	0.66	0.46	0.80	0.001
Pa 0.05:		-	1	0.05	1	-	-	-	0.97

The differences in the median values of the left dorsal premaxilla, the left ventral premaxilla, the right ventral premaxilla and the combined left and right ventral premaxilla and the mean value of the right dorsal premaxilla between the ostrich and emu were not great enough to reject the possibility that the differences were due to random sampling

variability (Table 5.2). There was no statistically significant difference between these five regions in the ostrich and emu (Table 5.2). However, the power of the performed test (0.05) was below the desired power of 0.8 in the right dorsal premaxilla (Table 5.2). This indicates that, due to the small sample size, a difference is less likely to be detected if one does actually exist. Therefore this result should be interpreted with caution.

The difference in the mean values of the *Culmen*, the combined left and right dorsal premaxilla and the combined dorsal and ventral premaxilla between the ostrich and the emu was greater than what would be expected by chance (Table 5.2). There was a statistically significant difference between these three regions in the ostrich and the emu (Table 5.2).

In summary the ostrich displayed more pits on the dorsal surface of the premaxilla than in the emu as well as on the premaxilla as a whole (Figs. 5.17-18 and Table 5.2). This difference was due to the bony region underlying the *Culmen* containing twice as many pits as the comparable region in the emu (Figs. 5.17-18 and Table 5.2). The remaining regions of the premaxilla contained a similar number of pits between the ostrich and emu (Figs. 5.17-18 and Table 5.2).

When considering the regions within each species, the differences in the mean values (\pm SD) of the dorsal (139.5 ± 19.67) and ventral (71.7 ± 10.43) premaxilla ($p < 0.001$) and the premaxilla (211.2 ± 22.04) and MR (138.8 ± 18.79) ($p < 0.001$) of the ostrich and the dorsal (92.4 ± 10.07) and ventral (70.6 ± 11.72) premaxilla ($p = 0.01$) in the emu as well as the median value of the dorsal (52) and ventral (88) MR ($p < 0.001$) in the ostrich were greater than what would be expected by chance. There was a statistically significant difference between these regions in the ostrich and the emu. However, the power of the performed test (0.75) was below the desired power of 0.8 in the emu. This indicates that, due to the small sample size, a difference is more likely to be detected when one does not actually exist. Therefore this result should be interpreted with caution.

The difference in the mean values of the ventral (82.2 ± 14.53) and dorsal (84.4 ± 10.31) MR ($p = 0.79$) and of the premaxilla (163 ± 19.88) and MR (166.6 ± 22.81) ($p = 0.8$) in the emu were not great enough to reject the possibility that the differences were due

to random sampling variability. There was no statistically significant difference between these regions in the emu. However, the power of the performed tests (0.05 and 0.05) was below the desired power of 0.8. This indicates that, due to the small sample size, a difference is less likely to be detected if one does actually exist. Therefore these results should be interpreted with caution.

When viewing the bill tip as a unit the ostrich displayed more pits on the outer surfaces (dorsal premaxilla (Table 5.2) and ventral MR (Table 5.1)) than on the inner (intra-oral) surfaces. The regional concentration of pits in the bony areas underlying the *Culmen* (Table 5.2) and *Gonys* (Table 5.1) appeared to be responsible for this effect in the ostrich. In both species the bony region underlying the *Culmen* (Table 5.2) contained twice as many pits as the corresponding *Gonys* (Table 5.1) of that species and that of the ostrich contained twice as many as that of the emu for these regions (Tables 5.1 and 5.2). The only region in which the emu displayed more pits than the ostrich was on the dorsal surface of the MR (Table 5.1). In the emu the premaxilla and MR contained a similar amount of pits.

The difference in the mean values of the total number of pits in the bill tip (premaxilla and mandibular rostra) of the ostrich (361.6 ± 45.10) and emu (329.6 ± 32.62) was not great enough to reject the possibility that the difference was due to random sampling variability. There was no statistically significant difference ($p=0.3$) between the number of pits in the bill tip in the ostrich and emu. However, their distribution differed significantly between the two birds with pits being more concentrated in the regions underlying the *Culmen* and *Gonys* in the ostrich whereas in the emu more pits were present on the dorsal surface of the mandible.

5.4. Discussion

5.4.1. Gross morphology

5.4.1.1. The mandible

The structure of the mandible revealed in the present study was similar to that previously described in the ostrich (Parker, 1866; Webb, 1957) and emu (Parker, 1866).

However, the origin of the mandibular neurovascular canal in both the ostrich and emu was not marked by a *Fossa aditus neurovascularis mandibulae*¹¹ as described in other birds (Baumel and Witmer, 1993) and it would appear that this bony feature is not present in these species. Another point of difference involved the structure of the mandibular neurovascular canal which remained partially open in the ostrich and emu (present study) and greater rhea (Müller, 1963) but is reportedly closed in other birds, for example, in the chicken (Hogg, 1983). The caudal mandibular fenestra noted in the greater rhea (Müller, 1963) was not present in the ostrich or emu, both of which displayed only one mandibular fenestra, which appeared equivalent to the rostral mandibular fenestra in the greater rhea (Müller, 1963).

A unique observation in this study was the presence and persistence of Meckel's cartilage through to adulthood (12-14 month-old birds) in both the ostrich and emu. The various bones forming the mandible and their fusion times have been studied in the chicken (from hatching to 182 days); however, Meckel's cartilage was not mentioned as being a part of the adult mandible (Hogg, 1983). The literature is silent (Bühler, 1981) on the persistence of Meckel's cartilage within the mandibular neurovascular canal of birds beyond the embryonal stage and there is no reference to a cartilage within the mandibular canal of adult mammals. However, Meckel's cartilage is present in adult lepidosaurs¹² (Holliday *et al.*, 2010) including the adult Texas blindsnake (*Leptotyphlops dulcis*) (Kley, 2006), Nile crocodile (*Crocodylus niloticus*) (personal observation) and broad-snouted caiman (*Caiman latirostris*) (Bona and Desojo, 2011).

Similar to that reported in some *Accipitres* (Webb, 1957), the rostral portion of Meckel's cartilage ossifies partly in the ostrich and emu. In birds the *Pars articularis* of Meckel's cartilage ossifies during embryonic development to form the articular bone while the rostral part is either absorbed or ossifies as the mentomandibular bone (Webb, 1957). Meckel's cartilage and its relationship to the intramandibular nerve has been described and depicted in the ostrich embryo; however, it was noted that Meckel's cartilage does not persist and is absorbed in the adult (Webb, 1957). In the ostrich (Webb, 1957), kiwi

¹¹ "Synonymy: *Fossa medialis mandibulae*. Depression on the internal aspect of *Pars caudalis* of the mandibular ramus that leads to the *aditus* or opening of the mandibular canal. The floor of the fossa often consists of thin bone, and may exhibit an opening (s), *Fenestra caudalis mandibulae*. The fossa is pronounced and extensive in many birds (e.g., *Pygoscelis*, *Gavia*, *Cathartes*, *Anser*)."
(Baumel and Witmer, 1993).

¹² "The **Lepidosauria** (from Greek meaning *scaled lizards*) are reptiles with overlapping scales. This subclass includes Squamata and Rhynchocephalia. The squamata includes snakes, lizards, and amphisbaenia. Lepidosauria is the sister taxon to Archosauria, which includes Aves and Crocodylia." (Anon, Lepidosauria. <http://en.wikipedia.org/wiki/Lepidosauria>. Accessed 18 January 2013)

(Parker, 1891) and greater rhea (Müller, 1963), Meckel's cartilage appears early in embryonic development and is essentially responsible for the framework (the dermal bones form around the *Collumela* of the cartilage (Parker, 1891)) and ensuing development of the mandible. By Day 34 in the ostrich embryo Meckel's cartilage begins to reduce in size (Webb, 1957) and, as reported by Parker (1866), the rostral two-thirds are resorbed soon after hatching. Webb (1957), based on the findings of Parker (1866) and Parker (1891), states that in the ostrich, rhea, emu and kiwi, only the caudal part of Meckel's cartilage ossifies as the articular bone while the remainder is resorbed. However, it is clear from the present study that Meckel's cartilage persists in the adult bird in both the ostrich and emu, and is also present in greater rhea chicks (Müller, 1963; personal observation). Based on the observation in the present study that Meckel's cartilage was a more robust structure in the emu, Webb's observation that it diminishes in size in the ostrich embryo may be correct; however, it does not finally disappear. Dissection of the mandibular neurovascular canal in an 8 month-old greater rhea (head length of 170 mm) revealed that Meckel's cartilage was still present and was composed of cartilage (personal observation), as in the ostrich and emu. However, in one ostrich specimen (at least 8 years old), Meckel's cartilage appears to have ossified (personal observation). This finding is similar to that of Müller (1963) in the adult rhea (head length of 180 mm) in which a rod of bone was present in the same location as that of Meckel's cartilage in greater rhea chicks. This would appear to indicate that Meckel's cartilage may ossify in ratites as they age.

In lepidosaurs the distal (rostral) aspect of Meckel's cartilage is closely linked to the complex functioning of the mandibular symphysis, which is in turn related to the specific feeding habits of the species (Holliday *et al.*, 2010). For example, in lingual feeders the distal aspect of Meckel's cartilage serves as an attachment for some of the muscles of the tongue (*M. genioglossus*) (Holliday *et al.*, 2010). However, in the ostrich and emu, there was no evidence of hyolingual muscles attaching to Meckel's cartilage, or of the distal ends forming part of the mandibular symphysis. The mandibular rami are completely fused at the symphysis in birds (Bühler, 1981); a situation also apparent in the ostrich and emu, and Meckel's cartilage would thus not play a role in this joint in these two species as it reportedly does in the lepidosaurs (Holliday *et al.*, 2010). Furthermore, the rostral ends of Meckel's cartilage in the ostrich and emu remained unfused, a feature shared by some lepidosaur species including Schneider's Skink

(*Eumeces schneideri*), Northern water snake (*Nerodia sipedon*), Ball python (*Python regius*), Sudan plated lizard (*Gerrhosaurus major*), yellow-spotted tropical night lizard (*Lepidophyma flavimaculatum*), gold tegu (*Tupinambis tequixín*), savannah monitor (*Varanus exanthematicus*) and Nile monitor (*Varanus niloticus*) (Holliday *et al.*, 2010). The insertion of the long tendon of *M. pseudotemporalis superficialis* onto the perichondrium of the caudal portion of Meckel's cartilage in the ostrich and emu has not previously been reported. Although Webb (1957) noted that the insertion of the superficial pseudotemporal muscle was on the medial surface of the surangular (supra-angular) bone, he did not mention the large, firm attachment to Meckel's cartilage. The insertion of this muscle in neognathous birds is on the *Tuberculum pseudotemporale* (Baumel and Witmer, 1993; Vanden Berge and Zweers, 1993), which is situated slightly rostral to the quadratomandibular joint near the base of the medial mandibular process of the mandible (Baumel and Witmer, 1993). The *Tuberculum pseudotemporale* was not identified to be present in the ostrich or emu. In crocodylians *M. pseudotemporalis superficialis* attaches to a large, fibrocartilaginous sesamoid cartilage, the *Cartilago transiliens* (Holliday and Witmer, 2007). Thus in both the crocodylians and the ostrich and emu *M. pseudotemporalis superficialis* displays an attachment to a cartilaginous structure. Although the ostrich was included in the study by Holliday and Witmer (2007), neither the attachment of *M. pseudotemporalis superficialis* to Meckel's cartilage, nor Meckel's cartilage itself, was mentioned. This interesting link between muscle attachments to, and the presence of, Meckel's cartilage between the ostrich and emu and lepidosaurs and crocodylia will need to be explored in future studies.

The presence and persistence through to adulthood of Meckel's cartilage would thus appear to be a unique feature of the ostrich and emu (and possibly of other ratite species such as the greater rhea (personal observation)) and may be a synapomorphic feature¹³ of the ratites. Additionally, the presence of Meckel's cartilage in the ostrich and emu may also be a symplesiomorphic¹⁴ trait, as it is shared with lepidosaurs and crocodylia. Apart from assisting in the embryological formation of the mandible, in particular that of the articular bone, and serving as an attachment site for *M. pseudotemporalis superficialis*, the persistence of Meckel's cartilage, at least until early

¹³ A synapomorphy is a character that is shared by all members of a particular group, but not with the members of other closely related groups (such as volant birds).

¹⁴ "An ancestral trait shared by two or more taxa. A symplesiomorphic trait is also shared with other taxa that have an earlier last common ancestor with the taxa under consideration. (<http://en.wikipedia.org/wiki/Symplesiomorphy>. Accessed 23 September 2013).

adulthood, may indicate additional functions for this structure. Furthermore, there is no mention in the literature of the relationship between the intramandibular nerve and Meckel's cartilage in the mandibular neurovascular canal of adult birds. The intramandibular nerve is homologous to the inferior alveolar nerve found in mammals (Bubień-Waluszewska, 1981), which runs within the mandibular canal (World Association of Veterinary Anatomists, 2012), a structure homologous to the mandibular neurovascular canal in birds. The mandibular neurovascular canal is partially open in the ostrich and emu and an obvious function for Meckel's cartilage would be to protect the intramandibular nerve, shielding it from mechanical trauma. Oddly, this does not appear to be a function of Meckel's cartilage in these two birds as it is situated lateral to the nerve (unlike that reported in the ostrich by Webb (1957)) leaving the canal still partially open. However, the close association of Meckel's cartilage with the intramandibular nerve (see Chapter 6) indicates it may fulfil a protective function by absorbing shockwaves produced during pecking which may interfere with signal transduction along the closely associated nerve (see Chapter 7).

5.4.1.2. The premaxilla

The structure of the premaxilla has been described in the ostrich (Parker, 1866; Webb, 1957) and emu (Parker, 1866). As both these authors conducted their studies on embryonic or newly hatched specimens their sketches (although not labelled) of early stage embryos appear to show a palatal process in the ostrich. However, in the adult bird there was no evidence of a palatal process. The remaining features described in the present study are similar to those of Parker (1866) and Webb (1957). To protect the braincase from dangerous concussive forces the bony palate needs to be a solid framework and in the emu "the main trajectory of compression stresses runs from the palatine process of the premaxillary bone to the vomer, then to the pterygoid, the quadrate, and finally via the quadrate's otic process to the braincase" (Dzerzhinsky, 1999) (see Fig. 5.6b). The palatal process of the premaxilla is absent in the ostrich (Webb, 1957; Dzerzhinsky, 1999; present study) and as a result the roof of the oropharynx displays a large gap unsupported by bone (Dzerzhinsky, 1999) (see Fig. 5.6a) while in the emu, the equivalent region is supported by bone, most notably the palatal process of the premaxilla. Thus in the ostrich "compression stresses run from the bill tip through the premaxillary and maxillary bones to the palatine and then almost

directly to the apex of the basipterygoid process” (Dzerzhinsky, 1999) (see Fig. 5.6a). The reason for the difference in the structure of the premaxilla in the ostrich and emu could not be determined in the present study. However, the absence of the palatal processes in the ostrich may be an adaptation to dissipating concussive forces away from the large, paired *R. medialis N. ophthalmicus* conveying sensory information from the maxillary rostrum. This is elaborated on in Chapter 7.

5.4.2. General microscopic features of the bill

There was an obvious difference in the trabecular organisation of the bill tips in the ostrich and emu. The trabeculae in the ostrich were more densely arranged than those in the emu, with the emu additionally displaying larger, fat-filled hollows in both the upper and lower bills. It has been shown that the trabeculae tend to be denser in those regions subjected to higher stress. Finches with probing bills, for example, display hollow spaces devoid of trabeculae (Genbrugge *et al.*, 2012). The larger hollows in the emu bill tips may either be related to lightening of the bill, as described in the toucan and hornbill (Seki *et al.*, 2005), or to the fact that the bill tips may experience less force while feeding than those of the ostrich, as noted for various finches (Genbrugge *et al.*, 2012). However, the ostrich and emu most likely experience similar concussive forces on the bill tips during feeding, and as shown by Dzerzhinsky (1999) these two birds display different pathways for dissipating this stress (see above). The fat filled cavities in the emu premaxilla may act in absorbing concussive forces before they travel along the palatal processes, and possibly interfere with signal transduction along the large, paired *R. medialis N. ophthalmicus*. This is elaborated on in Chapter 7.

Histology of the bill tips revealed that the bony pits seen macroscopically extend to the cavities within the premaxilla and mandibular rostra of the ostrich and emu. The pits contain groups of Herbst corpuscles and accompanying blood vessels and nerves (arrangement 1 of Herbst corpuscles as detailed in Chapters 3 and 7). The presence of macroscopic pits in the bone, which when viewed microscopically contain Herbst corpuscles, is positive confirmation of the presence of a bill tip organ as also identified in the kiwi (Cunningham *et al.*, 2007), Scolopacidae (see Cunningham *et al.*, 2007) and Threskiornithidae (Cunningham *et al.*, 2010a). The structure of the bill tip organ in the ostrich and emu is fully presented and discussed in Chapter 7.

5.4.3. The distribution and number and of pits in the bill tip

5.4.3.1. Distribution of pits

The basic pattern of bony pits in the premaxilla and mandibular rostrum was similar in the ostrich and emu. The pattern of pits in the kiwi premaxilla (Cunningham *et al.*, 2007), despite structural modifications (see below) also resemble that of the ostrich and emu. The intra-oral aspect of the kiwi mandible displays 1-2 rows of pits along the edges (Parker, 1891; Cunningham *et al.*, 2007) and rows of pits on the ventral surface, similar to that in the ostrich and emu. However, the mandible of the kiwi does differ from that of the ostrich and emu in that the lateral edges display a narrow groove which is also lined with pits. It was noted that the pattern of holes in the kiwi bill (a probe-foraging bird) was similar to that seen in Scolopacidae (also probing birds) (Cunningham *et al.*, 2007); however, the particular pattern was not mentioned.

The premaxilla of the kiwi (Parker, 1891; Martin *et al.*, 2007; Cunningham *et al.*, 2007) differs markedly from that of the ostrich and emu and the maxillary rostrum is reportedly highly specialised in this species. However, by analysing the pattern of the bony pits it is possible to draw an analogy between the ostrich, emu and kiwi (Fig. 5.19). The dorsal view of the kiwi bony premaxilla (Martin *et al.*, 2007; Cunningham *et al.*, 2007) (Fig. 5.19a) shows a similar distribution of pits to the bony region underlying the *Culmen* in the ostrich (Fig. 5.19c) and emu (Fig. 5.19d). In all three species pits are present on the lateral edges of the bony region underlying the *Culmen* and are separated by a median tract of non-pitted bone. In the kiwi these pits are referred to as “dorsal zones 3 and 4” (Fig. 5.19a) and correspond to the pits on the right (zone 3) and left (zone 4) side of the bony region underlying the *Culmen* in the ostrich (Fig. 5.19c) and emu (Fig. 5.19d). In the kiwi, the overlapping ventral surface (termed the sensory pad) has two zones, namely, the central circular tactile-disc (zone 1) and the semi-circular pre-oral zone (zone 2) (Cunningham *et al.*, 2007) (Fig. 5.19b). The so-called pre-oral zone in the kiwi appears to be homologous to the lateral portions of the body of the premaxilla in the ostrich and emu (zone 2) (Fig. 5.19b-d). It would appear that these two regions of the premaxilla (the body) in the kiwi are greatly reduced and fold in toward each other meeting ventrally (Fig. 5.19b). The so-called tactile disc (zone 1) (Fig. 5.19b) in the kiwi

appears to be either homologous to the rostral tip of the premaxilla in the ostrich and emu (zone 1) (Figs. 5.19c and d), which in the kiwi is folded ventrally, or to the immediate ventral surface of the rostral premaxilla in the ostrich and emu. The tactile disc is accentuated in the kiwi due to the slightly bulging nature of the ventrally folded pre-oral zones. The bill tip sensory pad is said to be unique to the kiwi, however, based on the above comparisons it would appear that it displays similar basic morphological components to those present in the ostrich and emu. The maxillary bill tip, with regards to the pattern/distribution of pits, is therefore similar in the ostrich, emu and kiwi, although, the various zones display different proportions.

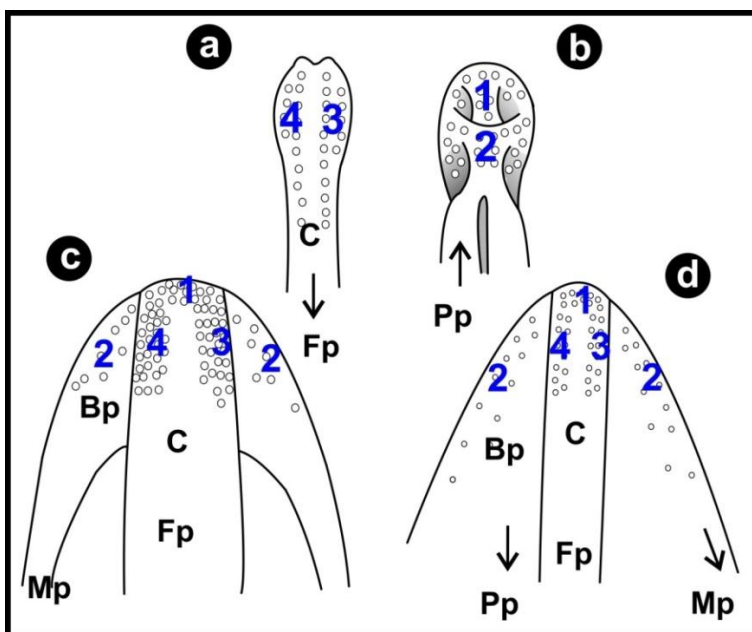


Figure 5.19. Schematic representation of the premaxilla in the kiwi chick (a and b) and adult ostrich (c) and emu (d). (a). **Dorsal premaxilla.** Dorsal zones (3 and 4), bony region underlying the *Culmen* (C) which caudally forms the frontal process (Fp). (b). **Ventral premaxilla.** Zone 1 represents the tactile disc and zone 2 the pre-oral zone. Palatal process (Pp). (c and d). **Dorsal views.** Bony area underlying the *Culmen* (C), body of the premaxilla (Bp), maxillary (Mp), frontal (Fp) and palatal (emu) (Pp) processes. The sketches are not drawn to scale. (Kiwi data adapted from original sketch by Parker (1891) and zones numbered as described by Cunningham *et al.*, 2007).

5.4.3.2. Number of pits

The only other ratite genus which has been studied with regards to the number and distribution of pits in the bill tip is the kiwi. The sensory pits were counted in 5 different kiwi species (*A. australis*, *A. haastii*, *A. mantelli*, *A. owenii*, *A. rowi*) (n=22) and the data presented as the average of the 22 specimens examined (Cunningham *et al.*, 2007). Taking into consideration that the counts in the kiwi (5 species), ostrich and emu were performed by different researchers any comparison should be interpreted with caution. Although this data cannot be submitted to statistical evaluation, it can, however, provide a basis for comparison between these three ratite genera (the 5 kiwi species are compared here as one). The 5 kiwi species displayed a slightly smaller total number of

pits in the bill (288 ± 58) (Cunningham *et al.*, 2007) compared to both the ostrich (361.6 ± 45.10) and emu (329.6 ± 32.62). Pit numbers in the mandible of the 5 kiwi species (142 ± 32) (Cunningham *et al.*, 2007) were similar to those of the ostrich (138.8 ± 18.79) and slightly less than in the emu (166.6 ± 22.81). The number of pits in the premaxilla of the 5 kiwi species (146 ± 35) (Cunningham *et al.*, 2007) was similar to that in the emu (163 ± 19.87) but markedly less than in the ostrich (211.2 ± 22.04). Thus, in terms of total number, the kiwi pit count (although slightly less) was similar in every respect to that of the emu, but differed from the ostrich in a similar fashion to that between the ostrich and emu. It was not possible from the available data on the kiwi's to determine whether there were any regional differences in distribution, as was seen in the ostrich and emu. It is interesting to note that the two Australasian ratites (the kiwi and emu) display affinities in respect of the number of pits present in the bill tips.

Sensory pits have also been counted in the bills of 9 ibis species (Cunningham *et al.*, 2010a). These birds, like the kiwi and shorebirds, use their long, slender bills for probe-foraging. As such they display a similar pattern of pits to the latter two families of birds (Cunningham *et al.*, 2010a). In the ibis, the largest number of pits was located on the outer surfaces of the upper (594.2 outside and 81.6 inside) and lower (505.5 outside and 83.3 inside) bills. Although the ostrich also displayed more pits on the outside of the upper (139.5 outside and 70.1 inside) and lower (88.6 outside and 50.2 inside) bills, the order of magnitude in respect of the difference between these surfaces was far less than that in the ibis. In the kiwi (Cunningham *et al.*, 2007) and emu the difference between the outer and inner surfaces was not as exaggerated as in the ostrich, except for the outside surface of the upper bill in the emu. The preferential placement of sensory pits on the outer surfaces of the bill in the ibis would indicate that the greatest degree of sensitivity exists on the outer surfaces of the bill; a suitable arrangement for probing. However, as the ostrich and emu do not probe it would appear, by the placement of the pits, that the inner and outer surfaces of the bill tip are equally important in these two birds.

The greater number of pits in the bill tip of the ostrich when compared to the emu may simply reflect the greater size of the bony regions underlying the *Culmen* and *Gonys* in this species. It has been noted that in different sized species of ducks, specialised dermal papillae (originating from the deep dermis and containing Herbst corpuscles in a

highly organise fashion in the bill), although of similar size, varied in number depending on the size of the duck (Berkhoudt, 1976). Thus the statistical significance in the number of pits present in these regions (ostrich>emu) may be directly related to the space available for the pits. Similarly, more pits were present in the dorsal part of the mandibular rostrum of the emu (which compared to the ostrich is larger in the emu).

The full significance of these results is discussed together with the relevant results from Chapters 4 and 6 in Chapter 7.

5.5. References

- Baumel, J.J. and Witmer, L.M. 1993. *Osteologia*. In: Handbook of Avian Anatomy: Nomina Anatomica Avium, 2nd edition. Edited by Baumel, J.J., King, A.S., Breazile, J.E., Evans, H.E. and Vanden Berge, C. Cambridge, Massachusetts: The Nuttall Ornithological Club, No. 23. pp. 45-132.
- Berkhoudt, H. 1976. The epidermal structure of the bill tip organ in ducks. *Netherlands Journal of Zoology*. **26**: 561-566.
- Berkhoudt, H. 1980. The morphology and distribution of cutaneous mechanoreceptors (Herbst and Grandry corpuscles) in bill and tongue of the mallard (*Anas platyrhynchos* L.). *Netherlands Journal of Zoology*. **30**: 1-34.
- Bock, W.J. 1963. The cranial evidence for ratite affinities. *Proceedings of the XIII International Ornithological Congress*. pp. 39-54.
- Bolze, G. 1968. Anordnung und Bau der Herbstchen Körperchen in Limicolenschnäbeln im Zusammenhang mit der Nahrungsfindung. *Zoologischer Anzeiger*. **181**: 313-355.
- Bona, P. and Desojo, J.B. 2011. Osteology and cranial musculature of *Caiman latirostris* (Crocodylia: Alligatoridae). *Journal of Morphology*. **272**: 780–795.
- Bubień-Waluszewska, A. 1981. *The Cranial Nerves*. In: Form and Function in Birds. Vol. 2. Edited by King, A.S. and McLelland, J. London: Academic Press. pp. 385-438.
- Bühler, P. 1981. *Functional Anatomy of the Avian Jaw Apparatus*. In: Form and Function in Birds. Vol. 2. Edited by King, A.S. and McLelland, J. London: Academic Press. pp. 439-468.

- Crole, M.R. and Soley, J.T. 2009. Comparative distribution of Herbst corpuscles within the oropharyngeal cavity of the ostrich (*Struthio camelus*) and emu (*Dromaius novaehollandiae*). *17th Congress of the International Federation of Associations of Anatomists*, Cape Town, South Africa. p. 361.
- Cunningham, S., Castro, I. and Alley, M. 2007. A new prey-detection mechanism for kiwi (*Apteryx* spp.) suggests convergent evolution between paleognathous and neognathous birds. *Journal of Anatomy*. **211**: 493-502.
- Cunningham, S.J., Alley, M.R., Castro, I., Potter, M.A., Cunningham, M. and Pyne, M.J. 2010a. Bill morphology of ibises suggests a remote-tactile sensory system for prey detection. *The Auk*. **127**: 308-316.
- Cunningham, S.J., Castro, I., Jensen, T. and Potter, M.A. 2010b. Remote touch prey-detection by Madagascar crested ibises *Lophotibis cristata urschi*. *Journal of Avian Biology*. **41**: 350-353.
- Dodd, J. 2013. *Struthio camelus*, Ostrich. *An NSF Digital Library at UT Austin*. Webpage: Accessed 14 May 2013. http://digimorph.org/specimens/Struthio_camelus/skull/
- Dzerzhinsky, F.Y. 1999. *Implications of the Cranial Morphology of Paleognaths for Avian Evolution*. In: Smithsonian Contributions to Paleobiology, number 89. Avian Paleontology at the Close of the 20th Century: Proceedings of the 4th International Meeting of the Society of Avian Paleontology and Evolution, Washington, D.C., 4-7 June 1996. Edited by Olson, S.L. Washington, D.C.: Smithsonian Institution Press. pp. 267-274.
- Franzosa, J. 2013. *Dromaius novaehollandiae*, Emu. *Digimorph*. *An NSF Digital Library at UT Austin*. Webpage: Accessed 14 May 2013. http://digimorph.org/specimens/Dromaius_novaehollandiae/skull/
- Genbrugge, A., Adriaens, D., De Kegel, B., Brabant, L., Van Hoorebeke, L., Podos, J., Dirckx, J., Aerts, P and Herrel, A. 2012. Structural tissue organization in the beak of Java and Darwin's finches. *Journal of Anatomy*. **221**: 383-393.
- Gentle, M.J. and Breward, J. 1986. The bill tip organ of the chicken (*Gallus gallus* var. *domesticus*). *Journal of Anatomy*. **145**: 79-85.
- Goglia, C. 1964. 'L'organa tattile apicale' del Becco di alcuni volatili. *Acta Medica Romana*. **11**: 243-262.
- Gottschaldt, K.-M. and Lausmann, S. 1974. The peripheral morphological basis of tactile sensitivity in the beak of geese. *Cell and Tissue Research*. **153**: 477-496.

- Gusseklou, S.W.S. and Bout, R.G. 2002. Non-neotenus origin of the palaeognathous (Aves) pterygoid-palate complex. *Canadian Journal of Zoology*. **80**: 1491–1497.
- Gusseklou, S.W.S. and Bout, R.G. 2005. The kinematics of feeding and drinking in palaeognathous birds in relation to cranial morphology. *The Journal of Experimental Biology*. **208**: 3395–3407.
- Halata, Z. and Grim, M. 1993. Sensory nerve endings in the beak skin of Japanese quail. *Anatomy and Embryology*. **187**: 131-138.
- Hogg, D.A. 1983. Fusions within the mandible of the domestic fowl (*Gallus gallus domesticus*). *Journal of Anatomy*. **136**: 535-541.
- Holliday, C.M. and Witmer, L.M. 2007. Archosaur adductor chamber evolution: integration of musculoskeletal and topological criteria in jaw muscle homology. *Journal of Morphology*. **268**: 457–484.
- Holliday, C.M., Gardner, N.M., Paesani, S.M., Douthitt, M. and Ratliff, J.L. 2010. Microanatomy of the mandibular symphysis in lizards: patterns in fiber orientation and Meckel's cartilage and their significance in cranial evolution. *The Anatomical Record*. **293**: 1350-1359.
- Johnston, P. 2011. New morphological evidence supports congruent phylogenies and Gondwana vicariance for palaeognathous birds. *Zoological Journal of the Linnean Society*. **163**: 959–982.
- Kelly, W.L. and Bryden, M.M. 1983. A modified differential stain for cartilage and bone in whole mount preparations of mammalian fetuses and small vertebrates. *Stain Technology*. **58**: 131-134.
- Kley, N.J. 2006. Morphology of the lower jaw and suspensorium in the Texas blindsnake, *Leptotyphlops dulcis* (Scolecopidia: Leptotyphlopidae). *Journal of Morphology*. **267**: 494-515.
- Krulis, V. 1978. Struktur und Verteilung von Tastrezeptoren im Schnabel-Zungenbereich von Singvögeln im besonderen der Fringillidae. *Revue Suisse de Zoologie*. **85**: 385-447.
- Martin, G.R., Wilson, K.-J., Wild, J.M., Parsons, S., Kubke, M.F. and Corfield, J. 2007. Kiwi forego vision in the guidance of their nocturnal activities. *PLoS ONE*. **2**: e198.
- Maxwell, E.E. 2009. Comparative ossification and development of the skull in palaeognathous birds (Aves: Palaeognathae). *Zoological Journal of the Linnean Society*. **156**: 184–200.
- Müller, H.J. 1963. Die morphologie und Entwicklung des Cranium von *Rhea americana* Linné. *Zeitschrift für Wissenschaftliche Zoologie*. **168**: 35-118.

Parker, T.J. 1891. Observations on the anatomy and development of apteryx. *Philosophical Transactions of the Royal Society of London, B*. **182**: 25-134.

Parker, W.K. 1866. On the structure and development of the skull in the Ostrich Tribe. *Philosophical Transactions of the Royal Society of London*. **156**: 113-183.

Rayfield, E.J. 2011. Strain in the ostrich mandible during simulated pecking and validation of specimen-specific finite element models. *Journal of Anatomy*. **218**: 47–58.

Richardson, M.K., Deeming, D.C. and Cope, C. 1998. Morphology of the distal tip of the upper mandible of the ostrich (*Struthio camelus*) embryo during hatching. *British Poultry Science*. **39**: 575–578.

Seki, Y., Schneider, M.S. and Meyers, M.A. 2005. Structure and mechanical behaviour of a toucan beak. *Acta Materialia*. **53**: 1093-1098.

Vanden Berge, J.C. and Zweers, G.A. 1993. *Myologia*. In: Handbook of Avian Anatomy: Nomina Anatomica Avium, 2nd edition. Edited by Baumel, J.J., King, A.S., Breazile, J.E., Evans, H.E. and Vanden Berge, C. Cambridge, Massachusetts: The Nuttall Ornithological Club, No. 23. pp. 189-247.

Webb, M. 1957. The ontogeny of the cranial bones, cranial peripheral and cranial parasympathetic nerves, together with a study of the visceral muscles of *Struthio*. *Acta Zoologica*. **38**: 81–203.

World Association of Veterinary Anatomists. 2012. *Nomina Anatomica Veterinaria*. 5th edition (revised version). Edited by the International Committee on Veterinary Gross Anatomical Nomenclature. Hannover, Germany: The Editorial Committee. http://www.wava-amav.org/Downloads/nav_2012.pdf

CHAPTER 6

MORPHOLOGY AND SENSORY SPECIALISATIONS OF THE BILL.

III. THE TRIGEMINAL NERVE BRANCHES SUPPLYING THE BILL TIP

6.1. Introduction

The trigeminal sensory system in birds is well developed (for review see Dubbeldam, 1998) and the trigeminal nerve (cranial nerve V) has been identified to innervate the bill and bill-tip organ (where present) (Dubbeldam and Veenam, 1978; Berkhoudt, 1980; Pettigrew and Frost, 1985; Dubbeldam *et al.*, 1995). It is common practise to de-beak chickens (Gentle, 1989; Dubbeldam *et al.*, 1995; Dubbeldam, 1998) and as a result of this procedure the sensory innervation to the bill of the chicken has been studied in detail (Gentle and Breward, 1986; Gentle, 1989; Dubbeldam *et al.*, 1995). Although the innervation of the bill in ratites has been poorly documented, the peripheral cranial nerves have been described and depicted in ostrich embryo's (Webb, 1957). This study included the two main nerves innervating the bill tip; however, their paths were only depicted schematically up to their entry into the bill tip. Although the terminal ramifications were noted to supply the maxillary and mandibular rostra, these branches were not illustrated (Webb, 1957). It was speculated that the large size of the main branch of the first division of the trigeminal nerve innervating the (upper) bill in the emu indicated the importance and significance of tactile cues received from this region (Cobb and Edinger, 1962). However, the above mentioned nerve was only shown within the orbit and no information on the innervation of the mandibular rostrum in the emu is available. The innervation of the bill in the kiwi has been briefly noted and the dorsal ramus of the orbitonasal nerve identified to supply end-organs concentrated in a honeycomb of small pits in the rostral maxilla (Parker, 1891). Of the above mentioned studies, that of Webb (1957) on the ostrich embryo represents the most complete account of the nerves innervating the bill tip in ratites although this description, coupled with a lack of illustrations of this region, remains inadequate.

All mechanoreceptors, including Herbst corpuscles, in the rostral part of the head region are innervated by branches of the trigeminal nerve, specifically by the large (myelinated) nerve fibres which supply the numerous end-organs in the bill-tip (Dubbeldam *et al.*, 1995). It has been reported that the number of myelinated fibres can be related to the number of end-organs supplied. This is based on the observation that the total number of myelinated nerve fibres decrease in the nerves of de-beaked chickens when these end-organs are removed (Dubbeldam *et al.*, 1995). Myelinated nerve fibres are visible using light microscopy whereas transmission electron microscopy (TEM) is necessary to view non-myelinated (autonomic) nerve fibres. Branches of the trigeminal nerve in the chicken, observed by TEM, have been shown to be composed of myelinated and non-myelinated nerve fibres (Dubbeldam *et al.*, 1995), similar to that reported for peripheral nerves in other avian species (Bubień-Waluszewska, 1985). As it has already been demonstrated that Herbst corpuscles are present in the bill tip of the ostrich and emu (Chapters 3, 4 and 5) it would be possible to count the number of nerve fibres in the branches of the trigeminal nerve supplying the bill-tip and relate this to the numbers of Herbst corpuscles in that region, thus determining the comparative sensitivity of the bill tip between these two species.

This Chapter identifies and describes the two main nerves innervating the bill tip in the ostrich and emu and compares the number of myelinated nerve fibres present in these nerves. This information is subsequently related to the presence and possible function of a bill tip organ in these two birds (see Chapter 7).

6.2. Materials and Methods

A total of 10 adult ostrich and 10 adult emu heads, from birds of either sex, were collected after slaughter from the Klein Karoo Ostrich abattoir (Oudtshoorn, Western Cape Province, South Africa), Oryx Abattoir (Krugersdorp, Gauteng Province, South Africa), Emu Ranch (Rustenburg, North-West Province, South Africa) and an emu farm (Krugersdorp, Gauteng Province, South Africa). All heads were thoroughly rinsed with either distilled water or running tap water to remove mucus, blood and regurgitated food.

6.2.1. Preparation of osseous elements of the head

For this part of the study the same two complete ostrich and emu skulls, from previous studies, utilised in Chapter 5.2.1 were used to plot the path of the ophthalmic nerve relative to the bony landmarks. The path of the nerve to the premaxilla was plotted on the skulls, described, digitally recorded with a Canon EOS 5D digital camera (Canon, Ōita, Japan) equipped with a Canon Macro 100mm lens, and annotated in Corel Draw X5.

6.2.2. Nerve dissection and light microscopy

Five adult ostrich and 5 adult emu heads were collected and fixed in 10% neutral-buffered formalin and transported to the Faculty of Veterinary Science, University of Pretoria. Care was taken to exclude air from the oropharynx by inserting a small block of wood between the bill tips. The heads were dissected to reveal branches of the trigeminal nerve. This was achieved by carefully removing the eye and associated muscles and fat, exposing the ophthalmic nerve and following the nerve to the premaxilla. Parts of the bony orbit were removed to trace the trigeminal nerve as it exited the orbit and the mandibular nerve was followed through the jaw muscles into the mandibular neurovascular canal to where it entered the mandibular rostrum. The rostral bill tips from 5 adult ostrich (protocol number V023/06, Faculty of Veterinary Science, University of Pretoria) and 5 adult emu (protocol number V040/08, Faculty of Veterinary Science, University of Pretoria) collected for previous studies were removed and decalcified (as described in Chapter 4.2.1). The dorsal part of the bone was removed and the fine nerve branches dissected and observed by stereomicroscopy. The topography of the finer branches of the trigeminal nerve in the bill tips was studied by light microscopy utilising the same histology slides studied in Chapter 4.2.3 (from 5 ostrich chicks and 1 emu chick).

6.2.3. Transmission electron microscopy

Five ostrich and 5 emu heads were sampled on-site and the tissues fixed in 2.5% gluteraldehyde (for at least 24 hours) in Millonig's phosphate buffer (pH 7.4, 0.13 M at

room temperature). The right medial branch of the ophthalmic nerve (exposed by removing the eye) and right intramandibular nerve (running in the mandibular neurovascular canal) were exposed, removed, fixed in 2.5% glutaraldehyde and processed routinely for TEM. The samples were rinsed in Millonig's phosphate buffer for 10 minutes, post-fixed for 1 hour at room temperature in similarly buffered 1% OsO₄ and given two final buffer washes of 10 minutes each. Samples were then rinsed in distilled water for 20 minutes and dehydrated through a graded series of ethanols (50%, 70%, 80%, 96% and 2 X 100% (with added Molecular sieve, Merck, Darmstadt, Germany) for 10 minutes per step. Samples were placed in 2X propylene oxide (PO) for 10 minutes each, followed by infiltration in PO: Epoxy resin (2:1) for 30 minutes to 1 hour and PO: Epoxy resin (1:2) for 1 hour to overnight. The tissue blocks were then embedded in 100% Epoxy resin in silicon moulds and cured in an embedding oven at 65°C overnight. Semi-thin sections were cut at 0.3 µm, mounted and stained with 1% toluidine blue and observed with the light microscope to identify areas of interest. The resin blocks were trimmed and ultra-thin sections (50-90 nm) cut using a diamond knife, mounted onto copper grids and stained with uranyl acetate and lead citrate. Nerve fibres were counted using the semi-thin sections (Figs. 6.8 and 6.9). The nerves were studied and compared in further detail using TEM. Samples were viewed, features of interest described and images digitally recorded using a Philips CM10 transmission electron microscope (FEI, Eindhoven, The Netherlands) equipped with a Mega View III Soft Imaging System camera and iTEM Soft Imaging System software. Images were digitally enhanced and annotated in Corel Draw X5.

6.2.4. Statistics

The null hypothesis, that the ostrich and emu are similar (in respect of the aspects studied), was tested by a Student's *t* test (a 2 sample assuming unequal variances) or the Mann-Whitney Rank Sum Test (where the normality test (Shapiro-Wilk) and/or equal variance test has failed (<0.05)). Values expressed were calculated using SigmaPlot, version 12.0 (Systat Software, San Jose, CA, USA) and comprised the mean, median, standard deviation, standard error of the mean, Mann-Whitney U statistic, significance and power of the test performed with alpha. Significance was set at $p=0.05$. A value of $p<0.05$ rejected the null hypothesis and a value of $p>0.05$ accepted the null hypothesis (Table 6.1).

6.3. Results

6.3.1. Gross morphology

In the ostrich and emu the branches of the *N. trigeminus* (cranial nerve V) innervating the maxillary and mandibular rostrum were the *N. ophthalmicus R. medialis* and the *N. intramandibularis*, respectively.

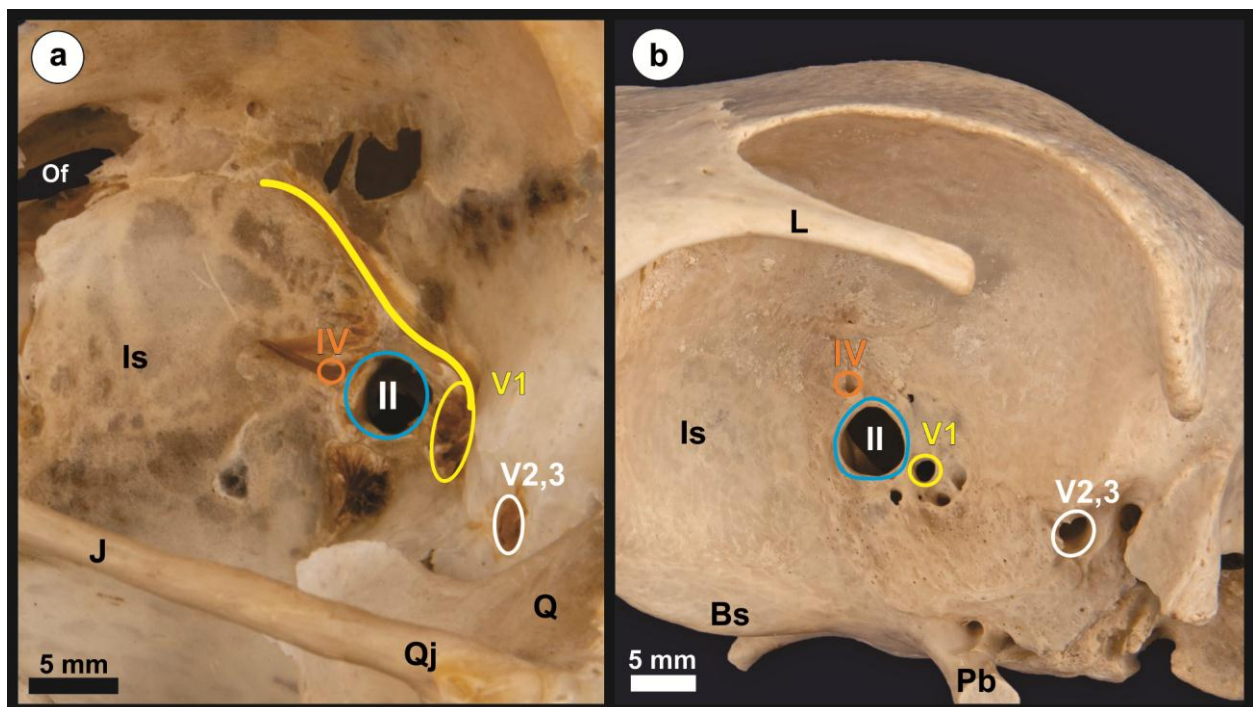


Figure 6.1. The bony orbit in the ostrich (a) and emu (b). The largest foramen in both the ostrich and emu is the *For. n. optici* (II) which in the above photographs remains separate from the adjacent *For. n. ophthalmici* (V1), which is larger in the ostrich than the emu. Part of the ophthalmic nerve (yellow line) is visible in the ostrich. *For. n. trochlearis* (IV), *For. n. maxillomandibularis* (V2,3) and interorbital septum (Is). **(a).** Orbitonasal foramen (Of), jugal (J), quadratojugal (Qj) and quadrate (Q) bones. **(b).** Lacrimal bone (L), basisphenoid bone (Bs) and basipterygoid process (Pb). The quadrate bone has been removed.

6.3.1.1. *N. ophthalmicus R. medialis*

The *N. ophthalmicus* exited the skull from the ophthalmic foramen which was positioned just lateral, and adjacent to, the optic foramen (Figs. 6.1 and 6.2). The ophthalmic foramen was larger in the ostrich than the emu (Fig. 6.1). In both species the foramen was either separate or continuous with the optic foramen, in the latter instance forming one common opening for the optic and ophthalmic nerves. The ophthalmic nerve ran

dorsal to the optic nerve (CN II), passed ventral to the dorsal rectus muscle, crossed the origin of the nasal rectus muscle and proceeded along the ventral margin of the dorsal oblique muscle (all medial to the eyeball) (Fig. 6.3). At the rostral margin of the orbit the ophthalmic nerve split into the smaller *R. lateralis* and the much larger *R. medialis*, both of which exited the orbit via the orbitonasal foramen. The medial branch moved from a dorsal position, ventral to the nasal and lacrimal bones, and proceeded at a steep angle rostro-ventrally, to a ventral position just dorsal to the maxilla (Figs. 6.2 and 6.3). The lateral branch moved laterally and supplied the nasal mucosa. The medial branch lay adjacent to the nasal septum and reached its ventral position near the junction of the bony and cartilaginous parts of the nasal septum (Figs. 6.2b and 6.3). The medial branch proceeded rostrally, adjacent to the cartilaginous nasal septum (Figs. 6.6d and 6.7d), and near the junction of the premaxilla and frontal process of the premaxilla, entered the premaxilla via the maxillary neurovascular canal (Fig. 6.3). This canal was represented by 1 to 3 openings in the emu and the nerve correspondingly split to enter through them. Only a single opening was present in the ostrich. Before entering the canal/s, although a single nerve was present, subdivisions (bundles), representing the premaxillary branches, were visible through the epineurium. This was also demonstrated microscopically in both birds (Figs. 6.6d and 6.7d). Within the premaxilla of the ostrich the nerve branched into a dorso-medial (presumably the *Ramus premaxillaris dorsalis*) and a ventro-lateral branch (presumably the *Ramus premaxillaris ventralis*) (Fig. 6.3a). In the ostrich these two branches were initially located in separate cavities (Fig. 6.6c) whereas in the emu multiple branches (2-3) (termed the premaxillary branches) were located within a single, large, fat-filled cavity (Fig. 6.7c). In both birds the nerves branched extensively within the cavities of the premaxilla (see Chapter 5) (Figs. 6.6 and 6.7). In the ostrich the dorso-medial branch innervated the tip of the premaxilla whereas the ventro-lateral branch innervated the lateral sides of the premaxilla (Fig. 6.3a). Similarly, in the emu, the more medial branches innervated the tip of the premaxilla and the more lateral branches innervated the lateral sides of the premaxilla. In both birds the branches within the cavities exited the premaxilla via the numerous neurovascular foramina (see Chapter 5) as the *Rr. rostri maxillaris* (Figs. 6.6 and 6.7).

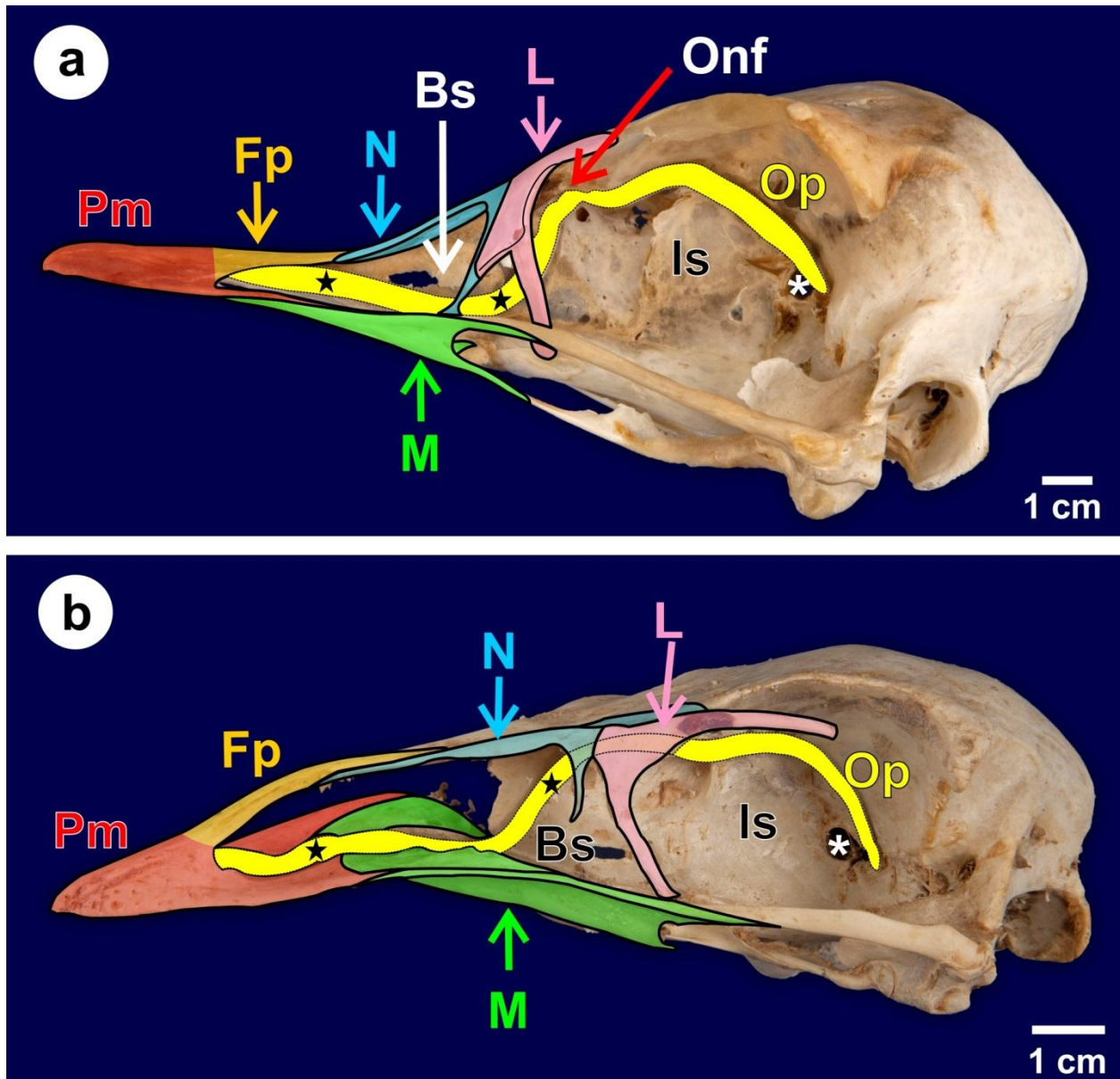


Figure 6.2. Lateral view of the ostrich (a) and emu (b) skull with a schematic to indicate the passage of the *N. ophthalmicus* (Op and in yellow) and its medial branch. The ophthalmic nerve is not drawn to scale. The nerve exits from the ophthalmic foramen situated lateral, and adjacent to, the optic foramen (*) and proceeds dorsally following the interorbital septum (Is). *R. medialis* (black star), orbitonasal foramen (Onf) (not shown in b), lacrimal (L) and nasal (N) bones, bony nasal septum (Bs), maxilla (M) and frontal process (Fp) of the premaxilla (Pm).

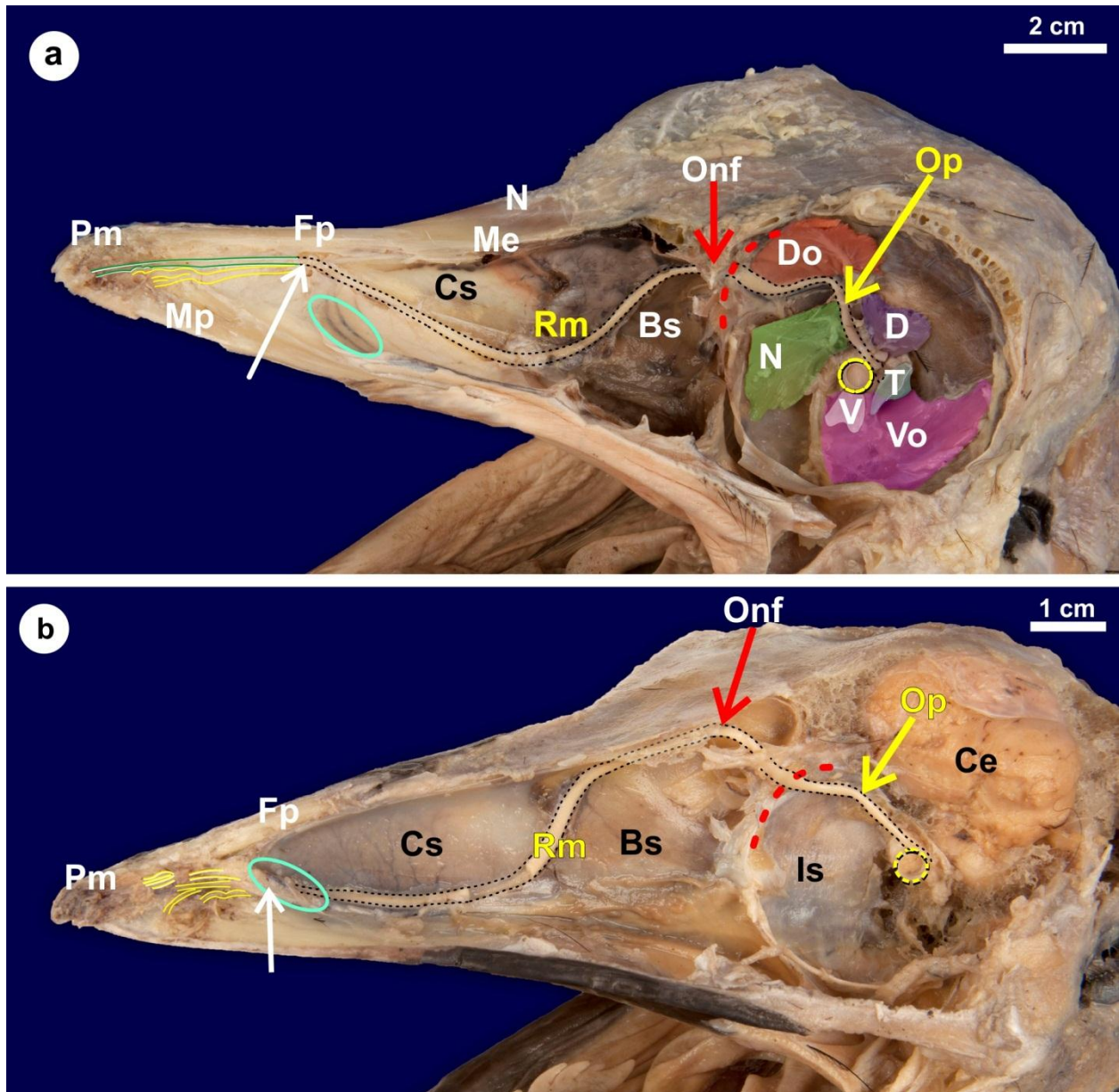


Figure 6.3. Dissected heads of the ostrich (a) and emu (b) revealing the path of the ophthalmic nerve (Op and outlined for clarity) and its medial branch to the premaxilla (Pm). The emu head has been dissected deeper to reveal the cerebrum (Ce). In the ostrich the eye muscles have been left in the orbit; the muscle stumps have been shaded for clarity and are the dorsal (D), temporal (T), ventral (V) and nasal (N) rectus muscles and the dorsal (Do) and ventral (Vo) oblique muscles. The ophthalmic nerve passes dorsal to the optic nerve (yellow circle) and follows the ventral border of the dorsal oblique muscle. At the orbitonasal foramen (Onf) it continues as the *Ramus medialis* (Rm) and the point of entry into the maxillary neurovascular canal is indicated (white arrow). In the ostrich a dorso-medial (green) and ventro-lateral (yellow) branch, of which the latter reaches the rostral extremity of the premaxilla, is present. In the emu, the premaxillary branches are indicated (yellow outlines). Interorbital septum (Is), rostral border of the orbit (red dotted line), bony (Bs) and cartilaginous (Cs) nasal septum, nasal (N) and mesethmoid (Me) bones, frontal process (Fp) of the premaxilla and approximate position of the external nares (light turquoise oval).

6.3.1.2. *N. intramandibularis*

In both birds the *N. mandibularis* exited the skull with the *N. maxillaris* through the *For. n. maxillomandibularis* (Fig. 6.1). In the ostrich the mandibular nerve emerged ventral to the *M. pseudotemporalis superficialis* and was sandwiched between the long tendon of the superficial pseudotemporal muscle and the deep pseudotemporal muscle. In the emu the mandibular nerve emerged lateral to the superficial pseudotemporal muscle and was located ventral to the *M. adductor mandibulae externus*. The nerve was positioned between the periosteum and the external mandibular adductor muscle and followed a course lateral to the long tendon of insertion of the superficial pseudotemporal muscle. In both birds, after supplying branches to the *Musculi mandibulae*¹, the mandibular nerve entered the mandibular neurovascular canal dorsally at a point just caudal to the rictus and between the insertion of the superficial pseudotemporal muscle and the medial aspect of the supra-angular bone (see Figure 5.3 of Chapter 5). In the emu, where the superficial pseudotemporal muscle also inserted onto the dorso-medial aspect of the supra-angular bone (see Chapter 5), the mandibular nerve ran through the tendon of this muscle. The main continuation of the mandibular nerve in the canal was the *N. intramandibularis*. The nerve proceeded rostro-ventrally within the canal dorsal to Meckel's cartilage (Fig. 6.4) but soon assumed a position dorso-medial to the cartilage. The intramandibular nerve continued into the mandibular rostrum where, especially in the emu, it formed an elaborate nerve plexus (Fig. 6.5b) encased in a fat body between the dorsal and ventral parts of the dentary bone. The intramandibular nerve in the ostrich did not branch as extensively within the mandibular rostrum; however, at the very rostral tip the nerve ramified into smaller branches (Fig. 6.5a). In the emu a small nerve was formed on the lateral edge of the plexus within the dentary bone and from this nerve arose many smaller branches (Fig. 6.5b) which corresponded to the positioning of the keratinised pegs described in Chapter 4. Numerous terminal branches of the intramandibular nerve exited the bone through the many neurovascular foramina as the *Rr. rostri mandibularis*. Light microscopy confirmed the findings observed macroscopically.

¹ "A collective term for those muscles which are involved in opening and closing jaws...." (Vanden Berge and Zweers, 1993).

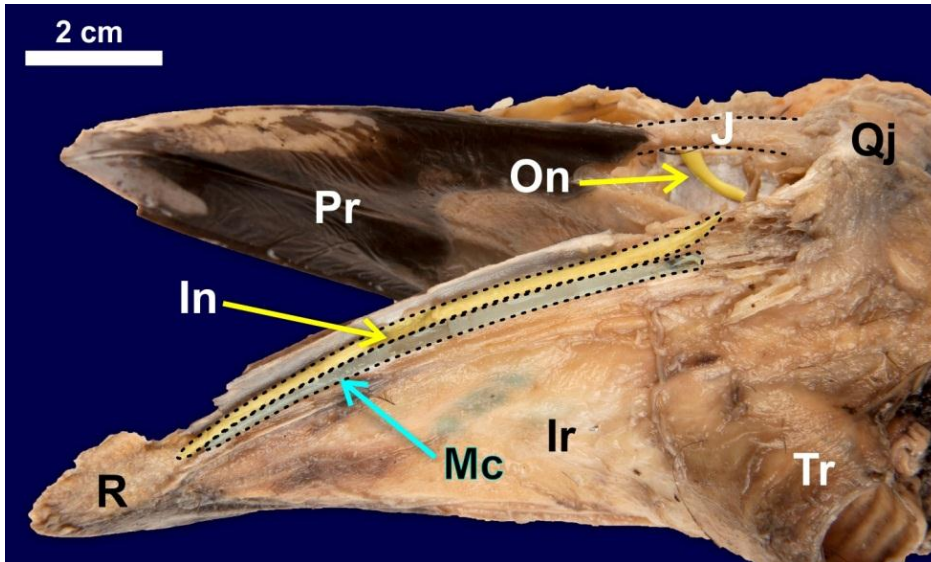


Figure 6.4. Ventro-lateral view of the intramandibular nerve (In) in the emu. The lateral portion of the mandibular ramus has been removed to reveal Meckel's cartilage (Mc) and the intramandibular nerve in the mandibular neurovascular canal. Mandibular rostrum (R), interramal region (Ir), trachea (Tr), pigmented roof (Pr), ophthalmic nerve (On), jugal bone (J) and quadrato-mandibular joint (Qj).

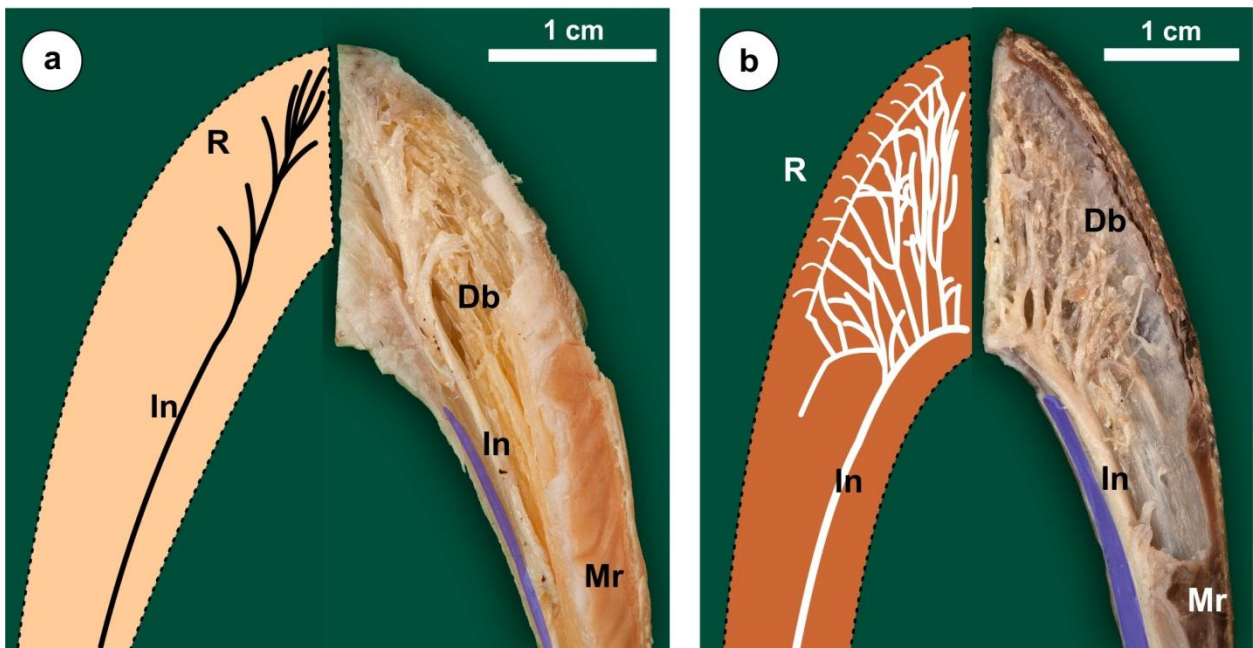


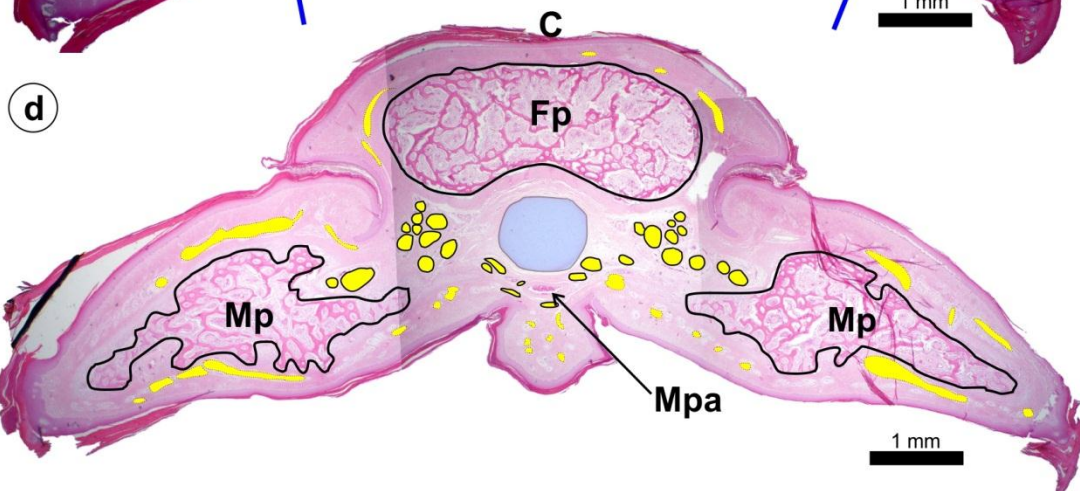
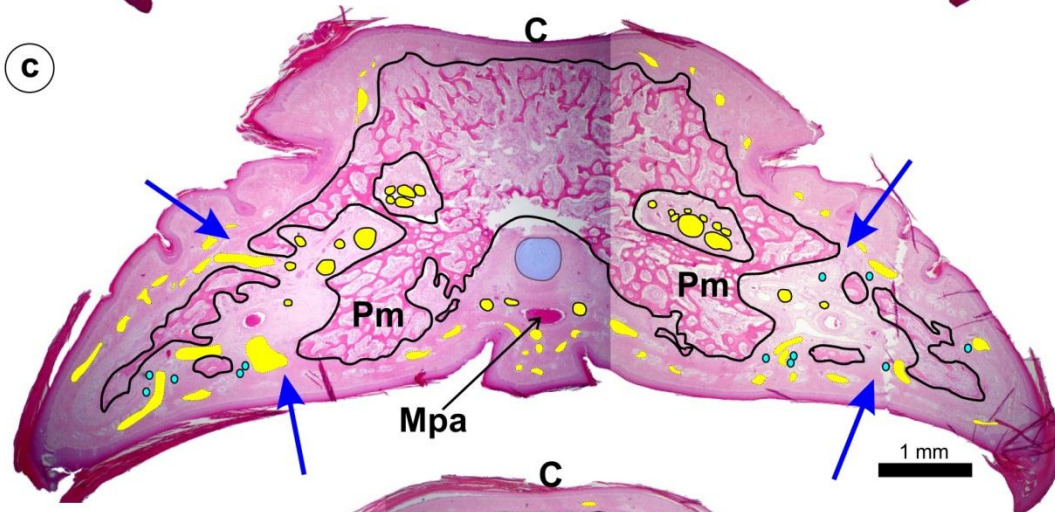
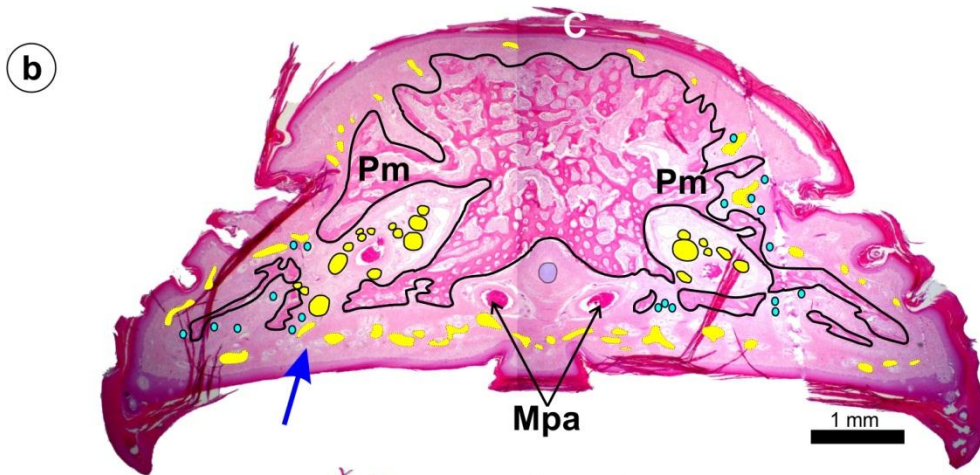
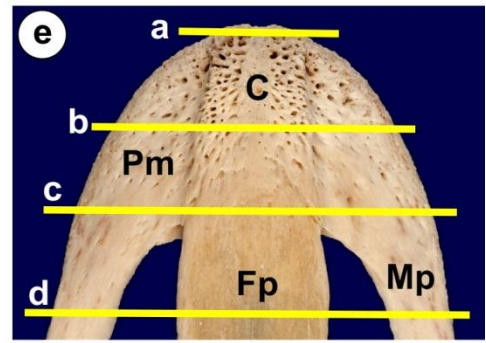
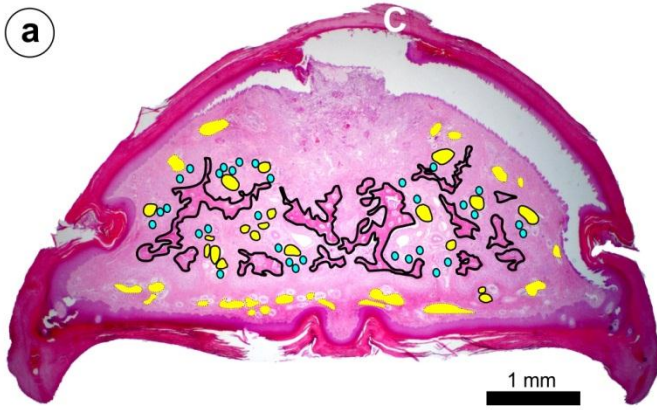
Figure 6.5. Dorsal view of the terminal branching of the *N. intramandibularis* (In) in the ostrich (a) and emu (b). The dorsal part of the dentary bone (Db) and the fat surrounding the nerves have been removed. The left side portrays a schematic of the nerve and its branching. Note the extensive branching of the *N. intramandibularis* in the mandibular rostrum (R) of the emu in comparison to the ostrich. Mandibular ramus (Mr) and Meckel's cartilage (shaded blue).

6.3.2. Light microscopy

6.3.2.1. Nerve topography in the upper bill-tip (Figs. 6.6 and 6.7)

The premaxillary branches were situated within the cavities of the premaxilla (see Chapter 5 and Figs. 6.6 and 6.7). In the ostrich the nerves were located in the cellular stroma which filled the cavities and in the emu they were situated within the fat body of the cavities. The nerves branched extensively and were situated in the many cavities present in the rostral extremity of the bill tip. The premaxillary branches exited through the neurovascular foramina of the premaxilla as the rostral maxillary branches (*Rr. rostri maxillaris*).

Figure 6.6. Composite micrographs of serial transverse-sections of the premaxilla (Pm) in an ostrich chick (a-d) with the location of each section indicated on an adult ostrich premaxilla (e). The bone has been outlined in black in a-d and only Herbst corpuscles (blue dots) associated with the bony cavities or holes are indicated. (a). The bone encloses numerous ill-defined cavities with Herbst corpuscles and terminal branches of the dorso-medial premaxillary branch (yellow dots in the bony cavities). *Rr. rostri maxillaris* (yellow dots outside the cavities) and *Culmen* (C). **(b).** The premaxilla (Pm) displays two main cavities, one on either side of the midline, carrying numerous ventral premaxillary branches (black outlined yellow dots). *Rr. rostri maxillaris* (yellow dots outside the cavities) can be seen exiting the premaxilla (blue arrow). The median palatine artery (Mpa) has split into two vessels. *Culmen* (C). **(c).** The dorso-medial branches (black outlined yellow dots) are situated in the dorsal cavity and the ventro-lateral branches (black outlined yellow dots) in the ventral cavities of the premaxilla. *Rr. rostri maxillaris* (yellow dots outside the cavities) can be seen exiting the premaxilla (blue arrow). Median palatine artery (Mpa) and *Culmen* (C). **(d).** The *N. ophthalmicus R. medialis* (already displaying subdivisions) (yellow dots) is shown just before it enters the premaxilla. Frontal process (Fp), maxillary processes (Mp) and median palatine artery (Mpa). The distal portion of the cartilaginous nasal septum is outlined and shaded light blue in b-d.



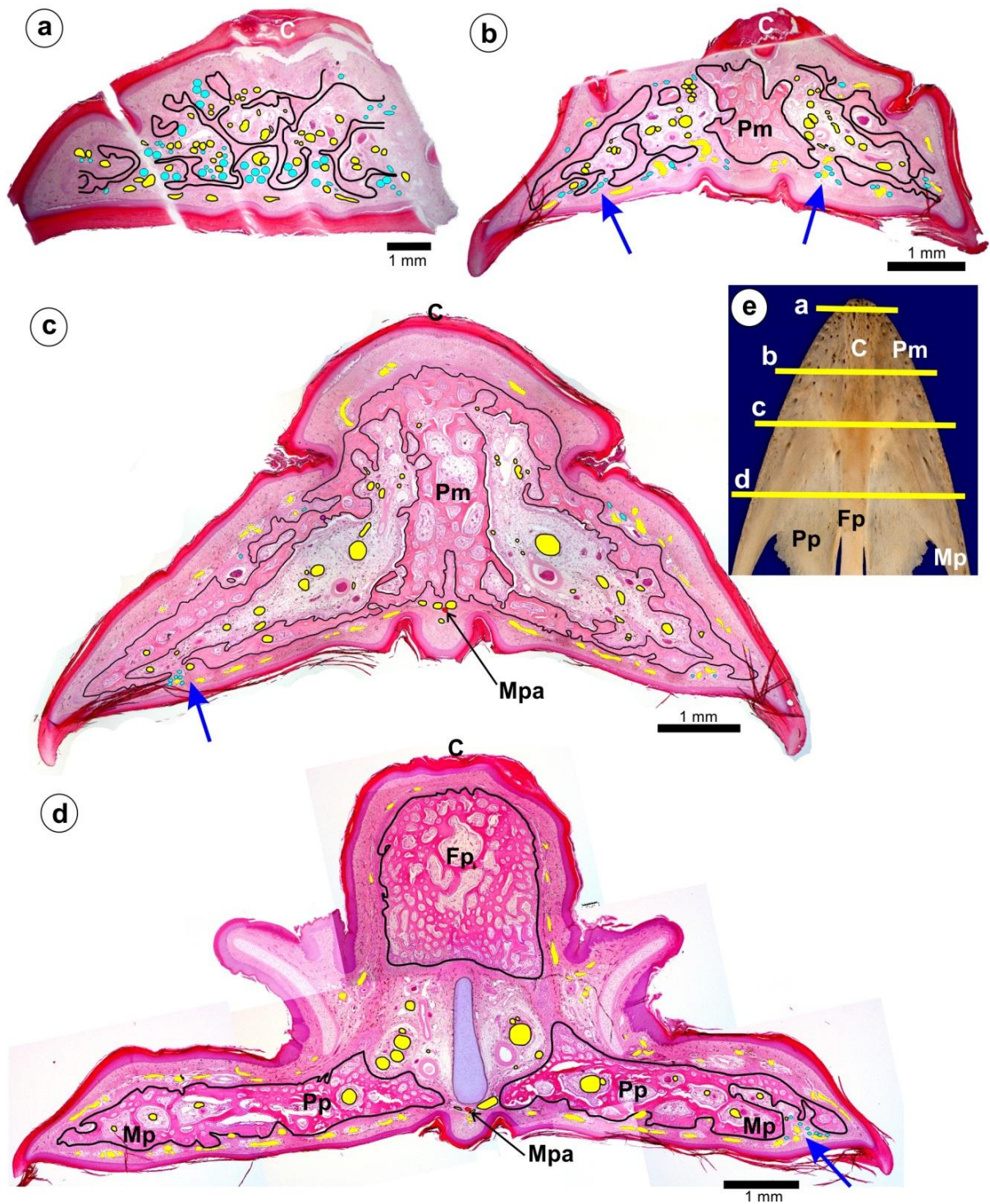


Figure 6.7. Composite micrographs of serial transverse-sections of the premaxilla (Pm) in an emu chick (a-d) with the location of each section indicated on an adult emu premaxilla (e). The bone has been outlined in black in a-d and only Herbst corpuscles (blue dots) associated with the bony cavities or holes are indicated. (a). The bone encloses numerous ill-defined cavities with Herbst corpuscles (blue dots) and terminal ramifications of the premaxillary branches (yellow dots in the bony cavities). *Rr. rostri maxillaris* (yellow dots outside the cavities) and *Culmen* (C). **(b).** The premaxilla (Pm) displays single bilateral cavities carrying numerous premaxillary branches (black outlined yellow dots). *Rr. rostri maxillaris* (yellow dots outside the cavities) can be seen exiting the premaxilla (blue arrows). *Culmen* (C). **(c).** The premaxilla at this level displays larger paired cavities with premaxillary branches (black outlined yellow dots). *Rr. rostri maxillaris* (yellow dots outside the cavities) can be seen exiting the premaxilla (blue arrow). Median palatine artery (Mpa) and *Culmen* (C). **(d).** The *N. ophthalmicus R. medialis* (yellow dots) is shown just before it enters the premaxilla. At this level the maxillary (Mp) and palatal (Pp) processes contain numerous fat-filled cavities carrying nerves (yellow dots) and blood vessels (red stars). Frontal process (Fp), median palatine artery (Mpa) and the distal portion of the cartilaginous nasal septum (outlined and shaded light blue).

6.3.2.2. Nerve fibre counts

The number of myelinated nerve fibres present in the respective branches of the trigeminal nerve supplying the premaxilla and mandible (Figs. 6.8 and 6.9, see next page) was counted in the ostrich and emu (Table 6.1).

Table 6.1. Myelinated nerve fibres present in the medial branch of the ophthalmic nerve and intramandibular nerve of the ostrich and emu. Yellow highlights indicate a significant difference and blue highlights indicate the power of the performed test with alpha (Pa) below the desired value of 0.8. Normality Test (Shapiro-Wilk) (NT), Equal Variance Test (EVT), Standard Deviation (SD), Standard Error of the Mean (SEM).

		Medial branch of the Ophthalmic nerve	Intramandibular nerve	Total
Ostrich n=5	1	5660	5241	10901
	2	6472	6146	12618
	3	5795	6406	12201
	4	5087	2720	7807
	5	6430	4820	11250
Mean		5888.80	5066.60	10955.40
Median		5795	5241	11250
SD		578.16	1462.61	1891.95
SEM		258.56	654.10	846.11
Emu n=5	1	6863	6275	13138
	2	7420	6232	13652
	3	6535	4932	11467
	4	5920	5485	11405
	5	7450	6054	13504
Mean		6837.60	5795.60	12633.20
Median		6863	6054	13138
SD		641.96	576.48	1109
SEM		287.09	257.81	495.96
NT		Pass	Pass	Pass
EVT		Pass	Pass	Pass
p value		0.04	0.33	0.12
Pa		0.50	0.06	0.22

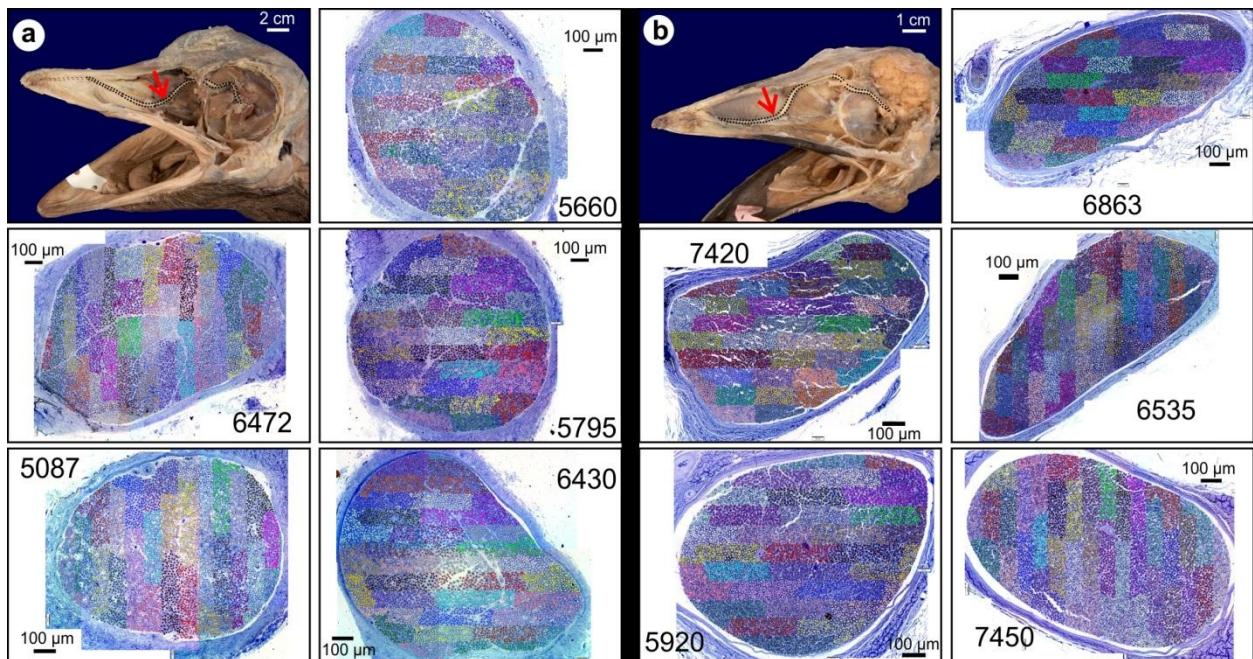


Figure 6.8. The *N. ophthalmicus R. medialis* of the Trigeminal nerve of the ostrich (a) and emu (b). The red arrow indicates the location from where the nerves were sampled. The five nerves on the left of the figure represent those from the ostrich (5888.8 ± 578.15) and the five on the right, those from the emu (6837.6 ± 641.96). The number of myelinated nerve fibres is indicated on each nerve (see also Table 6.1). Toluidine blue stained sections.

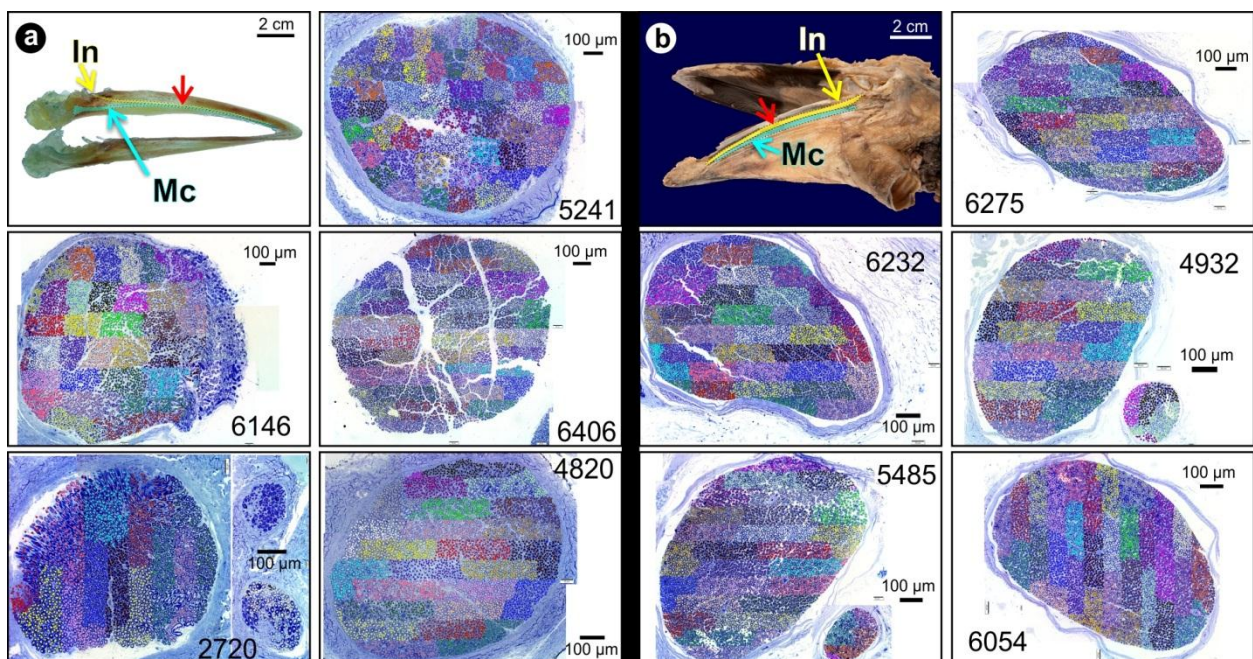


Figure 6.9. The *N. intramandibularis* of the Trigeminal nerve of the ostrich (a) and emu (b). The red arrow indicates the location from where the nerves were sampled. The five nerves on the left of the figure represent those from the ostrich (5066.6 ± 1462.61) and the five on the right, those from the emu (5795.6 ± 576.48). The number of myelinated nerve fibres is indicated on each nerve (see also Table 6.1). Toluidine blue stained sections. (a). The mandible stained with alcian blue (for cartilage) and cleared with glycerol. The intramandibular nerve (In) is outlined and shaded yellow and Meckel's cartilage (Mc) is outlined and shaded blue for clarity. (b). The intramandibular nerve (In) is outlined and shaded yellow. Meckel's cartilage (Mc) is not stained but outlined and shaded blue for clarity. The bony mandible has been removed.

The difference in the mean values of myelinated nerve fibres in the intramandibular nerve and the total number of myelinated nerve fibres (intramandibular nerve and medial branch of the ophthalmic nerve) between the ostrich and emu was not great enough to reject the possibility that the differences were due to random sampling variability (Table 6.1). There was no statistically significant difference between these specific myelinated nerve fibre counts in the ostrich and emu (Table 6.1). However, the power of the performed tests (0.06 and 0.22 respectively) was below the desired power of 0.8 for these nerve counts (Table 6.1). This indicates that, due to the small sample size, a difference is less likely to be detected if one does actually exist. Therefore these results should be interpreted with caution.

The difference in the mean value of the nerve count of the medial branch of the ophthalmic nerve between the ostrich and emu was greater than what would be expected by chance (Table 6.1). There was a statistically significant difference between the nerve counts for the above mentioned nerve in the ostrich and emu (Table 6.1). However, the power of the performed test (0.5) for the above nerve was below the desired power of 0.8 (Table 6.1). This indicates that, due to the small sample size, a difference is more likely to be detected when one does not actually exist. Therefore this result should be interpreted with caution.

When considering the numbers of myelinated nerve fibres within each species the difference in the mean values (\pm SD) of the medial branch of the ophthalmic nerve (5888.8 ± 578.16) and the intramandibular nerve (5055.6 ± 1462.61) in the ostrich was not great enough to reject the possibility that the differences were due to random sampling variability (Table 6.1). There was no statistically significant difference ($p=0.28$) between these two nerves in the ostrich. However, the power of the performed test (0.08) was below the desired power of 0.8. This indicates that, due to the small sample size, a difference is less likely to be detected if one does actually exist. Therefore this result should be interpreted with caution. In the emu, the difference in the mean values of the myelinated nerve fibres of the medial branch of the ophthalmic nerve (6837.6 ± 641.95) and the intramandibular nerve (5795.6 ± 576.48) was greater than what would be expected by chance (Table 6.1). There was a statistically significant difference ($p=0.03$) between these two nerves in the emu. However, the power of the performed test (0.6) was below the desired power of 0.8. This indicates that, due to the small

sample size, a difference is more likely to be detected when one does not actually exist. Therefore this result should be interpreted with caution.

6.3.3. Transmission electron microscopy (TEM) of the Trigeminal nerve branches

The medial branch of the ophthalmic nerve and the intramandibular nerve displayed similar features in both species. The description below therefore pertains to both nerve branches in the ostrich and emu. On low magnification, with both light microscopy using toluidine blue stained sections (Fig. 6.10a) and TEM (Fig. 6.10b), the most obvious feature of the nerve was the presence of large, myelinated nerve fibres (Fig. 6.10) which measured $13.17 \mu\text{m} \pm 2.17 \mu\text{m}$; range $9.38 - 18.41 \mu\text{m}$ in the ostrich ($n=24$) and $12.13 \mu\text{m} \pm 2.18 \mu\text{m}$; range $7.56 - 15.14 \mu\text{m}$ in the emu ($n=30$). Between the large myelinated nerve fibres were smaller myelinated nerve fibres (Figs. 6.10-13) which measured $4.47 \mu\text{m} \pm 2.23 \mu\text{m}$; range $1.32 - 8.89 \mu\text{m}$ in the ostrich ($n=30$) and $3.68 \mu\text{m} \pm 1.85 \mu\text{m}$; range $0.15 - 7.9 \mu\text{m}$ in the emu ($n=30$). The smaller myelinated nerve fibres displayed a thinner myelin sheath (Figs. 6.12 and 6.13) than the larger fibres, but were still visible using light microscopy due to the intense staining of the myelin sheath with toluidine blue (Fig. 6.10a). Non-myelinated fibres (Figs. 6.10b, 6.11 and 6.15) measured $1.58 \mu\text{m} \pm 0.55 \mu\text{m}$; range $0.69 - 2.89 \mu\text{m}$ in the ostrich ($n=25$) and $1.04 \mu\text{m} \pm 0.32 \mu\text{m}$; range $0.55 - 2.02 \mu\text{m}$ in the emu ($n=30$) and were located mainly in groups. These non-myelinated nerve fibres were individually surrounded by Schwann cell cytoplasmic processes (Fig. 6.15) and were only visible using TEM. Schwann cell nuclei were occasionally visible at the periphery of the nerve fibres (Figs. 6.11 and 6.12) and fibroblast nuclei were sometimes visible in the connective tissue stroma (Fig. 6.10b). Large blood vessels were located at the periphery of the nerve and in the connective tissue sheaths penetrating the nerve, whereas smaller vessels and capillaries were scattered between the nerve fibres (Fig. 6.10).

All nerve fibres were embedded in the endoneurium which was composed of bundles of collagen microfibrils with their long axis oriented parallel to the long axis of the nerve (Figs. 6.11-15). The endoneurium was surrounded/sub-divided by cytoplasmic processes of fibroblasts which formed an ill-defined perineurium (Fig. 6.11). In favourable sections, all the components of a typical, peripheral myelinated nerve were observed. The myelin sheath displayed major dense lines, representing the fused inner leaflets of the Schwann cell plasma membrane, intraperiod lines, indicating the fused outer plasma membrane leaflets and an extracellular space (Fig. 6.14). The outer mesaxon was present in the peripheral collar of Schwann cell cytoplasm and an inner mesaxon continuous with the axolemma could occasionally be observed. The Schwann cell nucleus was highly heterochromatic and displayed a prominent nucleolus (Fig. 6.11) and numerous nuclear pores (Fig. 6.12). The cytoplasm was rich in rough endoplasmic reticulum, smooth endoplasmic reticulum, Golgi fields, dense bodies, cytoplasmic vacuoles and mitochondria. A basal lamina was present around the Schwann cells of both myelinated and non-myelinated nerve fibres (Figs. 6.12-15). All axons typically displayed longitudinally oriented microtubules and neurofilaments (Figs. 6.13 and 6.15) and occasional mitochondria (Fig. 6.13).

In both the ostrich and emu the myelinated component of both nerves demonstrated various abnormalities, the most common being axonal degeneration. Hypermyelination and myelin ovoids were also present. This was a consistent feature in all the material studied.

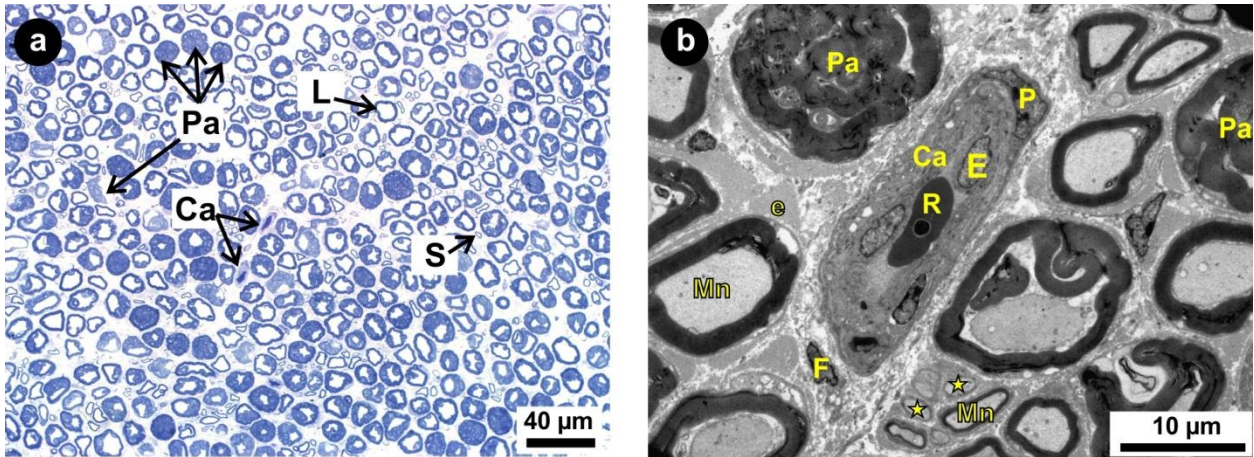


Figure 6.10. The *N. ophthalmicus R. medialis* of the Trigeminal nerve in the ostrich. (a). Toluidine blue stained section on which the nerve fibre counts were conducted. Only large (L) and small (S) myelinated nerve fibres were counted. A degree of nerve fibre pathology (Pa) was a normal feature in all the specimens. Capillaries (Ca). (b). TEM. Note the capillary (Ca), with a red blood cell (R) in the lumen, positioned amongst small myelinated (Mn) and non-myelinated (stars) nerve fibres. Fibroblast nuclei (F) are located in the perineurium. Nucleus of endothelial cell (E), nucleus of pericyte (P), endoneurium (e) and nerve pathology (Pa).

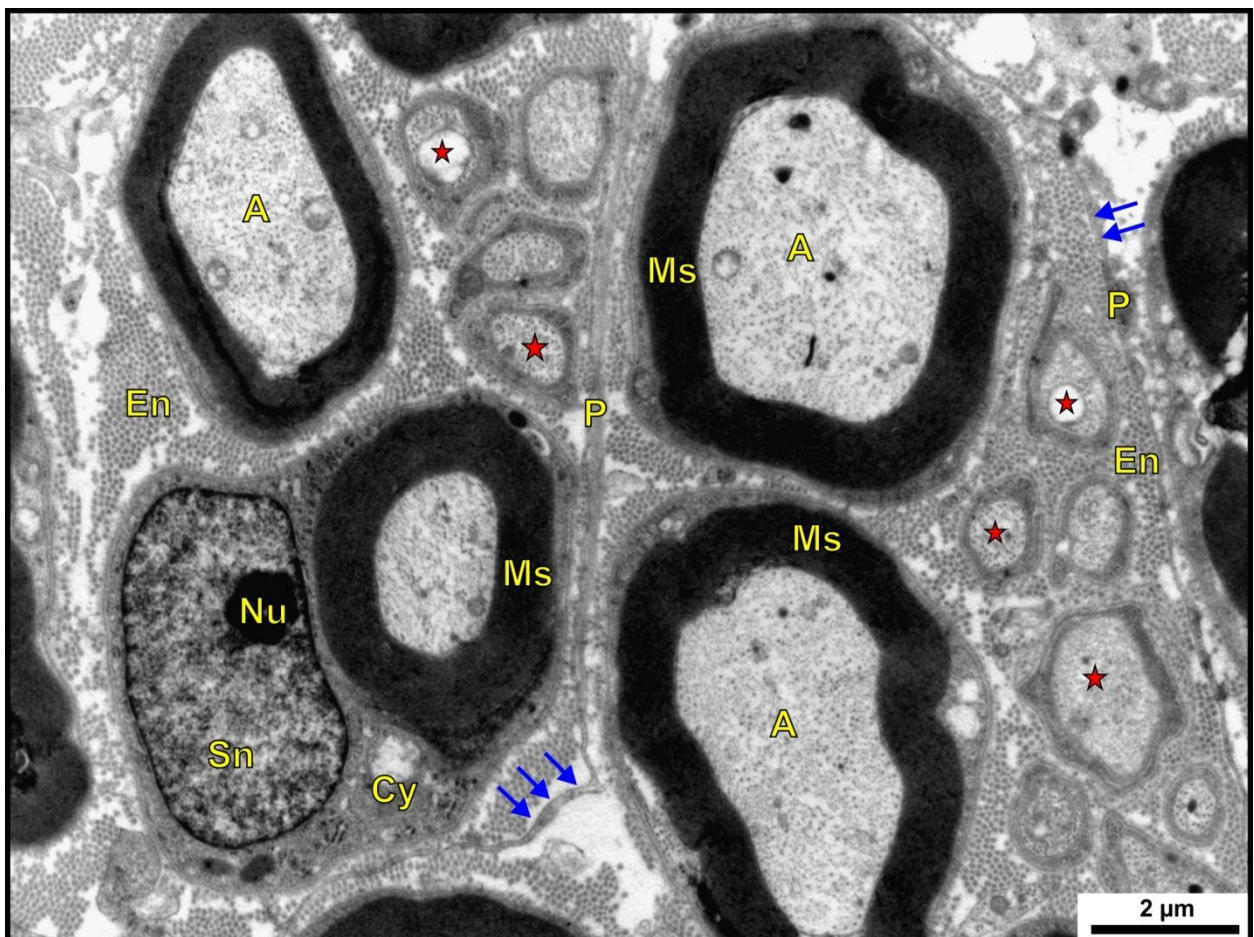


Figure 6.11. Transverse section of the *N. ophthalmicus R. medialis* in the ostrich. Note the presence of both small myelinated axons (A), with a myelin sheath (Ms), and non-myelinated (red stars) axons surrounded by Schwann cell cytoplasmic processes. Fibroblast cytoplasmic processes (blue arrows) form the perineurium (P) and surround the endoneurium (En). Large heterochromatic Schwann cell nucleus (Sn) with prominent nucleolus (Nu) and Schwann cell cytoplasm (Cy).

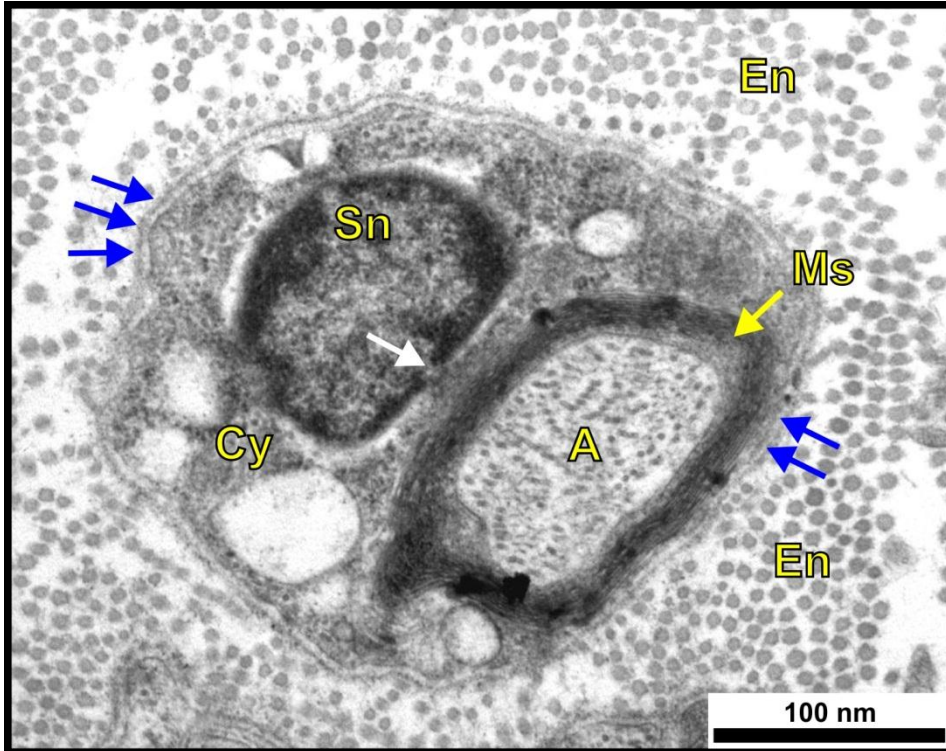


Figure 6.12. Transverse section of a very small myelinated nerve fibre from the *N. ophthalmicus R. medialis* in the emu. The axon (A) displays microtubules and neurofilaments and is surrounded by a thin myelin sheath (Ms). Schwann cell cytoplasm (Cy). Nuclear pore (white arrow), basal lamina (blue arrows), endoneurium (En) and Schwann cell nucleus (Sn).

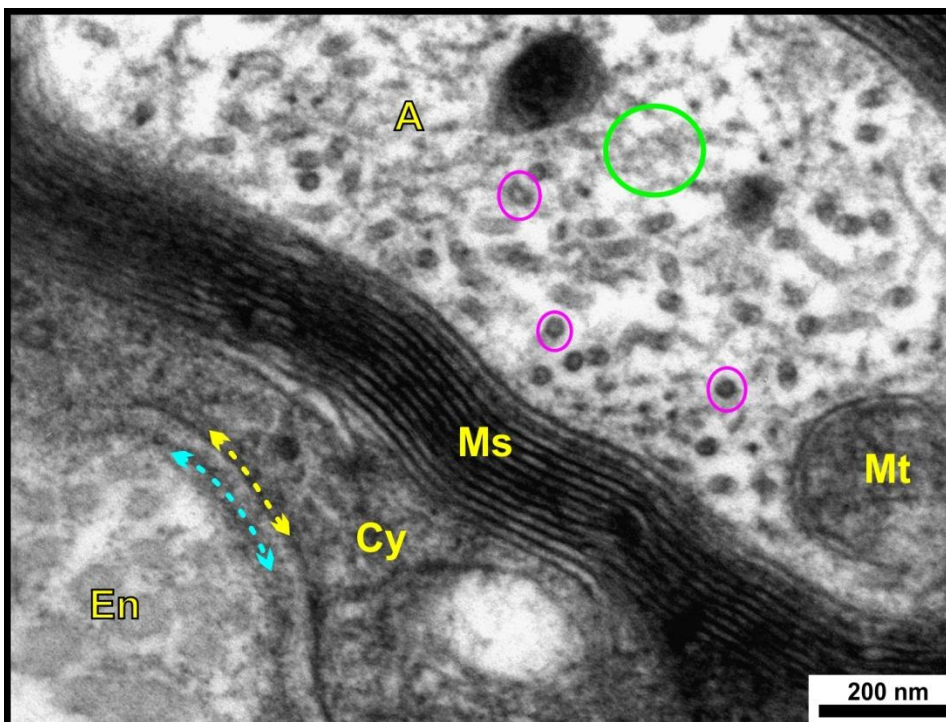


Figure 6.13. Transverse section of a small myelinated nerve fibre from the *N. ophthalmicus R. medialis* in the ostrich. The axon (A) contains microtubules (pink circles), neurofilaments (green circle) and mitochondria (Mt). Note the surrounding lamellated myelin sheath (Ms) and the Schwann cell cytoplasm (Cy). Schwann cell plasmalemma (yellow curved arrow), basal lamina (blue curved arrow) and endoneurium (En).

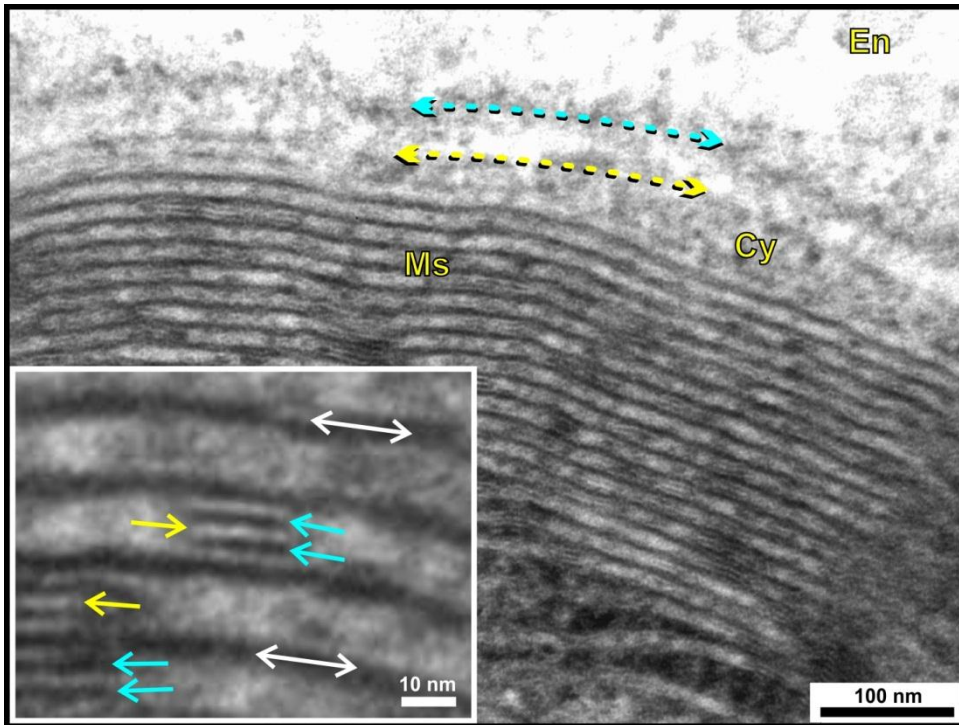


Figure 6.14. Transverse section of the myelin sheath from a nerve fibre of the *N. ophthalmicus R. medialis* of the emu. Note the regular and parallel arrangement of the myelin sheath (Ms) displaying major dense lines (white arrows), intraperiod lines (blue arrows) and an extracellular space (yellow arrows). Schwann cell cytoplasm (Cy) and plasmalemma (yellow curved arrow), basal lamina (blue curved arrow) and endoneurium (En).

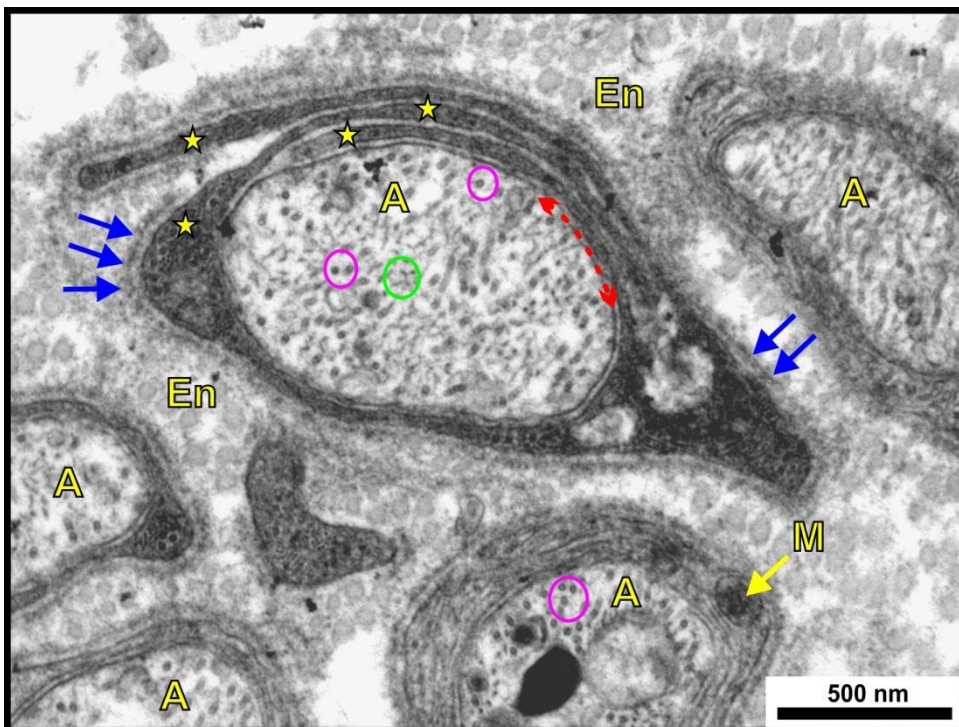


Figure 6.15. Transverse section of non-myelinated nerve fibres from the *N. intra-mandibularis* in the ostrich. The axons (A) are surrounded by cytoplasmic extensions (yellow stars) of Schwann cells. Microtubules (pink circles) and neurofilaments (green circle) are contained within the axons. Axolemma (red curved arrow), Schwann cell basal lamina (blue arrows), mitochondrion (M) and endoneurium (En).

6.4. Discussion

In birds the trigeminal nerve, cranial nerve number five (CN V), is largely sensory in nature and has three major divisions: the ophthalmic, maxillary and mandibular nerves (Bubień-Waluszewska, 1981). The ophthalmic nerve either enters the orbit ventro-lateral to the optic nerve, together with cranial nerves III and VI, or through its own ophthalmic foramen, as in Anatidae (Bubień-Waluszewska, 1981) and the ostrich and emu (present study). However, in the two ratites studied the ophthalmic and optic foramina were sometimes fused. The mandibular nerve may either exit from the skull with the maxillary nerve (through the maxillomandibular foramen), or through its own separate foramen (analogous to the *For. ovale* in mammals) (Bubień-Waluszewska, 1981), with the former being the situation in both the ostrich and emu. In the present study the medial branch of the ophthalmic nerve and the intramandibular nerve (the main continuation of the mandibular nerve) were the two main nerve trunks supplying terminal sensory branches to the premaxilla and mandibular rostrum, respectively, in both the ostrich and emu. The path followed by these nerves was similar between the two species and also to that described in other birds (Wight *et al.*, 1970; Krol and Dubbeldam, 1979; Berkhoudt, 1980; Bubień-Waluszewska, 1981; Dubbeldam *et al.*, 1995). The information presented on the trigeminal nerve in the ostrich embryo (Webb, 1957) and on the ophthalmic nerve in the emu (Cobb and Edinger, 1962) was similar to that observed in the present study in both species. However, some differences in terminology are apparent in the earlier studies. When compared to the terminology used in the current work based on Nomina Anatomica Avium (NAV) (Dubbeldam, 1993) the *N. ophthalmicus R. medialis* is referred to as the *R. praemaxillaris inferior (medialis)* and the *N. intramandibularis* is referred to as the *R. mandibularis internus* in the ostrich (Webb, 1957) and the *N. ophthalmicus R. medialis* as the orbitonasal nerve in the kiwi (Parker, 1891). The terminology of the nerves also differs in the mallard (Krol and Dubbeldam, 1979; Berkhoudt, 1980) where the *R. ophthalmicus* (Berkhoudt, 1980) appears to represent the *N. ophthalmicus R. medialis* referred to in this study, the *N. alveolaris inferior* (Berkhoudt, 1980) the *N. intramandibularis* in the ostrich and emu and the superior and inferior premaxillary branches (Krol and Dubbeldam, 1979) the dorsal and ventral premaxillary branches observed in the ostrich.

The ramifications of the medial branch of the ophthalmic nerve in the ostrich and emu appeared to differ slightly from that mentioned in the literature. Before entering the maxillary rostrum, the medial branch of the ophthalmic nerve in birds reportedly divides into dorsal and ventral premaxillary branches (Wight *et al.*, 1970; Berkhoudt, 1980; Bubień-Waluszewska, 1981; Dubbeldam, 1993). This division occurs near the rostral point of the external nares, which in the mallard (Krol and Dubbeldam, 1979), is positioned more caudally in relation to the maxillary rostrum than in the ostrich and emu (see Chapter 4). As a result, the dorsal and ventral premaxillary branches are considerably longer in the mallard (Krol and Dubbeldam, 1979) before they ramify at the rostral extremity of the maxillary rostrum, than the corresponding branches in the ostrich and emu. The dorso-medial and ventro-lateral premaxillary branches in the ostrich represent the dorsal and ventral premaxillary branches, respectively, as noted in other birds (Wight *et al.*, 1970; Bubień-Waluszewska, 1981; Dubbeldam, 1993) including the mallard (Krol and Dubbeldam, 1979; Berkhoudt, 1980). In the emu, with more rostrally positioned nostrils than the ostrich (see Chapter 4), the branching of the medial branch of the ophthalmic nerve was too extensive to identify specific components (dorsal and ventral premaxillary branches) and were collectively termed premaxillary branches. In contrast to the situation in other birds where the dorsal branch enters the premaxilla (Berkhoudt, 1980; Bubień-Waluszewska, 1981), the ventral premaxillary branch (or more lateral branches in the emu) enters the premaxilla together with the dorsal branch. Although the branching of the nerves rostral to the nares appears to differ slightly between the mallard (Krol and Dubbeldam, 1979; Berkhoudt, 1980), chicken (Wight *et al.*, 1970; Bubień-Waluszewska, 1981) ostrich and emu (most likely reflecting the differently shaped bills) they all commonly display extensive ramifications at the most rostral bill tip and project branches (*Rr. rostri maxillaris*) through bony canals and neurovascular foramina to the dermis surrounding the premaxilla.

The ramifications of the intramandibular nerve within the mandibular rostrum of the emu were far more complex than those of the ostrich. However, no significant difference in the number of nerve fibres forming this nerve was apparent between the two species (see below). The relatively simple branching pattern of the intramandibular nerve in the ostrich was restricted to the most rostral extremity of the mandibular rostrum in the vicinity of the concentration of pits in the dentary bone (see Chapter 5). Similarly, in the mallard (Berkhoudt, 1980), although the nerve within the dentary bone was described

as displaying explosive branching, the pattern appears more similar to that of the ostrich than of the emu, and thus less extensive. This observation would suggest that the mandibular bill tip in both the ostrich and mallard would have more tactile acuity at the most rostral extremity in contrast to the emu where the entire mandibular rostrum would have a more overall distribution of tactile sense. However, the MVR lends a midline sensitivity to this region in the ostrich. The proposed role of the keratinised pegs in conducting vibrational stimuli to Herbst corpuscles in pits in the dentary bone (see Chapter 4) is further strengthened by the presence of small nerves projecting laterally towards the pits. These lateral branches off the plexus within the mandibular rostrum would most likely represent a receptor unit receiving stimuli from a number of Herbst corpuscles around the periphery of the nerve thus forming part of the bill tip organ in the emu.

The structure of both the medial branch of the ophthalmic nerve and the intramandibular nerve in the ostrich and emu revealed light microscopic and ultrastructural features consistent with that reported in mammals (Bubień-Waluszewska, 1985; Beitz and Fletcher, 2006) and birds (Bubień-Waluszewska, 1985; Pavelka and Roth, 2010). TEM revealed that in both species these nerves were mixed, containing both large and small myelinated nerve fibres and non-myelinated nerve fibres similar to that noted in the chicken (Dubbeldam *et al.*, 1995).

It would appear that from the available literature that the only other avian species in which the nerve fibres of the medial branch of the ophthalmic nerve and the intramandibular nerve have been counted is the chicken (Dubbeldam *et al.*, 1995). Although the same nerve branches, sampled at similar locations to those in the present study, were examined in the chicken, the techniques used for their enumeration and determination of fibre size differed. Statistical evaluation indicated that a larger sample size was necessary in the present study to arrive at more accurate comparisons. However, the low sample sizes ($n=5$) of each species in the present study is similar to the sample size used in the chicken (Dubbeldam *et al.*, 1995). A total of 1325 nerve fibres were counted in the ophthalmic nerve of the pigeon (Graf, 1956); however, this number cannot be compared to the chicken (Dubbeldam *et al.*, 1995) or the ostrich and emu (present study) as the sampling site was more proximal and therefore may have included nerve fibres of the lateral and medial branches of the ophthalmic nerve. Larger

nerve fibre diameters were observed in the ostrich (up to 18 μm) and emu (up to 15 μm) compared to the upper calibre limit of nerve fibres in the pigeon of between 6-10 μm (Graf, 1956). As the ostrich and emu are considerably larger than the pigeon it is tempting to attribute the nerve fibre size difference to the difference in the size of the birds. However, as noted by Häggqvist (1948), there is no direct correlation between body size and the calibre spectra of nerve fibres. Thus the difference may be attributed to the well-developed sensory area of the bill tip in the ostrich and emu compared to that in the pigeon, with larger nerve fibres more effectively relaying sensory signals.

In the chicken, three types of nerve fibres were identified and counted using TEM; small and large myelinated fibres and non-myelinated fibres (Dubbeldam *et al.*, 1995). These fibres were enumerated by using grids placed on micrographs of the TEM sections, estimating surface areas of the nerves on light micrographs, measuring surface areas of nerve fibres and extrapolating the data to total numbers, whereas in the present study composite light micrographs were used to count all of the myelinated nerve fibres for each nerve in the ostrich and emu. Fibre size in the chicken was measured as a surface area of the axons and their myelin sheath (μm^2) whereas the present study measured the cross-sectional diameter of the fibres and myelin sheath (μm), thus comparison of the measurements is not possible. However, nerve fibre numbers could be compared. The total number of myelinated nerve fibres in the medial branch of the ophthalmic nerve in the chicken (2860) ($n=3$) was less than half that of the same nerve in the ostrich (5888.8 ± 578.15) ($n=5$) and emu (6837.6 ± 641.96) ($n=5$). Similarly, the number of myelinated nerve fibres in the intramandibular nerve in the chicken (1834) ($n=5$) was 2.5 – 3 times less than that of the same nerve in the ostrich (5066.6 ± 1462.61) ($n=5$) and emu (5795.6 ± 576.48) ($n=5$). To what extent these differences, as with the difference in nerve fibre calibre outlined above, simply reflect the physical size of the birds compared, or the extent of the bill tip organ between the chicken and the ratites studied, could not be determined.

The emu displays significantly more nerve fibres in the medial branch of the ophthalmic nerve (6838) when compared to the same nerve in the ostrich (5889). The same nerve also contains more fibres than the intramandibular nerve in both species (ostrich: 5067 and emu: 5796). This would indicate that the bill tip organ in the emu is better developed in the upper bill than in the ostrich or in the lower bill of both species. As the

basic design of the bill tip organ is similar in the ostrich and emu (arrangement of Herbst corpuscles around a nerve and the specific location of these structures) (see Chapter 7), the higher number of nerve fibres in the medial branch of the ophthalmic nerve would more likely indicate a greater tactile acuity in the maxillary rostrum of the emu as opposed to reflecting a better developed bill tip organ (see also Chapter 7). The similarity in the number of nerve fibres between the medial branch of the ophthalmic nerve and the intramandibular nerve of the ostrich, and the similarity between the number of fibres of the intramandibular nerve between the ostrich and emu, would suggest that the upper and lower bill of the ostrich and lower bill of the emu are equally sensitive. The relation between the number of nerve fibres in each species and the density of Herbst corpuscles is discussed in Chapter 7. Similar to the emu, the chicken also displays a higher proportion of myelinated nerve fibres in the medial branch of the ophthalmic nerve compared to the intramandibular nerve (Dubbeldam *et al.*, 1995). In the chicken this was postulated to reflect a better developed bill tip organ (arrangement of Herbst corpuscles) in the upper bill than in the lower bill (Dubbeldam *et al.*, 1995), despite the fact that a bill tip organ has only been described in the lower bill of this species (Gentle and Breward, 1986). However, as noted in the emu, the presence of more Herbst corpuscles may not necessarily reflect a better developed bill tip organ, but merely indicate a higher density of Herbst corpuscles.

The close association of the *N. intramandibularis* with Meckel's cartilage within the mandibular neurovascular canal was a unique feature in both birds. This association has not been reported in other adult birds (see Chapter 5), including the chicken (Bubień-Waluszewska, 1981) and mallard (Berkhoudt, 1980). It is unlikely that Meckel's cartilage would add any structural support to the mandible in the adult bird, although it is possible that this cartilage ossifies with advancing age thus fulfilling such a function (see Chapter 5). A protective function is also not indicated as it is not positioned on the open, medial part of the mandibular neurovascular canal. Excluding the function of Meckel's cartilage acting as an attachment site for *M. pseudotemporalis superficialis* (see Chapter 5), its persistence through to adulthood is an enigma that has three possible explanations. It is either a non-functional embryonal remnant carried through to adulthood and therefore a pedomorphic trait (this is unlikely); or it is a symplesiomorphic trait, strengthening a closer link between the ostrich and emu (ratites) and the lepidosaurs and crocodylia; or it represents a functional structure that possibly plays a

role in absorbing shockwaves produced by pecking against hard substrates. Meckel's cartilage would possibly prevent nerve fibres within the *N. intramandibularis* from creating action potentials by direct mechanical stimulation as opposed to transporting action potentials initiated by mechanoreceptors in the bill tip. The end result would be better isolation of tactile cues received from the mandibular rostrum. Cartilage is also present along the greater length of the medial branch of the ophthalmic nerve, in the form of the cartilaginous nasal septum (see Figs. 6.3, 6.6d and 6.7d). This cartilage may act in a similar fashion to that described for Meckel's cartilage and afford better isolation of tactile cues received from the maxillary rostrum. This proposed function would need to be explored in future studies.

6.5. References

- Beitz, A.J. and Fletcher, T.F. 2006. *Nervous Tissue*. In: Dellmann's Textbook of Veterinary Histology. 6th edition. Edited by Eurell, J.-A., Frappier, B.L. Ames, Iowa: Blackwell Publishing. pp. 91-116.
- Berkhoudt, H. 1980. The morphology and distribution of cutaneous mechanoreceptors (Herbst and Grandry corpuscles) in bill and tongue of the mallard (*Anas platyrhynchos* L.). *Netherlands Journal of Zoology*. **30**: 1-34.
- Bubień-Waluszewska, A. 1981. *The Cranial Nerves*. In: Form and Function in Birds. Vol. 2. Edited by King, A.S. and McLelland, J. London: Academic Press. pp. 385-438.
- Bubień-Waluszewska, A. 1985. *Somatic Peripheral Nerves*. In: Form and Function in Birds. Vol. 3. Edited by King, A.S. and McLelland, J. London: Academic Press. pp. 149-193.
- Cobb, S. and Edinger, T. 1962. The brain of the Emu (*Dromaeus novaehollandiae*, Lath) I. Gross anatomy of the brain and pineal body. *Breviora Museum of Comparative Zoology*. **170**: 1-18.
- Dubbeldam, J.L. 1993. *Systema Nervosum Periphericum*. In: Handbook of avian anatomy: Nomina Anatomica Avium, 2nd edition. Edited by Baumel, J.J., King, A.S., Breazile, J.E., Evans, H.E. and Vanden Berge, C. Cambridge, Massachusetts: The Nuttall Ornithological Club, No. 23. pp. 555-584.
- Dubbeldam, J.L. 1998. The sensory trigeminal system in birds: input, organization and effects of peripheral damage. A review. *Archives of Physiology and Biochemistry*. **106**: 338-345.
- Dubbeldam, J.L. 2009. The trigeminal system in birds and nociception. *Central Nervous System Agents in Medicinal Chemistry*. **9**: 150-158.

- Dubbeldam, J.L. and Veenman, C.L. 1978. Studies on the somatotopy of the trigeminal system in the mallard, *Anas platyrhynchos* L.: I. the Ganglion trigeminale. *Netherlands Journal of Zoology*. **28**: 150-160.
- Dubbeldam, J.L., de Bakker, M.A.G. and Bout, R.G. 1995. The composition of trigeminal nerve branches in normal adult chickens and after debeaking at different ages. *Journal of Anatomy*. **186**: 619-627.
- Gentle, M.J. 1989. Cutaneous sensory afferents recorded from the nervus intramandibularis of *Gallus gallus* var *domesticus*. *Journal of Comparative Physiology A*. **164**: 763-774.
- Gentle, M.J. and Breward, J. 1986. The bill tip organ of the chicken (*Gallus gallus* var. *domesticus*). *Journal of Anatomy*. **145**: 79-85.
- Graf, W. 1956. Caliber spectra of nerve fibers in the pigeon (*Columba domestica*). *Journal of Comparative Neurology*. **105**: 355-363.
- Häggqvist, G. 1948. Nervenfaserkaliber bei Tieren verschiedener Grösse. *Anatomischer Anzeiger*. **96**: 398-412.
- Krol, C.P.M. and Dubbeldam, J.L. 1979. On the innervation of taste buds by the *N. facialis* in the mallard, *Anas platyrhynchos* L. *Netherlands Journal of Zoology*. **29**: 267-274.
- Parker, T.J. 1891. Observations on the anatomy and development of apteryx. *Philosophical Transactions of the Royal Society of London, B*. **182**: 25-134.
- Pavelka, M. and Roth, J. 2010. *Functional Ultrastructure. Atlas of Tissue Biology and Pathology*. 2nd edition. Austria: SpringerWienNewYork.
- Pettigrew, J.D. and Frost, B.J. 1985. A tactile fovea in the *Scolopacidae*? *Brain Behavior and Evolution*. **26**: 185-195.
- Vanden Berge, J.C. and Zweers, G.A. 1993. *Myologia*. In: Handbook of Avian Anatomy: Nomina Anatomica Avium, 2nd edition. Edited by Baumel, J.J., King, A.S., Breazile, J.E., Evans, H.E. and Vanden Berge, C. Cambridge, Massachusetts: The Nuttall Ornithological Club, No. 23. pp. 189-247.
- Webb, M. 1957. The ontogeny of the cranial bones, cranial peripheral and cranial parasympathetic nerves, together with a study of the visceral muscles of *Struthio*. *Acta Zoologica* **38**: 81-203.
- Wight, P.A.L., Siller, W.G. and Mackenzie, G.M. 1970. The distribution of Herbst corpuscles in the beak of the domestic fowl. *British Poultry Science*. **11**: 165-170.

CHAPTER 7

MORPHOLOGY AND SENSORY SPECIALISATIONS OF THE BILL.

IV. THE BILL TIP ORGAN

7.1. Introduction

The bill can be described as a highly specialised sensory organ which has the ability to discriminate between edible and non-edible items (Widowski, 2010), the morphology of which can be linked to foraging behaviour, diet and habitat selection (see Nebel *et al.*, 2005; Widowski, 2010; Piersma, 2011). Pacinian corpuscles are numerous in human fingers as are Herbst corpuscles in the beaks of birds, strengthening the suggestion that the bill serves many of the purposes of a human hand and is used amongst others for defense, feeding, preening, nest building (Wight *et al.*, 1970) and exploration (Demery *et al.*, 2011). Therefore, an understanding of bill morphology in a particular species of bird, as well as their perceptual systems (Piersma, 2011) such as the bill tip organ, may be important in interpreting the habits and food selection of the bird itself. The bill is covered by a tough, keratinised epithelium (rhamphotheca) and is supported by the premaxillary and mandibular bones (Widowski, 2010). The dermis, situated between the epithelium and bone, is richly supplied with blood vessels, nerves and sensory receptors (Widowski, 2010). The bill has been studied extensively in domestic poultry (Gottschaldt and Lausmann, 1974; Gentle and Breward, 1986; Berkhoudt, 1976, 1980; Halata and Grim, 1993). In contrast, information on bill morphology in ratites is scarce and has been addressed in Chapters 4-6 as part of this study.

A complex sensory structure known as the bill tip organ (*Terminationes sensorium apicis rostri*)¹, and which was originally noted in parrots (Goujan, 1869), has been described at length mostly in birds which forage by probing such as the woodcock and snipe (Goglia, 1964), *Limicolae* (shorebirds) (Bolze, 1968; Nebel *et al.*, 2005),

¹ "The "bill-tip organ" is not really an "organ" but rather an aggregation of sensory structures (Grandry and Herbst-type cells) in the bill, best developed in charadriiforms and anseriformes. It has been seen in the shorebirds such as snipe (Bolze, 1968; Goglia, 1964) and sandpipers (Gerritsen, 1988), and studied extensively in ducks and geese...." (Evans and Martin, 1993).

Scolopacidae (sandpipers) (Pettigrew and Frost, 1985), kiwi species (Cunningham *et al.*, 2007) and ibis (Cunningham *et al.*, 2010a, b), or in birds which use their beak for straining (ducks and geese) (Gottschaldt and Lausmann, 1974; Berkhoudt, 1976, 1980). A bill tip organ has, however, been described in a few other species of birds which use their bills for pecking. These include the chicken (Gentle and Breward, 1986) and Japanese quail (Halata and Grim, 1993). This structure has also been classified as a somatosensory organ (Evans and Martin, 1993). In probing birds the bill tip organ serves as a remote sense of touch by detecting vibrotactile and/or pressure cues from prey in the substrate (Piersma *et al.*, 1995; Zweers and Gerritsen, 1997; Nebel *et al.*, 2005; Cunningham *et al.*, 2010b). However, a less complex arrangement of Herbst corpuscles may still constitute a bill tip organ but one which functions by direct touch (Gerritsen and Meiboom, 1986). Amongst the extant ratites, the kiwi is the only bird to have a long, slightly down-curved bill which it uses for probing (Cunningham *et al.*, 2007). It has been demonstrated that, in similar fashion to other probing birds such as the *Scolopacidae*, the kiwi also possesses a bill tip organ (Cunningham *et al.*, 2007). In part, the existence of the bill tip organ was identified in the kiwi by the presence of numerous, obvious bony pits in the rostrum of the bill (Cunningham *et al.*, 2007), the *Foveae corpusculorum nervosorum* (Baumel and Witmer, 1993). Similar bony pits have been identified in the ostrich and emu (see Chapter 5) and, furthermore, Herbst corpuscles are encountered in the same region (see Chapters 3-6). However, it still remains to be determined whether or not the ostrich and/or emu possess a collection of Herbst corpuscles concentrated in the rostral bill tip which could be specifically classified as a bill tip organ.

This Chapter essentially collates and expands on the results from Chapters 3-6 to confirm, describe and compare the bill tip organ in the ostrich and emu.

7.2. Materials and Methods

The specimens collected and dissected/prepared as detailed in Chapters 4.2.1, 4.2.2, 5.2.1, 5.2.2 and 6.2.2 were used to demonstrate the macroscopic features of the bill tip organ in the ostrich and emu. For microscopic observations the same histology slides utilised in Chapter 3.2.3 (from 5 adult ostrich and 5 adult emu) and Chapter 4.2.3 (from

5 ostrich chicks and 1 emu chick) were examined in order to describe the microscopic features of the bill tip organ. Histological sections were viewed, features of interest described and digitally recorded using an Olympus BX63 light microscope (Olympus Corporation, Tokyo, Japan) equipped with a DP72 camera and Olympus cellSens imaging software (Olympus Corporation, Tokyo, Japan), and annotated in Corel Draw X5.

7.3. Results

7.3.1. The bill tip organ

Based on the localisation of bony pits and the distribution of Herbst corpuscles, as well as the presence of specialised epidermal structures, the bill tip organ in the ostrich and emu was defined in this study as follows: In the upper bill it was confined to the region underlying the sensory cap in the ostrich (Fig. 7.1a) and to the region extending from the maxillary nail up to the nostrils in the emu (Fig. 7.1c) as well as the corresponding intra-oral regions. In the lower bill it occupied the mandibular rostrum and distal portions of the mandibular arms (Figs. 7.1b, d) and the corresponding intra-oral region, in both birds. Although the external features of that part of the bill housing the bill tip organ differed slightly between the two species, the basic microscopic structure of the bill tip organ was similar between the two birds, with each displaying unique specialisations (see below).

The bill tip organ of the upper bill was characterised externally by a prominent maxillary nail which continued caudally as the *Culmen* (Figs. 7.1a, c, 7.5 and 7.6). The *Culmen* was a raised epidermal structure bordered on either side by the rhamphotheca (*Str. corneum* of the epithelium) (Figs. 7.1a, c, 7.5 and 7.6). The portion of rhamphotheca rostral to the nostrils and lateral to, and including the rostral aspect of the *Culmen*, was considered to represent the bill tip organ of the upper bill (Figs. 7.1a, c). In the ostrich, the rhamphotheca rostral to the nostrils, adjacent to the *Culmen* and stretching to the tomia, was termed the sensory cap (Fig. 7.1a) and was characterised by the presence of oblique striations representing specialised adaptations, the epidermal troughs (see Discussion below and Chapter 4). Although a similar-shaped region was present in the

emu (Fig. 7.1c), it was not as obvious an external feature or as large as in the ostrich. The corresponding ventral aspect of the above mentioned regions represented the intra-oral portion of the bill tip organ in both birds. However, in the ostrich, a prominent median palatine ridge packed with Herbst corpuscles was present (see Chapter 3).

The bill tip organ of the lower bill was characterised externally by a prominent mandibular nail (Fig. 7.4) which continued caudally as the *Gonys* (Figs. 7.1b, d and 7.9a). Similar to the *Culmen*, the *Gonys* was a raised epidermal structure bordered on either side by rhamphotheca (*Str. corneum* of the epithelium) (Figs. 7.1b, d, and 7.9a). The portion of rhamphotheca adjacent to, and including the *Gonys*, and those parts overlying the regions of bony pits (Fig. 7.8) (see Chapter 5) located in the dentary bone were considered to represent the bill tip organ of the lower bill (Figs. 7.1b, d). In the ostrich, oblique striations similar to those seen in the upper bill were visible in the rhamphotheca and represented epidermal troughs (see Discussion and Chapter 4). In the emu, the tomium displayed rhamphothecal serrations with keratinised pegs positioned between each serration (see Chapter 4), representing a specialisation of the bill tip organ (see below). The corresponding dorsal aspect of the above mentioned regions represented the intra-oral portion of the bill tip organ in both birds. However, in the ostrich, a prominent median ventral ridge was present which, like the median palatine ridge, displayed a high density of Herbst corpuscles (see Chapter 3).

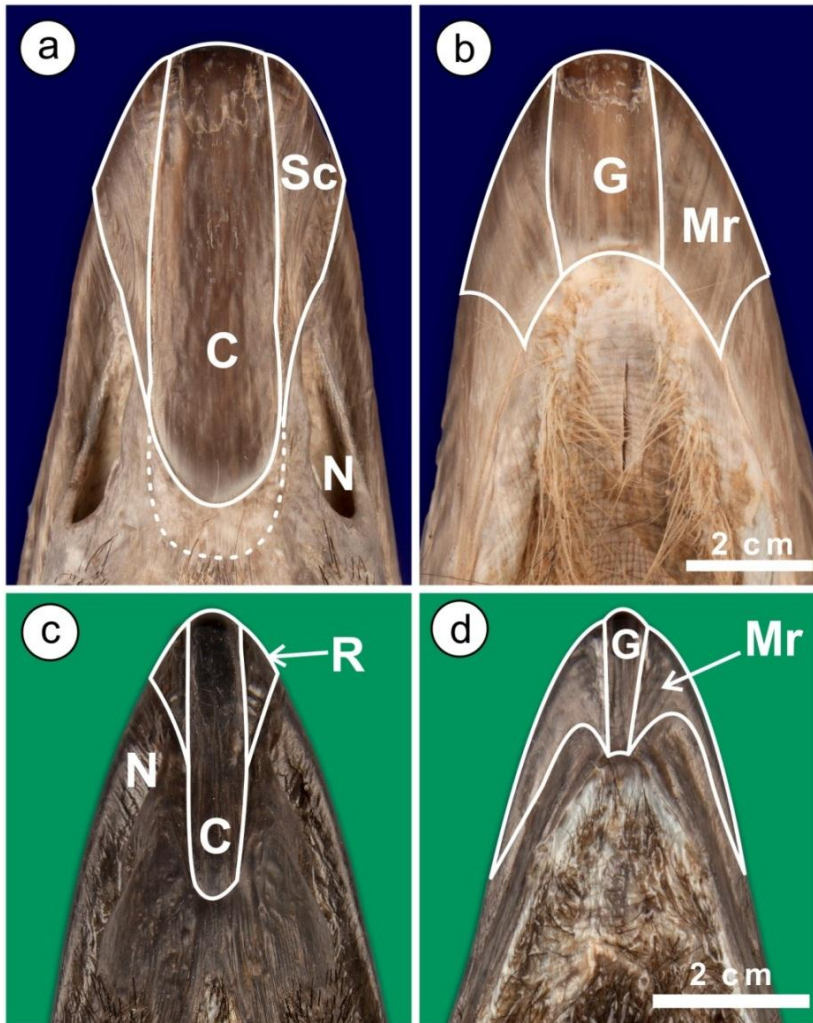


Figure 7.1. Location of the bill tip organ in the ostrich (a-b) and emu (c-d). The outlined regions show the approximate location of the underlying bony pits and Herbst corpuscles in the upper (a and c) and lower (b and d) bill. The entire *Culmen* (C) and *Gonys* (G) are outlined although only the rostral portions contain pits (see Chapter 5). Sensory cap (Sc), maxillary rostrum (R), nostril (N) and mandibular rostrum and distal portion of mandibular arms (Mr). The dotted line represents the caudal extent of the *Culmen* in the ostrich.

Herbst corpuscles formed the receptor units of the bill tip organ and were mostly oriented with their long axis running rostro-caudally. The corpuscles were almost always situated in groups around the periphery of a nerve or nerves (Figs. 7.2, 7.4 and 7.8-11). However, depending on the plane of section, some individual Herbst corpuscles or groups of corpuscles appeared isolated within the dense, irregular connective tissue. In some instances profiles of nerves appeared without associated Herbst corpuscles indicating that the corpuscles formed discontinuous groups along the length of the nerve. This represented the first type of arrangement of Herbst corpuscles, as described in Chapter 3, and was generally seen as lighter staining areas within the connective tissue stroma. These areas were composed of peripheral collections of Herbst corpuscles and blood vessels grouped around myelinated nerve fibres (Fig. 7.3) and encased in a thin layer of fine, irregular connective tissue and occasional adipose cells. The Herbst corpuscles located at the periphery of the groups were generally in direct contact with the surrounding dense, irregular connective tissue (Figs. 7.2-7.4 and 7.8-

11). This arrangement of Herbst corpuscles was observed within the bone and bony pits (Figs. 7.2 and 7.5-9) and in the dense, irregular connective tissue (Figs. 7.4-7 and 7.9-11) which surrounded all surfaces of the premaxilla and dentary bone. Based on these findings the bill tip organ could be divided into two main parts, namely, the collection of Herbst corpuscles housed within the bone and bony pits (the bony bill tip organ) and the peripheral bill tip organ composed of sheets of Herbst corpuscles sandwiched between the bone and the surface epithelium. A combination of the bony and peripheral bill tip organ was located under the maxillary and mandibular nails.

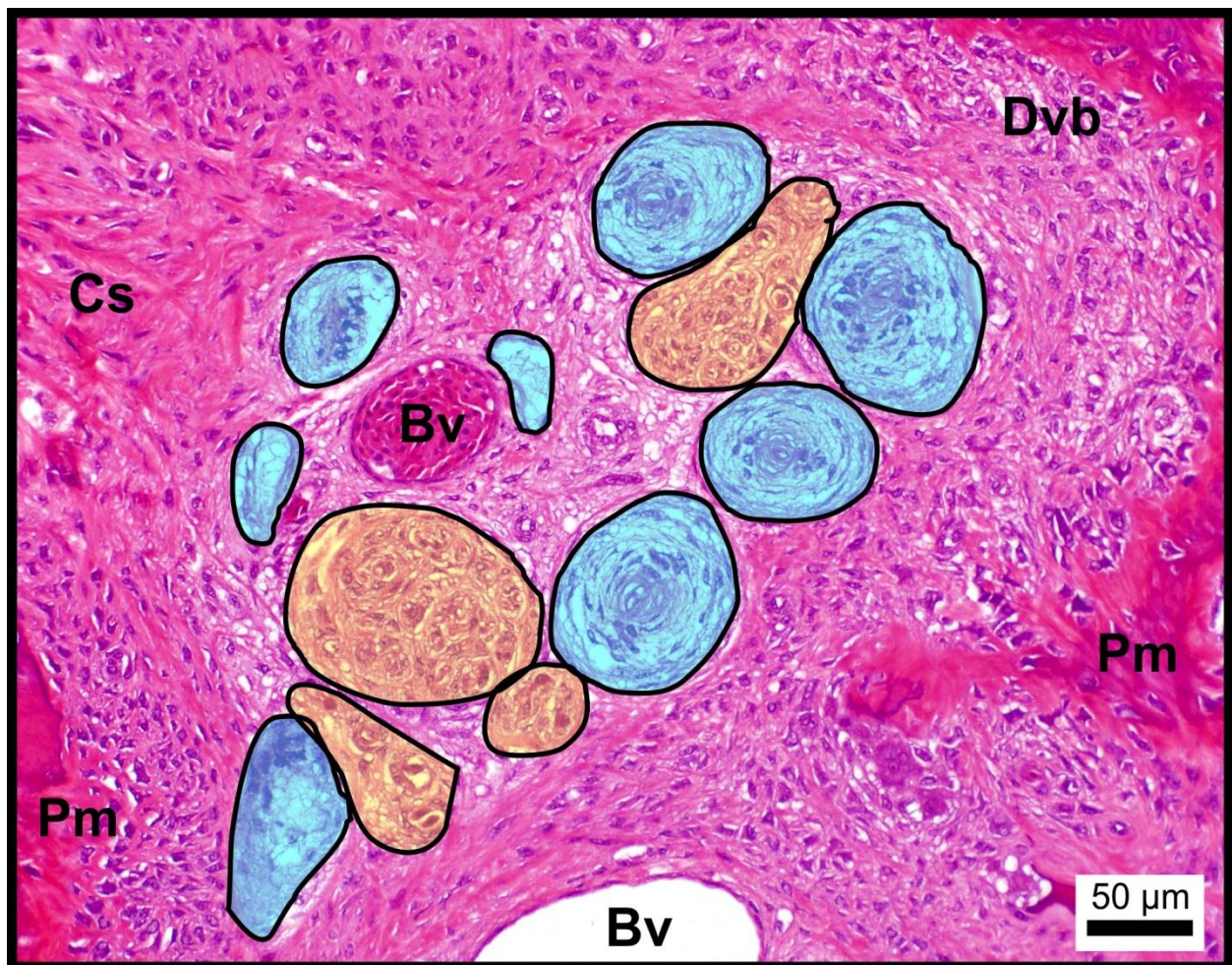


Figure 7.2. Transverse section of Herbst corpuscles and related structures within the premaxilla (Pm) in an ostrich chick. Note the peripheral arrangement of Herbst corpuscles (blue) around myelinated nerves (yellow) and a blood vessel (Bv). The Herbst corpuscles have been sectioned at different levels. Developing bone (Dvb) and connective tissue stroma (Cs).

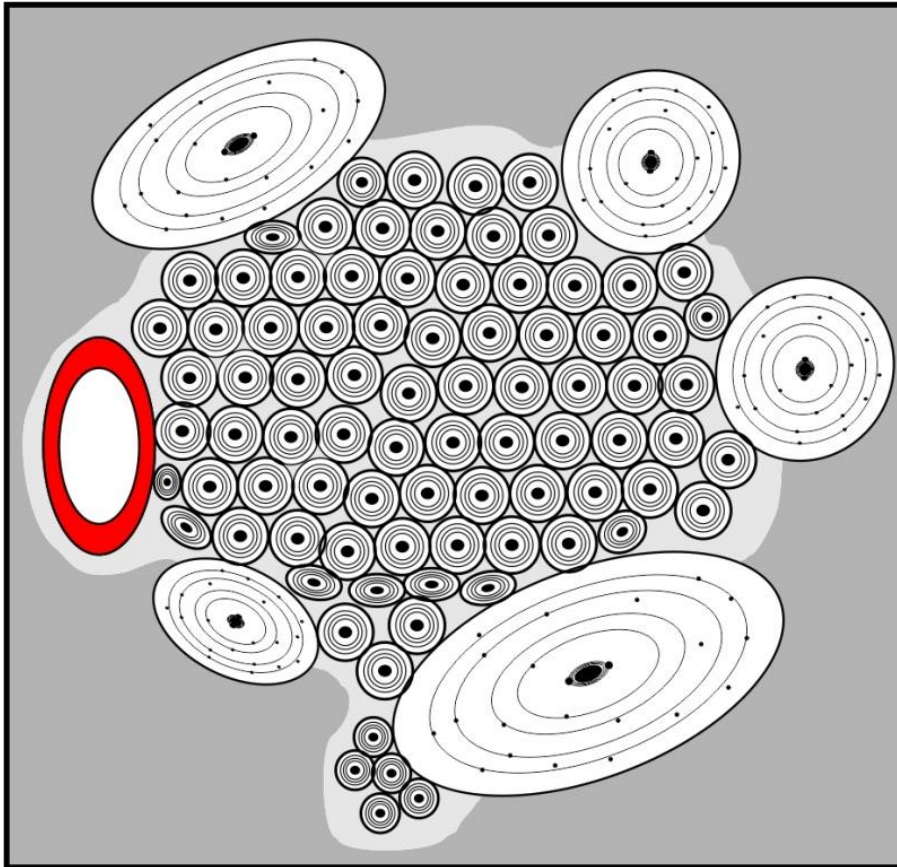


Figure 7.3. Schematic diagram showing the arrangement of Herbst corpuscles around a myelinated nerve. The nerve fibres (small circles), associated Herbst corpuscles (large circles) and a blood vessel (red circle) are all enclosed by fine, irregular connective tissue (light grey). The entire structure is located within a layer of dense irregular connective tissue (dark grey). The structures are not drawn to scale.

The most rostral extremity of the bill tip organ, that part under the nails, was formed by Herbst corpuscles embedded in the dense, irregular connective tissue situated between the maxillary nail and the premaxilla and between the mandibular nail and the dentary bone (Fig. 7.4). Numerous Herbst corpuscles were positioned in the connective tissue between the bone and nails while fewer corpuscles were present between the bone and the intra-oral epithelium (Fig. 7.4).

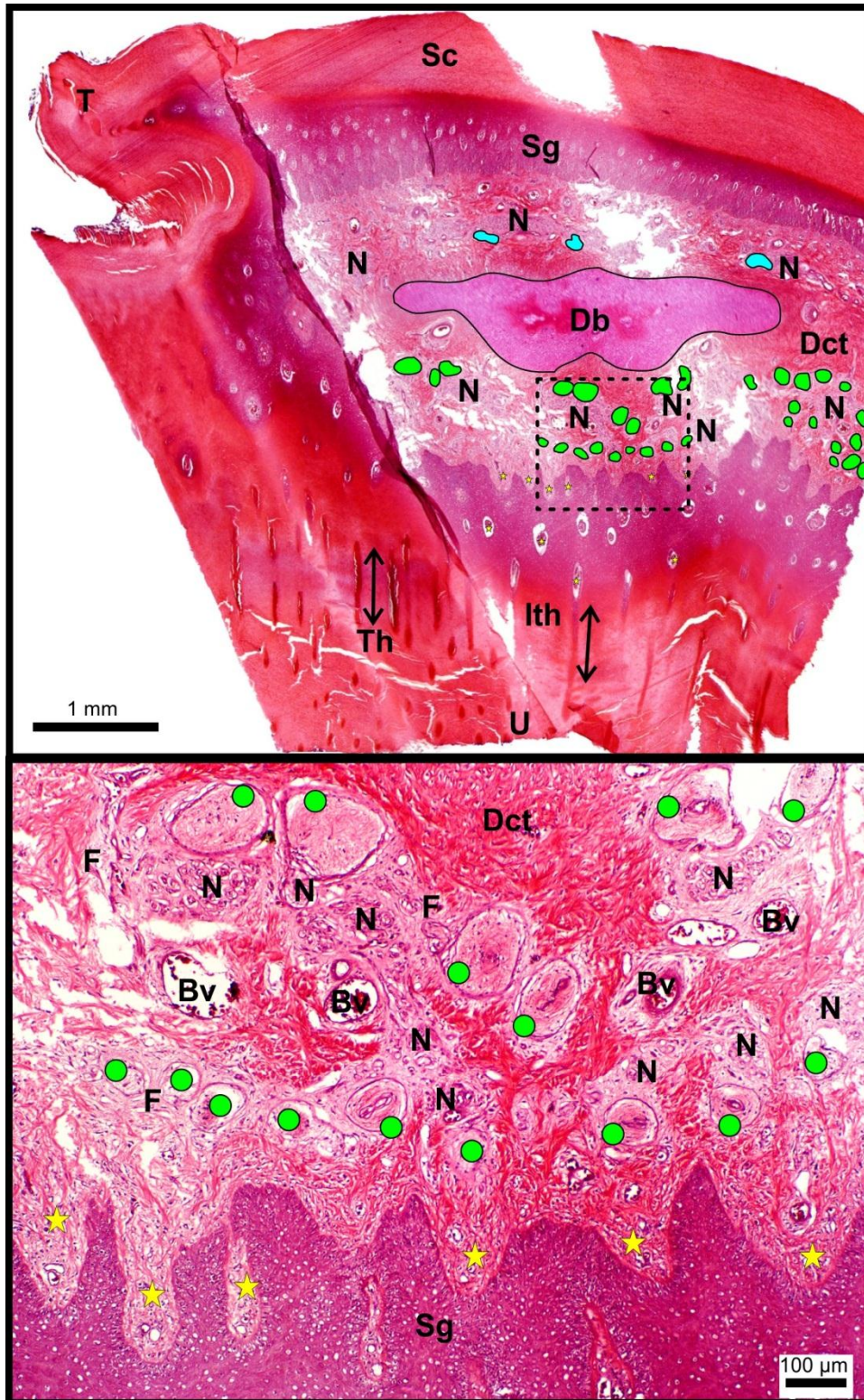


Figure 7.4. Rostral extremity of the mandibular bill tip in the adult ostrich. The square is enlarged below. The section is distorted due to the hardness of the horn forming the mandibular unguis (U). Herbst corpuscles (green dots) are numerous between the dentary bone (Db) and unguis. Less Herbst corpuscles (blue dots) are present in the dense connective tissue (Dct) above the dorsal surface of the dentary bone. Tubular horn (Th and arrows), dermal papillae (stars), inter-tubular horn (lth), *Tomium* (T), *Str. corneum* (Sc), *Str. germinativum* (Sg) and nerves (N). **Enlargement:** Note the arrangement of the Herbst corpuscles (green dots) peripheral to the nerves (N). Fine (F), loosely arranged connective tissue, blood vessels (Bv), dermal papillae (stars), dense irregular connective tissue (Dct) and *Str. germinativum* (Sg).

The bony bill tip organ was formed by Herbst corpuscles located within the cavities of the premaxilla and dentary bone and in the bony pits adorning the surfaces of these bones. The bony pits of the most rostral extremity of the bill, particularly those portions underlying the *Culmen* and *Gonys*, displayed a higher density of Herbst corpuscles than in other regions of the bony bill tip organ (Figs. 7.2 and 7.5-7). The Herbst corpuscles were arranged around myelinated nerves as described above. However, the connective tissue stroma within the bone was mainly cellular in the ostrich (Figs. 7.7 and 7.9a) but displayed a high content of adipose tissue in the emu (Figs. 7.6 and 7.8) (see also Chapter 5). In transverse section the rostral premaxilla (Fig. 7.5) and dentary bone appeared fragmented as a result of the numerous pits present. Further caudally, large cavities were present bilaterally in the bone (Figs. 7.6, 7.8 and 7.9a) (see Chapter 5) and from this level caudally only occasional Herbst corpuscles were encountered within these cavities (Fig. 7.6) but continued to be present in the bony pits (Figs. 7.6, 7.8 and 7.9). Nerve branches traversed the bony canals (Figs. 7.7-9) to exit the pits and supply Herbst corpuscles in the vicinity of the pit openings. Herbst corpuscles were not seen in each pit which was sectioned. This may indicate that not all pits contained aggregations of Herbst corpuscles, or simply that the corpuscles did not appear in the plane of section, particularly if the size of the pits is taken into consideration. The Herbst corpuscles varied in size from large to small, which could either be a reflection of the plane of sectioning (Fig. 7.7, 7.9b and 7.10) or an actual difference in size. In the emu, the rhamphothecal serrations with intervening keratinised pegs (Chapter 4) leading to Herbst corpuscles in pits at the lateral edge of the dentary bone (Chapters 4 and 5) represented an integration of the bony bill tip organ with epidermal specialisations which possibly assist in directing vibrational stimuli to the pits in the bone (see below). Only a thin layer of intervening connective tissue was present between the tip of the keratinised peg and the dentary bone.

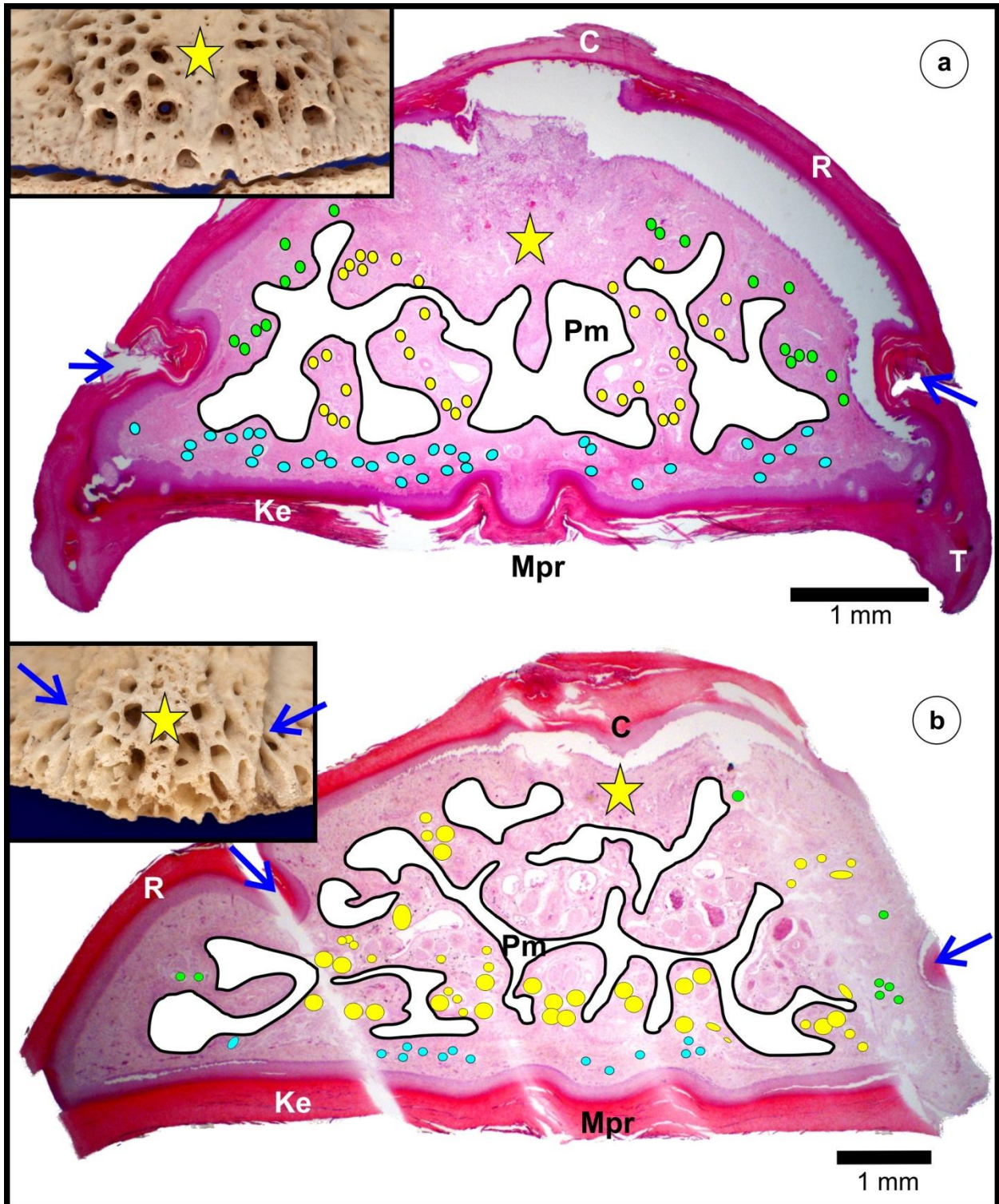


Figure 7.5. Transverse sections of the rostral extremity of the upper bill in ostrich (a) and emu (b) chicks. The premaxilla (Pm, outlined and coloured white) appears discontinuous as a result of numerous pits (see insets). Herbst corpuscles (yellow dots) inside the premaxilla. Peripheral Herbst corpuscles (blue dots) located ventrally in the connective tissue between the premaxilla and keratinised epithelium (Ke) and dorso-laterally (green dots) between the premaxilla and *Rhamphotheca* (R). Epithelial invaginations (blue arrows) on the lateral edges of the *Culmen* (C), median palatine ridge (Mpr), *Tomium* (T) and central part (yellow star) of the premaxilla underlying the *Culmen*. The insets illustrates a rostral view of the premaxilla in an adult ostrich (a) and adult emu (b).

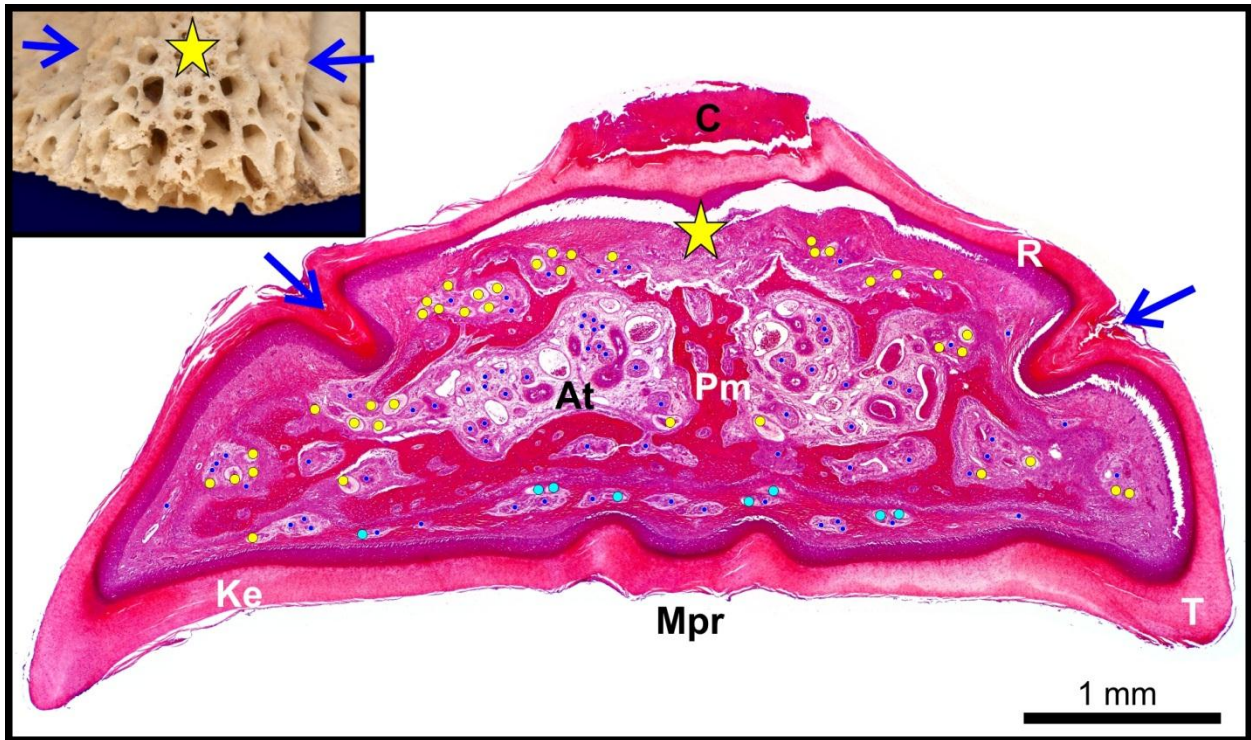


Figure 7.6. Composite micrograph of a transverse section of an emu chick upper bill, immediately caudal to Fig. 7.5.b. At this level the premaxilla (Pm) displays a cavity on either side of the midline (see Chapter 5) which contains adipose tissue (At) housing a plexus of nerves (small blue dots) and blood vessels. Groups of Herbst corpuscles (yellow dots) occupy the bony pits and are also present peripherally (light blue dots) in the connective tissue ventral to the premaxilla. The epidermal invaginations (blue arrows) bordering the *Culmen* (C) extend close to the premaxilla. Keratinised stratified squamous epithelium (Ke), *Rhamphotheca* (R), *Tomium* (T), median palatine ridge (Mpr) and central part of the premaxilla (yellow star) underlying the *Culmen*. The inset is a rostral view of the premaxilla in an adult emu.

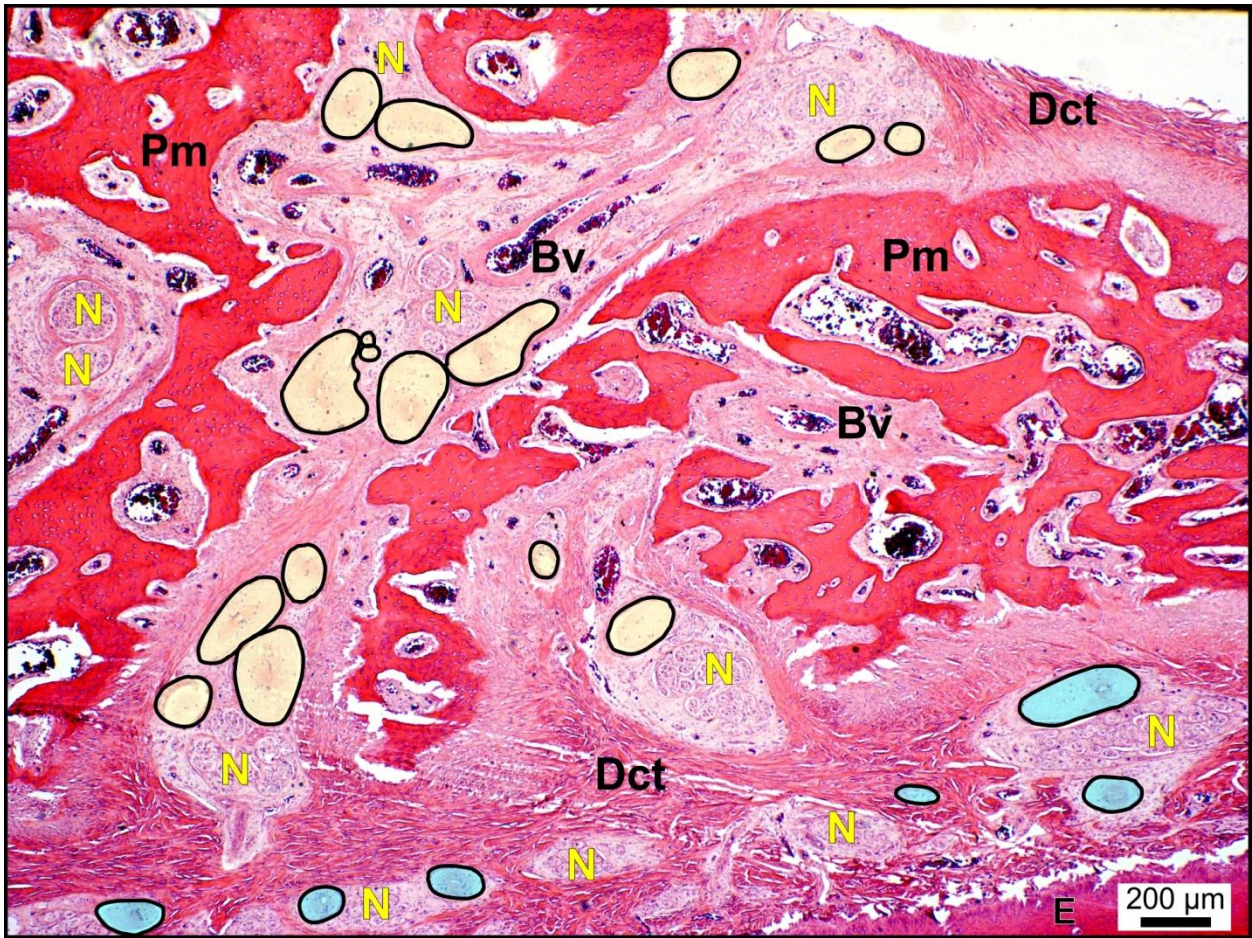


Figure 7.7. Transverse section of the rostral premaxilla in the adult ostrich demonstrating the bony component of the bill tip organ. Herbst corpuscles (yellow) of varying sizes occupy the stroma within the bony cavities of the premaxilla (Pm) and are situated peripherally to the nerves (N). Fine connective tissue encases the nerves and Herbst corpuscles and is interspersed between tracts of dense irregular connective tissue (Dct). Epithelium (E), blood vessel (Bv) and Herbst corpuscles (blue) not situated within the premaxilla.

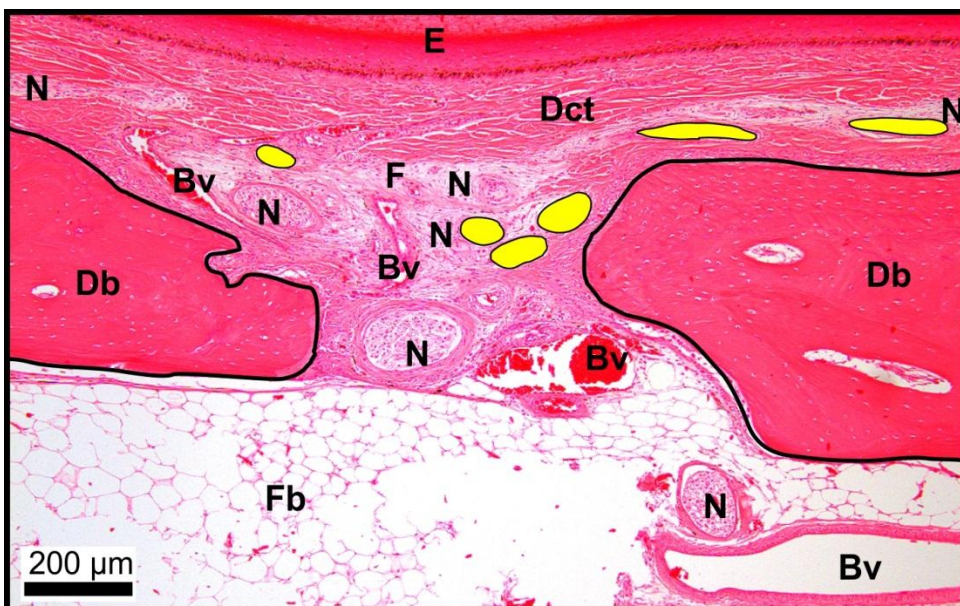


Figure 7.8. Transverse section of the mandible showing a bony pit in the dorsal part of the dentary bone (Db) in an adult emu. Nerves (N), blood vessels (Bv) and Herbst corpuscles (yellow) lie in a bony pit surrounded by fine (F) connective tissue. Fat body (Fb), dense irregular connective tissue (Dct) and keratinised stratified squamous epithelium (E).

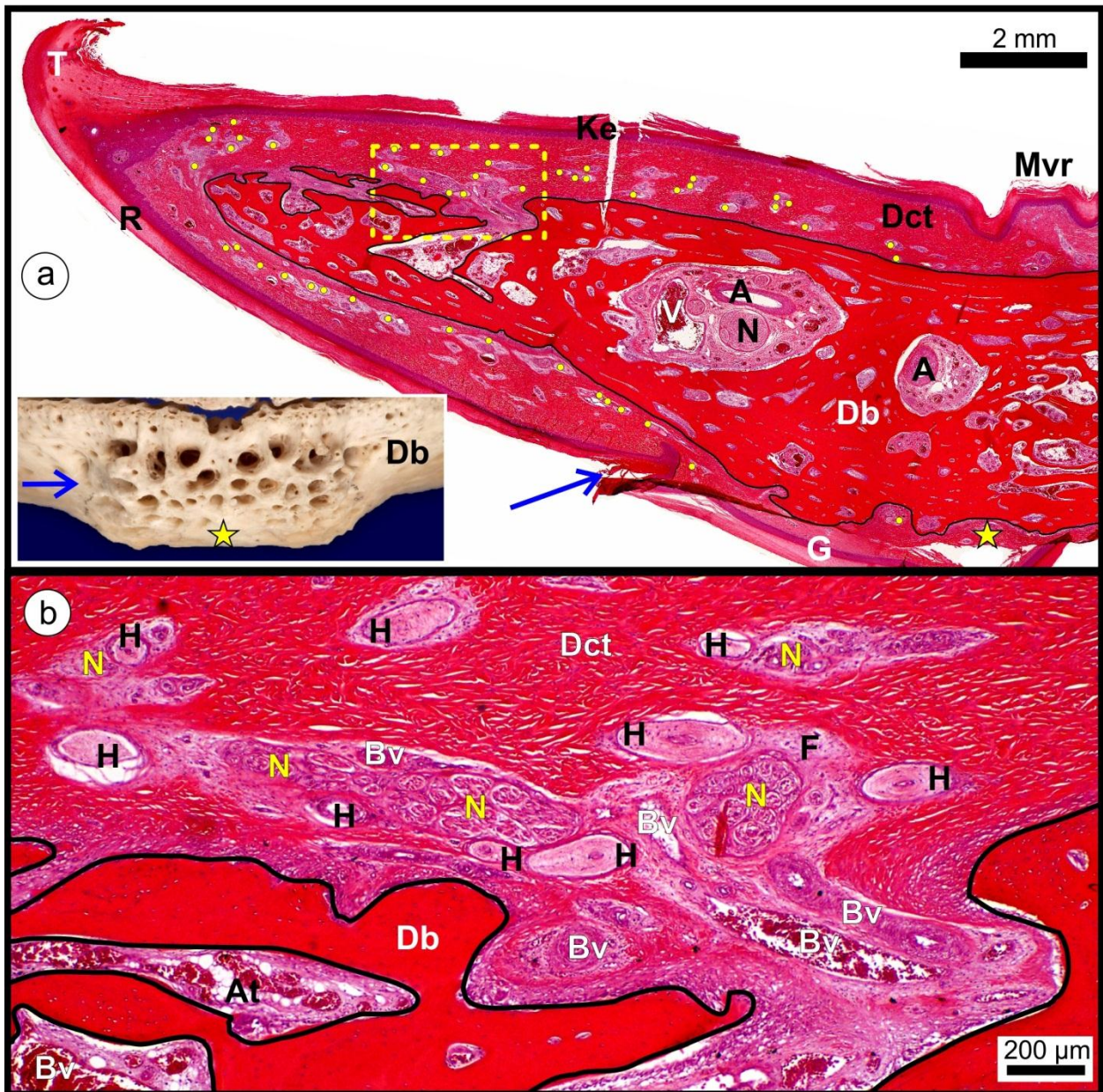


Figure 7.9. Composite micrograph (a) of a transverse section of the mid region of the mandibular rostrum in an adult ostrich with the yellow square enlarged in (b).

(a). Note the large pit (enlarged in the figure below) on the dorsal surface of the dentary bone (Db). Herbst corpuscles (yellow dots) are abundant peripherally in the dense irregular connective tissue (Dct) surrounding all surfaces of the dentary bone. The Herbst corpuscles appear within lighter areas which represent the associated nerve fibres embedded in fine, irregular connective tissue. A large cavity is present in the bone and carries a terminal branch of the intramandibular nerve (N), an artery (A) and vein (V). *Tomium* (T), keratinised stratified squamous epithelium (Ke), *Rhamphotheca* (R), median ventral ridge (Mvr), epidermal invagination (blue arrow) bordering the *Gonys* (G) and central region (yellow star) underlying the *Gonys*. The inset is a rostral view of the dentary bone in an adult ostrich.

(b). Numerous blood vessels (Bv), nerves (N) and Herbst corpuscles (H) exit a pit in the dentary bone (Db). The structures are surrounded by a fine, irregular connective tissue (F) which appears paler than the surrounding dense irregular connective tissue (Dct). Adipose tissue (At) in a cavity of the dentary bone.

The peripheral bill tip organ was formed by those Herbst corpuscles situated in the dense, irregular connective tissue surrounding the bony component of the bill tip organ underlying the external features outlined above (Figs. 7.5-7 and 7.9-11). The impression gained when viewing transverse sections of the bill tip was that of a continuous chain or sheet of Herbst corpuscles within the dermis/connective tissue of the bill tip (Figs. 7.5, 7.6, 7.9a and 7.10). The nerve branches present in the connective tissue were those which exited from the bony pits of the premaxilla (Fig. 7.7) and dentary bone (Figs. 7.8 and 7.9) (see Chapter 5), namely, the *Rr. rostri maxillaris* and *Rr. rostri mandibularis*, respectively (see Chapter 6). Each nerve branch was composed of numerous myelinated nerve fibres which at intervals supplied groups of surrounding Herbst corpuscles. This part of the bill tip organ was associated with epidermal specialisations in the form of epithelial invaginations and troughs (see below). At the borders of the *Culmen* and *Gonys* in both birds the epithelium was deeply invaginated and as a result extended close to the underlying bone (Figs. 7.5, 7.6, 7.9a and 7.11). These invaginations were structurally similar to the epidermal troughs present in the ostrich bill tip (see Chapter 4) and referred to as epidermal invaginations. Very little connective tissue was present between the *Str. basale* and the bone in the region of the invaginations and troughs, and the *Str. germinativum* appeared compressed (Fig. 7.11). Herbst corpuscles were observed in the thin layer of connective tissue present between the epidermal troughs (in the ostrich) (see Chapter 4) and the invaginations bordering the *Culmen* and *Gonys* (in both the ostrich and emu) (Figs. 7.5-6 and 7.11) and the underlying bone.

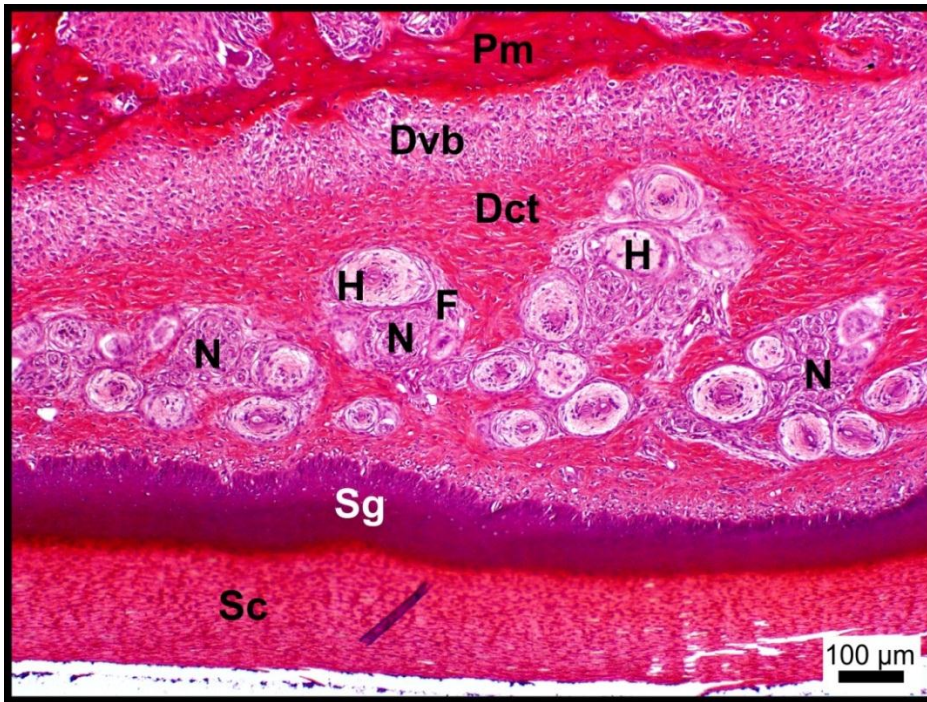


Figure 7.10. Transverse section of the ventral surface of the upper bill tip in an ostrich chick demonstrating the peripheral bill tip organ. Note the peripheral arrangement of the Herbst corpuscles (H) around the nerves (N) which represent the *Rr. rostri maxillaris*. The structures are encapsulated by fine (F) connective tissue and located in a layer of dense irregular connective tissue (Dct). Premaxilla (Pm), developing bone (Dvb), *Str. germinativum* (Sg) and *Str. corneum* (Sc).

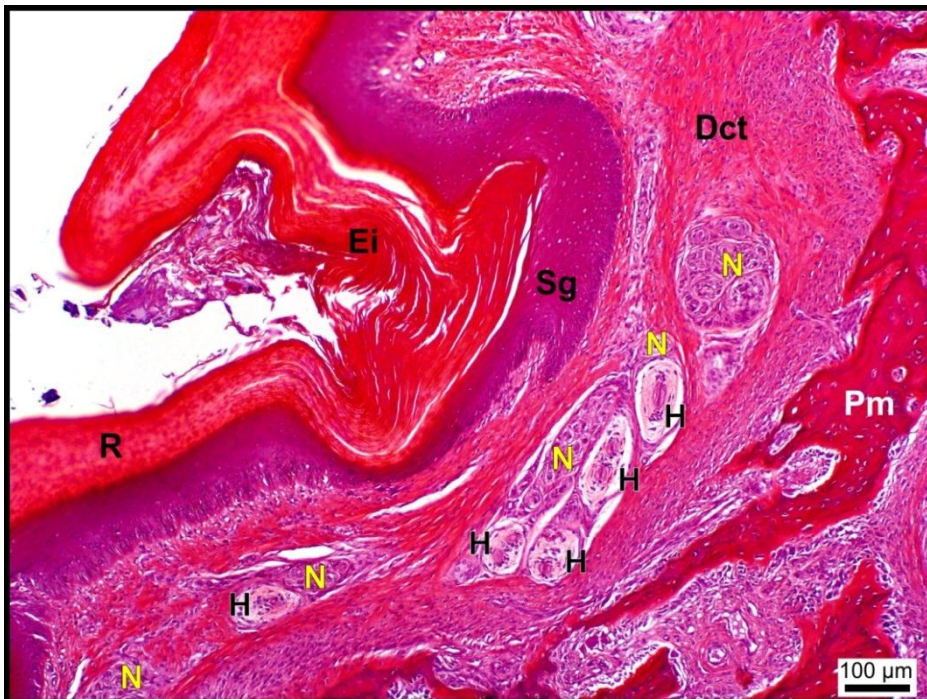


Figure 7.11. Epidermal invagination (Ei) in the upper bill of an ostrich chick. Note the Herbst corpuscles (H) which are located between the epidermal invagination and the premaxilla (Pm). The *Str. germinativum* (Sg) of the epidermis is compressed in the region of the invagination. Nerves (N) are closely associated with the Herbst corpuscles. Dense irregular connective tissue (Dct) and *Rhamphotheca* (R).

7.3.2. Accessory components of the bill tip organ

Numerous elements were noted in the preceding Chapters which, in addition to the bony pits and Herbst corpuscles, appeared to contribute to the structure and functioning of the bill tip organ. These included epidermal specialisations (Chapter 4), Meckel's cartilage (Chapter 5) and the nerve supply (Chapter 6). The relevant results from each chapter are listed below (Table 7.1) and their role analysed in the discussion.

Table 7.1. Comparative data on the structures contributing to the bill tip organ in the ostrich and emu. Values are rounded to the nearest whole number.

	Ostrich		Emu	
	Premaxilla	Mandible	Premaxilla	Mandible
Herbst corpuscle % relative density (intra-oral) (n=5) (Fig. 3.1)	(Region L1) 9%	(Region A) 7%	(Region L) 18%	(Region A) 10%
Number of pits (intra-oral) (Figs. 5.17-18)	72 (n=10)	50 (n=10)	71 (n=5)	84 (n=5)
Number of pits (externally) (Figs. 5.17-18)	140 (n=10)	89 (n=10)	92 (n=5)	82 (n=5)
Nerve fibre counts (n=5) (Figs. 6.8-9)	5889	5067	6838	5796
Epidermal specialisations (Chapter 4)	Epidermal troughs	Epidermal troughs	-	Rhamphothecal serrations and keratinised pegs
Cavities in the bone (Chapter 5)	Small and filled with cellular stroma	Small and filled with cellular stroma	Large and fat-filled	Large and fat-filled
Cartilage (Chapter 5)	Cartilaginous bony septum	Meckel's cartilage	Cartilaginous bony septum	Meckel's cartilage

The data suggests that the upper and lower bill of the emu may be more sensitive to tactile cues than that of the ostrich. This is supported by the significantly higher myelinated nerve fibre count in the medial branch of the ophthalmic nerve and the

slightly higher count in the intramandibular nerve in the emu compared to that of the ostrich as well as the higher relative percentage of Herbst corpuscles present in the intra-oral portion of the maxillary and mandibular rostra (Table 7.1). Although the externally located Herbst corpuscles were not counted, they appeared, based on histological observations, to be similarly distributed in both birds. As the nerve counts were only performed unilaterally, and assuming a correlation between nerve fibre count and the number of Herbst corpuscles, the values would have to be doubled to represent the total number of receptors in the bill tip. Based on this assumption the maxillary rostrum in the emu would possess about 2000 more Herbst corpuscles than that in the ostrich and in the mandibular rostrum, about 1400 more Herbst corpuscles. The nerve fibre counts and the relative distribution of Herbst corpuscles appear to be more correlated than when comparing either of these values to the pit counts (Table 7.1). Thus it would seem that pit numbers do not necessarily indicate increased general sensitivity, but may, however, reflect regional sensitivity.

7.4. Discussion

7.4.1. Extent of the bill tip organ

It is evident from the present study that the ostrich and emu display sensory structures arranged in a consistent manner in the bill tips which classify these two species as possessing a bill tip organ. The bill tip organ reportedly occupies only the most rostral extremities of the bill tip, such as the first 3 mm in Dunlin (*Calidris alpina pacifica*) (Pettigrew and Frost, 1985), the first 2 mm in Western sandpipers (*Calidris mauri*), Dunlin (*Calidris alpina*) and Least sandpipers (*Calidris minutilla*) (Nebel *et al.*, 2005) and the first few millimetres of the rostral tip of the upper bill in the Senegal parrot (*Poicephalus senegalus*) (Demery *et al.*, 2011). Within this limited region of the bill tip the Herbst corpuscles often show a particular concentration favouring the outer surfaces of the bill as in the Dunlin, with a concentration on the dorsal surface of the upper bill (Pettigrew and Frost, 1985), and the ibis, with higher concentrations on the outside surfaces of the upper and lower bills (Cunningham *et al.*, 2010a). The bill tip organ is limited to the maxillary and mandibular nails in the duck (Berkhoudt, 1976), mallard (Berkhoudt, 1980) and goose (Gottschaldt and Lausman, 1974), and to the rostral lower

bill tip in the chicken (Gentle and Breward, 1986) and Japanese quail (Halata and Grim, 1993). In contrast, although restricted to the rostral extremity of the bill, the bill tip organ occupied a much larger portion of the bill tips in the ostrich and emu, incorporating all surfaces of the maxillary and mandibular rostra, both intra-orally and externally. Similarly, the bill tip organ in the kiwi (Cunningham *et al.*, 2007) appears to occupy the entire region of the premaxilla and mandibular rostrum. Thus the bill tip organ of ratite species would seem to encompass a larger region of the bill tip than in other bird species.

A concentration of Herbst corpuscles has been reported in the tomium of finches (Krulis, 1978) and a similar concentration was observed in the tomium and lateral part of the beak in the black-capped chickadee (*Poecile atricapillus*) (Van Hemert *et al.*, 2012), although these birds are not recognised to possess a bill tip organ. A collection of Herbst corpuscles localised in a particular region, is, however, reminiscent of a bill tip organ and as the tomia do not represent the bill tip, their occurrence at other locations would still constitute a form of bill organ. Furthermore, as Herbst corpuscles in the tomium of finches aid in the dehusking of seeds (Krulis, 1978), their presence would thus fulfil the function of a bill organ and may aptly be named the tomial organ. Similarly, the concentration of Herbst corpuscles in the median palatine ridge and median ventral ridge in the ostrich may constitute a palatal ridge organ and ventral ridge organ, respectively, in this species.

7.4.2. Structural organisation of the bill tip organ

The structure of the bill tip organ differs between the various groups of birds. In the probing shorebirds (Bolze, 1968), kiwi (Cunningham *et al.*, 2007) and ibis (Cunningham *et al.*, 2010a) the bill tip organ consists of large, polygonal bony pits at the most rostral extremity of the bill tip which house Herbst corpuscles. A single row of shallow pits, situated on the intra-oral aspect of the mandibular rostrum, and corresponding to the tips of dermal papillae, have been described in the chicken (Gentle and Breward, 1986) and a similar situation is apparent in the Japanese quail (Halata and Grim, 1993). The distribution and pattern of bony pits in the bill tips is important for the specific functioning of the bill tip organ and, as with the number and distribution of Herbst corpuscles, varies between species (Cunningham *et al.*, 2007). Therefore it would be expected that birds

with differing diets and foraging behaviour would show differences in the arrangement of the bill tip organ. It was found that the kiwi shares some foraging patterns with, and displays analogous structures in the bill tip to, the Scolopacidae family (Cunningham *et al.*, 2007) and ibises (Threskiornithidae) (Cunningham *et al.*, 2010a). The Scolopacidae display forward-facing pressure detecting pits (Piersma *et al.*, 1998) and outward-facing vibrational detecting pits (Gerritsen and Meiboom, 1986; Nebel *et al.*, 2005), whereas in the kiwi both sets of pits are present, as well as backward facing pits (Cunningham *et al.*, 2007). Thus kiwis would appear to use their bill tip organ during probe foraging to detect both pressure and vibrational cues from any direction (Cunningham *et al.*, 2007). The shape of the sensory pits is important and a polygonal shape allows for the maximum density of pits within the bill (Nebel *et al.*, 2005). The pits in the ostrich and emu display an oval to round shape as space does not appear to be a limiting factor in these birds. Although the pits in the ostrich and emu display a slight directionality it is unlikely that these two birds would rely on a bill tip organ which is highly sensitive to directional cues, and as such, differ from the kiwi. The similarity in foraging behaviour of the ostrich and emu accounts for the similarity in the pattern of bony pits in these two birds. As the ostrich bill tip displays more pits than in the emu it may be tempting to conclude that the ostrich possesses a better developed bill tip organ than the emu. However, the emu, being a smaller bird, may simply reflect proportionally less pits in comparison to the ostrich. Despite displaying fewer pits, the higher nerve counts in the emu would indicate that this species possesses a greater number of Herbst corpuscles in the bill tip organ thus calling into question any correlation between pit numbers and sensitivity. However, based on the regional concentration of pits, the ostrich may possess a greater sensitivity around the *Culmen* and *Gonys* and the emu a greater sensitivity on the dorsal aspect of the mandibular rostrum.

The presence of bony pits in the bill tips indicates a propensity for the presence of a bill tip organ (Bolze, 1968; Cunningham *et al.*, 2007) and Cunningham *et al.* (2010a) speculate that the presence of this organ is favoured by a probe-foraging lifestyle as it occurs in three different families of probe-foraging birds, namely the Apterygidae, Scolopacidae and Threskiornithidae. The presence of a bill tip organ has been confirmed in three of the five palaeognathae orders (Apterygiformes (Cunningham *et al.*, 2007), Casuariiformes and Struthioniformes (present study)). Of the Casuariiformes, the emu (present study) displays a bill tip organ, whereas the status of the cassowary

(various species) is still undetermined. However, sketches of the bill tips of the cassowary and the remaining two orders, Rheiformes (Parker; 1866; Müller, 1963) and Tinamiformes (Parker; 1866), and images of palaeognath skulls available on the website Digital Morphology (<http://digimorph.org/index.phtml>), all display numerous pits in the rostral bill tips. If the connection between bony pits and the existence of a bill tip organ is valid, it may be reasonable to assume that a bill tip organ is synapomorphic for the Palaeognathae. Pits in the bill tips of extinct palaeognaths (Dinornithidae, Aepyornithidae and Dromornithidae) may also indicate that these birds possessed a bill tip organ. For example, bony pits in the bill tip of the extinct Australian “Demon Duck of Doom” (*Bullockornis planei*) (Murray and Megirian, 1998), are strongly suggestive that this bird possessed a bill tip organ. Histological studies on the bills of the remaining extant palaeognathous birds would confirm the common presence of a bill tip organ in this group.

It was noted by Cunningham *et al.* (2007) that the number and orientation of Herbst corpuscles within bony pits are important considerations in respect of the specific function of the bill tip organ and thus varies between species. In the ostrich and emu there was no noticeable consistency in the pattern and arrangement of Herbst corpuscles, other than that the majority of the corpuscles were situated with their long axis running rostro-caudally. Herbst corpuscles were mostly situated in the connective tissue between the epithelium and bone and although pits were present in the bill tips, Herbst corpuscles were not present in every pit and were not as densely packed as described in probing birds. In contrast, the Herbst corpuscles in the bill tip organ of probe-foraging birds are highly organised and would appear to be limited in location to the pits, within which they are densely stacked (Goglia, 1964; Bolze, 1968; Pettigrew and Frost, 1985; Nebel *et al.*, 2005). The ibis (Cunningham *et al.*, 2010a) also displays a large concentration of Herbst corpuscles within sensory pits in the bill tips, with the majority of the corpuscles occurring in the pits and fewer situated in the surrounding dermis. In the kiwi up to 70 Herbst corpuscles were counted in a single sensory pit (Cunningham *et al.*, 2007) which differs markedly from that observed in the ostrich and emu. This striking difference between these ratites most likely relates to the fact that the kiwi relies heavily on the sensory function of its bill for finding food rather than on vision (Martin *et al.*, 2007) when compared to the ostrich and emu which possess well-developed eyes for locating food (see also below). In the goose (Gottschaldt and

Lausman, 1974), duck (Berkhoudt, 1976) and mallard (Berkhoudt, 1980) for example, the bill tip organ is represented by keratin capped dermal papillae housing Herbst (and Grandry) corpuscles underlying the maxillary and mandibular nails. However, bony pits also occur in the rostral extremity in the bill tip of the duck which house Herbst corpuscles (Quilliam, 1966), although it is not clear if this arrangement is considered to form part of the bill tip organ in these birds. Dermal papillae with nerves, blood vessels and Herbst corpuscles have also been described in the beak of the parrot (Schildmacher, 1931); however, no traces of the components of the bill tip organ were found in the (pre)maxilla or mandible (Demery *et al.*, 2011). Stacking of Herbst corpuscles within dermal papillae was never observed in the ostrich and emu. The structure of the bill tip organ in the ostrich and emu places this particular type of bill tip organ (a combination of bony and peripheral components) in a class of its own, separate from that of probing or water-birds. It would appear as if the basal pattern exists for the palaeognathous bill tip organ, which in the kiwi (Cunningham *et al.*, 2007) has specialised in such a manner as to resemble that of probing birds. Future studies involving other palaeognathous birds may shed further light on this hypothesis.

The close relationship between sensory nerves and Herbst corpuscles observed in the ostrich and emu is shared with all birds described as possessing a bill tip organ. As noted in the pigeon wing (Hörster, 1990) the arrangement of numerous Herbst corpuscles in the ostrich and emu converging onto single nerves essentially created receptor fields. In the ostrich and emu the only sensory units are Herbst corpuscles. These structures are located in the bony pits and in the surrounding connective tissue both intra-orally and externally, being concentrated in the pits underlying the mandibular and maxillary nails.

7.4.2.1. Accessory components of the bill tip organ

The ostrich and emu possess additional structures which enhance and enable the functioning of the bill tip organ, and which have not been reported in other birds. In probing birds, specificity (localisation) regarding the origin of vibratory signals is gained through the stacking of Herbst corpuscles in bony pits which are mechanically isolated from one another. In the duck, mallard, goose and chicken, mechanical isolation is achieved by concentrating the corpuscles in dermal papillae which are separated by the

keratinised cells of the intervening *Str. corneum*. The ostrich and emu display a combination of structures which allow enhancement, specificity (localisation) and mechanical isolation of vibrational stimuli. Enhancement of stimuli conduction would be a role of the epidermal troughs in the ostrich and the keratinised pegs in the emu (see Chapter 4). Isolation and localisation of stimuli would be a function of the bony pits as well as the fat bodies (mainly in the emu) or the smaller fat bodies and cavities filled with cellular stroma (in the ostrich) in the bony bill tips. Large amounts of adipose tissue have also been described in the premaxilla of the black-capped chickadee; however, the possible function of this tissue was not alluded to (Van Hemert *et al.*, 2012).

7.4.2.1.1. Epidermal specialisations (Chapter 4)

A well-defined region of the rhamphotheca of the maxillary rostrum in the ostrich has been termed the sensory cap (see Chapter 4) and is that part of the upper bill which displays keratin-filled epidermal troughs projecting into the underlying connective tissue and which delineates the bill tip organ in the upper bill. Herbst corpuscles were located in the compressed dermis, between the epidermal troughs and the underlying bone. This arrangement strongly points to the advanced conduction ability of the keratin-filled troughs. In both the ostrich and emu, similar structures were present flanking the *Culmen* and *Gonys* which at places also displayed Herbst corpuscles at their base. These grooves would also enhance the conduction of vibrational stimuli to the underlying corpuscles. The epidermal troughs are clearly visible externally in the ostrich and indicated areas of increased sensitivity of the bill tip organ in this species. The rhamphothecal serrations and keratinised pegs are a feature unique to the emu. The sum of the structures involved in this specialisation points to a synergy to enhance and detect vibrational stimuli. The proximal aspect of each tapered keratinised peg is located near the opening of a pit on the lateral edge of the dentary bone. Each pit houses Herbst corpuscles (although not visible in every plane of section), nerves and blood vessels and each unit is supplied by a small nerve which originates from the nerve plexus within the fat body of the dentary bone. The region of the rhamphothecal serrations in the emu represents a highly sensitive region of the bill tip organ.

7.4.2.1.2. Cartilage and bone modifications (Chapter 5)

As noted in Chapter 5, cartilage is present along each of the major nerve trunks carrying impulses from the bill tip organ, in the form of Meckel's cartilage and the cartilaginous nasal septum. These structures provide mechanical isolation by absorbing forces from pecking and thereby prevent direct stimulation of the nerve trunks. Gussekloo and Bout (2005) demonstrated that the forces experienced by the bill tips of the greater rhea during pecking were not great and were sufficiently spread over the bony surface area of the bill tips. However, the forces generated would still travel to the braincase as described by Dzerzhinsky (1999). Incidentally, the dissipation of force away from the *R. medialis N. ophthalmicus* may be an explanation for the difference in palatal conformation between the ostrich and emu (see Chapter 5). The premaxillary body is flattened in the ostrich, whereas in the emu it is larger and contains sizeable fat bodies. The premaxillary rostrum in the emu would thus act as a more efficient shock absorber due to the large amount of adipose tissue present. The remaining force from pecking would travel along the palatal processes of the premaxilla, as well as being absorbed by the cartilaginous nasal septum. In the ostrich, the absence of the palatal processes of the premaxilla would compensate for the lack of dissipation of forces from pecking by the compact, flattened premaxillary body. The forces from pecking would bypass the *R. medialis N. ophthalmicus* and instead travel laterally along the only existing route of the maxillary processes (see Fig. 5.6 of Chapter 5).

7.4.2.1.3. Neural component (Chapter 6)

Although not essentially involved in enhancing the function of the bill tip organ, the nerve supply to the bill tip confirmed the sensory importance of this region. The bill tips in the ostrich and emu were richly supplied with nerves which formed a plexus within the bill tips in a matrix of adipose tissue. This was particularly evident in the emu. The importance of the sensory function of the bill tip is reflected by the size of the ophthalmic nerve which maintains a large diameter all the way to the maxillary rostrum (Cobb and Edinger, 1962; Pettigrew and Frost, 1985). Similarly, the medial branch of the ophthalmic nerve in the ostrich and emu maintained its diameter as it coursed to the premaxilla, before ramifying extensively within the structures of the maxillary rostrum. The main factor determining the degree of branching is the morphology of the bill and

specifically the sensory area (Bubień-Waluszewska, 1981). For example, the sensory corpuscles are abundant in the rhamphotheca of Anatidae and Scolopacidae, and birds from these families display well-developed, extensive branching of nerves in the maxillary rostrum (Bubień-Waluszewska, 1981). The extensive branching of the intramandibular nerve in the mandibular rostrum in the emu and the rostral mandibular bill tip in the ostrich similarly indicates a region of high sensitivity. The high concentration of Herbst corpuscles in the bill tips (see Chapter 3) follow the path of the extensive nerve branching. The large size of the nerves, and their extensive branching within the bill tips, support the existence of a well-developed sensory region in the bill tips of the ostrich and emu.

7.4.3. Function of the bill tip organ

The ostrich and the emu do not hunt. They are mainly herbivorous, although the emu is known to eat insects (Davies, 1978) when available. As a consequence, neither the ostrich nor emu have a need to source food via remote touch as this is only necessary for detecting movement of prey (Gerritsen and Meiboom, 1986). This would explain why the arrangement of Herbst corpuscles in the bill tip organ of the ostrich and emu is structurally different to that of probing and straining birds. Furthermore, the bill tip organ of probing birds which forage in wet or water substrates is more complex than those which forage in drier substrates (Cunningham *et al.*, 2010a). Neither the ostrich nor the emu are known to forage in water which further explains the presence of a structurally different bill tip organ in these birds. Gerritsen and Meiboom (1986) note that Herbst corpuscles in moderate numbers, and which are more loosely arranged (within grooves and widely spaced hollows in the bone) is suggestive of a bill tip organ which functions via direct touch as opposed to a honeycomb arrangement of holes densely packed with Herbst corpuscles which would imply a bill tip organ that functions via remote touch. The arrangement of bony pits and Herbst corpuscles in the ostrich and emu fit the former description and support the function of their bill tip acting as an organ of direct touch. Although the very rostral tips of the bill display the arrangement noted for remote touch (honeycomb of holes with many Herbst corpuscles) they probably represent the area of greatest sensitivity for direct touch in both birds. The bill tips in the ostrich and emu are thus an organ of direct touch and fulfil a similar function to the fingertips of the human hand which work by direct touch.

A bill tip organ allows the fine tactile discrimination necessary to enable numerous, complex oral tasks (Gentle and Breward, 1986) and those birds that use their beak mainly for pecking grain do not possess a bill tip organ (Gottschaldt, 1985). Although no 'complex oral tasks' have been described or noted in these birds, the arrangement and content of Herbst corpuscles present in the bill tip certainly indicates that these two birds would possess the ability for fine tactile discrimination. This makes these two species unusual amongst birds as they would appear to be the only pecking birds which display such a well-developed bill tip organ. In *Calidris alba* (Gerritsen and Meiboom, 1986) it was demonstrated that in searching for prey, tactile cues took preference over visual cues. The eyes of the ostrich and the emu are extremely large with the eye of the ostrich being larger than its brain. Thus it is unlikely that these two birds would rely on tactile senses (the bill tip organ) to locate food, especially as these two birds do not probe-forage. This is supported by the opposite situation in the kiwi, whereby this species has foregone vision in preference to tactile cues received from the bill tip organ and other sensory information, and as a result displays small eyes (Martin *et al.*, 2007). The bill tip organ in the ostrich and emu may assist in the discrimination of different food types by touch once they have been located visually or by smell. It was noted in the ostrich how rapidly discrimination took place between similar food items by just a single touch of the mandible (Anon, 1922). Feeding studies, similar to those conducted in other birds (Gerritsen and Meiboom, 1986), would be necessary to determine the importance of the various sensory inputs in foraging in these two birds.

An interesting personal observation in the ostrich and also noted by Martin and Katzir (1995), but which has not been confirmed in the emu, is the action of the third eyelid which is often drawn across the eye when the bird pecks. This action would appear to be linked to a reflex which can perhaps be consciously overridden. As the ostrich possesses a bill tip organ, a reflex may be present between the Herbst corpuscles in the bill tip and the muscles (*M. quadratus membranae nictitantis* and *M. pyramidalis membranae nictitantis* (Evans and Martin, 1993)) which draw the third eyelid across the eye. There appears to be a link between visual and tactile information in birds and their foraging ecology (Martin and Portugal, 2011). To better comprehend the function of the bill tip organ in the ostrich and emu and to relate it to their natural behavioural ecology, it will be necessary to perform studies incorporating the visual fields of these two birds,

such as in the parrot (Demery *et al.*, 2011) and Threskiornithidae (Martin and Portugal, 2011).

The following two links have been provided which demonstrate the pecking action of the ostrich and emu. These video clips do not show any form of obvious discrimination performed by the bill tip organ in these two birds. However, they do demonstrate the enigma of two birds which perform relatively simple tasks with their bills, yet possess a well-developed bill tip organ. If time is spent watching the ostrich and emu performing exploratory behaviour it is clear that both of these birds use their bill to constantly 'feel' and explore their surroundings. Based on their behaviour it can be concluded that the ostrich and emu do not possess a bill tip organ to assist them in performing complex oral tasks. The bill tip organ of these two birds functions in the discrimination of food items and serves as an organ for exploring and interpreting their environment.



Ostrich pecking (<https://www.youtube.com/watch?v=9M12ky4M-dQ>)



Emu eating (<http://www.youtube.com/watch?v=6P65kqnmr9g>)

7.5. References

- Anon, T.H.G. 1922. *Taste or Scent in the Ostrich*. In: The Scottish Naturalist. Edited by Ritchie, J. Edinburgh: Oliver & Boyd. pp.168.
http://archive.org/stream/scottishnaturali1922arbr/scottishnaturali1922arbr_djvu.txt
- Baumel, J.J. and Witmer, L.M. 1993. *Osteologia*. In: Handbook of Avian Anatomy: Nomina Anatomica Avium, 2nd edition. Edited by Baumel, J.J., King, A.S., Breazile, J.E., Evans, H.E. and Vanden Berge, C. Cambridge, Massachusetts: The Nuttall Ornithological Club, No. 23. pp. 45-132.
- Berkhoudt, H. 1976. The epidermal structure of the bill tip organ in ducks. *Netherlands Journal of Zoology*. **26**: 561-566.
- Berkhoudt, H. 1980. The morphology and distribution of cutaneous mechanoreceptors (Herbst and Grandry corpuscles) in bill and tongue of the mallard (*Anas platyrhynchos*. L). *Netherlands Journal of Zoology*. **30**: 1-34.
- Bolze, G. 1968. Anordnung und Bau der Herbstchen Körperchen in Limicolenschnäbeln im Zusammenhang mit der Nahrungsfindung. *Zoologischer Anzeiger*. **181**: 313-355.
- Bubień-Waluszewska, A. 1981. *The Cranial Nerves*. In: Form and Function in Birds. Vol. 2. Edited by King, A.S. and McLelland, J. London: Academic Press. pp. 385-438.
- Cobb, S. and Edinger, T. 1962. The brain of the Emu (*Dromaeus novaehollandiae*, Lath) I. Gross anatomy of the brain and pineal body. *Breviora Museum of Comparative Zoology*. **170**: 1-18.
- Cunningham, S., Castro, I. and Alley, M. 2007. A new prey-detection mechanism for kiwi (*Apteryx* spp.) suggests convergent evolution between paleognathous and neognathous birds. *Journal of Anatomy*. **211**: 493-502.
- Cunningham, S.J., Alley, M.R., Castro, I., Potter, M.A., Cunningham, M. and Pyne, M.J. 2010a. Bill morphology of ibises suggests a remote-tactile sensory system for prey detection. *The Auk*. **127**: 308-316.
- Cunningham, S.J., Castro, I., Jensen, T. and Potter, M.A. 2010b. Remote touch prey-detection by Madagascar crested ibises *Lophotibis cristata urschi*. *Journal of Avian Biology*. **41**: 350-353.
- Davies, S. J. J. F., 1978. The food of emus. *Australian Journal of Ecology*. **3**: 411–422.

Demery, Z.P., Chappell, J. and Martin, G.R. 2011. Vision, touch and object manipulation in Senegal parrots *Poicephalus senegalus*. *Proceedings of the Royal Society B*. **278**: 3687-3693.

Dzerzhinsky, F.Y. 1999. *Implications of the Cranial Morphology of Paleognaths for Avian Evolution*. In: Smithsonian Contributions to Paleobiology, number 89. Avian Paleontology at the Close of the 20th Century: Proceedings of the 4th International Meeting of the Society of Avian Paleontology and Evolution, Washington, D.C., 4-7 June 1996. Edited by Olson, S.L. Washington, D.C.: Smithsonian Institution Press. pp. 267-274.

Evans, H.E. and Martin, G.R. 1993. *Organa Sensuum [Organa Sensoria]*. In: Handbook of Avian Anatomy: Nomina Anatomica Avium, 2nd edition. Edited by Baumel, J.J., King, A.S., Breazile, J.E., Evans, H.E. and Vanden Berge, C. Cambridge, Massachusetts: The Nuttall Ornithological Club, No. 23. pp. 585-611.

Gentle, M.J. and Breward, J. 1986. The bill tip organ of the chicken (*Gallus gallus* var. *domesticus*). *Journal of Anatomy*. **145**: 79-85.

Gerritsen, A.F.C. 1988. Feeding techniques and the anatomy of the bill in sandpipers (*Calidris*). PhD Thesis, University of Leiden, The Netherlands.

Gerritsen, A.F.C. and Meiboom, A. 1986. The role of touch in prey density estimation by *Calidris alba*. *Netherlands Journal of Zoology*. **36**: 530-562.

Goglia, C. 1964. 'L'organa tattile apicale' del Becco di alcuni volatili. *Acta Medica Romana*. **11**: 243-262.

Gottschaldt, K.-M. 1985. *Structure and Function of Avian Somatosensory Receptors*. In: Form and function in birds. Vol. 3. Edited by King, A.S. and McLelland, J. London: Academic Press. pp. 375-462.

Gottschaldt, K.-M. and Lausmann, S. 1974. The peripheral morphological basis of tactile sensitivity in the beak of geese. *Cell and Tissue Research*. **153**: 477-496.

Goujan, E. 1869. Sur un appareil de corpuscles tactiles suite dans le bec des perroquets. *Journal of Anatomy and Physiology*. **6**: 390-395.

Gussekkoo, S.W.S. and Bout, R.G. 2005. The kinematics of feeding and drinking in palaeognathous birds in relation to cranial morphology. *The Journal of Experimental Biology*. **208**: 3395–3407.

Halata, Z. and Grim, M. 1993. Sensory nerve endings in the beak skin of Japanese quail. *Anatomy and Embryology*. **187**: 131-138.

- Hörster, W. 1990. Histological and electrophysiological investigations on the vibration-sensitive receptors (Herbst corpuscles) in the wing of the pigeon (*Columba livia*). *Journal of Comparative Physiology A*. **166**: 663-673.
- Krulis, V. 1978. Struktur und Verteilung von Tastrezeptoren im Schnabel-Zungenbereich von Singvögeln im besonderen der Fringillidae. *Revue Suisse de Zoologie*. **85**: 385-447.
- Martin, G.R. and Katzir, G. 1995. Visual fields in ostriches. *Nature*. **374**: 19-20.
- Martin, G.R. and Portugal, S.J. 2011. Differences in foraging ecology determine variation in visual fields in ibises and spoonbills (Threskiornithidae). *Ibis*. **153**: 662-671.
- Martin, G.R., Wilson, K.-J., Wild, J.M., Parsons, S., Kubke, M.F. and Corfield, J. 2007. Kiwi forego vision in the guidance of their nocturnal activities. *PLoS ONE*. **2**: e198.
- Müller, H.J. 1963. Die morphologie und Entwicklung des Cranium von *Rhea americana* Linné. *Zeitschrift für Wissenschaftliche Zoologie*. **168**: 35-118.
- Murray, P.F. and Megirian, D. 1998. The skull of dromornithid birds: anatomical evidence for their relationship to Anseriformes. *Records of the South Australian Museum*. **31**: 51-97.
- Nebel, S., Jackson, D.L. and Elner, R.W. 2005. Functional association of bill morphology and foraging behaviour in calidrid sandpipers. *Animal Biology*. **55**: 235-243.
- Parker, W.K. 1866. On the structure and development of the skull in the Ostrich Tribe. *Philosophical Transactions of the Royal Society of London*. **156**: 113-183.
- Pettigrew, J.D. and Frost, B.J. 1985. A tactile fovea in the Scolopacidae? *Brain Behavior and Evolution*. **26**: 185-195.
- Piersma, T. 2011. From spoonbills to Spoon-billed sandpiper: the perceptual dimensions to the niche. *Ibis*. **153**: 659-661.
- Piersma, T., Aelst, R.V., Kurk, K., Berkhoudt, H. and Maas, L.R.M. 1998. A new pressure sensory mechanism for prey detection in birds: the use of seabed-dynamic principles? *Proceedings of the Royal Society of London, B*. **265**: 1377-1383.
- Piersma, T., van Gils, J., de Goeij, P. 1995. Holling's functional response model as a tool to link the food-finding mechanism of a probing shorebird with its spatial distribution. *Journal of Animal Ecology*. **64**: 493-504.

Quilliam, T. A., 1966. *Unit Design and Array Patterns in Receptor Organs*. In: Touch, Heat and Pain. London: Churchill. pp. 86-116.

Schildmacher, H. 1931. Untersuchungen über die Funktion der Herbstschen Körperchen. *Journal für Ornithologie*. **79**: 374-415.

Van Hemert, C., Handel, C.M., Blake, J.E., Swor, R.M. and O'Hara, T.M. 2012. Microanatomy of passerine hard-cornified tissues: beak and claw structure of the black-capped chickadee (*Poecile atricapillus*). *Journal of Morphology*. **273**: 226-240.

Widowski, T. 2010. *The Physical Environment and its Effect on Welfare*. In: The Welfare of Domestic Fowl and Other Captive Birds. Edited by Duncan, I.J.H. and Hawkins, P. Dordrecht, Heidelberg, London, New York: Springer. pp. 137-164.

Wight, P.A.L., Siller, W.G. and Mackenzie, G.M. 1970. The distribution of Herbst corpuscles in the beak of the domestic fowl. *British Poultry Science*. **11**: 165-170.

Zweers, G.A. and Gerritsen, A.F.C. 1997. Transitions from pecking to probing mechanisms in waders. *Netherlands Journal of Zoology*. **47**: 161-208.

CHAPTER 8

DISTRIBUTION AND STRUCTURE OF TASTE BUDS

8.1. Introduction

The sense of taste in birds is an important motivator for feeding as well as initial food selection (Gentle, 1971a). However, food selection is also based on size, shape, colour and texture (Berkhoudt, 1985) as well as taste and olfaction (Gerritsen *et al.*, 1983; van Heezik *et al.*, 1983; Berkhoudt, 1985). Birds possess a very low number of taste buds in comparison to other vertebrates (Berkhoudt, 1985; Ganchrow and Ganchrow, 1985; Evans and Martin, 1993; Brand and Gous, 2006) and their presence or absence in the avian oropharynx has been heavily debated due to the different eating habits and diet of birds (Moore and Elliott, 1946). However, despite their low numbers, birds do possess an acute sense of taste (Berkhoudt, 1985). Taste buds have been positively identified in numerous species (Bath, 1906; Botezat, 1910; Warner *et al.*, 1967; Berkhoudt, 1985) including domestic poultry (Lindenmaier and Kare, 1959; Saito, 1966; Gentle, 1971b; Berkhoudt, 1977; Kurosawa *et al.*, 1983; Ganchrow and Ganchrow, 1985, 1987, 1989), of which the chicken has been most extensively researched. The capacity for chemoreception has also been identified in *Calidris* species (sandpipers) (Gerritsen *et al.*, 1983; van Heezik *et al.*, 1983), based on feeding trials; however, the physical presence of taste buds was not demonstrated.

Conclusive evidence of a sense of taste in ratites has remained elusive. Various investigations have yielded negative results in both the ostrich (see Brand and Gous, 2006; Jackowiak and Ludwig, 2008; Tivane, 2008) and greater rhea (Feder, 1972; Santos *et al.*, 2011). In the emu, structures resembling taste buds have been identified and were located in the tongue root (Crole and Soley, 2009b), oropharyngeal floor and proximal oesophagus (Crole, 2009) and constitute the first report of a sense of taste in ratites. However, these structures remained putative and were never positively confirmed. McCann (1973) interpreted openings in the kiwi oropharynx as “taste pores”. However, it is more probable that the pores represent the openings of underlying

glands, as no histological evidence of taste buds was supplied. Ratites swallow their food whole, employing the 'catch and throw' (Gussekkloo and Bout, 2005) or cranioinertial feeding method (Bonga Tomlinson, 2000) in which the food lands near or into the esophageal entrance before swallowing. As a result of this method of food intake there would be a limited need or opportunity for taste during the intra-oral transport of food. It would thus seem appropriate that any taste receptors found in the oropharynx would be sparse and located in the most caudal regions, as was noted in the emu (Crole, 2009).

This study aims to confirm the presence of taste buds in the emu by using conventional light microscopy as well as immunohistochemical labelling for neurofilament protein to identify the gustatory nerve fibres supplying the taste buds. By using this method this study also aims to confirm the presence or absence of taste buds in the ostrich as well as in determining their distribution and structure in the ostrich (if present) and emu. Knowledge of a sense of taste in these two commercially important birds may have an impact on the composition of feed rations as well as providing a more holistic view on food selection in these two species.

8.2. Materials and Methods

To identify regions in the oropharynx containing taste buds the same histology slides utilised in Chapter 3.2.3 (from 5 adult ostrich and 5 adult emu) were examined. A study of these slides revealed that only certain regions of the emu oropharynx contained taste buds. The taste buds from the above histological sections were viewed, and features of interest described and digitally recorded using an Olympus BX63 light microscope (Olympus Corporation, Tokyo, Japan) equipped with a DP72 camera and Olympus cellSens imaging software (Olympus Corporation, Tokyo, Japan), and annotated in Corel Draw X5. The structures of the oropharynx (see below) (Fig. 8.1) was digitally recorded with a Canon EOS 5D digital camera (Canon, Ōita, Japan) equipped with a Canon Macro 100mm lens.

A total of 5 adult ostrich and 5 adult emu heads, from birds of either sex, were collected after slaughter from the Klein Karoo Ostrich abattoir (Oudtshoorn, Western Cape

Province, South Africa) and the Oryx Abattoir (Krugersdorp, Gauteng Province, South Africa). All heads were thoroughly rinsed with either distilled water or running tap water to remove mucus, blood and regurgitated food. The heads were immersion fixed in 10% neutral-buffered formalin and transported to the Faculty of Veterinary Science, University of Pretoria. Care was taken to exclude air from the oropharynx by inserting a small block of wood between the bill tips. The heads remained in the 10% neutral-buffered formalin for a maximum of 4 days before being processed for light microscopy.

The regions previously identified to contain taste buds in the emu, as well as the proximal esophagus (Crole, 2009), were sampled from the 5 emu and the 5 ostrich heads (Fig. 8.1). In both species the left and right quadratomandibular joints were disarticulated and the oesophagus incised to separate the upper and lower parts of the head. The soft interramal region was removed from the bony mandible by sharp incision following the inside mandibular edge. The non-keratinised roof and non-keratinised floor of the oropharynx, the tongue root and the proximal esophagus were excised (Fig. 8.1) and then serially sectioned in the transverse plane at approximately 2-4mm intervals. The samples were dehydrated through 70%, 80%, 96%, and 2X 100% ethanol and further processed through 50:50 ethanol: xylol, 2X xylol and 2X paraffin wax (60-120 minutes per step) using a Shandon model 2LE Automatic Tissue Processor (Shandon, Pittsburgh, PA, USA). Tissue samples were then manually serially imbedded (this was ensured by cutting a notch on the side not to be imbedded) into paraffin wax in plastic moulds. Sections were cut at 3 μ m and stained with Haematoxylin and Eosin (H&E) (Bancroft and Gamble, 2002). Taste buds were viewed, and features of interest described and digitally recorded using an Olympus BX50 equipped with the analysis CC12 Soft Imaging System (Olympus Corporation, Tokyo, Japan) and an Olympus BX63 light microscope (Olympus Corporation, Tokyo, Japan) equipped with a DP72 camera and Olympus cellSens imaging software (Olympus Corporation, Tokyo, Japan), and annotated in Corel Draw X5.

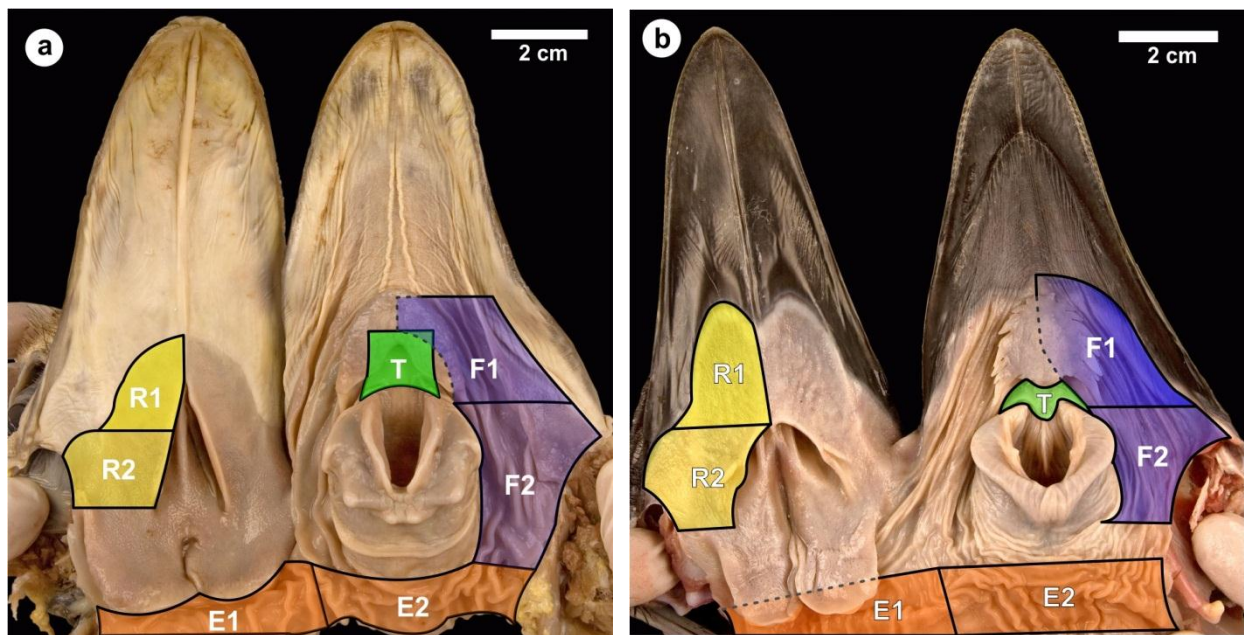


Figure 8.1. Ostrich (a) and emu (b) head opened to display the regions sampled to identify taste buds in the oropharynx. Rostral part of the non-keratinised floor (F1), caudal part (F2), tongue root (T), dorsal esophagus (E1), ventral esophagus (E2), rostral part of non-keratinised roof (R1) and caudal part (R2).

8.2.1. Immunohistochemistry (IHC)

The wax blocks corresponding to sections where taste buds were identified in the emu, were re-cut at 4 μm . The first section was picked up on a glass slide and processed for immunohistochemical labelling of neurofilament to identify nerve fibres supplying the taste buds. Although no taste buds were identified in the ostrich, wax blocks from the oropharyngeal roof from the 5 specimens mentioned above were processed according to the same protocol as the emu specimens. Sections for immunostaining were mounted on positively-charged microscope slides (SuperFrost® Plus, Menzel-Glasser®) and dried overnight in a 38-40°C oven. Routine dewaxing took place in xylene for 10 minutes, followed by rehydration through a graded ethanol and distilled water series (100%, 96% and 70%). Sections were subsequently rinsed in distilled water, incubated with 3% hydrogen peroxide in methanol for 10 minutes at room temperature and then rinsed in distilled water. Heat-induced epitope retrieval (HIER) was performed via microwave heating (96°C) in a plastic container in Tris-EDTA Buffer (pH 9.0) for 21 minutes. Thereafter the test sections (still in buffer) were allowed to cool for 15 minutes on the bench before rinsing in distilled water (3 times) and then in phosphate buffered saline/Bovine serum albumin (PBS/BSA) buffer (pH 7.6) for 5 minutes. Sections were

incubated with the primary monoclonal mouse anti-human Neurofilament protein antibody (Cat. No. M0762, Dako, Denmark) at a dilution of 1:50 for 30 minutes in a humidified chamber at room temperature. The antibody labels neurons (axons) of the central and peripheral nervous system by binding to the neurofilament in the cells. Sections were rinsed in distilled water and then kept in buffer for 10 minutes. The labelled streptavidin biotin plus (LSAB+) System-horse radish peroxidase (HRP) reagents were applied according to the manufacturer's instructions (catalogue no. K0679, Dako, Denmark). The biotinylated link was incubated for 15 minutes, followed by rinsing for 10 minutes in PBS buffer. Sections were then incubated in streptavidin-HRP for 15 minutes and rinsed in PBS buffer for 10 minutes. Sections were incubated for less than a minute in 3,3' diaminobenzidine plus (DAB+) substrate buffer and chromogen combination. They were then rinsed in distilled water, counterstained with Mayer's haematoxylin for 1 minute and rinsed under running tap water for 10 minutes to remove excess substrate. Sections were routinely dehydrated through increasing ethanol concentrations and xylol, and mounted with cover slips. Large peripheral nerves present in the sections served as a positive internal control (Fig. 8.5c).

8.3. Results

Taste buds (*Caliculus gustatorius*) were only identified in the emu and no structures resembling taste buds were found in the ostrich with H&E staining or immunohistochemical labelling.

8.3.1. Distribution

In the present study taste buds in the emu were located in the non-pigmented oropharyngeal roof (Figs. 8.2, 8.4, 8.5, 8.8 and 8.9) and the caudal oropharyngeal floor (Figs. 8.3, 8.6 and 8.7), corresponding to the regions labelled R1, R2 and F2 in figure 8.1b. The highest incidence of taste buds was evident in the rostral part of the oropharyngeal roof, between the pigmented part of the roof and the choana (Region R1) (Fig. 8.1b). Most of the taste buds were located adjacent to the openings of the large, simple branched tubular mucus-secreting glands (Fig. 8.2). When positioned adjacent to the gland opening the taste bud was angled towards the opening. When situated away from the glands, the taste bud lay perpendicular to the surface of the oropharynx.

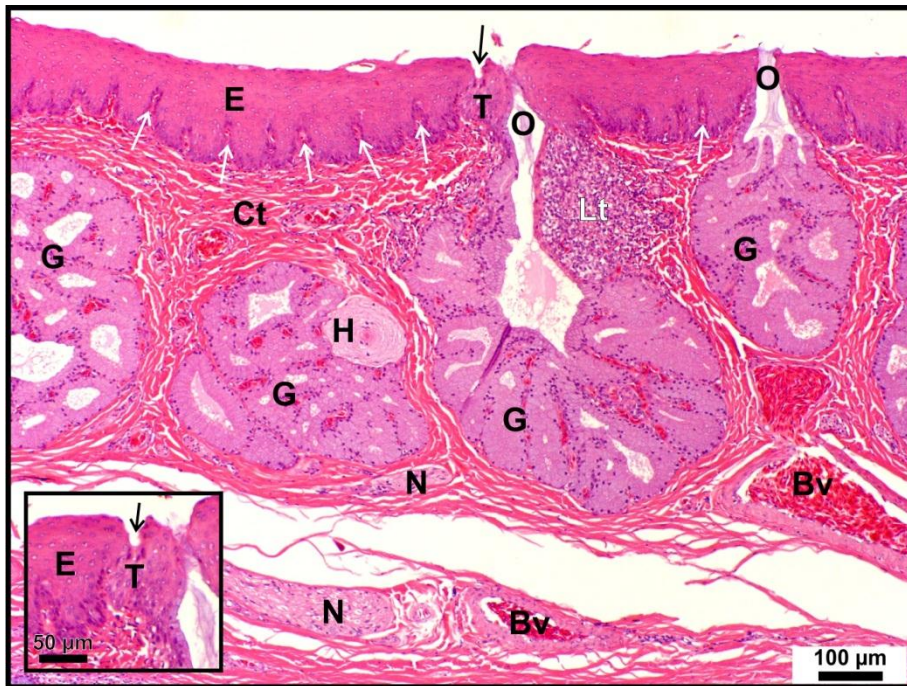


Figure 8.2. Taste bud (T) located near the opening (O) of a large, simple branched tubular gland (G) in the non-pigmented oropharyngeal roof. The taste pore (black arrow) opens near the gland opening. Epithelium (E), connective tissue papillae (white arrows), connective tissue (Ct), Herbst corpuscle (H), blood vessel (Bv), nerve (N) and lymphoid tissue (Lt). **Inset:** Enlargement of the taste bud. H&E stained section.

8.3.2. Structure

The taste buds in the emu extended the full depth of the epithelium in which they were located (Figs. 8.2-8). They were mostly teardrop-shaped (Figs. 8.4 and 8.8); however, depending on the plane of section, they could also appear as round (Figs. 8.2 and 8.9), elliptical (ovoid) (Figs. 8.6 and 8.7) or rectangular (Fig. 8.5) structures. The proximal two thirds of the taste bud was surrounded by connective tissue (Figs. 8.4 and 8.8). The connective tissue encasing the perimeter of the taste bud had a similar appearance to the adjacent connective tissue papillae, which stretched deep into the epithelium (Figs. 8.2, 8.5a and 8.9). However, the connective tissue surrounding the taste bud extended further into the epithelium, carried capillaries in their distal tips (Figs. 8.4 and 8.6-8) and, as demonstrated with positive IHC labelling for neurofilament, contained many fine nerve fibres (perigemmal fibres) (Figs. 8.5, 8.7 and 8.8). As a result of the plane of sectioning it was not possible to accurately measure every taste bud. Based on a total of 9 'usable' taste buds and rounded to the nearest whole number, the average height was calculated as $96 \mu\text{m} \pm 15 \mu\text{m}$ with a width of $51 \mu\text{m} \pm 7 \mu\text{m}$.

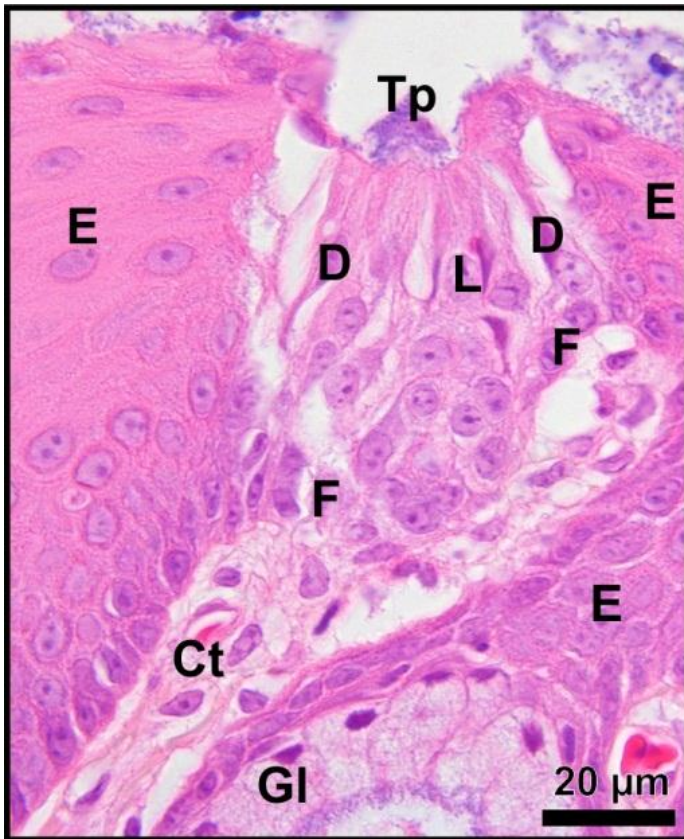


Figure 8.3. Taste bud from the middle region of the non-pigmented oropharyngeal floor (F2 in Fig. 8.1b) in the emu.

Note the elongated dark (D) and light (L) cells with large, round nuclei opening into the taste pore (Tp). As a result of the plane of sectioning, not many follicular cells (F) are present. Connective tissue (Ct), stratified squamous epithelium (E) and mucus-secreting gland (G). H&E stained section.

The taste bud was composed of light and dark cells and follicular cells (Figs. 8.3, 8.4 and 8.6-8). The light and dark cells were vertically oriented and were situated as a group in the centre of the taste bud, surrounded by the follicular cells (Figs. 8.3, 8.4 and 8.6-8). The light cells were rounded and displayed a large, pale-staining nucleus with a prominent nucleolus, whereas the dark cells were slender, elongated and the nucleus was not clearly visible (Figs. 8.3, 8.4 and 8.6-8). The follicular cells were continuous with the surrounding *Str. germinativum* of the stratified squamous epithelium and formed the outer component of the taste bud (Figs. 8.3, 8.4 and 8.6-8). The taste pore (*Porus gustatorius*) (Figs. 8.3, 8.4 and 8.6-8) displayed a wider outer region (Fig. 8.8) ($25 \mu\text{m} \pm 3 \mu\text{m}$) ($n=9$) which was formed by a shallow depression in the epidermis and a narrower inner pore (Fig. 8.8) ($10 \mu\text{m} \pm 4 \mu\text{m}$) ($n=9$) into which components of the centrally located cells opened directly. The taste pore was generally filled with basophilic mucus. Clear, circular openings of unknown origin were rarely observed in the centre of the taste bud (Fig. 8.8).

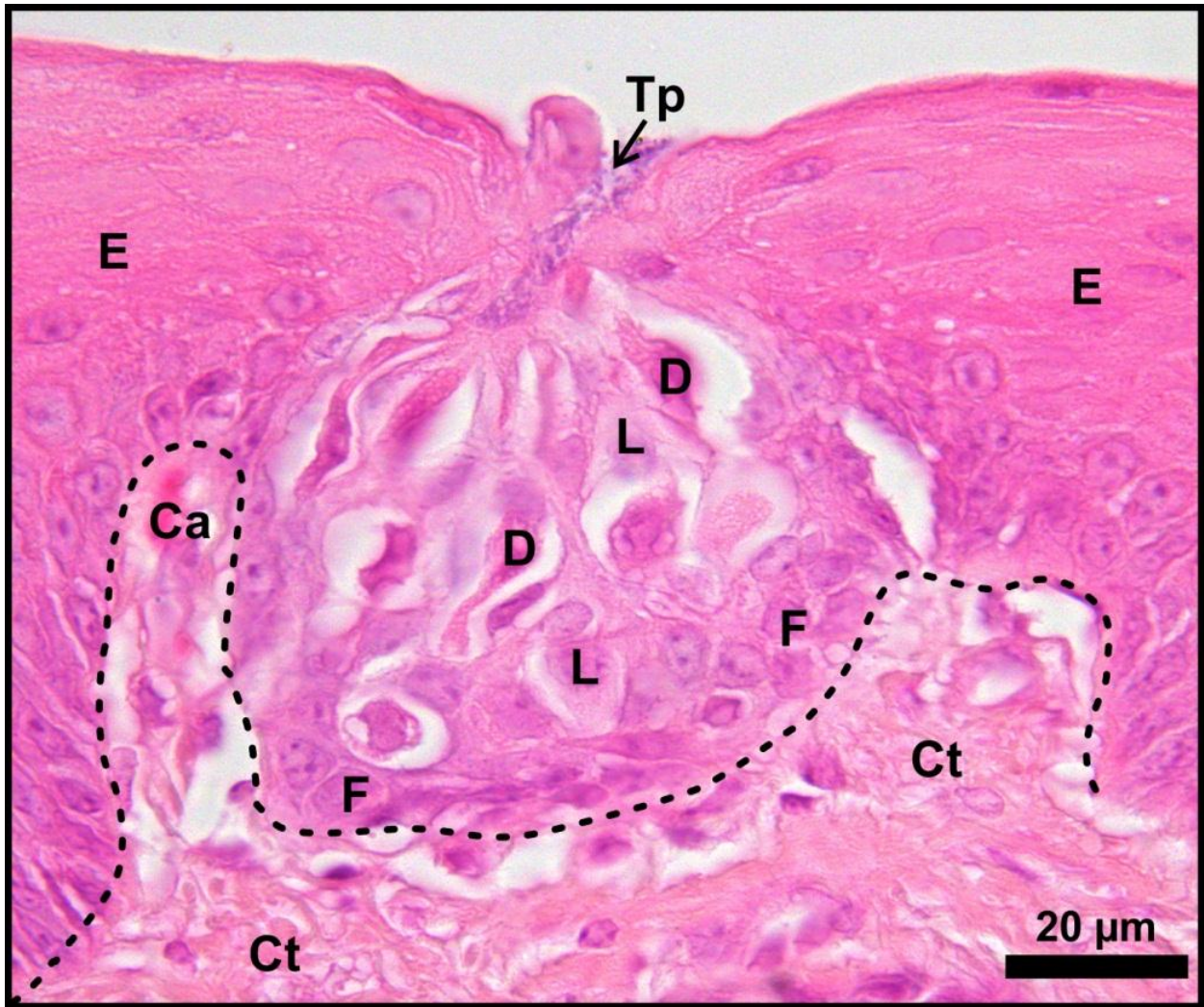


Figure 8.4. Taste bud from the non-pigmented oropharyngeal roof (R1 in Fig. 8.1b) in the emu. The round taste bud displays a taste pore (TP), which is long, narrow and filled with mucus and debris, elongated dark cells (D), light cells (L) with large, round nuclei and follicular cells (F). Connective tissue (Ct) surrounds the base of the taste bud and is demarcated from the taste bud by the dotted line. Stratified squamous epithelium (E) and capillary (Ca). H&E stained section.

Positive IHC labelling for neurofilament (Figs. 8.5 and 8.7-9) demonstrated numerous fine nerve fibres (*Neurofibra gustatoria*) at the base of the taste bud (subgemmal fibres) (Figs. 8.5 and 8.7-9), within the connective tissue immediately surrounding the taste bud (perigemmal fibres) (Figs. 8.5, 8.7-9) and between the follicular and light and dark cells (intragemmal fibres) (Fig. 8.7). IHC labelling for neurofilament allowed the identification of taste buds which were not favourably sectioned and which would not have been visualised with H&E staining (Fig. 8.9). For example, in taste buds which had been sectioned obliquely, the existence of such a structure was only made obvious by the presence of subgemmal and perigemmal nerve fibres which had reacted positively with

IHC labelling for neurofilament (Fig. 8.9). With H&E staining, such a taste bud would have appeared as a part of the surrounding stratified squamous epithelium (Fig. 8.9).

No structures resembling taste buds were found in the ostrich in the samples submitted for immunohistochemical labelling for neurofilament. Although the slides also demonstrated positive labelling for neurofilament in the peripheral nerves and axons of Herbst corpuscles, there was no evidence of sub-, peri- and intragemmal nerve fibres in the surrounding stratified squamous epithelium.

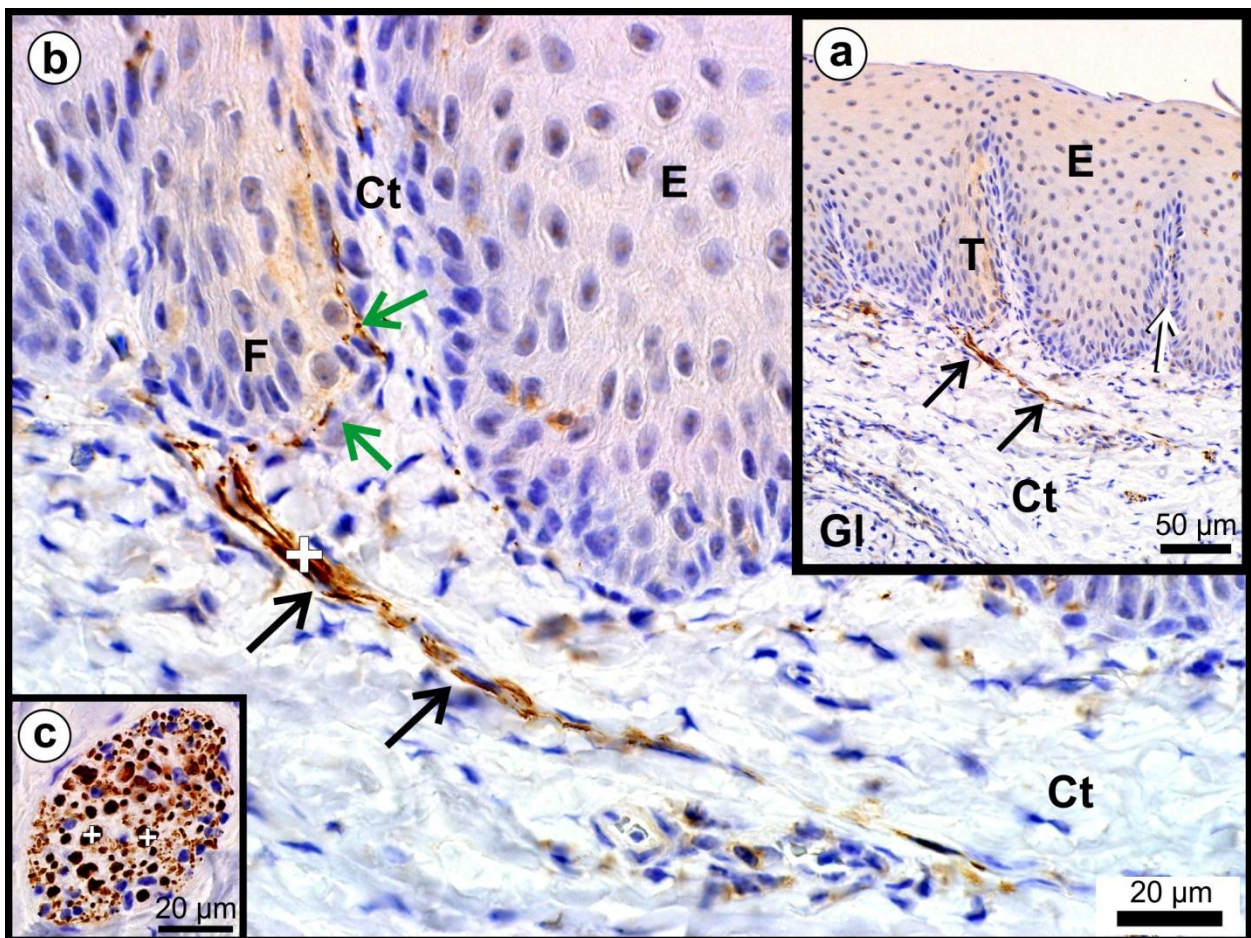


Figure 8.5. Positive (+) IHC labelling for neurofilament. (a) and (b – enlargement from a). Taste bud from the non-pigmented oropharyngeal roof (R1 in Fig. 8.1b) in the emu. The taste bud (T) has been sectioned superficially and only follicular cells (F) can be identified. The subgemmal (black arrows) and perigemmal (green arrows) divisions of the gustatory nerve fibres are clearly demonstrated with the brown staining. Stratified squamous epithelium (E), connective tissue (Ct), connective tissue papilla (white arrow) and mucus-secreting gland (Gl).

(c). Peripheral nerve. Note the positive (+) IHC labelling for neurofilament in a nerve present in the connective tissue in the non-pigmented roof.

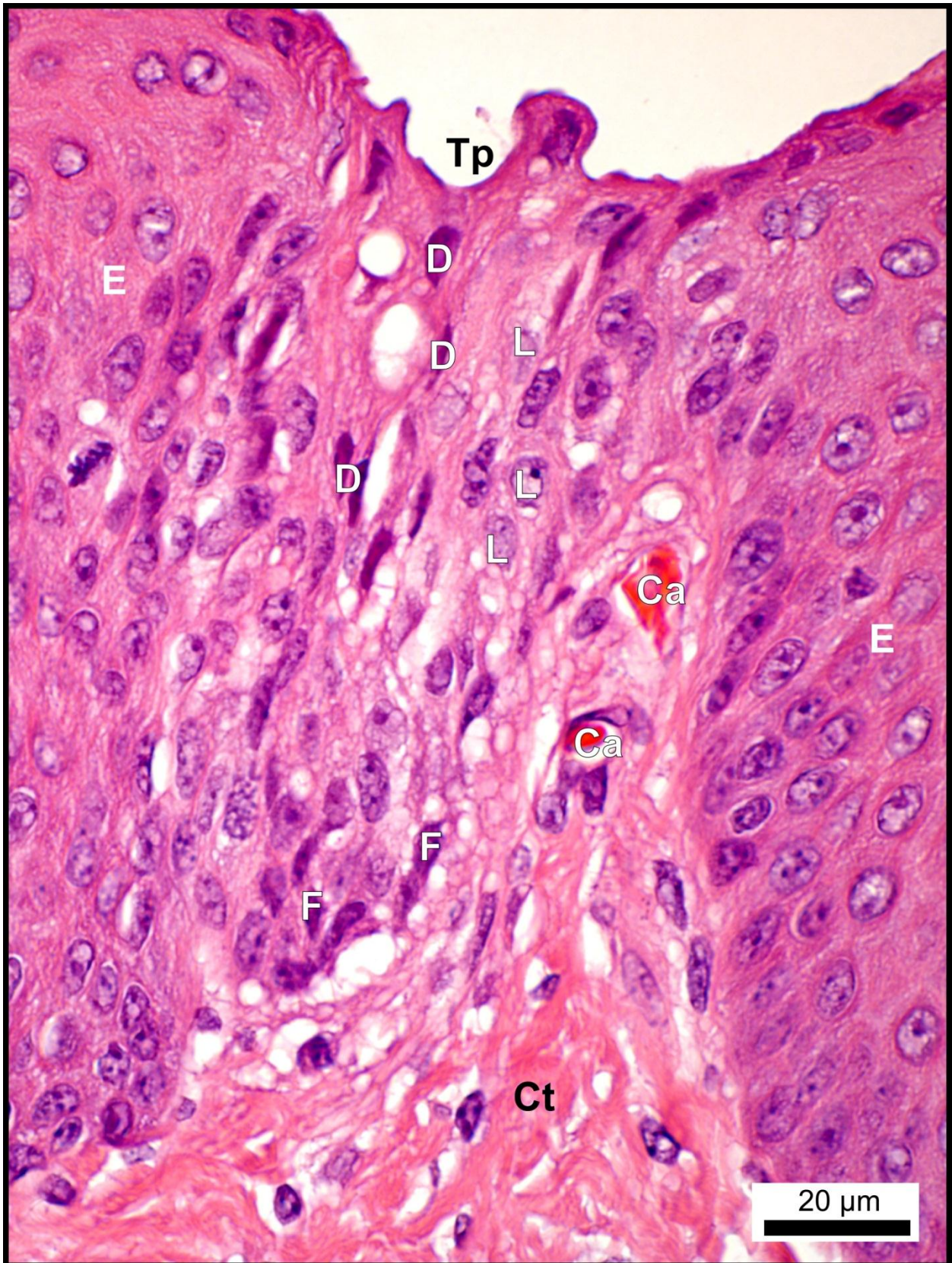


Figure 8.6. Taste bud on the caudal non-pigmented oropharyngeal floor (F2 in Fig. 8.1b) in the emu. Note the less obvious morphology of the taste bud with H&E staining compared to the IHC labelling of an adjacent section of the same taste bud illustrated in Fig. 8.7. Dark cells (D), light cells (L), follicular cells (F), taste pore (Tp), stratified squamous epithelium (E), capillary (Ca) and connective tissue (Ct).

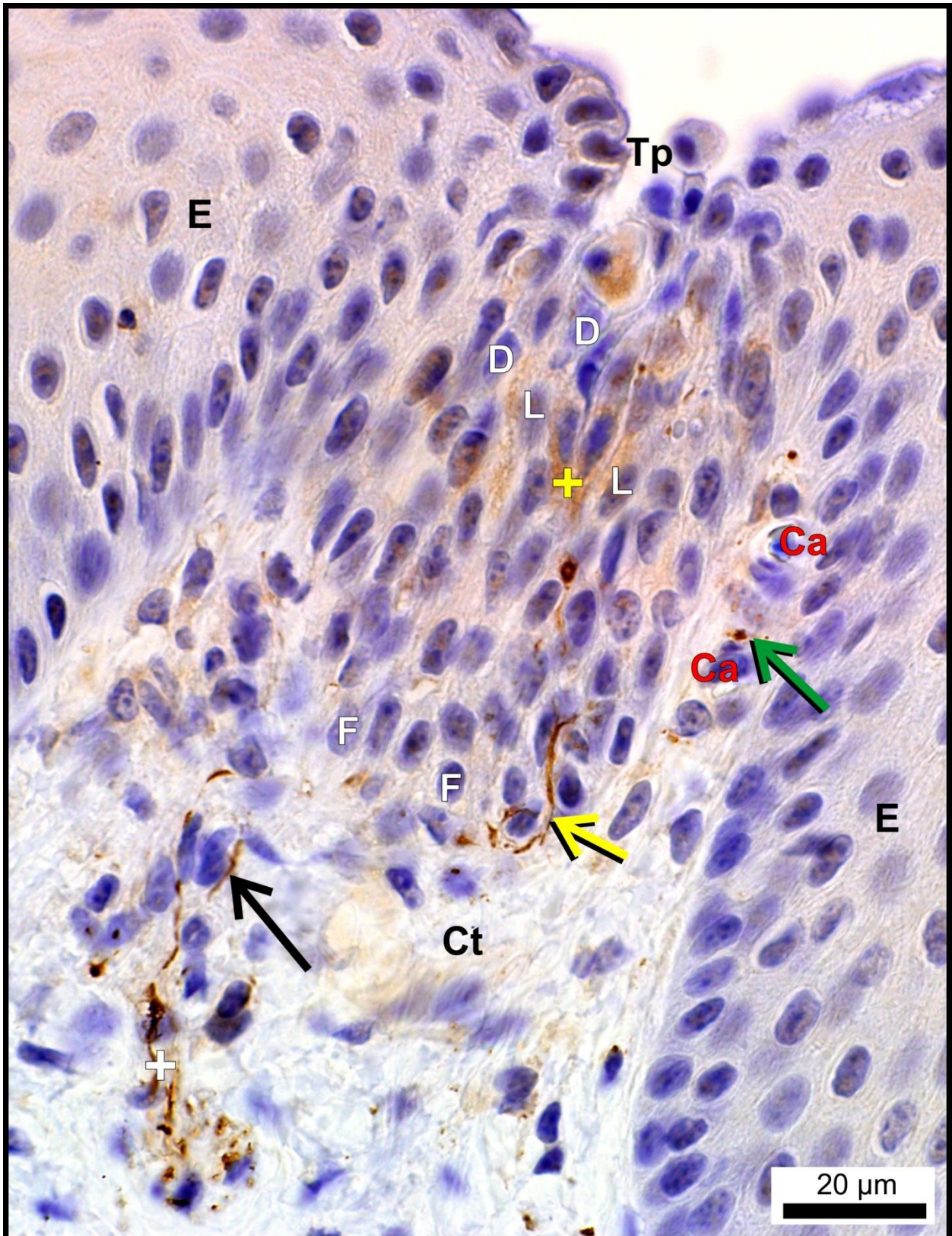


Figure 8.7. The same taste bud as in Fig. 8.6 but from an adjacent section demonstrating positive (white +) IHC labelling for neurofilament. Division of the gustatory nerve fibre into subgemmal (black arrow), perigemmal (green arrow) and intragemmal (yellow arrow) fibres is obvious using this technique. The light cells show a degree of non-specific staining (yellow +). Dark cells (D), light cells (L), follicular cells (F), taste pore (Tp), stratified squamous epithelium (E), capillary (Ca) and connective tissue (Ct).

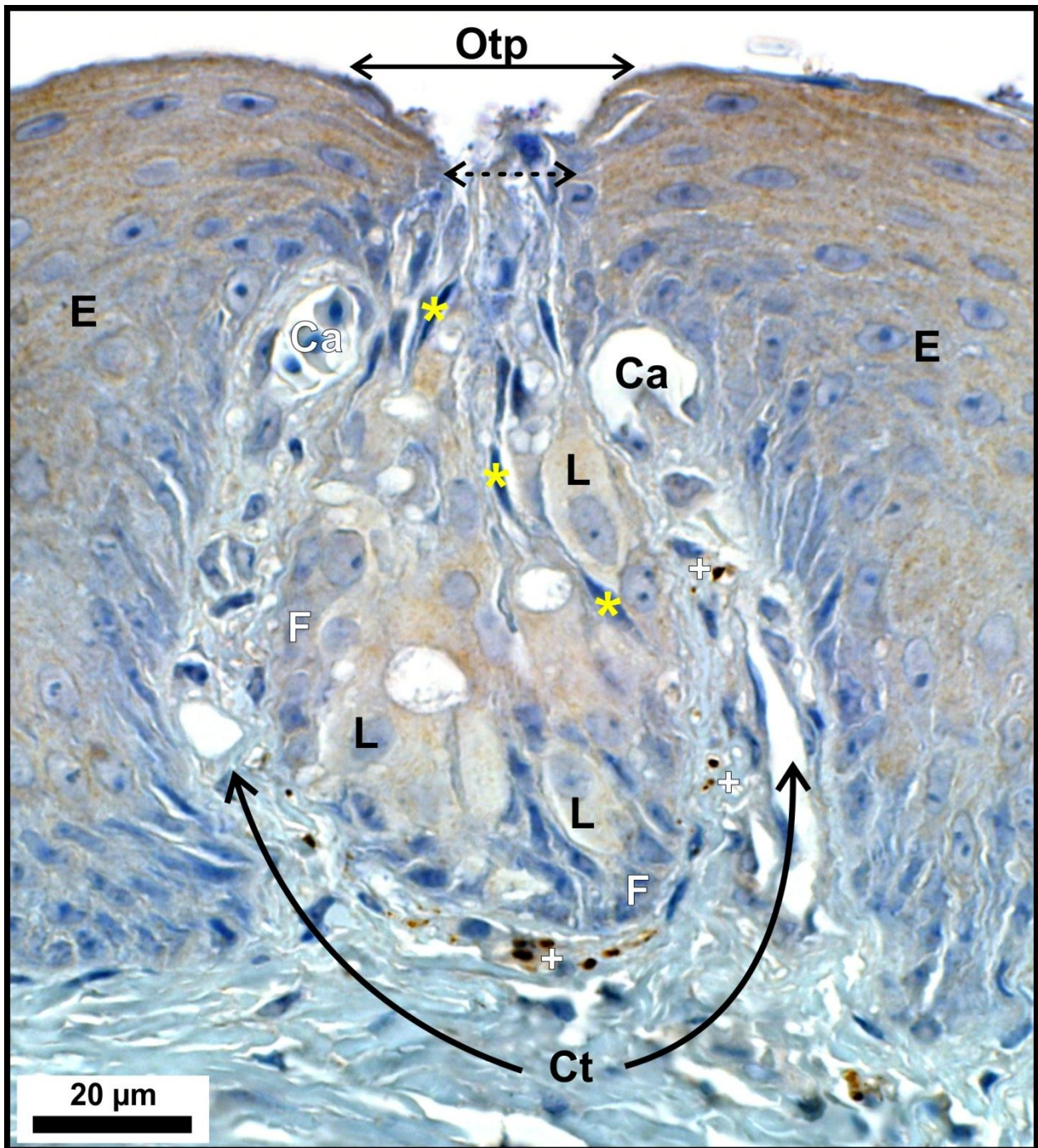


Figure 8.8. Taste bud in the caudal non-pigmented oropharyngeal roof (R2 in Fig. 8.1b) in the emu demonstrating positive (white +) IHC labelling for neurofilament. Note the connective tissue (Ct) which encapsulates the taste bud and carries capillaries (Ca) distally. Dark cells (yellow *), light cells (L), follicular cells (F), outer taste pore (Otp), inner taste pore (dotted double-headed arrow) and stratified squamous epithelium (E). Clear, circular openings are present in the region of the light cells.

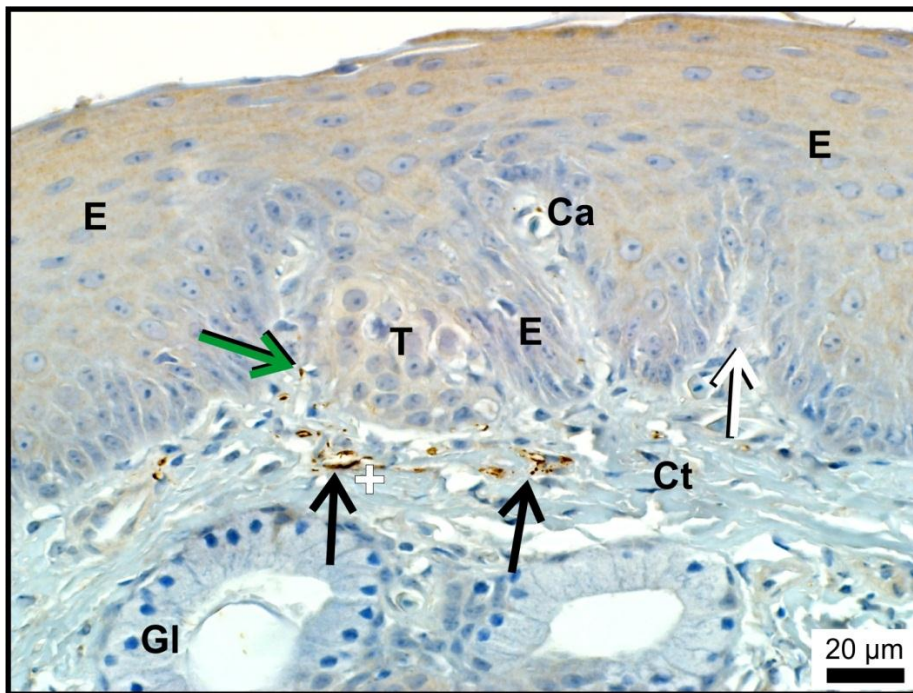


Figure 8.9. Positive (+) IHC labelling for neurofilament in a taste bud in the caudal non-pigmented oropharyngeal roof. Note the similarity in appearance of the obliquely sectioned taste bud (T) to the surrounding stratified squamous epithelium (E). Subgemmal (black arrow) and perigemmal (green arrow) nerve fibres, connective tissue (Ct), capillary (Ca), mucus-secreting gland (Gl) and connective tissue papilla (white arrow).

8.4. Discussion

8.4.1. Distribution

This study confirmed the presence of taste buds previously reported in the emu (Crole, 2009; Crole and Soley, 2009). In light of the fact that no structures resembling taste buds were observed in the ostrich oropharynx, this study identifies the emu as the only ratite studied which displays a known sense of taste. When sectioned tangentially, taste buds were indistinguishable from the surrounding epithelium with H&E staining. Taste buds are inherently difficult to identify in all bird species as they are obscured by the connective tissue papillae and the ducts of glands traversing the epithelium (Moore and Elliott, 1946). Depending on the plane of section, submucosal papillae and salivary ducts can also be mistaken for taste buds (Lindenmaier and Kare, 1959). By using IHC labelling for neurofilament, concentrations of nerve fibres could be demonstrated beneath apparently non-descript epidermal structures, thus indicating the presence of a taste bud and overcoming the above mentioned difficulties in locating these structures. IHC labelling for neurofilament protein therefore proved to be a more reliable method of accurately identifying taste buds in the emu than conventional H&E staining. However, despite the use of this technique, no structures resembling taste buds were identified in the ostrich oropharynx.

The conventional method for determining the distribution of taste buds by rapid surface staining, as applied in the mallard (Berkhoudt, 1977), was not used in the present study. Although this method is superior for determining the total number and distribution of taste buds, the presence in some birds of a high number of small salivary gland openings obscures their identification, as was noted in the pigeon and chicken (Berkhoudt, 1985). The ostrich (Tivane, 2008) and emu (Crole and Soley, 2011) both possess an oropharynx with densely packed large and small salivary gland openings, and which occur in those locations where taste buds are found (in the emu). Furthermore, surface studies using scanning electron microscopy in these regions of the ostrich (Tivane, 2008) and emu (Crole, 2009) have also failed to identify taste buds. For this reason, as noted above, it would appear that the best method of identifying taste buds in the ratites would currently be with IHC labelling for neurofilament protein. A practical method of detailing the exact distribution and number of taste buds in large birds such as the adult emu (and other large ratites) remains to be determined.

Based on the present study and previous putative reports in the emu (Crole, 2009; Crole and Soley, 2009), taste buds in this species are present in the following non-keratinised regions of the oropharynx; the non-pigmented oropharyngeal roof, the non-pigmented oropharyngeal floor, the proximal esophagus (Crole, 2009) and the tongue root (Crole and Soley, 2009). However, the present study could not confirm the presence of taste buds in the proximal esophagus and tongue root of the emu reported in earlier studies (Crole, 2009; Crole and Soley, 2009), indicating that these structures are most likely very scarce in these regions. The distribution of taste buds in birds has been well summarised and presented by Berkhoudt (1985). Based on numerous studies (see Berkhoudt, 1985) it has been demonstrated that taste buds in birds are located in the base of the tongue (tongue root) and the oropharyngeal roof and floor. Thus the distribution of taste buds in the emu follows the general pattern noted in avians. However, the emu is the only bird in which taste buds have been reported in the proximal esophagus (Crole, 2009). Additionally, some birds possess taste buds in the keratinised regions of the oropharynx (which are usually more rostrally situated), including the hoopoe and sparrow (Botezat, 1910) and mallard (Berkhoudt, 1985) whereas *Calidris* species (Gerritsen *et al.*, 1983) reportedly possess taste buds in the bill.

8.4.2. Structure

An extensive collection of literature exists on the structure of the avian taste bud and the earlier work has been summarised by Berkhoudt (1977). In general, the structural characteristics of taste buds in the emu resemble those of other birds (Botezat, 1910; Moore and Elliott, 1946; Lindenmaier and Kare, 1959; Gentle, 1971b; Berkhoudt, 1977; Ganchrow and Ganchrow, 1985) particularly in respect of their ovoid shape and outer component of follicular cells. Although mammalian taste buds, as in birds, extend throughout the entire thickness of the stratified squamous epithelium in which they are housed, they differ in a number of respects from those of birds. The outer layer of follicular cells is absent and only a single layer of elongated chemoreceptor (taste) cells and sustentacular (supporting) cells is present (Frappier, 2006). The taste buds of the emu and other birds, for example the mallard (Berkhoudt, 1977), also differ in respect of the connective tissue sheath surrounding much of the taste bud and which displays a well-developed capillary supply. This would suggest that the taste bud in the emu occupies a deep, widened dermal papilla, thus isolating it from the surrounding epithelium.

Based on the structural characteristics of taste buds from a number of avian species, Bath (1906) defined three distinct groups. Group I were noted in five species of song birds (common starling (*Sturnus vulgaris*), house sparrow (*Passer domesticus*), common blackbird (*Turdus merula*), yellowhammer (*Emberiza citronella*), European greenfinch (*Chloris chloris*)), the barn swallow (*Hirundo rustica*), European swift (*Cypselus apus*), great hornbill (*Buceros bicornis*), lesser spotted woodpecker (*Dendrocopus minor*), two birds of prey (common kestrel (*Falco tinnunculus*) and pallid harrier (*Circus macrurus*)), and the chicken and pigeon (Bath, 1906). These taste buds were ovoid in shape and the receptor cells were enveloped by a peripheral sheath of follicular cells. Group II taste buds were identified in the mallard duck (*Anas boschas*), Northern shoveller (*Spatula clypeata*), greater flamingo (*Phoenicopterus roseus*) and oyster-catcher (*Haematopus ostralegus*). They were much longer than those of Group I and demonstrated a more prominent follicular cell layer (Bath, 1906). Group III, present in the budgerigar (*Melopsittacus undulates*) and parakeet (*Palaeornis rufirostris*), were more similar in structure to those of Group I but lacked the surrounding follicular cells

(Bath, 1906). Due to the absence of follicular cells these taste buds more closely resemble mammalian the taste buds than those from the other two groups.

Based on the criteria used by Bath (1906), the taste buds in the emu can be categorised as belonging to Group I. The diameter of the taste buds in the emu ($51 \mu\text{m} \pm 7 \mu\text{m}$) places them within the range of those birds belonging to this group (Bath, 1906), including the chicken (40-69 μm) (Ganchrow and Ganchrow, 1985). The height of the taste buds in many of the birds in Group I (Bath, 1906) was greater than that of the emu ($96 \mu\text{m} \pm 15 \mu\text{m}$), although the chicken (73-99 μm) and pigeon (78-109 μm), also from this group, appeared to have a similar height. The taste pore in the mallard is divided into an outer pore (100 μm) and an inner pore (10 μm) (Berkhoudt, 1977), similar to that noted in the present study. Although the inner pore in the emu (10 μm) was comparable to that of the mallard, the outer pore was only a quarter of the width (25 μm). The small size of the outer pore in the emu may partially explain why these structures were not identified in previous studies using scanning electron microscopy (Crole, 2009). Taste canals have been described in the taste buds of the chicken (Gentle, 1971b; Kurosawa *et al.*, 1983; Ganchrow and Ganchrow, 1985, 1987) and Japanese quail (Warner *et al.*, 1967). Although similar structures appeared to be present in some of the taste buds in the emu (see Fig. 8.8), it was not clear whether these openings represented canals or artefacts. Their presence in only a few sections suggests the latter to be true.

A feature of the inner cell component of the emu taste buds was the presence of both light and dark elongated cells. Transmission electron microscopy (TEM) of taste buds in the chicken revealed light cells (gustatory cells displaying afferent synaptic contacts with axon terminals), dark cells (supporting cells displaying extensive axonal contacts with no synapses) and peripheral (follicular) cells (flattened cells with filaments and free ribosomes) (Kurosawa *et al.*, 1983, cited by Berkhoudt, 1985). Future ultrastructural studies on taste buds in the emu will be required to more accurately determine the fine structure of light and dark cells in order to postulate their function. However, the scarcity of taste buds in the emu oropharynx would make their detection by blind sampling almost impossible. A method to accurately sample taste buds in the emu and to prepare them for TEM remains a challenge.

The nerve fibres supplying the taste buds of the emu, the subgemmal, perigemmal and intragemmal fibres, were a distinguishing feature in this species. The presence of these nerve fibres, as demonstrated with the IHC labelling for neurofilament, allowed for the positive identification of taste buds in the present study. Twenty to thirty intragemmal axons reportedly supply the taste bud in the mallard (Evans and Martin, 1993). Although the gustatory nerve fibres were not counted in the present study, they did not appear to be as numerous in the emu as those reported in the mallard. This may be a reflection of the smaller size of the taste buds in the emu (Group I) compared to those of the mallard (Group II). The lingual nerve from the glossopharyngeal nerve reportedly supplies taste buds in the tongue of birds and was originally considered to be the only cranial nerve transmitting gustatory impulses to the brain (see Berkhoudt, 1985). However, later studies demonstrated that branches of the facial nerve innervated taste buds located in the rostral tips of the bill in the mallard (Krol and Dubbeldam, 1979) and the palate and rostral mandible of the chicken (Gentle, 1987). Future functional studies will need to be performed to determine the innervation of taste buds in the emu.

8.4.3. Function

The distribution of taste buds in the mallard (Berkhoudt, 1977) and chicken (Ganchrow and Ganchrow, 1985) has been linked to their particular feeding habits. Similarly, it would appear that the distribution of taste buds reflects their strategic placement in the oropharynx which can be linked to the feeding method of the emu (Bonga Tomlinson, 2000). In this species the food is accelerated through the oropharynx from the bill tip to land in the proximal esophagus, after which the tongue scrapes the oropharyngeal roof during retraction and swallowing (Bonga Tomlinson, 2000). This action would clear the oropharyngeal roof of loose food particles which did not reach the proximal esophagus and simultaneously expose the ingested food to the largest concentration of taste buds in the oropharynx. A search in GenBank revealed that the emu possesses two bitter taste receptor sequences and one amino acid receptor (personal communication, H. Rowland). Thus the relatively few taste buds present in the emu oropharynx would mainly function in distinguishing bitter taste. As bitter-tasting compounds can cause a negative association with a particular food type (Rowland *et al.*, 2013) it would appear that the sense of taste in the emu would be predominantly for protection and not for food selection. Emu's enjoy a varied diet, including insects (Davies, 1978), and the

ability to taste bitter compounds could protect the emu from ingesting noxious insects and plants. Furthermore, as previously postulated (Crole, 2009), the ability to distinguish bitter tasting compounds would aid in detecting potable water, an especially important trait in the emu's natural, arid environment. Thus, in the emu, taste buds on the oropharyngeal roof would be ideally positioned to aid in tasting ingested food, whereas those on the oropharyngeal floor and proximal esophagus would be best positioned for detecting potable water. The density of taste buds in the above mentioned regions supports this view. Kare and Pick (1960) noted in chicks that fewer taste buds were necessary to taste liquids; whereas fewer taste buds were stimulated by dry food. The oropharyngeal roof of the emu would mainly come into contact with dry food, which necessitates a higher amount of taste buds, whereas those on the oropharyngeal floor would mainly be in contact with liquids (water), and hence the reason for fewer taste buds in this region. Due to their commercial importance many studies have been performed in the chicken to determine the effect of taste on food intake (see Gentle, 1971a). As the emu industry is based on farming these birds for their body fat, the importance of encouraging food intake in these birds is self-evident. The effect of taste on feed intake in the emu would be a topic for future studies.

Proof of a sense of taste in the ostrich has long been sought (Anon, 1922; Brand and Gous, 2006; Jackowiak and Ludwig, 2008; Tivane, 2008) and the various studies in this regard have yielded only negative results (including the present study). However, a search of the ostrich genome for any of the taste genes (bitter, sweet, sour and salty) should finally clarify this matter. However, the potential for chemoreception in the oropharynx of the ostrich, through mechanisms other than taste buds, cannot be ruled out. For example, substances inactivating one or more enzymes in the oral mucosa may give rise to a characteristic sensation (Lindenmaier and Kare, 1959). A well-developed bill tip organ is present in the ostrich (see Chapter 7) and there is little doubt that these birds display a high tactile acuity (as does the emu) in their bill tips. Additionally, the median palatine and ventral ridges in the ostrich would contribute to this heightened sense of touch. If the ostrich truly does not possess a sense of taste, then it would appear that this bird relies more heavily on the bill tip organ to discriminate food. Selection of food in the ostrich would most likely be based on vision and smell. The ostrich displays a small field of binocular vision which enables it to visualise the bill tip and afford a high accuracy during pecking (Martin and Katzir, 1995). Although lower

than in the emu (26.3) the ostrich possesses a relatively high olfactory bulb: cerebral hemisphere ratio (19.2) and which can be correlated to a good sense of smell (Zelenitsky *et al.*, 2011). A possible reason for the absence of taste buds in the ostrich may be that it is an adaptation to enable the ingestion of less palatable food. The ostrich appears well-equipped for selection (vision and smell) and discrimination (bill tip organ) of food items, which may compensate for an absence of taste in this species. Numerous studies have been performed on feed composition in ostriches (see Brand and Gous, 2006). However, the current lack of information on anatomical features such as the existence of a bill tip organ may adversely affect these formulations. The results of the present study would seem to indicate that texture, as opposed to taste, would be a factor to consider in formulation of feed for ostriches.

8.5. References

- Anon, T.H.G. 1922. *Taste or Scent in the Ostrich*. In: The Scottish Naturalist. Edited by Ritchie, J. Edinburgh: Oliver & Boyd. pp.168.
http://archive.org/stream/scottishnaturali1922arbr/scottishnaturali1922arbr_djvu.txt
- Bath, W. 1906. Die Geschmacksorgane der Vögel und Krokodile. *Archiv für Biontologie*. **1**: 5-47.
- Berkhoudt, H. 1977. Taste buds in the bill of the mallard (*Anas platyrhynchos* L.). Their morphology, distribution and functional significance. *Netherlands Journal of Zoology*. **27**: 301-331.
- Berkhoudt, H. 1985. *Structure and Function of Avian Taste Buds*. In: Form and Function in Birds. Vol. 3. Edited by King, A.S. and McLelland, J. London: Academic Press. pp. 463-491.
- Bonga Tomlinson, C.A. 2000. *Feeding in Paleognathous Birds*. In: Feeding: Form, Function, and Evolution in Tetrapod Vertebrates. Edited by K. Schwenk. San Diego: Academic Press. pp. 359-394.
- Botezat, E. 1910. Morphologie, Physiologie und phylogenetische Bedeutung der Geschmacksorgane der Vögel. *Anatomischer Anzeiger*. **36**: 428-461.
- Brand, T.S. and Gous, R.M., 2006. *Feeding Ostriches*. In: Feeding in Domestic Vertebrates: From Structure to Behaviour. Edited by Bels, V. Wallingford, England: CAB International. pp. 136-155.
- Crole, M.R. 2009. A gross anatomical and histological study of the oropharynx and proximal oesophagus of the emu (*Dromaius novaehollandiae*). MSc dissertation, University of Pretoria, South Africa.

- Crole, M.R. and Soley, J.T. 2009. Morphology of the tongue of the emu (*Dromaius novaehollandiae*). II. Histological features. *Onderstepoort Journal of Veterinary Research*. **76**: 347-361.
- Evans, H.E. and Martin, G.R. 1993. *Organa Sensuum*. In: Handbook of Avian Anatomy: Nomina Anatomica Avium, 2nd edition. Edited by Baumel, J.J., King, A.S., Breazile, J.E., Evans, H.E. and Vanden Berge, C. Cambridge, Massachusetts: The Nuttall Ornithological Club, No. 23. pp. 585-611.
- Feder, F.-H. 1972. Zur mikroskopischen Anatomie des Verdauungsapparates beim Nandu (*Rhea americana*). *Anatomischer Anzeiger*. **132**: 250-265.
- Frappier, B.L. 2006. *Digestive System*. In: Dellmann's Textbook of Veterinary Histology. 6th edition. Edited by Eurell, J.-A., and Frappier, B.L. Ames: Blackwell Publishing. pp. 170-211.
- Ganchrow, D. and Ganchrow, J.R. 1985. Number and distribution of taste buds in the oral cavity of hatchling chicks. *Physiology and Behaviour*. **34**: 889-894.
- Ganchrow, D. and Ganchrow, J.R. 1987. Taste bud development in chickens (*Gallus gallus domesticus*). *The Anatomical Record*. **218**: 88-93.
- Ganchrow, D. and Ganchrow, J.R. 1989. Gustatory ontogenesis in the chicken; an avian-mammalian comparison. *Medical Science Research*. **17**: 223-228.
- Gentle, M.J. 1971a. Taste and its importance to the domestic chicken. *British Poultry Science*. **12**: 77-86.
- Gentle, M.J. 1971b. The lingual taste buds of *Gallus domesticus*. *British Poultry Science*. **12**: 245-248.
- Gentle, M.J. 1987. Facial nerve sensory response recorded from the geniculate ganglion of *Gallus gallus* var. *domesticus*. *Journal of Comparative Physiology*. **160**: 683-691.
- Gerritsen, A.F.C., van Heezik, Y. M. and Swennen, C. 1983. Chemoreception in two further *Calidris* species (*C. maritima* and *C. canutus*) with a comparison of the relative importance of chemoreception during foraging in *Calidris* species. *Netherlands Journal of Zoology*. **33**: 485-496.
- Gussekkloo, S.W.S. and Bout, R.G. 2005. The kinematics of feeding and drinking in palaeognathous birds in relation to cranial morphology. *The Journal of Experimental Biology*. **208**: 3395-3407.
- Kare, M. R. and Pick, H.L. 1960. The influence of the sense of taste on feed and fluid consumption. *Poultry Science*. **39**: 697-705.

- Krol, C.P.M. and Dubbeldam, J.L. 1979. On the innervation of taste buds by the *N. facialis* in the Mallard, *Anas platyrhynchos*. *Netherlands Journal of Zoology*. **29**: 267-274.
- Kurosawa, T., Niimura, S., Kusuhara, S. and Ishida, K. 1983. Morphological studies of taste buds in chickens [In Japanese]. *Japanese Journal of Zootechnical Science*. **54**: 502-510.
- Lindenmaier, P. and Kare, M.R. 1959. The taste end-organs of the chicken. *Poultry Science*. **38**: 545-549.
- Martin, G.R. and Katzir, G. 1995. Visual fields in ostriches. *Nature*. **374**: 19-20.
- McCann, C. 1973. The tongues of kiwis. *Notornis*. **20**: 123-127.
- Moore, D.A. and Elliott, R. 1946. Numerical and regional distribution of taste buds on the tongue of the bird. *Journal of Comparative Neurology*. **84**: 119-131.
- Rowland, H.M., Ruxton, G.D. and Skelhorn, J. 2013. Bitter taste enhances predatory biases against aggregations of prey with warning coloration. *Behavioral Ecology*. **24**: 942-948.
- Saito, I. 1966. Comparative anatomical studies of the oral organs of the poultry. V. Structure and distribution of taste buds of the fowl. *Bulletin of the Faculty of Agriculture, Miyazahi University*. **13**: 95-102.
- Santos, T.C., Fukuda, K.Y., Guimarães, J.P., Oliveira, M.F., Miglino, M.A. and Watanabe, I.-S. 2011. Light and scanning electron microscopy study of the tongue in *Rhea americana*. *Zoological Science*. **28**: 41-46.
- Tivane, C. 2008. A morphological study of the oropharynx and oesophagus of the ostrich (*Struthio camelus*). M.Sc. thesis, University of Pretoria, South Africa.
- van Heezik, Y. M., Gerritsen, A.F.C. and Swennen, C. 1983. The influence of chemoreception on the foraging behaviour of two species of sandpiper, *Calidris alba* and *Calidris aplina*. *Netherlands Journal of Sea Research*. **17**: 47-56.
- Warner, R.L., McFarland, L.Z. and Wilson, W.O. 1967. Microanatomy of the upper digestive tract of the Japanese quail. *American Journal of Veterinary Research*. **28**: 1537-1548.
- Zelenitsky, D., Therrien, F., Ridgely, R.C., McGee, A.R. and Witmer, L.M. 2011. Evolution of olfaction in non-avian theropod dinosaurs and birds. *Proceedings of the Royal Society B*. **278**: 3625–3634.

CHAPTER 9

GENERAL CONCLUSIONS

A number of interesting and unique observations were made during this study on the comparative morphology of mechanical and sensory specialisations in the upper digestive tract of the ostrich and emu that further emphasise the special position these ratites hold within the avian phylogenetic tree. This information and the hypotheses presented should form the basis for interpreting future functional and behavioural studies in the ostrich and emu, and of ratites in general.

Unlike mammals, birds do not possess an epiglottis to protect the glottis while swallowing. However, the ostrich and emu display specialisations of the tongue and laryngeal mound which work synergistically while swallowing to cover and protect the adducted glottis. This novel mechanism was termed the linguo-laryngeal apparatus and functionally replaces an epiglottis in the ratites studied. This apparatus may also be present in other avian species and represents a novel mechanism which should be incorporated into the field of avian biology.

Herbst corpuscles are widely spread throughout the oropharynx of the ostrich and emu. This is in contrast to the situation in most birds where the distribution of these mechanoreceptors is mostly limited to those regions supported by bone. Additionally, concentrations of Herbst corpuscles are present at various strategic locations in the oropharynx of the ostrich and emu. The differences in distribution of Herbst corpuscles between comparable regions of the oropharynx in these two birds can be linked to their specific feeding habits. The ostrich, unlike the emu, displays prominent median palatine and ventral ridges which have a high relative percentage of Herbst corpuscles, effectively denoting these two ridges as sensory structures, the palatal and interramal organs, respectively. The location of these structures, and the specific orientation of the

assembled Herbst corpuscles, may enable them to distinguish directional stimuli. The higher relative percentage of Herbst corpuscles present in the rostral oropharyngeal floor in the ostrich compared to the emu, coupled with the palatal and interramal organs present in the ostrich, indicate that the part of the oropharynx caudal to the mandibular and maxillary rostra are an important sensory region in the ostrich. This study also established a link, in both birds, between the concentration and positioning of Herbst corpuscles and adaptations of the tongue and laryngeal mound for cleaning the choana. In the ostrich a concentration of Herbst corpuscles is present along the edges of the choana whereas corpuscles are absent from the tongue and very scarce in the laryngeal mound. The opposite situation is apparent in the emu where Herbst corpuscles are present in the tongue and laryngeal mound but absent from the perimeter of the choana. In both instances the corpuscles would be able to provide feedback on the correct positioning of the structures involved in cleaning the choana. A connection was also revealed between glandular tissue and Herbst corpuscles which may indicate an additional role for these corpuscles.

Visualised at the ultrastructural level, the intra-oral Herbst corpuscles in the ostrich and emu displayed the same basic components (capsule, outer zone, inner core and axon) described in other neognathous birds. However, some important specific differences were noted between the ostrich and emu and other birds, notably, the presence of myofibroblasts in the capsule, sensory cilia in cells of the outer layers, a relatively larger, less organised outer zone and narrower inner core, and variations in the shape of the axon. The previously unreported presence of myofibroblasts in the capsule indicates the ability for the capsule to contract, thus altering the tension of the capsule, which in turn has implications for the conduction of vibrational stimuli. The sensory cilia in the myofibroblasts of the capsule bordering the outer zone, and in the fibroblasts of the outer zone, may themselves function as mechanoreceptors and play a role in regulating the contraction of the capsule. Such a function has not previously been reported for Herbst corpuscles.

Epidermal specialisations were present in both the ostrich and emu bill. Epidermal troughs (keratin-filled invaginations of the epidermis with underlying Herbst corpuscles) were a feature in the ostrich and would appear to function in transmitting and enhancing vibrational stimuli. Epidermal invaginations, similar in structure and function to the

epidermal troughs, were present in both birds and bordered the *Culmen* and *Gonys*. Similarly, groups of Herbst corpuscles were present at the base of the invaginations. Rhamphothecal serrations with intervening keratinised pegs were a feature of the rostral mandibular tomia in the emu. While perhaps representing a form of pseudo-tooth, these structures could also function to transmit and enhance vibrational stimuli to groups of Herbst corpuscles in pits in the underlying dentary bone. The above mentioned epidermal specialisations would seem to represent important structural adaptations that assist in transmitting and enhancing vibrational stimuli for the bill tip organ. This is the first report of epidermal specialisations functioning to enhance the role of the bill tip organ.

The distribution of Herbst corpuscles in the premaxilla and rostral mandible differs between the ostrich and emu, being less pronounced between the upper and lower bill in the ostrich than in the emu. This finding is reflected in the respective nerve fibre counts. In the ostrich there was no significant difference between the average number of nerve fibres present in the *N. ophthalmicus R. medialis* and *N. intramandibularis*, whereas in the emu a significant difference was present between the two nerves. Considering the significantly greater amount of nerve fibres present in the *N. ophthalmicus R. medialis* of the emu, compared to that of the ostrich, it would appear that the upper bill of the emu is more sensitive than that of the ostrich. However, the region of the *Culmen* in the ostrich (based on the significantly greater amount of bony pits in this region) is likely to be more sensitive than the corresponding region in the emu. The ostrich would thus appear to possess a more specific sensitivity (including also the Herbst corpuscle-rich median palatine and ventral ridges), and the emu a greater, but more general, sensitivity. When comparing nerve fibre counts, the upper bill in the emu would appear to be more sensitive than the lower bill, although this was not supported by the number of bony pits in the upper and lower bill of the emu. In the ostrich the upper and lower bills seem equally sensitive and both the nerve count and pit counts support this conclusion. Although the presence of bony pits indicated the presence of a bill tip organ in the ostrich and emu, the number of pits did not appear to correlate with overall sensitivity in these species.

The persistence through to adulthood of Meckel's cartilage in the ostrich and emu is a feature not previously reported in any avian species. Although this structure may ossify

at a much later stage in life, the function in young and adult birds may be to dampen shockwaves along the intramandibular nerve that result from the action of pecking. Cartilage is present along the main nerves relaying sensory information to the brain in both the upper and lower bill. The cartilaginous nasal septum is associated with the medial branch of the ophthalmic nerve and Meckel's cartilage runs with the intramandibular nerve in the mandibular neurovascular canal. The persistence of Meckel's cartilage in adult lepidosaurs and crocodylians strengthens a closer link between the ratites and extant members of the above groups.

A bill tip organ, characterised by the presence of bony (sensory) pits, has been demonstrated in three extant orders of palaeognathous birds, the Apterygiformes, Casuariiformes and Struthioniformes. Similar bony pits described or illustrated in the bill tips of the remaining extant and extinct orders strongly suggest that these birds also possess a bill tip organ. The kiwi (Apterygidae) was the first palaeognath in which a bill tip organ was described and the similarity observed between the bill tip anatomy and bill tip organ of this bird and probing shorebirds (Scolopacidae of the superorder Neognathae) prompted the conclusion that this feature was more likely a result of convergent evolution across a deep taxonomic divide rather than an indication of a shared phylogeny. As a bill tip organ may be a synapomorphic feature of the Palaeognathae, an explanation for this apparent 'convergent evolution' seen in the kiwi may be the specialisation of an already present anatomical feature shared amongst the palaeognaths. Following this line of reasoning, the question arises as to whether the bill tip organ of the kiwi (more complex and specialised) or that of the ostrich and emu, represents the basal form of bill tip organ in the Palaeognathae.

A bill tip organ is generally present in birds which probe-forage or strain their food (remote touch) and therefore perform more 'complex oral tasks'. A well-developed bill tip organ does not appear to be a prominent feature in pecking birds. Thus an enigma exists as to why the ostrich and emu, which primarily peck their food, possess such a well-developed bill tip organ. A possibility to be explored in future studies is the link between the eye and the bill. The eyes of both birds, and especially the ostrich, are quite prominent and would require some degree of protection from thorny plants and potentially dangerous objects during pecking. This is achieved by long eye lashes, a reinforced lower eyelid and a third eyelid which can be actively drawn across the eye.

The eyes would be necessary for aiming during pecking; however, once the bill is in motion towards the 'target', it may be beneficial to protect the eye by drawing the third eyelid over the cornea and allowing the tactile sense of the bill tip organ to complete the action of procuring the food item, rather than using vision and exposing the eye to potential harm. This could, in part, explain why both birds display such a well-developed bill tip organ.

This study concluded that taste buds were only present in the emu and that no structures resembling taste buds, employing the methods used in the present study, could be identified in the ostrich. Immunohistochemical labelling for neurofilament proved to be a superior method in identifying taste buds in the emu and this method is advocated for future studies on taste buds in other ratite species. The distribution of taste buds in the emu matched strategic locations in the oropharynx along which food could be sampled, according to the emu's specific feeding method. More taste buds were present on the oropharyngeal roof where sampling of dry food would occur and fewer taste buds were present in the oropharyngeal floor where liquids would travel. The morphological features of taste buds in the emu were similar to those described in other avian species, including the chicken. However, a taste canal system was not confirmed in the present study. The emu possesses genes indicating the ability to distinguish bitter and certain amino acid compounds. The ability to discriminate bitter tasting compounds is usually associated with a protective function and prevents consumption of noxious insects, plants and brackish water. In view of the emu's natural diet and arid environment it would appear that the main function of taste in this bird is that of protection. The emu would likely rely on senses other than taste, such as sight, smell and touch (bill tip organ), in discriminating everyday food. Future feeding studies would be necessary in the emu to determine the importance of taste discrimination in their diet. Similarly, in the ostrich, which apparently does not possess a sense of taste; sight, smell and touch (the bill tip organ) would be the most important factors determining food intake in these birds.

This study provided a number of new insights into the structure and function of specific elements of the upper digestive tract in the ostrich and emu. Functional implications ranged from new anatomical mechanisms (linguo-laryngeal apparatus) to an enigmatic, heightened sense of touch in the bill tips (bill tip organ), the phylogenetically important

persistence of Meckel's cartilage, and finally, a sense of taste (in the emu only). The various structural peculiarities identified in the ostrich and emu oropharynx during this study may form a basis for future functional studies, including electrophysiological experiments, feeding and behavioural trials as well as phylogenetic comparisons. Recent studies have integrated the various sensory systems present in birds to enable a better understanding of their behavioural ecology. Similar studies on the ostrich and emu, incorporating the visual fields, smell, touch and taste, are advocated to fully understand the function of the structures described in this study.

APPENDICES

APPENDIX I

Published article

Crole, M.R. and Soley, J.T. 2012. What prevents *Struthio camelus* and *Dromaius novaehollandiae* (Palaeognathae) from choking? A novel anatomical mechanism in ratites, the linguo-laryngeal apparatus. *Frontiers in Zoology*. **9**: 11.

APPENDIX II

1. Papers presented at local conferences

Crole, M.R., Soley, J.T. and du Plessis, L. 2009. The ultrastructure of Herbst corpuscles in the oropharynx of the emu (*Dromaius novaehollandiae*) and ostrich (*Struthio camelus*). *Proceedings of the Microscopy Society of Southern Africa*. **39**: 27. Durban, South Africa.

Crole, M.R. and Soley, J.T. 2012. Abstracts. A selection of abstracts presented at the 40th Annual Conference of the Anatomical Society of Southern Africa (ASSA) at the University of Namibia, Windhoek, Namibia, 14–18 April 2012. “What prevents ratites from choking?”. *Clinical Anatomy* **25**: 918-928 (920).

Crole, M.R. and Soley, J.T. 2012. As rare as emu “teeth”. *Proceedings of the Microscopy Society of Southern Africa*. **42**: 18. Cape Town, South Africa.

Crole, M.R. and Soley, J.T. 2013. Rostral nostrils: a unique feature distinguishing the Australasian ratites. 41st Annual Conference of the Anatomical Society of Southern Africa (ASSA). Durban, South Africa.

Crole, M.R., Soley, J.T. and van Wilpe, E. 2013. Distribution and structure of taste buds in the emu. *Proceedings of the Microscopy Society of Southern Africa*. **43**: in press. Pretoria, South Africa.

2. Poster presented at an international conference

Crole, M.R. and Soley, J.T. 2009. Comparative distribution of Herbst corpuscles within the oropharyngeal cavity of the ostrich (*Struthio camelus*) and emu (*Dromaius novaehollandiae*). *17th Congress of the International Federation of Associations of Anatomists*, Cape Town, South Africa. p. 361.